Effect of natural biofilm on transport and retention behavior of nanoparticles and microorganisms in limestone sediments: implications for managed aquifer recharge

by

Amirhosein Ramazanpour Esfahani

M.Sc.

Thesis Submitted to Flinders University

for the degree of

Doctor of Philosophy

College of Science and Engineering

20 April 2020

Table of Contents

List of Tables

List of Figures

List of Plates

Summary

Managed aquifer recharge (MAR) is increasingly becoming a component of water resource management in water stressed arid and semi-arid countries. Surface waters e.g. stormwater or treated wastewaters injected into the aquifer for storage may contain pathogenic bacteria and viruses and engineered nanoparticles, which pose a risk to public health upon subsequent surface reuse. Understanding the behavior of enteric pathogens and engineered nanoparticles in aquifers contributes to the management of this human exposure risk.

In this study, MS2 F-RNA bacteriophage, *Escherichia coli* (*E.coli*) and graphene oxide nanoparticles were applied as model virus, bacteria and nanoparticles, respectively. Physically simple and chemically clean sand grains, quartz sediments and limestone sediments were also used as collectors in batch and column studies. RO water with desired pH and ionic strength and treated wastewater obtained from Mount Barker, South Australia were used as aqueous media. Additionally, batch experiments of MS2 inactivation by attachment onto the surfaces of pristine and biofilm-conditioned limestone sediments were conducted at different contact times, initial virus concentrations (10^3-10^7 PFU/mL), limestone particle size distributions (0.25-0.5, 0.5-1 and >1 mm), temperatures (4 and 22 °C), agitation status (static and dynamic) and aqueous media (RO water and treated wastewater). The column experiments were conducted in saturated water conditions to mimic the real aquifers. The convection-dispersion equation (CDE) model was used to describe the experimental data of tracer (bromide) transport in sand and limestone columns.

The results of batch studies revealed higher affinity of MS2 to the biofilm-conditioned limestone sediments than the pristine ones. Furthermore, in column experiments of tracer and virus transport, higher biofilm accumulation in sand columns caused higher virus attachment onto the collectors. However, long-term irrigation of limestone columns led to more discharge of virus into the

effluents, due to changing the structure of limestone column by causing heterogeneities, due to calcite dissolution. Moreover, the biofilm growth and proliferation increased the physical and biological clogging of porous media, caused decreasing saturated hydraulic conductivity of columns.

GONPs transport and retention was significantly governed by mineralogical features of porous media, in which higher metal oxide/hydroxides enhanced their retention in columns. Moreover, high ionic strength of solution not only decreased the transport of GONPs in all columns, but also changed the shape of retention profiles (RPs) of GONPs from linear, at low ionic strength, to hyper-exponential at high ionic strength. The presence of biofilm in columns also not only increased the attachment of nanoparticles onto the surfaces of collectors, but also led to physical straining in the column.

The co-presence of microorganisms in nanoparticle suspension may have a significant influence on the transport and retention of GONPs. At high ionic strength, no changes were observed in the transport behavior of GONPs, due to the aggregation of microorganisms and nanoparticles. However, at low ionic strength, simultaneous enhanced transport and decreased retention of GONPs were obtained in the columns, due, primarily, to the competition between microorganisms and nanoparticles to occupy surface reactive sites of collectors.

The presence of biofilm onto the surfaces and interpores of columns, at both batch and columns systems, caused higher virus and nanoparticle attachment which can be acted as a biofilter in a real MAR site for prevention of pathogenic and engineered nanoparticles discharge in the groundwater.

Declaration

I certify that this thesis does not incorporate without acknowledgement any material previously submitted for a degree or diploma in any university, and that to the best of my knowledge and belief it does not contain any material previously published or written by another person except where due reference is made in the text.

Name: Amirhosein Ramazanpour Esfahani

Date: 20.04.2020

Acknowledgments

With completion of my thesis, I want to express my sincere thanks to all the people who have motivated, advised, appreciated and helped me throughout this long and interesting journey. Now, I would like to give special mention to the following persons:

For the first, my kind, humble and respectable principal supervisor Prof. Howard Fallowfield for inspiring me in using the novel ideas and methods in my thesis. The advice and ideas that you gave me in this journey were immensely appreciated. Frankly speaking, it was one of my greatest achievements in my life that become a PhD student of Howard. I also appreciate Prof. Okke Batelaan and Prof. John Hutson for their critical comments and advices about hydrogeology and soil science during PhD study which led to the improvement of the quality of my works.

I would like to thank Flinders University for providing academic and financial supports via Australian Government Research and Training Program (RTP) which made the research possible.

Special thanks to my genius friend, a very talented expert Mr. Raj Indela for his great knowledge in laboratory works and providing guidance and assistance in the experiments of my thesis.

I would like to show my sincere gratitude to Dr. Jennifer Fendler (Flinders Microscopy and Microanalysis) for assistance in taking CLSM images, Prof. Jason Gascooke (Flinders University) for his assistance with SEM analysis, Prof. Allan Pring for supports his guidance in spectroscopic analysis and Mr. Michael Ferraro, Olympic Drilling, South Australia for provision of authentic aquifer substrates.

Thanks to honors and PhD students at School of the Environmental Health department for creating unforgettable and memorable moments during the study of PhD. Particularly, however, I would like to acknowledge Mr. Peter Reeve for helping me in collecting wastewater samples from a water

and wastewater plant in Mount Barker, South Australia and Mrs. Farah Jafarpisheh and her husband Mr. Kiumars Shafiei that helped me so much in settling in via providing the accommodation.

And finally, to my family, my mother for her patience that motivated me whenever I became disappointed in this way. And also, my brother and father which supported me.

1. Introduction

Managed aquifer recharge (MAR) is increasingly becoming a component of water resource management in water stressed arid and semi-arid countries. Surface waters e.g. stormwater or treated wastewaters injected into the aquifer for storage may contain pathogenic bacteria, viruses and emerging contaminants, which pose a risk to public health upon subsequent surface reuse. Suspended solids and nutrients cause severe physical, chemical and biological clogging of aquifers via the production of biofilm. Understanding the behavior of enteric pathogens and emerging contaminants e.g. engineered nanoparticles in aquifers conditioned with biofilm contributes significantly to the management of this human exposure risk. The following chapter reviews effect of different mechanisms on attachment and transport behavior of microorganisms and nanoparticles in aquifer sediments.

1.1. Managed aquifer recharge (MAR)

One of the principal areas proposed by Integrated Water Resources Management (IWRM) is reusing wastewater resources to achieve the environmental sustainability (Lazarova et al., 2001). In recent years, there is an increasing trend towards reclamation and reuse of wastewater in different parts of the world. Extensive growth in population, urbanization and climate change, has caused a significant change in the balance between water supply and human demand (e.g., agricultural, industrial and domestic) which has led to an increasing demand for drinking water resources (Connor et al., 2017). To supply required demand for human water resources, groundwater has attracted the attention of hydrologists (Angelakis and Gikas, 2014). Managed aquifer recharge (MAR) has been a particular focus, which is a combination of different techniques

such as aquifer storage, transfer, and recovery (ASTR) or aquifer storage and recovery (ASR) (Ayuso-Gabella et al., 2011). In Australia, there is widespread growth in application of recycling urban stormwater via ASR and irrigation of agricultural lands (Vanderzalm et al., 2016). Stormwater harvesting and ASR was started in 2003 at Parafield Airport, South Australia at the city of Salisbury. The conventional method of water storage such as dam construction has several drawbacks including high evaporation, land availability for constructing dam, sediment accumulation and spreading human diseases (Bouwer, 2002). However, MAR is a water management approach in which a huge volume of low quality water resources such as stormwater and treated wastewater are injected directly into the aquifers for compensating groundwater scarcity (Dillon et al., 2010). Furthermore, it has been shown that the quality of influents can be improved via various, chemical, physical and biological processes in the aquifers (Dillon et al., 2012). This practice has been applied in different countries such as Israel, the Netherlands, the United States and Australia (Rinck-Pfeiffer et al., 2000). In those countries, treated water resources are injected into the aquifers and stored for subsequent reuse. The MAR design is site specific. Direct injection at predefined aquifer depths, water infiltration ponds, river bank filtration (RBF) and farm flooding are considered the most applicable processes applied in MAR schemes. The principal benefits of MAR techniques are (a) natural filtration of pathogenic contaminants, (b) excessive recharge rates for small surface areas and (c) preventing pollution and loss by evaporation of water resources (Tzoraki et al., 2018).

1.2. Different approaches to MAR

Different approaches in groundwater recharge have been applied in MAR schemes. Generally, increasing the groundwater resources using MAR was achieved thereby recharging water in

confined and unconfined aquifers via, i) vadose zone infiltration, ii) direct injection and iii) surface infiltration. In injection in vadose zone and surface infiltration methods, the subsurface layer plays an important role in improvement the water quality of influent through various physical, chemical and biological filtration mechanisms (Stuyfzand, 2011). The subsurface infiltration of recharge water decreases the amount of total organic carbon, nutrients and chemical pollutants with simultaneous saving in the cost of energy and system maintenance (Drewes, 2009). Surface infiltration systems are applicable in some zones with highly permeable top layer and a subsurface layer without presence of fine particles which limited vertical water movement (Bouwer, 2002). Furthermore, in some urban areas, where an increase in the level of the water table may cause damage to the infrastructure, the application of surface infiltration is not suitable. In some zones which lack top soil, vadose zone infiltration systems such as multiple recharge trenches and vadose zone wells can be implemented (Bouwer, 2002). When top soil is not permeable whereas the layer 2-3 m below the surface is permeable, the application of recharge trenches would be economical. The quality of applied water for vadose zone infiltration is critical which should have negligible amounts of suspended particles, nutrients and microorganisms, so the pre-treatment of water resources is of great importance (Bouwer, 2002). Both surface and vadose zone infiltration systems are economical and applicable for sites with lower lands. However, there is a restriction is application of these approaches in aquifers with high water table. Therefore, the application of direct injection is common where, i) no permeable top soils and sufficient land areas present for surface infiltration, ii) the vadose zone conditions are not appropriate for infiltration and iii) aquifers are confined and deep (Bouwer, 2002). It may have two wells for separate injection and recovery or single well for doing both of them at the same time.

1.3. MAR in limestone aquifer sites in Australia

In South Australia, there is a widespread consumption of surface and groundwater resources for irrigated horticulture and urban populations. Therefore, the abundance of water resources is a critical factor for future development in majority regions of the state. In South Australia, the research on improving the groundwater resources via MAR has been foregone because of restricted and site specific knowledge of water quality to inject into the unconsolidated aquifers (Page et al., 2011, Page et al., 2014). The practical application of MAR have focused on fractured rock and limestone aquifers (Page et al., 2011). From the point of view of clogging, limestone aquifers have higher tolerance toward low quality influent water because matrix dissolution maintains hydraulic conductivity (Page et al., 2011). Although fractured rock aquifers have shown more complexity for characterization of permeability, no comprehensive study has been carried out in Australia. Difficulties have been observed in maintaining injection rates in ASR wells in unconsolidated, fine-grained aquifers (Jeong et al., 2018).

Dissolution or precipitation of minerals in limestone aquifer sites change the media permeability at various temporal and spatial scales (Dijk et al., 2002). Many studies have reported the presence of preferential flow paths in limestone columns, due to mineral dissolution (Buijse, 1997, Hill et al., 1995, Dijk et al., 2002). The created macropores and preferential flow paths have a significant role in accelerating transport of solutes, microorganisms and engineered nanoparticles and changing their breakthrough curves (BTCs) (Eriksson et al., 1997). The rapid transport processes decrease the chemical degradation and retardation with matrix media and increase the risk of pathogenic and engineered nanoparticle transport from influent to the groundwater resources (Morris and Mooney, 2004). Understanding the effect of treated wastewater or stormwater on

mineral dissolution in limestone aquifers and the consequent changes to their hydraulic properties and structure is a critical for the sustainability of MAR schemes.

1.4. The drawbacks of MAR

Treated wastewater would be an appropriate MAR alternative source in urban environment, although several practical and public health issues have been identified (Page et al., 2018). The practical restrictions include clogging of aquifers via the presence of high volumes of suspended organic and inorganic materials, microbial mass growth and proliferation and particle precipitation by changing pH and redox potentials. Public health considerations are groundwater contamination by pathogenic and chemical contaminants such as engineered nanoparticles present in the injected water resources. Therefore, if water is not well treated, it may lead to the quick failures of this technique. Moreover, the presence of pathogenic contaminants and engineered nanoparticles in the wastewater pose a potential risk to humans (Symonds et al., 2009). The nature and dosages of microbial contaminants in a typical wastewater is highly dependent on various agents such as, the pathogen occurrence in the community, the seasonality of most of pathogens and social economic factors where in low socio-economic groups the rate of infection by microbial contaminants is high (Toze, 1999).

1.4.1. Aquifer clogging mechanisms

The term "clogging" which is one of the most critical disadvantages of MAR technique is defined as a reduction in porosity and permeability of porous media via different physical chemical and biological processes (Bouwer, 2002). The processes operating in porous media clogging are

complicated and diverse and the related mechanisms are categorized into three different sections physical clogging, chemical clogging and biological clogging, (Rinck-Pfeiffer et al., 2000, Mays and Hunt, 2007). The related processes associated with MAR clogging are as follows: the accumulation of suspended particles in the collectors (Rinck-Pfeiffer et al., 2000), mineral precipitation via either chemical or biological processes (Baveye et al., 1998), clays swelling and dispersion (Konikow et al., 2001), the production of biofilm via growth and proliferation of microbial mass by nutrient elements present in the influent (Rinck-Pfeiffer et al., 2000) and air and gas entrapment. Results of research on 40 aquifer wells show that over 80 % of them suffer from clogging where the role of suspended solids and gas bubbles, microbial mass and chemical precipitations is around 70, 15 and 10 %, respectively (Dillon et al., 1994).

1.4.1.1. Physical clogging

In general, physical clogging occurs by entrapment and attachment of fine suspended solid materials into the aquifer grains interpores and surfaces, clay materials dispersion and fine materials rearrangement within the porous media (Platzer and Mauch, 1997). The most important factor affecting physical clogging is the size of suspended particles in the stormwater and porous media (Wang et al., 2012). The intensity of physical clogging has a direct relationship with the diameter of suspended solids (Siriwardene et al., 2007). The clogging caused by suspended solids can be further categorized as superficial, inner and mixed clogging based on the ratio of effective medium pore diameter and suspended solids median grain size (Du et al., 2014). Clay minerals are the other ubiquitous particles in aquifers, which exacerbate porous media physical clogging by swelling, migration and swelling-induced migration (Konikow et al., 2001). In addition to suspended particles size, the ionic strength of solution and hydrodynamics alter the media

hydraulic conductivity thereby changing the morphology and stability of retained colloidal particles (Mays and Hunt, 2005). The higher permeability happens when larger fluid velocity transport a huge mass of suspended solids (Veerapaneni and Wiesner, 1997).

Gas bubbles produced by entrapped air and biogenic activities is another factor contributing in porous media physical clogging (Beckwith and Baird, 2001). The clogging by gas bubbles can be inferred by a significant increase in water level after injection of stormwater (Martin, 2013). The biogenic gases (e.g., CO_2, N_2, H_2S and CH_4) can be produced by microorganism's metabolism which clog the pore throat of large pores, causing increasing water level and decreasing permeability of media. The sum of entrapped air and biogenic gases may occupy 7-20 % of pore space (Beckwith and Baird, 2001).

1.4.1.2. Chemical clogging

The concentrations of different ions, solution pH, redox potential and mineralogical characteristics of aquifer materials influence pore stability and shape and also determine the saturated hydraulic conductivity of aquifers. A decrease in ionic strength of solution and enhancement of the sodium adsorption ratio (SAR) causes dispersion of clay particles leading to the pore clogging (Rengasamy et al., 1996). The precipitation of different minerals such as carbonate, sulfate and phosphate may lead to the chemical clogging of porous media. In most cases, it is not the major cause of porous media clogging and may develop after a very long time (Martin, 2013). The presence of microorganisms in iron and manganese-bearing media causes the precipitation of Fe(III) and Mn oxides. In a typical medium, either carbonate and sulfate or iron and manganese precipitation can be observed. Carbonates are easily dissolving in acidic conditions, but sulfate minerals are resistant against dissolution, even at low pH values. The iron precipitation has a firm relationship with the

concentration of dissolved oxygen in solution. Indeed, mixing aerated shallow groundwater with anoxic deep groundwater leads to oxidation of two to three valent iron and subsequently iron oxide precipitation, as shown in equations below (Majkić-Dursun et al., 2015):

$$Fe^{2+} + O_2 + 2H^+ \leftrightarrow Fe^{3+} + 2OH^- \quad (1\text{-}1)$$

$$Fe^{3+} + 3H_2O \leftrightarrow Fe(OH)_3(s) + 3H^+ \quad (1\text{-}2)$$

As discussed above, the precipitation of iron is highly depended on redox potential and calcium dissolution is closely related to the solution pH. Therefore, to better understand the chemical clogging processes, the measurement of pH and redox potential has to be performed.

1.4.1.3. Biological clogging

Microbial activities in the aquifers can produce some solid, gas and gel phases. The solid materials are their cells and by-products precipitated from their activities such as iron sulfide and iron hydroxides (Van Beek and Van der Kooij, 1982). While, the gas phase includes some soluble gaseous compounds like dinitrogen or methane (Oberdorfer and Peterson, 1985, Lance and Whisler, 1972). The gel phase may be the extracellular polymers, which are known as exo-polymers that are intrinsically polysaccharide (Cagle, 1975). This phenomenon is extensively observed in in-situ bioremediation of different contaminants, aquifer storage management and permeable reactive barriers (PRB) construction (Liang et al., 2000, Calderer et al., 2014). Bio-clogging can be triggered by discharge of recycled water containing large amount of organic carbon, nitrogen and phosphorous. The 'traditional' view was that the microbial biomass was as a biofilm distributed uniformly onto the solid surfaces (Seifert and Engesgaard, 2007). While, others stated that microbial micro-colonies are mainly responsible of bio-clogging. Baveye and Valocchi,

(1989) proposed three different models for distribution of biofilm in porous media: (i) the unique uniform distribution of biofilm, (ii) the non-uniform distribution of micro-colonies and (iii) a microscopic approach which assumes that biomass is in a bulk state. Some studies stated that bacterial biomass can be non-uniformly -as an aggregate- attached to the porous media (Baveye and Valocchi, 1989). Therefore, they attributed the saturated hydraulic conductivity (K_s) reduction in porous media to the accumulation of bacterial mass (either as biomass or microbial colonies) into the pore structures (Vandevivere and Baveye, 1992a, Vandevivere and Baveye, 1992b). Plate 1-1 is a schematic diagram that shows different steps of bio-clogging where micro-colonies grew from initial phase (Phase I) to the Phase II and III that led to the bio-clogging of porous media (Seifert and Engesgaard, 2007). Accordingly, the growth of micro-colonies are observed in which the continuous attachment and detachment cause changing the water flow and hydrological features of porous media. Additionally, in other articles, the reduction of K_s by 2-3 orders of magnitude as a results of pore-clogging with biomass has been reported (Seki et al., 2002). In nearly all studies, a similar trend for K_s reduction was reported where it dropped suddenly then was followed by a constant trend until the end of experiments. Indeed, there was a remarkable drop in K_s ascribed to the accumulation of biomass near the injection point which decrease K_s in the inlet end, compared to the outlet end (Baveye et al., 1998). The amount of microbial mass and bacteria has a pivotal role on the extent of biological clogging of porous media. Research has been performed to find a correlation between number of bacteria and reduction in K_s. Gupta and Swartzendruber, (1962) found no significant changes in the K_s of column, when the concentration of bacteria was 0.4×10^6 CFUg, while by increasing the bacteria concentration to 1.3×10^6 CFU/garound 100 times reduction was seen in K_s (Gupta and Swartzendruber, 1962). Furthermore, Vandevivere and Baveye, (1992d) studied the role of biomass densities of *Arthrobacter* sp. biofilm

on K_s reduction, in which no reduction was seen in K_s at 4 mg/cm^3 of biomass density (Vandevivere and Baveye, 1992d). However, as biomass densities increased to 10, 20 and 35 mg/cm^3, the reduction rates of K_s were one, two and three orders of magnitude, respectively. The percentages of amount of microbial mass occupied in the columns were 2.4, 4.8 and 8.5 %, respectively.

As it is obvious, although microbial mass occupied a negligible fraction of pore space, they could cause huge reductions in the K_s of columns. So, it can be postulated the specific and direct influence of microbial mass on the hydraulic properties of columns (Seki et al., 2002). The microbial mass can trigger severe clogging if they grow in the grain contacts or at pore necks of columns. Results of Vandevivere and Baveye, (1992d), Vandevivere and Baveye, (1992a), Vandevivere and Baveye, (1992c) revealed that the strategic localization of bacterial cells would be due to the characteristics of lots of microorganisms to create aggregates of different sizes (Vandevivere and Baveye, 1992d, Vandevivere and Baveye, 1992a, Vandevivere and Baveye, 1992c). Particularly, no biofilm was produced by *Arthrobacter* AK19 onto the surfaces of sand grains, while three-dimensional aggregates were formed at the pores lumen (Vandevivere and Baveye, 1992d).

Furthermore, bio-clogging of porous media in bioremediation initiatives will not only prevent or at least inhibit contaminant transport, but also deviate groundwater flow from its paths to the contaminated area (Taylor and Jaffé, 1990). The economic damage of bio-clogging should also be considered. For example, in Microbial-Enhanced Hydrocarbon-Recovery (MEHR) treatment approach, it can potentially cause significant economic loss to the well bores (Brown, 2010). Moreover, biological factors like growth of microbial mass into the aquifers cause huge operational costs such as increase in energy required for pumping and well re-development and disinfection of microorganisms to prevent clogging (McCarty, 1993, McCarty et al., 1998).

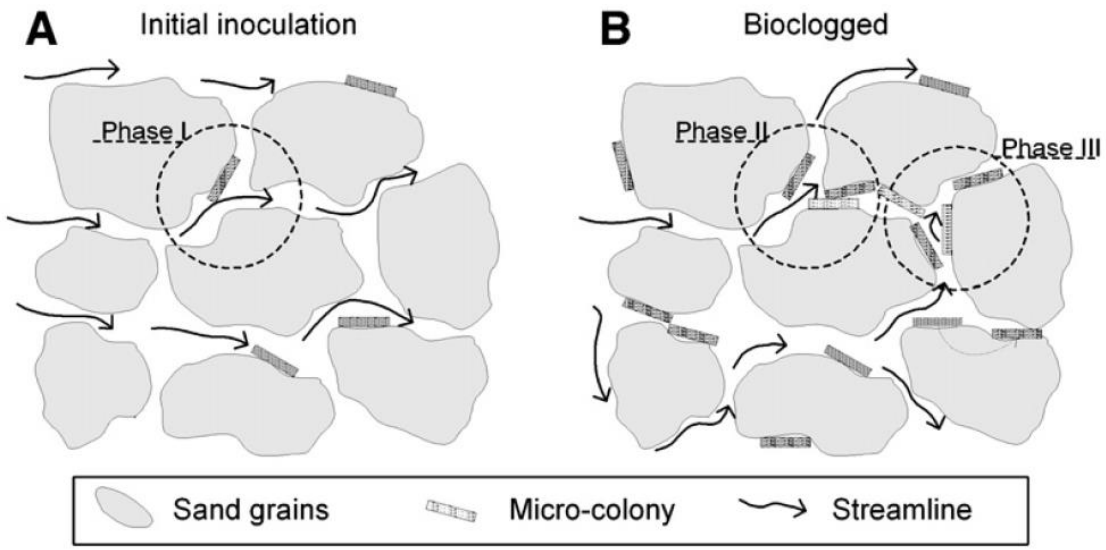

Plate 1-1. Schematic diagram depicting biomass growth in porous media (Seifert and Engesgaard, 2007) (Reproduced with permission).

1.4.2. Water quality criteria

All water resources used as influents for MAR need some degree of treatment, due to the presence of different chemicals and contaminants. A large number of organic and inorganic colloidal particles namely, bacteria, viruses, clay minerals, engineered nanoparticles, humic materials and iron and aluminum oxides present in subsurface environment. Groundwater contamination by pathogenic microorganisms has led to the pollution of drinking water resources causing a risk to human health (Fontes et al., 1991, Scandura and Sobsey, 1997). In confined aquifers, the recharge source water is the major source of enteric pathogens. In unconfined aquifers, however, the other sources such as manure spread over pastures and sewage contamination would contribute to contamination with pathogens (Dillon, 2009). The applied water resources in MAR sites including treated wastewater, stormwater and grey water may have different types and concentrations of

pathogenic factors which caused serious risks to human health. Between 1971 and 2002, in the United States, around 575,457 cases of diseases and 79 deaths related to drinking fecal polluted potable water have been reported (Reynolds et al., 2008). Virus can be discharged into the subsurface environment either intentionally or accidentally. Some activities like fractured sewer lines, application of polluted municipal wastewater for agricultural irrigation, and constructed landfill may accelerate the entrance of viruses into the groundwater (Yates et al., 1985, Chrysikopoulos and Sim, 1996). Pathogenic organisms can enter the surface water either by runoff or discharged into the groundwater by transport through soil profiles and aquifers. The transport and retention behavior of microorganisms in soils and aquifers may be influenced by the following factors: (1) attachment to porous media particles, (2) transport into the deeper layers or discharge into the groundwater resources and (3) death due to undesired environmental conditions. The importance of potable water sanitation and the prevention of microbial pollution, transport and retention of bacteria, viruses and pathogenic agents has resulted in extensive investigations over last decades.

Besides viruses and bacteria, the other colloidal-sized particles that are ubiquitous either in suspended or deposited states in the environment are engineered nanoparticles. The increasing application of engineered nanoparticles, specifically the metal oxides, has been drawn significant attention to their interactions with soil and marine environment (Babaei et al., 2015). A group of these particles such as zero-valent iron nanoparticles (ZVIN), because of their small diameters and immense surface areas, which is an advantage to reduce various contaminants, have widely been applied for environmental clean-up (Esfahani et al., 2014). Furthermore, in recent years, graphene oxide nanoparticles (GONPs) has attracted the attention of environmentalists, since they are being used more extensively in medical, energy and environmental fields (Dreyer *et al*., 2010).

According to the literature, GONPs have potential for bacterial toxicity, cytotoxicity and causing lung illness in humans. Therefore, knowledge about transport and retention of GONPs in porous media and related mechanisms governing their retention is critical. Transport and retention behavior of GONPs have been studied in last decade which exhibited a firm relationship with physicochemical features of porous media and aqueous solution. However, there is lack of information about GONPs transport in natural aquifers, since most research have been carried out in artificial porous media or physically simple and chemically clean sand grains. Therefore, the related mechanisms of GONPs retention in real aquifer materials have not been elucidated.

Until some decades ago, a general belief was that only aqueous and gaseous phases can influence the transport behavior of chemicals and particles in the porous media. However, it is totally accepted that the suspended solid particles can either facilitate or prevent the mobility of other chemicals and particles, depending on the chemical conditions of porous media (Saiers, 2002). The majority of research on transport of colloidal particle such as bacteria, viruses and metal nanoparticles were performed on individual transport behavior of these particles in porous media (Esfahani et al., 2014, Saha et al., 2019, Kanel et al., 2015). However, the presence of either suspended or deposited manufactured colloidal particles which are quite ubiquitous in aquifers may influence their transport and deposition behavior (Malgaresi et al., 2019). In addition, colloidal particles, due to their extensive surface area, enhance adsorption of chlorinated organic substances like polychlorinated biphenols (PCBs), polycyclic aromatic hydrocarbons (PAHs), heavy metals, and radionuclides (Puls and Powell, 1992).

Several studies have revealed that bio-colloidal particle (i.e., bacteria and virus) transport and retention kinetics was significantly dependent on the presence of either suspended or deposited colloids like clay minerals (Vasiliadou and Chrysikopoulos, 2011, Cai et al., 2013), natural organic

matter (NOM) (Yang et al., 2012a, Yang et al., 2012b) and metal/metal oxide nanoparticles (Yang et al., 2013). Colloid-facilitated transport of bio-colloids may improve their transport to larger distance, compared to the absence of inorganic colloids. In addition, nanoparticle transport and retention are highly affected by co-presence of colloids, due to changing their agglomeration status. In other words, the agglomeration status of nanoparticles can be altered by presence of other colloids either with similar or different surface charges (Chowdhury et al., 2012).

Among these effective particles, clay minerals are the most abundant inorganic particles in subsurface environment with over thirty different classes namely, bentonite, montmorillonite, elite, kaolinite and so forth (Wilson *et al*., 2014). Regarding their high specific surface area, abundant surface charges and influential environmental factors, clay colloidal particles can either facilitate or prevent bio-colloids or nanoparticle transport in porous media (Schroth and Sposito, 1996). Vasiliadou and Chrysikopoulos, (2011) studied cotransport of suspended kaolinite and *E. coli* in water-saturated glass beads packed columns (Vasiliadou and Chrysikopoulos, 2011). They found that bacteria deposition was increased in the presence of kaolinite particles, due to their retention onto the solid matrix. Virus transport may also be affected by colloidal clay particles at different experimental conditions. Syngouna and Chrysikopoulos, (2013) reported that kaolinite and montmorillonite, as two model clay colloids, had significant influence of two bacteriophage MS2 and ϕX174 transport in saturated columns packed with glass beads at different pore water velocities (Syngouna and Chrysikopoulos, 2013). According to their research, irreversible deposition of bacteria onto the porous media surfaces happened in the presence of suspended clay particles. Moreover, MS2 compared to ϕX174, exhibited more inclination to be attached to clay particles. As mentioned above, not only bio-colloids transport may be affected by clay particles, but also metal/metal oxide nanoparticle transport is relatively dependent on the type and amount

of suspended clay particles. Unlike the findings in cotransport of bio-colloids and clay minerals, Cai et al., (2014) found that the presence of bentonite and kaolinite enhanced titanium dioxide nanoparticles ($nTiO_2$) transport in sand column with NaCl (Cai et al., 2014). However, in $CaCl_2$ solutions, a different pattern was observed. The breakthrough curves of $nTiO_2$ were lower and higher in the presence of kaolinite and bentonite, respectively.

Additionally, the huge application of engineered nanoparticles in various manufactures have led to their widespread release into the environment. These nanoparticles are ubiquitous in aquatic environment and may have some physical or chemical interactions (Qi et al., 2014b, Wang et al., 2013a). To the best of our knowledge, the majority of research have been conducted on transport of one type of nanoparticles. However, releasing various sorts of engineered nanoparticles simultaneously into the environment would expected to have influence on their transport. Therefore, the simultaneous transport of different nanoparticles deserves greater attention. In this regards, Cai et al., (2013) investigated transport of $nTiO_2$ and fullerene nanoparticles (nC_{60}) in saturated porous media at various ionic strength and two pH values (i.e. 5 and 7) (Cai et al., 2013). They found that at pH of 5, in all the studied ionic strengths, cotransport of nC_{60} had not significant effect on $nTiO_2$ breakthrough curves and retention profiles. While, at pH of 7 a decrease was observed in BTCs and retention profiles of $nTiO_2$ in the presence of nC_{60}.

Another facet of cotransport study would be the interactions between engineered nanoparticles and bio-colloids. Not surprisingly, bio-colloids will interact with engineered nanoparticles and their transport would be either hindered or facilitated. Yang et al., (2013) studied transport of *E.coli* and carbon nanotubes in saturated porous media at different ionic strengths and compositions (Yang et al., 2013). Their results revealed that at low ionic strength, no significant changes were observed for BTCs of bacteria transport affected by carbon nanotubes, compared to the absence of

nanotubes. On the other hand, with increasing ionic strength, the BTCs of *E.coli* effected by carbon nanotubes showed a considerable decrease. Recently, co-transport of *E.coli* as model bacteria with both carboxyl and hydroxyl functionalized multi-walled carbon nanotubes were performed in saturated porous media under various ionic strength and compositions (Han et al., 2016). The analysis of BTCs and retention profiles of nanoparticles revealed that without consideration of ionic strength, nanoparticle retention was high in the presence of bacteria. On the other hand, the most recent paper published on cotransport of microorganisms and engineered nanoparticles studied the effect of *E.coli* on multi-walled carbon nanotubes (MWCNTs) (Yang et al., 2013). The most important finding of that was the significant effect of bacteria on enhanced transport of MWCNTs and a decrease in their retention, due to high inclination of bacteria to occupy surface reactive sites.

Although transport of engineered nanoparticles and microorganisms in pristine sand grains have been performed previously, there is a lack of understanding on interaction between GONPs and microorganisms in natural porous media and transport and retention behavior.

1.5. Mechanisms influencing colloidal particle transport and retention in porous media

1.5.1. Attachment/Detachment

The retention of colloidal particles onto the surfaces of substrate is known as attachment. Derjaguin- Landau- Verwey - Overbeek (DLVO) is an approach that has been used for explanation of colloidal particle attachment process (Derjaguin and Landau, 1993). Based on DLVO theory, it is assumed that the attachment of particles occurs in both short ($\leqslant$1 nm) and long (5–10 nm)

distances which are termed as primary and secondary energy minima, respectively. The zone between these two spaces, the maximum electrostatic repulsion forces can be obtained, which has an indirect relationship with the ionic strength of solution (Abbott et al., 1983). The attachment of colloidal particles on solid surfaces is divided into reversible and irreversible processes. The reversible attachment is derived from a weak bonding between colloidal particles and porous media via electrostatic and van der Waals forces (Mozes et al., 1987). While, the irreversible attachment is considered as a permanent interaction with significant energy (Marshall, 1971). Factors influencing the attachment of colloidal particles onto the substrate surfaces are physical (e.g., temperature, biofilm and pore water velocity), chemical (e.g., pH and ionic strength and composition) and biological (e.g., hydrophobicity and cell surfaces) (Stevik et al., 2004).

The term detachment is opposite of attachment of colloidal particles in substrate which is defined as separation of colloidal particles from a solid matrix. In some cases, the detachment of particles from solid surfaces would be impossible, even by decreasing the ionic strength of solution, because of increasing the energy well depth which means that the particles should overcome more attractive forces in primary energy minimum. In some cases, decreasing ionic strength thereby diluting the concentrations of cations in the solution can lead to the detachment of particles. For example study of Wang et al., (2017a) showed detachment of graphene oxide nanoparticles from sand column by decreasing ionic strength (Wang et al., 2017a). In general, ionic strength of solution has a significant influence on the retention of nanoparticles onto the surfaces of substrate. Based on the classic DLVO theory, by increasing the ionic strength a reduction will happen in the electrostatic double layer and repulsive forces between nanoparticles and substrate, which causes enhanced retention of nanoparticles. When both colloidal particles and solid surfaces have negative charges, there is large electrostatic repulsion between the particles and substrate, which is derived from

ineffective screening at low ionic strength conditions (Chowdhury et al., 2013). Increasing the ionic strength decreases the diffuse double layer thickness and electronegativity of particles, which causes simultaneous decrease in the repulsive electrostatic interaction and increases deposition behavior.

1.5.2. Blocking and ripening

These are two opposite mechanisms governing on particle attachment behavior which cause decreasing and increasing nanoparticle retention in porous media, respectively. Blocking is considered as a decrease in further nanoparticle deposition onto the substrate surfaces caused by previously attached nanoparticles occupying the limited reactive surface area. One of the most significant index to recognize the role of blocking on retention of nanoparticles is the shape of BTC. The shape of BTC of a non-reactive tracer is symmetrical, which is close to 1 without skewness. However, the shape of BTC of nanoparticles affected by blocking would be ascending which reflects higher eluted particle in the effluents by further injection. Similar papers have reported role of blocking on transport and retention behavior of different nanoparticles in porous media (Fan et al., 2015). Dong et al., (2017) found that the main mechanism affected graphene oxide nanoparticles (GONPs) in limestone-packed columns was blocking (Dong et al., 2017). The shape of retention profile (RP) of nanoparticles is one of the most important factors which shows the governing mechanisms on nanoparticle retention in porous media. In most studies, the linear shape which shows the equal retained nanoparticles in different parts of porous media has been obtained for blocking of nanoparticles in collectors. In contrast, ripening occurs when attached nanoparticles act as further attachment sites for suspended nanoparticles (Nascimento et al., 2006). Irrespective of the contrast between blocking and ripening mechanisms, they can occur

simultaneously within a column, due to chemical and physical heterogeneities. A typical BTC of nanoparticle transport affected by ripening shows a decreasing trend with time, because of an enhancement in the attachment of suspended nanoparticles with recently deposited particles onto the collector surfaces. The RP of deposited nanoparticles by repining would be either exponential or hyper-exponential in which higher nanoparticles are attached close to the column inlet, due to the attachment to the deposited particles or enhanced aggregation. Findings of Chen et al., (2018) showed the exponential shape of retained graphene oxide nanoparticles (GONPs) onto the sand columns at high ionic strength (Chen et al., 2018).

1.5.3. Straining

Straining is a process where suspended nanoparticles are trapped in the pore spaces between porous media collectors, preventing their passage through the solid phase. Straining affects physical filtration of particles with a wide range of diameters (Tufenkji et al., 2004, Bradford et al., 2002). In subsurface environment, there is a wide range of sand or soil particles with different size distributions, orientation and configuration. There is, however, a linear relationship between the intensity of straining and the diameter of colloidal particles and collectors (Bradford et al., 2013). The effect of straining on particle deposition occurs when the ratio of colloidal particles to collector diameters is over 0.002 (Torkzaban et al., 2008b). In most of the time the breakthrough curve of nanoparticles affected by physical straining is relatively flat which is completely different with BTCs when blocking and ripening happen. However, in most studies, different RP shape was obtained for straining in comparison with ripening in which majority of nanoparticles were attached in the inlet end of columns which decreased hyper-exponentially with depth. Plate 1-2 shows different mechanisms affecting colloidal particle retention in porous media.

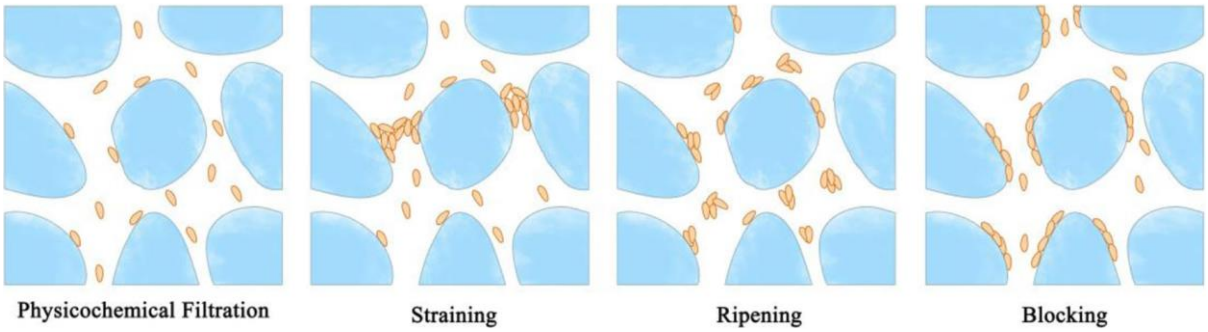

Plate 1-2. Schematic diagram of different mechanisms on colloidal particle retention in porous media (Ma et al., 2018) (Reproduced with permission).

1.6. Factors affecting interaction between nanoparticles and biofilm in porous media

Various factors affect the interactions between colloidal particles and biofilm onto the surfaces of porous media such as environmental conditions, colloidal particles and biofilm characteristics.

1.6.1. Effect of colloidal particle characteristics on interaction between colloidal particles and biofilm

The characteristics of colloidal particles including chemical composition, size distribution, dosage and surface charges, especially engineered nanoparticles have a significant influence on biofilm-porous media systems. Regarding the size of nanoparticles, it affects the antimicrobial ability of colloidal particles. Results of Morones et al., (2005) revealed that the size and antimicrobial activities of nanoparticles had an indirect relationship (Morones *et al*., 2005). Further research, Pal et al., (2007) reported that the changes in biocidal features of nanoparticles were moderated by changing the size of the nanoparticle (Pal et al., 2007). Previous research have showed that

engineered nanoparticles penetrated easily into the biofilm when their sizes and negative charges were high; the larger size and higher negative charges decreased self-aggregation of nanoparticles (Peulen and Wilkinson, 2011). Furthermore, findings of Tripthi et al., (2011) showed that the size, charge and surface chemistry of nanoparticles have a significant influence on the behavior of nanoparticles in biofilm-conditioned substrate (Tripathi et al., 2011). In terms of nanoparticle concentration, it is so hard to determine the exact concentrations of nanoparticles present in the environment, estimations have been carried out based on the production and release rates, which suggest nanoparticle concentration as µg/L (Mueller and Nowack, 2008, Zänker and Schierz, 2012). Findings of Agarwala et al., (2014) showed the effect of CuO nanoparticle on biofilm formation inhibition when the concentration of nanoparticles was in the range of 0.5 to 2 MIC (Agarwala et al., 2014). While, at concentrations of less than 0.5 MIC, a reduction was observed in the effect of nanoparticles on biofilm. The surface properties of nanoparticles is another important factor influencing the interaction between nanoparticles and biofilm (Jastrzębska et al., 2012). Indeed, there is a high attraction between positively-charged colloidal particles and negatively-charged biofilm surfaces by electrostatic forces.

1.6.2. Effect of biofilm features on interaction between colloidal particles and biofilm

The main part of biofilm would be extracellular polymeric substances which controls the features and functions of biofilm. EPS contains 10-82 % protein, 30-60 % humic substances, 7-30 % carbohydrates, 3-22 % uronic acids and 2-15 % DNA (Jahn and Nielsen, 1995). EPS components, surface irregularities and charges, density and thickness of biofilm determine its interaction with colloidal particles. It is apparent that the thinner biofilm more easily attracts colloidal particles

than the thicker ones (Sahle-Demessie and Tadesse, 2011). The roughness of biofilm surfaces is a critical factor which rougher biofilm entraps higher number of the pathogenic agents from aqueous media (Janjaroen et al., 2013). The age of biofilm would be effective on the interaction with colloidal particles in which the chance toxicity of nanoparticles to young biofilm is higher than the older ones due to the lower thickness and density of EPS protected cells. The surface charges of biofilm determined the electrostatic interactions between biofilm and nanoparticles. The surface charge expresses by zeta potentials and electrophoretic mobility in which by the attachment of positive charges nanoparticles onto the biofilm the negative charges would be decreased (Joo and Aggarwal, 2018).

1.6.3. Effect of environmental conditions on interaction between colloidal particles and biofilm

The surfaces of nanoparticles can be functionalized in the aqueous matrix which changes their surface features. Several studies have reported the creation of "corona" layer onto the nanoparticle surfaces when discharged into the aqueous media (Cedervall et al., 2007). For example, the presence of humic materials in natural organic matters would be adsorbed onto the surfaces of ENPs which changes the stability of nanoparticles in aqueous solution (Jastrzębska et al., 2012). The biofilm with higher density may limit nanoparticle and solute diffusion in biofilm body (Renslow et al., 2010). Results of Tong et al., (2010) showed higher attachment of C_{60} nanoparticles onto the silica surfaces conditioned with EPS at different ionic strength and fluid velocity in which the deposition of nanoparticles was more influenced by flow rate and ionic strength than EPS (Tong et al., 2010). In addition, the nanoparticle retention on biofilm-conditioned collectors were not interpreted by DLVO forces, revealing the role of non-DLVO

forces such as surface roughness and irregularities and C_{60}-protein interaction on enhanced nanoparticle deposition. Findings Fabrega et al., (2009) of showed that the presence of Suwannee River Fulvic Acids (SRFA) caused higher silver nanoparticles uptake and bioaccumulation on *Pseudomonas putida* biofilm, due to the long-term influence of biofilm structure and function (Fabrega et al., 2009). However, in the absence of SRFA, the interaction between silver nanoparticles and *P.putida* biofilms led to considerable biofilm sloughing from the surface. Sahle-Demessie and Tadesse, (2011) reported the effect of pH on the interaction between TiO_2 nanoparticles and biofilm prepared as superporous spherical beads from agarose in controlled environmental conditions (Sahle-Demessie and Tadesse, 2011). Their results showed that the attachment of nanoparticles by biofilm at acidic conditions was 40 % higher than neutral conditions due to the high colloidal stability of nanoparticles at alkaline environment.

1.7. Effect of biofilm on mechanistic approach of retention of colloidal particles in porous media

Surface conditioning of porous media collectors with biofilm alters transport and retention behavior of nanoparticles. Recently, there has been a widespread interest on working on the effect of surface conditioning of porous media grains on mechanisms of particle retention. According to the literature, the enhanced retention of colloidal particles onto the surfaces of biofilm-conditioned porous media can be attributed to the changes in DLVO forces, increasing surface roughness of collectors and physical straining.

1.7.1. Changing DLVO interaction energies

The sum of attractive or repulsive forces between nanoparticles and collector surfaces is described by classical Derjaguin-Landau-Verwey-Overbeek (DLVO) theory (Deraguin and Landau, 1941). In general, high values of maximum energy barriers (Φ_{max}) and less negative value of secondary (Φ_{min2}) energy minimum show higher electrostatic repulsive forces between colloidal particles and substrate, which prevent particle retention in substrates. The zeta potential of particles shows the dominant surface charges in which the more negative values represent the higher negative surface charges on the surfaces of collectors. According to the literature, less negative values of zeta potential of biofilm-conditioned collectors have been reported, compared with pristine ones, which was attributed to the charge neutralization of surfaces by biofilm growth. Therefore, colloidal particles in the presence of biofilm-coated collectors experienced less negative surface charges, which decrease the electrostatic repulsive forces between colloidal particles and collectors and consequently higher attachment (according to classical DLVO considerations). Figure 1-1 shows the calculated DLVO interaction energies between graphene oxide nanoparticles (GONPs) and (a) pristine and (b) biofilm-conditioned sand grains at different ionic strengths. Accordingly, higher Φ_{max} and less negative Φ_{min2} were observed in pristine columns than the biofilm-conditioned ones, which indicate the role of biofilm on enhanced retention of GONPs by changing the DLVO forces (He et al., 2017).

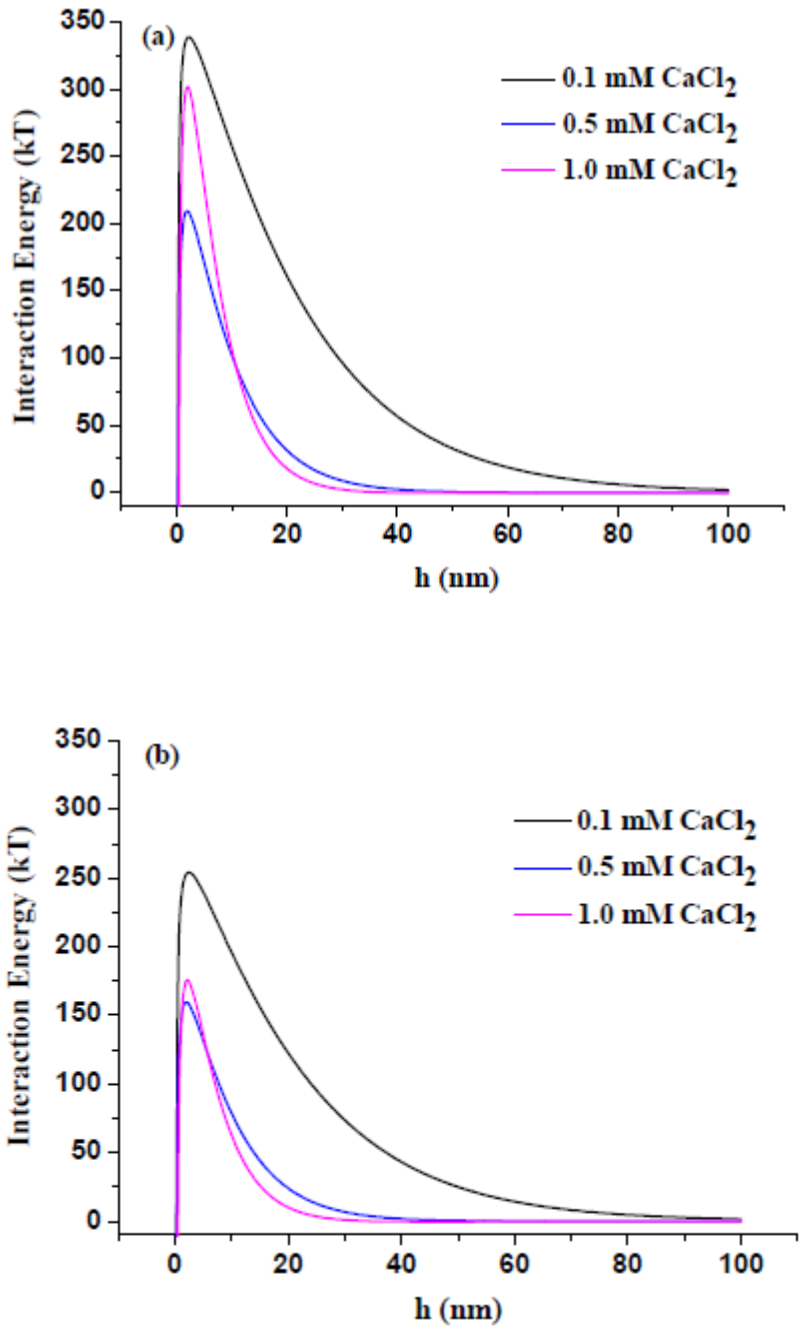

Fig 1-1. Calculated DLVO interaction energies between GONPs and (a) pristine and (b) biofilm-conditioned sand grains (He et al., 2017) (Reproduced with permission).

1.7.2. Surface properties

Chemical and physical heterogeneities of collector surfaces have been recognized as the most critical factors affecting particle retention behavior, even at unfavorable attachment conditions (Tufenkji and Elimelech, 2005a). Biofilm growth on collector surfaces increase physical heterogeneities by producing higher irregularities and surface roughness which produce favorable attachment sites for nanoparticle retention at both favorable and unfavorable attachment conditions. The produced regions caused less hydrodynamic forces and torques and flow vortices for nanoparticles (Taneda, 1979, Vaidyanathan and Tien, 1988). Findings of He et al, (2017) showed that the SEM images of biofilm-conditioned sand grains had higher surface irregularities than pristine ones which led to the enhancement in GONPs retention in porous media (He et al., 2017). However, a contradictory result has been reported in the literature. In some cases, biofilm growth onto the surfaces of substrates occupies the reactive surface sites, which decrease the attachment efficiency of the adsorbent. Findings of Mayotte et al., (2017) showed that the sand grains obtained from a MAR site containing 15 times higher organic carbon than the sand from the same source had lower MS2 sorption rate (Mayotte et al., 2017). Furthermore, the mechanisms of attachment of MS2 onto the sand grains with higher and lower organic was reversible and irreversible, respectively.

1.7.3. Physical straining

It is widely reported in the literature that the growth of microbial biofilm inside of columns, especially in pore vacancy causes decreasing porosity and permeability (Dupin and McCarty, 2000). However, higher microbial biofilm growth and proliferation has been observed in the

column inlet, compared to the other parts, which decreases significantly with increasing distance from column inlet. Rinck-Pfeiffer et al., (2000) found that total biomass in the inlet end of limestone-packed columns was higher than the deeper areas, because of the abundance of oxygen and required nutrient elements (e.g., N, P, K and etc) for biofilm growth (Rinck-Pfeiffer et al., 2000). He et al., (2017) used X-ray micro-computed tomography to find the changes in porosity of sand columns conditioned with different sorts of biofilm which obtained a considerable decrease in the porosity of biofilm-conditioned columns than pristine ones (He et al., 2017). The critical condition for physical straining of colloidal particles is the diameter of the colloidal particles and porous media. When the ratio of colloidal particle diameter to the porous media collector is less than 0.002, physical straining of particles is insignificant (Torkzaban et al., 2008a). The presence of biofilm in columns with a higher ratio than 0.002 causes trapping of particles into the inter spaces. The key factor in determining the effect of physical straining on colloidal particle retention in porous media is when the retention profiles (RPs) of nanoparticles changes from linear to hyper-exponential, which indicates the higher attachment of colloidal particle close to the inlet end of column. Numerous studies have shown that the presence of biofilm changed the RP shape of nanoparticles in comparison with pristine columns. Han et al., (2016) reported the hyper-exponential shape of RPs for ZnO nanoparticle in biofilm-conditioned sand columns. But, the shape of RPs of ZnO in pristine columns was exponential at high ionic strength (Han et al., 2016). So, the similarity of RPs of nanoparticles in biofilm-conditioned columns with fine columns in which the ratio of nanoparticles to collector diameter is higher than 0.002 shows the similar mechanism Therefore, it shows that the physical straining of nanoparticles in biofilm-conditioned columns in independent of ratio of nanoparticles to collector, in which nano-sized particles were physically trapped in coarse biofilm-conditioned columns.

1.8. Comparison with previous literature

From the review above, it is obvious that the application of treated wastewater in aquifers not only triggers porous media physical, chemical and biological clogging, but also causes groundwater contamination via pathogens and engineered nanoparticles. However, the effect of biofilm on limestone aquifers, as a chemical and geological reactive aquifer, is likely different to that of non-reactive aquifers. Previous studies on porous media clogging in a simulated managed aquifer recharge system mainly focused on the artificial or chemically and physically simple porous media (Cunningham et al., 1991). Clean and simple porous media was used in studies focusing on the role of biofilm in decreasing the porosity and hydraulic permeability of porous media. Therefore, the role of porous media chemical and mineralogical features on clogging of MAR sites, either via microbial growth and proliferation or media dissolution, was overlooked. Rinck-Pfeiffer, (2000) in a study on limestone aquifer sediments described the role of biofilm on calcite dissolution, which maintained a higher saturated hydraulic conductivity, in comparison with sand grains similarly modified with biofilm (Rinck-Pfeiffer, 2000). Furthermore, they found that the amount of produced microbial mass in authentic aquifer materials was higher than sand grains. This phenomenon was due to the preferential attachment of bacteria to the rich-nutrient substrates. Furthermore, the surface charges of bacteria and porous media collectors would be another possible reason for higher production of microbial mass in native aquifer materials. Therefore, the significant difference in the amount of biofilm in native substrates and the subsequent effects on porous media dissolution, supports the need for further research using native aquifer materials for simulation of a managed aquifer recharge sites.

In addition, in most transport studies of colloidal particles in porous media, clean sand grains or glass beads have been applied as collectors, which are not the representatives of natural aquifers (Sasidharan et al., 2017b, Wang et al., 2018). A native aquifer material contains different species and quantities of metal oxide/hydroxides, which have an influence on the attachment behavior of colloidal particles, due to the grain surface charge heterogeneities. This is exemplified by the finding that 5 % of calcite in the media caused a significant retention of *Escherichia coli* in columns (Foppen and Schijven, 2005). In addition, in some studies the distribution of metal oxides (Fe_2O_3, Al_2O_3, MgO and CaO) onto the surfaces of collectors increases the attachment of microorganisms by one or two orders of magnitude (Schijven and Hassanizadeh, 2000). Moreover, regarding matrix dissolution in carbonaceous aquifers, the created preferential flow paths and macropores accelerate the transport of microorganisms and engineered nanoparticles in columns, which poses a significant risk for groundwater resources. In the literature of colloidal particle transport in limestone-packed porous media, no significant attention has been paid on the role of preferential flow paths on particle transport in the columns (Stevenson et al., 2015).

Furthermore, production of natural biofilm in the columns through long-term application of treated wastewater containing high amount of total organic carbon (TOC), nutrients and suspended solids and microorganisms significantly affects attachment/detachment, transport and retention behavior of colloidal particles. In addition to the changing of surface properties of biofilm-conditioned aquifer substrate, the growth and proliferation of biofilm in aquifers by application of treated wastewater changes the structure of aquifers via either decreasing porosity and permeability or increasing the preferential paths by matrix dissolution. Therefore, there is lack of information about the relationship between biofilm-induced clogging, transport and retention behavior of microorganisms and engineered nanoparticles. The overall conclusion of this review is that much

research has been performed on porous media clogging and transport/retention behavior of colloidal particles, further research is required on microorganisms and engineered nanoparticle retention in native aquifer materials to determine any relationship between transport and retention behavior of colloidal particles in a limestone-based managed aquifer recharge site in the presence of biofilm.

Aims and objectives

The main aim of this research was understanding the attachment/detachment behavior of microorganisms and nanoparticles using natural aquifer substrates in batch and continuous systems. Furthermore, this research focused on the role of natural biofilm produced by treated wastewater on hydrogeological features of porous media and transport behavior of microorganisms and nanoparticles. Finally, the specific objectives of this thesis are outlined below:

1- Investigate the attachment and detachment of MS2 virus to/from limestone aquifer material at different temperature, agitation status, initial virus concentrations and substrate particle size distributions. Moreover, study the role of attached biofilm onto the surfaces of aquifer material on either enhanced or decreased attachment of virus at different temperature and agitation status.

2- Study effect of short and long-term irrigation of sand and limestone-packed columns with treated wastewater on physical, chemical and biological properties of porous media. Furthermore, investigate the surface and morphological characteristics of sand and limestone aquifer material conditioned with treated wastewater to facilitate growth of natural biofilm. Finally, finding the effect of production of natural biofilm on transport of virus in limestone-packed column in saturated conditions.

3- Study the effect of mineralogical features, temperature, ionic strength and composition on transport and retention behavior of graphene oxide nanoparticles (GONPs) in saturated porous media. In addition, study the role of biofilm on surface and hydrological features of porous media and transport behavior of GONPs in saturated porous media.

4- Investigation of cotransport of GONPs with MS2 and *E.coli* to find the role of microorganisms on transport and retention behavior of GONPs in limestone aquifer

material. Furthermore, identifying the mechanisms governing GONPs retention in porous media with and without co-presence of microorganism in suspension.

2. Materials and methods

This chapter outlines the details of experiments performed in whole parts of this study including preparation of colloidal particles (e.g., virus, bacteria and nanoparticles) and porous media (e.g., sand, quartz and limestone aquifer materials), batch experiments of MS2 inactivation via attachment onto the collectors, virus transport, nanoparticle transport and retention and co-transport of nanoparticles with virus and bacteria in porous media.

2.1. Preparation of aquifer materials and clean sand grains

The tertiary limestone aquifer materials were obtained from a site in Virginia, South Australia from depth -102 to -108 m at latitude -34 ° 42 ' 44 " and longitude 138 ° 34 ' 9". Furthermore, quartz sediments were obtained from Muno Para West, South Australia at latitude -34 ° 40 ' 5" and longitude 138 ° 40 ' 31". The obtained materials from sites were loose and disturbed with different size distributions containing small grains to larger blocks and plants and animal residues. The materials were extracted, rinsed with reverse osmosis (RO) water (Milli Q) and dried in an oven at 40˚C. Then, the materials were crushed using a hammer, ground and passed through a stainless steel sieve to attain three different size distributions (e.g., small: 0.25-0.50 mm, medium: 0.5-1 mm and coarse: 1-2 mm). Although in natural carbonaceous aquifers, water containing colloidal particles may pass through fractures, in this study, we used packed columns with disturbed limestone grains with specific size distributions to study the interaction between aquifer materials, surfaces and colloidal particles. For all transport experiments, uniform limestone grains with 0.25-0.50 mm particle size were used as porous media, while recognizing this size distribution does not represent the natural conditions of obtained materials. The raw materials were used in column

experiments without further pre-treatment, except the other materials were conditioned with treated wastewater for production of biofilm. The specific gravity of samples was obtained using pycnometer method (Gee and Bauder, 1986). Plate 2.1 shows the borehole site from which the limestone aquifer materials were obtained.

In addition, sand grains were applied as a simple and model porous medium and prepared as discussed in the literature (Mattison et al., 2011). In this regards, the sand grains were rinsed using reverse osmosis (RO) water (Milli Q), 0.1 M hydrochloric acid and 5 % (v/v) hydrogen peroxide for removal of organic matter, metal and metal oxide impurities. Then, sand grains were washed with RO water for pH equilibration and dried at 90 °C in an oven.

Plate 2.1. Borehole site (Virginia, South Australia) from which the limestone aquifer materials were collected.

2.2. Preparation of colloidal particle suspension

2.2.1. Bacteriophage

MS2, F-RNA bacteriophage (ATCC # 15597-B1) was used in all experiments to study its inactivation via attachment onto the substrate surfaces. MS2 host *Escherichia coli* (*E. coli*) was grown (37 °C, overnight) in a 10 mL suspension of tryptone soya broth (TSB) containing 0.15 g ampicillin sodium salt and streptomycin sulphate antibiotic stock solution. The ampicillin and streptomycin stock solution was prepared by addition of 0.15 g of both ampicillin sodium and streptomycin sulphate to 100 mL RO water followed by mixing using a magnetic stirrer. The obtained solution was passed through a 0.2 µm syringe filter and kept into some 10 mL yellow-capped tubes and frozen (-20 °C) for future use.

To prepare MS2 stock solution, 5 mL of *E.coli* suspension, grown in TSB and 5 mL of MS2 suspension was added to 10 mL double strength 1.5% tryptone soya agar (TSA) containing 1% of the ampicillin/streptomycin antibiotic stock solution. This suspension was added to a Petri dish containing a base layer of TSA, mixed, allowed to set and incubated overnight at 37^0C.

Following incubation, MS2 was harvested by flooding the plate with 5 mL 0.5 % tryptone water (Oxoid), incubated for 45 min at 37^0C, over which time the plate was gently swirled 3-4 times. The resulted suspension was passed through a 0.22 µm syringe filter to remove of *E.coli*. The obtained MS2 stock solution was kept in 100 mL solution containing 90 mL half strength solution and 10 mL glycerol at freezer at -20 °C.

The concentration of MS2 in the stock solution and in suspensions from experimental treatments was measured using the TSB double layer agar (DLA) method adapted from (Noble et al., 2004) and (Debartolomeis and Cabelli, 1991). Finally, the grown MS2 were reported as plaque forming units (PFU) per 1 mL.

2.2.2. Bacteria

Escherichia coli: Escherichia coli (ATCC # 700891) was used as model bacteria to study its effect on transport and retention behavior of GONPs. The *E.coli* suspension was prepared by addition of an *E.coli* colony to 100 mL tryptone soya broth (TSB; Oxoid) and 0.15 g ampicillin sodium salt and streptomycin sulphate antibiotic stock solution and grown at 37 °C overnight. Then, the obtained bacteria suspension was centrifuged at 3000 rpm for 15 min. The concentration of *E.coli* in the stock solution was determined (10^8 MPN/100 mL) using Colilert (IDEXX Laboratories, Maine, USA) according to the manufacturer's instructions.

2.2.3. Graphene oxide nanoparticle (GONPs)

Single layer graphene oxide with thickness 0.8-1.2 nm prepared by Hummer's method (according to the manufacture) were purchased from ACS Material, Medford, MA. The stock solution of nanoparticles was prepared by addition of 100 mg GONPs to 1000 mL RO water which was sonicated for 2 h using an ultrasonic bath (Cooper surgical 895, USA). GONPs stock solution was diluted to a working solution (25 mg GONP/L) and at different ionic strengths (10 and 50 mM NaCl and 1 and 5 mM $CaCl_2$) and used for all transport studies. The pH of nanoparticle suspension was adjusted to 7.5 using 0.1 M NaOH and 0.1 M HCl solutions. Finally, the zeta potentials of GONPs suspension were determined using a zetasizer instrument (Malvern, Zetasizer Nano Series, Nano-ZS) at 4 and 22°C.

The concentration of GONPs in the solution was measured using a UV-visible spectrophotometer (UV-1800 Shimadzu, Japan) at 226 nm wavelength. In this regards, the calibration line was

prepared for GONPs by measuring the absorbance at 226 nm of different concentrations of GONPs (0-50 mg/L). The residual GONPs concentrations in each effluent sample was determined using the linear regression equation of calibration curve. The lack of interference by MS2 (10^7 PFU/mL) and *E.coli* (10^8 MPM/100 mL) on the measurement of GONPs was confirmed by comparison of absorption at 226 nm following their addition to calibration concentrations of GONPs. The calibration curves of GONPs either individually or with co-presence of microorganisms are shown in Figure 2-1.

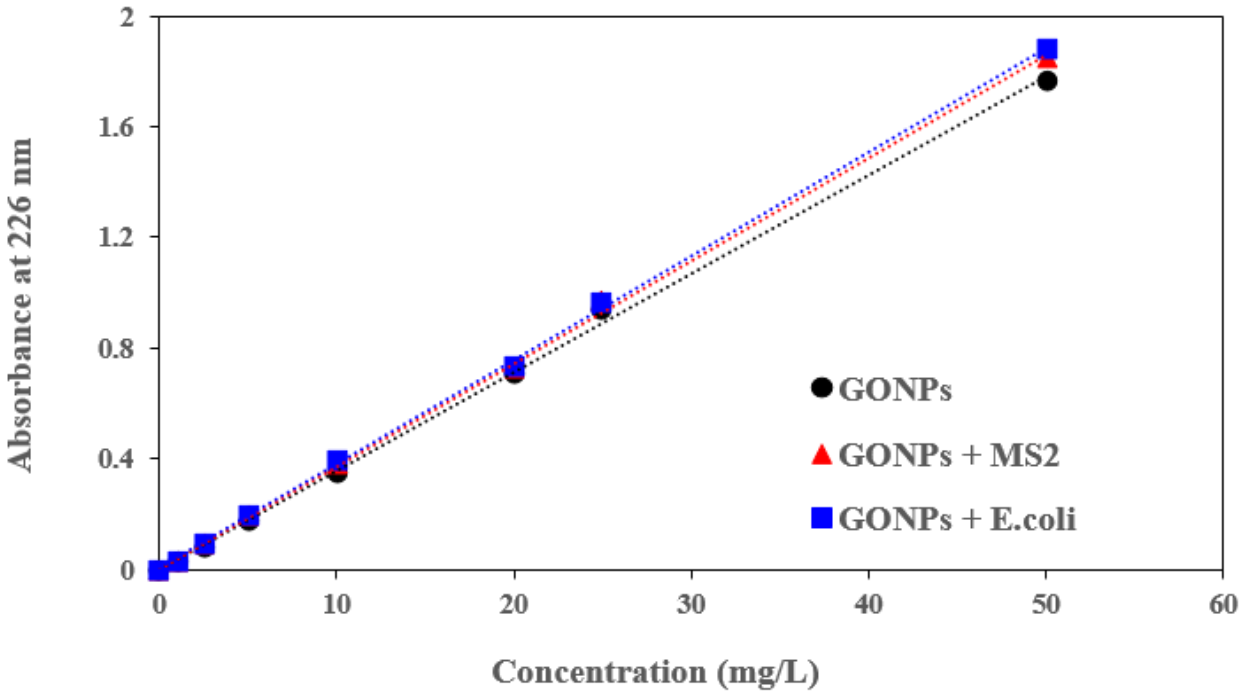

Fig 2-1. Calibration curves of GONPs (mg/L) either individually or with co-presence of microorganisms (The initial concentrations of MS2 and E.coli were 10^7 PFU/mL and 10^8 MPN/100 mL, respectively).

2.3. Analyses of nanoparticles, microorganisms and porous media

The surface and morphological features of GONPs, pristine and biofilm-conditioned (see below) porous media were examined using scanning electron microscopy (SEM, Inspect D50). In this regards, for nanoparticles, the suspensions of GONPs either individually or with the co-presence of microorganisms at different ionic strengths were prepared. Then, 1 mL of suspension was extracted using a pipette and dropped on a grid for drying. However, in terms of porous media, samples were first fixed via 2.5 % (v/v) glutaraldehyde solution. Afterwards, a series of ethanol with different concentrations (30-100 %) were used to dry the sample. Finally, several grains of samples were poured on a grid and their SEM images were taken. The crystalline characteristics of porous media grains were also determined using a Bruker Advance D8 Eco XRD instrument (Co-Kα radiation, $\lambda = 1.79$ Å). Furthermore, X-ray fluorescent (XRF, PANalytical Axios Advanced instrument) was applied for determination of the amount of metal oxides in the structure of porous media. The presence of different surface functional groups on the porous media grains was determined by application of Fourier transformed infrared spectroscopy (FTIR- PerkinElmer/ Frontier) technique. Energy dispersive X-ray spectroscope (EDS) installed on a SEM instrument was also applied to characterize the elemental analysis of porous media grains.

The structural visualization of the biofilm on porous media was studied using a confocal laser scanning microscope (CLSM, Leica TCS SP5 at Flinders Microscopy and Microanalysis). The process of preparation of samples was performed by washing with phosphate buffer solution (PBS) and staining via carbohydrate-recognizing lectin concanavalin A (ConA)-Alexa Fluor 488 (Molecular Probes, Inc., Eugene, OR) for 30 min and then washing with RO water to remove the excess ConA. Then, the detection of fluorescent sediments was performed at 488 nm and a PMT

detector set to capture 510-610 nm emission. The processing of the initial images to obtain 3-dimensional images was performed using Imaris software (version 8.3).

2.4. Measurements of the composition of treated wastewater

In this study, in order to create biofilm onto the surfaces of aquifer materials, treated wastewater was obtained from Mount Barker, South Australia. Several chemical and biological characteristics of treated wastewater were measured as follows:

2.4.1. Acidity (pH)

pH of treated wastewater was measured using a pH-meter (Eutech) at room temperature (22±2 °C)

2.4.2. Nutrient analysis

Total nitrogen (TN) and total organic carbon (TOC) were measured using a total organic carbon and nitrogen analyzer (TOC-LCSH TNM-L analyzer, Shimadzu). However, the concentrations of nitrate (NO_3^-), nitrite (NO_2^-), ammonium (NH_4^+) and phosphorous (PO_4-P) were determined using a Foss instrument (FIAstar 5000 Analyzer, Sweden) based on the APHA Standard Methods for the Analysis of Water and Wastewater.

2.4.3. Cation and anion analysis

The concentrations of several cations including calcium (Ca^{2+}), magnesium (Mg^{2+}), sodium (Na^{+}) and potassium (K^{+}) and several anions such as chloride (Cl^{-}) and bromide (Br^{-}) were determined using ion chromatography (Metrohm, Switzerland).

2.4.4. Turbidity and total suspended solids (TSS)

The turbidity of treated wastewater samples, before and after experiments were measured using a Hach spectrophotometer (DR 2000) at 450 nm wavelength. In this regards, first, 25 mL RO water was added to the glass tubes to auto zero instrument. Afterwards, the turbidity of sample was measured and reported as FTU.

The TSS of treated wastewater was measured by filtering 100 mL through a pre-dried (105ºC overnight) and weighed a filter pad (GF/C, 90 mm, Whatman, 1822-090). Afterwards, the filter pad was dried and weighed again. Then, the TSS of treated wastewater sample was obtained via equation below:

$$TSS(mg/L)=W_{final}-W_{initial}\times\left(\frac{1000}{V}\right) \quad (2\text{-}1)$$

where, $W_{initial}$ and W_{final} are the initial and final weigh of filter pad (g), respectively. V is the volume of solution (mL).

2.4.5. Alkalinity

A specific volume of water sample before and after experiments was poured into a conical flask. Then, several drops of phenolphthalein indicator were dropped into the sample which turned the color into pink. Afterwards, the titration was performed by 0.02 M HCl solution while the pink color was disappeared. However, for samples which did not show any changes with phenolphthalein indicator, some drops of methyl orange indicator were added into the samples which changed the color to orange. Then, the titration of sample was done using 0.02 M HCl while the solution color turned into red. The amounts of consumed acid were measured and used to determine the alkalinity. Finally, the amount of alkalinity was reported based on the concentration of calcium carbonate (mg $CaCO_3$/L).

2.5. Batch experiments of virus inactivation

MS2 inactivation by attachment onto limestone grains was studied in a series of batch experiments at different particle size distributions with both treated wastewater and RO water under static and dynamic conditions at 4 and 22 ˚C temperatures. A working virus solution was prepared by addition of 1 mL of virus stock solution (above) to 1 L RO water and then shaken vigorously to create homogeneous virus suspension. Where a range of MS2 concentrations (10^3-10^7 PFU/mL) were used in the experiments they were prepared from the working solution diluted to the desired concentrations with RO water. The pH of the suspension was adjusted to 7.5 using 0.1 M NaOH and 0.1 M HCl solutions. The concentration of virus in the solution was measured immediately after preparation of virus suspension.

To prevent or at least minimize virus inactivation by attachment onto the internal walls, acid washed (6 N HCl) sterile (121˚C for 16 min) Pyrex™ glass screw-cap tubes were used in all incubations. The sterilized glass tubes were filled with 2.5 g limestone and 25 mL virus suspension (1:10 w/v), to ensure absence of air bubbles to prevent the effect of air-water interface (AWI) on virus inactivation (Chrysikopoulos and Aravantinou, 2012). In addition, parallel control experiments, in the absence of limestone, were incubated under the same conditions using 25 mL virus suspension. All incubations were conducted in the dark (Sinton et al., 2002). The static experiments were conducted in quiescent conditions at both 4 and 22 ˚C. In contrast, in the dynamic experiments, the tubes containing virus suspension with limestone aquifer grains and the respective control incubations were gently shaken using a rotary shaker for 24 h to establish an equilibrium between the aquifer material and MS2. On completion of the incubations, the tubes were centrifuged (1000 × g for 10 min; Phonix, Australia) to separate limestone from aqueous solution. Then, 1 mL virus suspension was pipetted from the tubes and the equilibrium MS2 concentration in the suspensions was determined using double layer agar method (Noble et al., 2004). All experiments were carried out in triplicate and the mean values ± standard deviation were reported. The virus inactivation by attachment onto the limestone surfaces was reported as $\log_{10}$ fraction removal using Equation (2-2):

$$Log_{10}\frac{N(t)}{N(0)} \qquad (2\text{-}2)$$

where, N(t) is the virus concentrations (PFU/mL) at time *t* in reactor and control tubes. While, N(0) is the initial virus concentration (PFU/mL).

Additional batch incubations were performed with limestone ‘conditioned’ by incubation with wastewater obtained from Mount Barker, South Australia, to encourage biofilm development. The

wastewater was stored in non-reactive plastic containers in a cold room at 4 ˚C prior to use. 100 g of limestone grains were added to 1 L (10 % w/v) conical flasks containing treated wastewater. Then, the flasks were sealed with aluminum foil and shaken (22 °C, 100 rpm, Innova 4) for two months to enable the formation of biofilm on the surfaces of limestone particles. In addition, in order to keep 10 % w/v solid/solution ratio, the specific amounts of fresh treated wastewater were added into the bottles to compensate for evaporative loss. Following the two month incubation the wastewater was decanted and used to prepare MS2 suspensions (25 mL) for use in batch incubations with the conditioned limestone (2.5 g). The methods where then as described above for the RO water incubations. The amount of produced biofilm was measured via a total organic carbon (TOC, SSM-5000A, Shimadzu, Japan) analyzer instrument. In addition, the organic matter of both pristine and biofilm-conditioned limestone grains as an index of biofilm was measured using loss on ignition (LOI) method (Dean, 1974). In this regards, the samples were dried in an oven at 105 °C overnight in pre-weight ceramic boats, equilibrated in a desiccator at room temperature and weighted (D_{105}). Then, the samples were combusted in a muffle furnace at 550 °C, followed by reweighting (D_{550}). Finally, the amount of produced microbial mass was obtained via the differences between D_{105} and D_{550}. In order to prevent intervention of biomass of native materials, parallel control LOI determinations were conducted on samples from columns containing pristine substrates. During the experiments, care was taken on the experimental factors which could possibly intervene into the results such as humidity and organic matters attached onto the surfaces of the ceramic boats. Therefore, before weighting samples, all ceramic boats were first washed with 1 M HCl and RO water, dried in an oven at 105 °C for 12 h and burnt in a muffle furnace at 900 °C for 4 h.

2.6. Virus transport experiments

The plexiglass columns with 9 cm length and 2.5 cm inner diameter, with stainless steel mesh screens at either end, were wet-packed in separate 1 cm increments with porous media grains, gently vibrated and also tapped simultaneously using a small rod in order to prevent preferential flow paths and to release air trapped in the interpores. The columns were wrapped in aluminum foil to prevent virus inactivation as a result of light penetration (Sinton et al., 2002). Treated wastewater from the wastewater treatment plant in Mount Barker, South Australia was passed through a filter pad (GF/C, 90 mm, Whatman, 1822-090) and kept in a non-reactive plastic container at 4 $^{\circ}$C, prior to conducting experiments. Wastewater was injected, at a constant flow rate using a peristaltic pump (Watson Marlow, UK), upward through the column over different durations, short (2 weeks) and long (8 weeks) (Godinez and Darnault, 2011). The specific gravity (ρ_s) of limestone and sand grains was calculated using the pycnometer method (Gee and Bauder, 1986). The porosity (n) of columns was obtained from the particle density and the bulk density (Equation 2-3)

$$n = 1 - \frac{\rho_b}{\rho_s} \tag{2-3}$$

where, ρ_b and ρ_s respectively represent the bulk density (g/cm^3) and particle density (g/cm^3) of the aquifer material.

In addition, the saturated hydraulic conductivity (K_s) of columns was determined using the falling head method, before and after the column experiments (Bagarello et al., 2004). The wastewater effluent from the columns was gathered at different time intervals to determine the chemical and biological composition. Calcium carbonate and bicarbonate concentrations were also determined using the titration method (Federation and Association, 2005).

Transport behavior of tracers was studied in saturated sand and limestone-packed columns fed with treated wastewater for different time periods (2 and 8 weeks). Breakthrough curves (BTC) were constructed by injecting a 10 pore volume (PV) pulse of tracer (10 mg/L Br^-) in a background solution upward into the column, followed by 10 PVs background solution (treated wastewater) to complete the Br^- BTCs. The concentrations of Br^- in the samples collected were determined by ion chromatography (Metrohm, Switzerland).

10 PVs of MS2 suspension containing 10^9 plaque forming units (PFU)/mL in treated wastewater was prepared and injected upward into the column at a similar flow velocity as that used to construct the BTC. After feeding columns with virus suspension, background solution (treated wastewater) equivalent to 10 PVs was injected into the columns to complete the MS2 BTCs. To determine the detachment behavior of MS2, 10 PVs RO water were injected followed by 10 PVs 3 % Beef Extract solution (Oxide, UK) at pH 10. Effluents were gathered at every half pore volume in 25 mL glass tubes. The obtained data were used to plot BTCs of tracer and MS2 transport as a function of dimensionless relative concentration (C/C_0), where C_0 and C are the initial and measured Br^- (mg/L) or MS2 concentrations (PFU/mL), respectively, against pore volume. All transport experiments were carried out at room temperature ($22 \pm 2\ ^{\circ}C$).

Upon completion of the experiments, the columns were excavated and divided to 9 sections each of 1 cm length. The produced biofilm was measured using loss on ignition (LOI) method (Dean, 1974). The porous media grains of different parts of the columns were analyzed using SEM technique (SEM, Inspect D50) to visualize their surface morphological characteristics. The CLSM analysis was also used for finding the production of biofilm onto the surfaces of biofilm-conditioned substrates. The apparatus used for the transport experiments is shown in Plate 2.2.

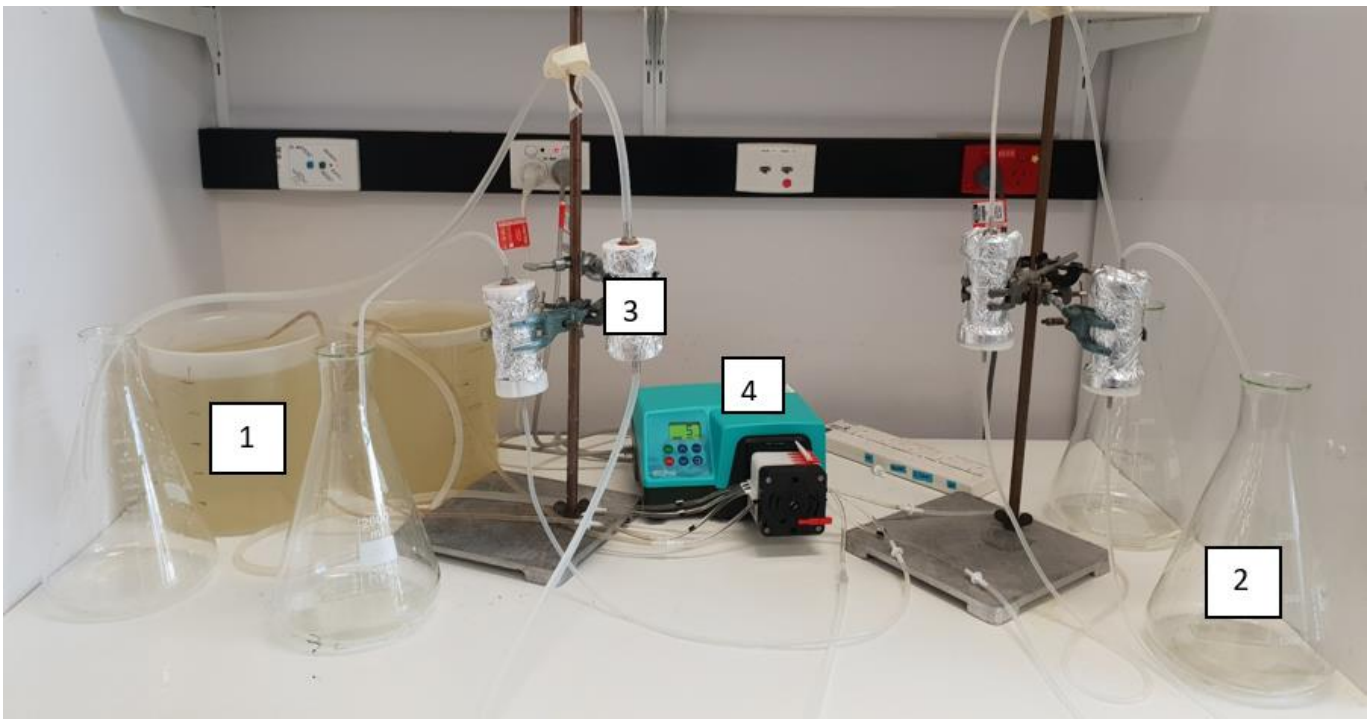

Plate 2.2. The experimental setup of virus transport experiments in different porous media (1: influent containing treated wastewater, tracer and virus, 2: effluents, 3: experimental column and 4: peristaltic pump).

2.7. Saturated hydraulic conductivity measurement using falling head method

To find the saturated hydraulic conductivity of pristine and biofilm-conditioned sand and limestone-packed columns, the falling head method was applied. In this regards, columns were filled completely with porous media grains. Then, a head of water with burette was produced on the top of column which was connected to the inlet end of column and the other side of column was closed by a clamp. Afterwards, the column was saturated using RO water to maintain a steady-state flow rate. Then, the water was discharged into the column from burette at specific time periods. The decrease in the height of water in burette at different time-intervals were measured. Finally, the hydraulic conductivity was measured, based on the following formula:

$$k = \frac{aL}{At} \ln \frac{h_0}{h_1} \tag{2-4}$$

where, a is surface area of burette (cm^2), A is surface are of column (cm^2), L is length of column (cm), t is time of decreasing height of water (min). h_0 and h_1 are the initial and final heights of water in the burette (cm), respectively. The schematic diagram of measuring K_s has been illustrated in Figure 2.2.

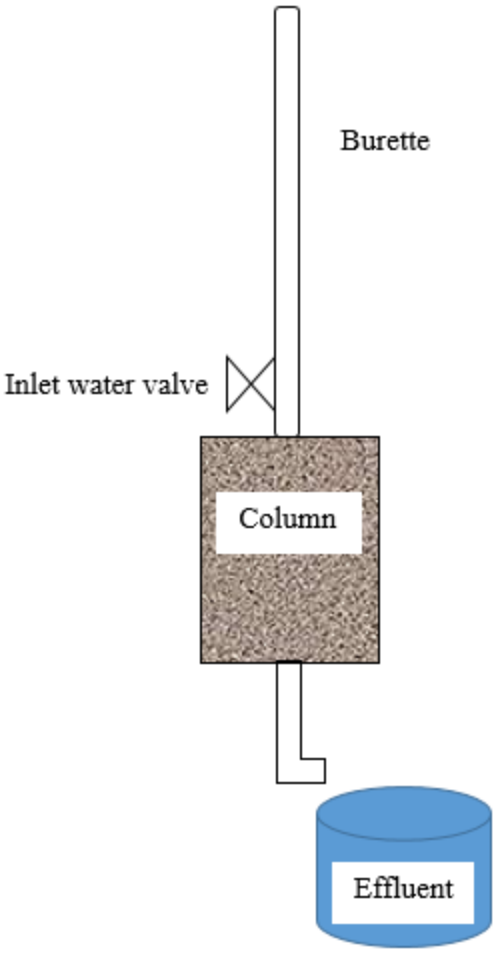

Fig 2.2. Schematic diagram of measurement of saturated hydraulic conductivity using falling head method.

2.8. Batch sorption of GONPs

Batch sorption experiments of GONPs onto the surfaces of sand, quartz and limestone sediments were carried out at different temperatures (4 and 22 °C) and ionic strengths and compositions (10 and 50 mM NaCl and 1 mM $CaCl_2$). The experiments were carried out by changing one factor and keeping the other factors constant. In this regards, 2.5 g adsorbents were added to acid washed (6 N HCl), sterile (121˚C for 16 min) PyrexTM glass screw-cap tubes containing 25 mL of 25 mg GONP/L at pH 7.5, which was adjusted using 0.1 M NaOH and 0.1 M HCl to the desired ionic strength. The tubes were shaken on a rotary shaker for 3 h, which is similar to the time of transport experiments (below). At the end of reaction, the residual concentrations of GONPs in supernatants were measured using a UV-visible spectrophotometer (UV-1800 Shimadzu, Japan) at 226 nm wavelength (Jian-Zhou et al., 2015). Parallel control experiments were performed without adsorbents to determine the attachment of GONPs onto the internal surfaces of glass tubes. The experiments were performed in triplicate and the results were reported as mean ± standard deviation.

2.9. Graphene oxide transport experiment

In order to perform the transport experiments of GONPs in saturated porous media, initially, the columns were flushed with approximately 10 pore volumes (PV) of the respective background solution (10 and 50 mM NaCl and 1 mM $CaCl_2$ ionic strength, pH 7.5) at a constant flow rate of 1.7 mL/min. 10 PVs of the conservative tracer bromide (10 mg/L Br^-) were injected, followed by 10 PVs of the respective background solution to complete the breakthrough curve (BTC) of tracer, to obtain the pore volume of column and assess the presence or absence of preferential flow paths

within the column. The columns were flushed with 10 PVs of the respective background solution to provide a homogeneous surface charge throughout the column.

The column experiments were conducted, in a thermostatically controlled cold room at 4°C and at room temperature (22°C) both at various ionic strengths. A flask containing 25 mg GONP/L was sonicated for 30 min to obtain a homogeneous suspension of nanoparticles. Then, 10 PVs of GONPs suspension –with the same pH and ionic strength of background solution- were injected into the column followed by addition of 10 PVs background solution. The column effluents were gathered at different time intervals in 50 mL plastic tubes to determine the GONPs residual concentrations. At the end of each breakthrough curve experiment, the spatial distribution of retained GONPs in porous media was determined, as discussed in section 2-10 (Lanphere et al., 2013). The residual GONPs concentrations were measured using a UV-visible spectrophotometer (UV-1800 Shimadzu, Japan) at 226 nm wavelength (Jian-Zhou et al., 2015) from calibration curves obtained using 0-50 mg GONP/L concentrations (R^2=0.99). Finally, the breakthrough curves of GONPs were plotted based on relative GONP concentration (C/C_0) against pore volume (PV). The measurements were performed three times and the results were reported as mean ± standard deviation. Furthermore, the colloidal stability of GONPs was measured at 4 and 22 °C in 10 and 50 mM NaCl and 1 mM $CaCl_2$ solutions. In this regards, 3 mL of 25 mg GONP/L suspension at the respective ionic strengths were added in a quartz cuvette and the absorbance was measured every 6 min for 3 h under quiescent conditions.

Similar experiments were also conducted in biofilm-conditioned porous media at 22°C. To establish a natural biofilm in the columns, the columns were saturated by upward injection of the treated wastewater at 1.7 mL/min for approximately 10 days to ensure that a layer of biofilm was generated on the surfaces of substrates. Then, 5 PVs of background solution was injected into the

columns to remove any loose bacterial colonies and the adsorption of the effluents at 226 were measured using a UV-visible spectrophotometer (UV-1800 Shimadzu, Japan) to ensure low background absorbance values of effluents at volumes equivalent to 5 PVs. The other stages of transport experiments of GONPs in biofilm-conditioned porous media were as for those described above for the pristine porous media.

2.10. Dismantling columns

After end of each breakthrough curve experiment, the spatial distribution of retained GONPs in porous media was determined. In this regards, the columns were excavated in 1 cm increments and the material transferred into 50 mL plastic vials, following addition of 20 mL 1 mM NaOH solution the vials were shaken using a rotary shaker for 2 h. The supernatants were extracted for measuring the residual GONPs concentrations and hydrodynamic diameters and the porous media grains were dried in an oven at 60 ^{o}C for over 12 h to find their quantities (Lanphere et al., 2013). Different steps of dismantling of limestone-packed column after end of GONPs transport tests are shown in Plate 2.3.

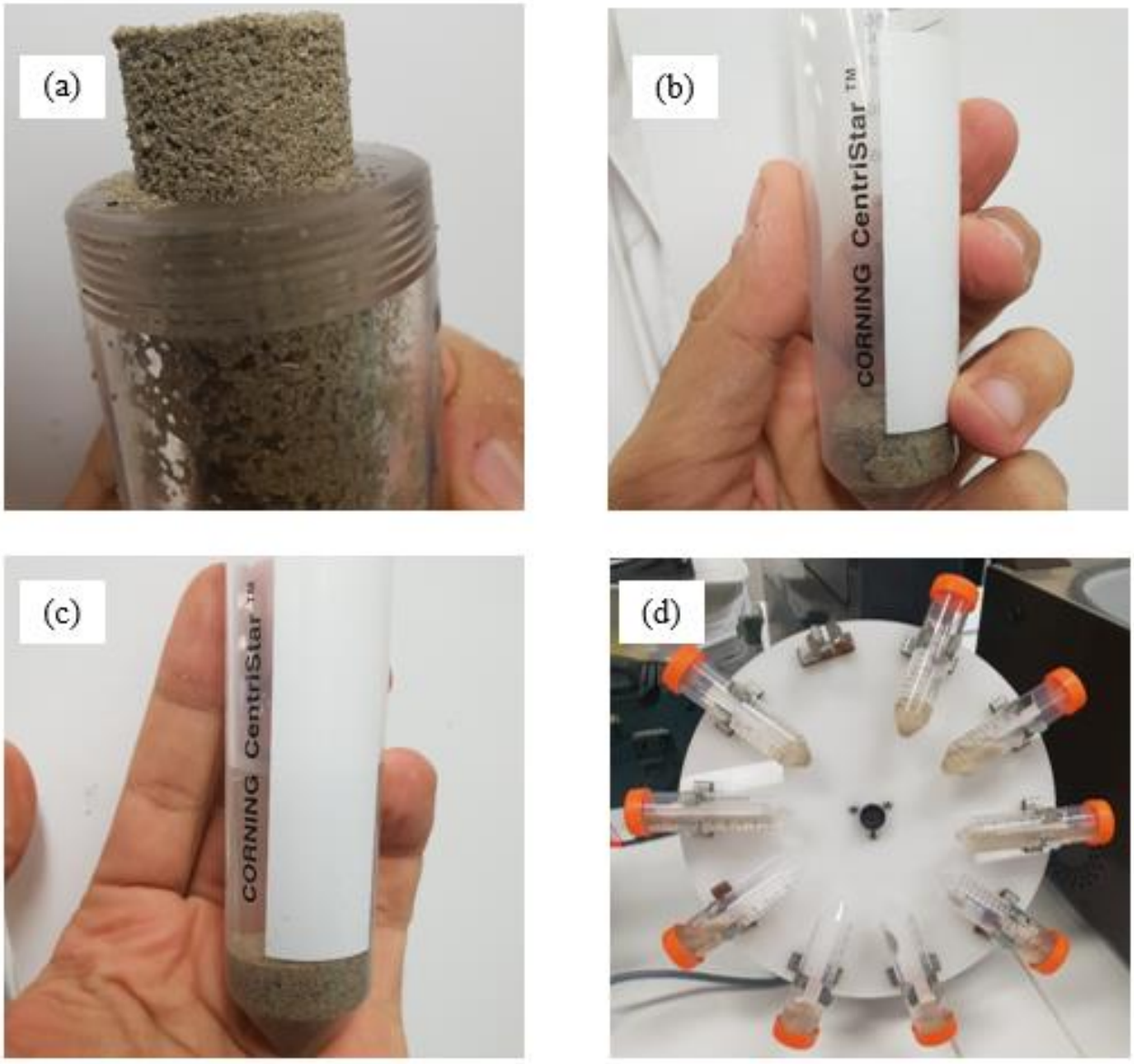

Plate 2.3. Different steps of dismantling limestone-packed columns after end of transport experiments (a: extraction of each centimeter of column, b: addition of separated porous media in plastic tubes, c: addition of 1 mM NaOH into plastic tube and d: shaking plastic tubes containing porous media and 1 mM NaOH for GONPs detachment).

2.11. Cotransport experiments of graphene oxide and microorganisms

The transport experiments of graphene oxide nanoparticles (GONPs) were commenced by injection of 5 PVs GONPs either with or without presence of *E.coli* (10^8 MPM/ 100 mL) and MS2 (10^7 PFU/mL), followed by 5 PVs of particle-free solution to flush all GONPs at 10 mM NaCl and 5 mM $CaCl_2$. Several experiments were conducted using columns pre-saturated with MS2 or *E.coli*, followed by injection of GONPs at the desired ionic strength to determine the role of surface collector's blockage on nanoparticle retention rate.

Additional experiments were carried out using porous media conditioned with biofilm developed using treated wastewater obtained from Mount Barker, South Australia. In this regard, the columns were fed continuously with treated wastewater for 10 days to stimulate biofilm development onto the surfaces of collectors. Afterwards, similar experiments as described above were performed at low ionic strength. Furthermore, following the completion of transport experiments, the columns were dissected to find the spatial distribution of retained GONPs. After end of experiments, the amount of produced biofilm was measured using LOI method and the residual concentrations of retained and eluted GONPs were measured using a UV-visible spectrophotometer at 226 nm (UV-1800 Shimadzu, Japan) as described above. The surface morphological of collectors and the biofilm structure were also studied using SEM (SEM, Inspect D50) and CLSM (Leica TCS SP5) instruments, respectively. Finally, the hydrodynamic diameter of retained GONPs were measured using a dynamic light scattering instrument (Malvern, Zetasizer Nano Series, Nano-ZS). All measurements were performed in triplicate and the results are presented as mean ± standard deviation.

2.12. Data analysis

2.12.1. Kinetic studies

In order to study the kinetics of MS2 inactivation under various experimental conditions, the Geeraerd and Van Impe (Geeraerd et al., 2005) inactivation model-fitting tool was applied (GinaFit, Version 1.5; KU Leuven, Belgium). Following inspection, a non-linear model with shoulder and tail was used as shown in Equation 2-5 (Geeraerd et al., 2005):

$$N_t = (N_0 - N_{res})e^{-k_{max}t}\left(\frac{e^{k_{max}Sl}}{1+(e^{k_{max}Sl}-1)e^{-k_{max}t}}\right) + N_{res} \quad (2\text{-}5)$$

where, k_{max} is the virus inactivation rate (h^{-1}), N_0 and N_{res} are the initial and residual virus concentrations in the solution (PFU/mL), Sl is the shoulder length (h) which is the required time for beginning the inactivation of virus and t is the reaction time (min).

2.12.2. Statistical analysis

Analysis of variance (ANOVA) was applied for evaluation of the role of agitation status, temperature, initial virus concentrations, adsorbent particle size distributions and biofilm on MS2 inactivation rate. Mean differences were compared through LSD test ($p < 0.05$). The statistical analysis was performed by SPSS software (version 16) for Windows and the Figures were plotted using Microsoft Excel.

2.12.3. Transport of tracer

The tracer transport (Br^-) in this study was described using an advection-dispersion equation (ADE) (Mallants, 2014).

The dispersivity (λ) and dimensionless Peclet number (P_e) were obtained via the following equations:

$$\lambda = D/v \quad (2\text{-}6)$$

$$P_e = L/\lambda \quad (2\text{-}7)$$

where, v is the pore water velocity (cm/min), D is the hydrodynamic dispersion (cm/min^2) and L is the length of column (cm).

2.12.4. DLVO theory

Total interaction energy, which is defined as the sum of the attractive Lon-don van der Waals (VDW) interaction and the repulsive electrostatic double layer (EDL) interaction was obtained via classical Derjaguin-Landau-Verwey-Overbee (DLVO) theory, assuming sphere-plate interaction (Derjaguin and Landau, 1993). The zeta potentials of minerals and nanoparticles at different ionic strength and conditions in place of surface potentials were measured using a Zetasizer instrument (Malvern, Zetasizer Nano Series, Nano-ZS) and used for calculation of interaction energy profiles. The calculations for applied energies are as follows:

$$\Phi_{TOT} = \Phi_{VDW} + \Phi_{EDL} \quad (2\text{-}8)$$

$$\Phi_{vdw}(h) = -\frac{A_{123} r_p}{6h}\left[1 + \left(\frac{14h}{\lambda}\right)\right]^{-1} \quad (2\text{-}9)$$

$$\Phi_{dl}(h) = \pi \varepsilon_r \varepsilon_0 r_p \left[2\Psi_p \Psi_s \ln\left(\frac{1+e^{-kh}}{1-e^{-kh}}\right) + (\Psi_p^2 + \Psi_s^2)\ln(1-e^{-2kh})\right] \quad (2\text{-}10)$$

where, A_{123} is the overall Hamaker constant of the interacting media, which was obtained using

the equation below:

$$A_{123} = (\sqrt{A_{11}} - \sqrt{A_{22}})(\sqrt{A_{33}} - \sqrt{A_{22}}) \quad (2\text{-}11)$$

where, A_{water}, A_{sand} and A_{GONPs} are the individual Hamaker constants for water (3.70×10^{-20}) (Israelachvili, 1992), sand (8.86×10^{-20}) (Bergström, 1997) and GONPs (6.34×10^{-20}) (Feriancikova and Xu, 2012). Furthermore, h is the separation distance between collectors and nanoparticles (nm), r_p is the hydrodynamic radius of particles (m), λ is the characteristics wavelength (100 nm), ε_0 is the vacuum dielectric permeability (8.85×10^{-12} $CV^{-1}m^{-1}$), ε_r is the water dielectric constant (78.5). ψp and ψs are the zeta potentials of particles and collectors (mV), respectively, κ is the reciprocal of Debye length, which can be obtained using the following equation:

$$k = \left[\frac{2I_s N_A 1000 e^2}{\varepsilon_r \varepsilon_0 k_B T} \right]^{1/2} \quad (2\text{-}12)$$

where, T is the temperature (K), k_B is the Boltzmann constant (1.38×10^{-23} J/K), N_A is the Avogadro number (6.02×10^{23} mol^{-1}), I_s is the ionic strength of solution and e is the electron charge (1.602×10^{-19} C).

3. Role of biofilm on virus inactivation in limestone aquifers: Implications for managed aquifer recharge

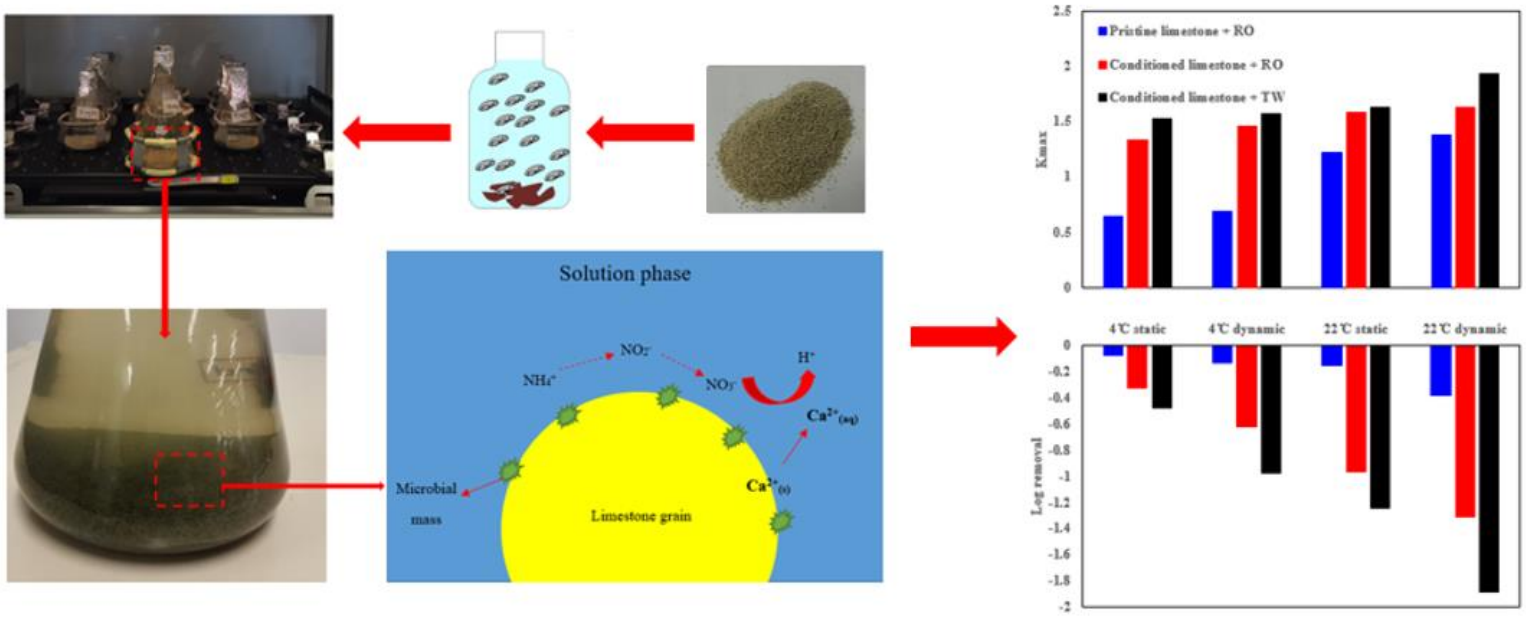

Graphical abstract

3.1. Highlights

- MS2 inactivation by attachment on limestone aquifer at different experimental conditions.
- Effect of biofilm on MS2 inactivation by attachment onto the surfaces of limestone aquifer materials.
- Role of treated wastewater on inactivation of MS2 on limestone aquifer materials.

This Chapter is based on the following publication: Amirhosein Ramazanpour Esfahani, Okke Batelaan, John L. Hutson and Howard J. Fallowfield. Role of biofilm on virus inactivation in limestone aquifers: Implications for managed aquifer recharge. Journal of Environmental Health Science and Engineering (in-press, DOI: 10.1007/s40201-019-00431-5).

3.2. Abstract

Virus, as nano-sized microorganisms are prevalent in aquifers which threaten the groundwater resources quality and human health wellbeing. Virus inactivation by attachment onto the limestone surfaces is a determining factor in the transport and retention behavior of virus in carbonaceous aquifers. In the present study, the inactivation of MS2 -as a model virus- by attachment onto the surfaces of limestone grains was investigated in a series of batch experiments under different conditions such as limestone particle size distribution (0.25-0.50, 0.5-1 and 1-2 mm), treated wastewater and RO water, temperature (4 and 22˚C), initial MS2 concentrations (10^3-10^7 PFU/mL) and static and dynamic conditions. The experimental data of MS2 inactivation was also fitted to a non-linear kinetic model with shoulder and tailing. The characteristics of biofilm onto the surfaces of limestone aquifer materials were assessed using scanning electron microscopy (SEM) and confocal laser scanning microscopy (CLSM). The inactivation rate of virus decreased with increasing the adsorbent diameter. Furthermore, virus inactivation was greater at room temperature (22˚C) than 4 ˚C, in both static and dynamic conditions. The inactivation of virus via attachment onto the limestone aquifer materials in dynamic conditions was higher than under static conditions. In addition, fitting the experimental data with a kinetic model showed that virus inactivation was high at higher temperature, smaller limestone grains and dynamic conditions. Moreover, the experiments with treated wastewater showed that in authentic aqueous media, the virus inactivation was considerably higher than in RO water, due to the presence of either monovalent or divalent cations and surface roughness created by biofilms. Finally, in terms of managed aquifer recharge systems, the presence of biofilm increases bacteria and virus retention onto the aquifer surfaces.

3.3. Introduction

Recently, the human demand for clean and safe drinking water resources is strongly increasing (Esfahani et al., 2013, Abuzerr et al., 2018). Although groundwater resources, compared to the surface waters, are more tolerant of pollution, the discharge of treated wastewater and stormwater containing microbial pollutants into the aquifers has been recently considered a great threat for subsurface water resources (Macler and Merkle, 2000). Human pathogenic viruses (and various surrogates, MS2,PRD1,ϕX174) are quite ubiquitous in the subsurface environment, which may be derived from either intentional or accidental discharges (Hundesa et al., 2006). Virus can enter groundwater resources through discharge of municipal wastewater, wide application of faecally contaminated water and sewage sludge for agricultural activities and leakage of septic tanks (Anders and Chrysikopoulos, 2005); (Bradford et al., 2006). In addition, the practice of artificial groundwater recharge has grown in order to compensate for the fast depletion of aquifers, which has led to the discharging of microbial-polluted water into the subsurface environment (Maxwell et al., 2003). Indeed, the release of viruses into the environment is a potential danger for public health (Lipson and Stotzky, 1983). Furthermore, their presence in high concentrations in groundwater resources can be ascribed to a lack of efficient conventional water treatment techniques (Lee and Kim, 2002) (Chen and Elimelech, 2007). Therefore, in order to prevent viral diseases, it is critical to identify the various environmental factors influencing virus transport and retention in aquifers.

In general, a large number of factors such as inactivation by attachment and detachment to/from solid collectors and environmental factors potentially influences on virus interactions with solid surfaces (Anders and Chrysikopoulos, 2006). Additionally, the intensity of interaction between viruses and collector surfaces can be determined by different environmental factors such as pH of

solution, temperature, ionic strength and composition (e.g., presence of mono or divalent cations), the amount of organic matter and metal oxides (Sasidharan et al., 2016) (Pham et al., 2009) (Bhattacharjee et al., 2002) (Chrysikopoulos and Aravantinou, 2014).

Furthermore, virus inactivation may demonstrate different behaviors depending upon the physical, chemical, mineralogical and surface characteristics of the porous media. Chrysikopoulos and Aravantinou (2014) reported that quartz sand grains had an interaction with MS2 and ϕX174 viruses under different experimental conditions such as temperature, adsorbent size distributions and agitation status (Chrysikopoulos and Aravantinou, 2014). Clay particles are ubiquitous in the subsurface environment, which can adsorb viruses, due to their high specific surface areas, expandability and ion exchange capacity (Zhang et al., 2010). Bellou *et al*., (2015) and Zhou, (2011) showed, at different temperatures and ionic strengths, the significant effect of kaolinite and montmorillonite on the attachment of human adenoviruses and coliphages (Zhou, 2011, Bellou et al., 2015).

Carbonaceous (limestone and dolomite) aquifers are globally important resources for potable water (Mondal and Sleep, 2013). In these aquifers, the groundwater pH is generally buffered at 7. However, the surface charges of aquifer minerals at either neutral or high pH values are negative which is quite unfavorable for virus removal. Therefore, these aquifers pose a risk for drinking water resources from the point of view of pathogenic pollution. In order to manage the risk of groundwater resources pollution in carbonaceous aquifers, the interaction between limestone material and viruses, under different experimental conditions, needs to be understood. In majority of studies on virus interaction with substrate, the surfaces of substrate have been considered physically clean and simple. However, natural porous media contains different microbes that can produce biofilm on the surfaces of aquifer grains. Biofilm consists of several layers of bacteria

which can be accumulated on a surface and surrounded by a matrix of extracellular polymeric substances (EPS) (Smirnova et al., 2010). Surprisingly, little attention has been paid by hydrogeologists to the interaction between microorganisms and biofilm in the subsurface environment. An exception was a laboratory study of the transport of colloidal particles through biofilm-conditioned porous media, where the biofilm was produced using a culture of *Pseudomonas putida* (Jian-Zhou et al., 2015). However, in real MAR sites, the natural biofilm derives from a plethora microorganisms with different features. Therefore, in this study, we used treated wastewater obtained from a wastewater treatment plant in Mount Barker to produce natural biofilm on the limestone aquifer grains

The MS2 virus, which is not a pathogenic agent and has also been studied in previous research (Thompson et al., 1998, Weng et al., 2018, Hijikata et al., 2016), was used in this study as a surrogate for pathogenic viruses. It is an *F*-specific RNA virus with a size of 24–26 nm (Pang et al., 2014), a hydrophobic protein coat and an isoelectric point of 4.1. Its host is *Escherichia coli* (*E.coli*) (Chrysikopoulos and Syngouna, 2012). Although the study of virus attachment onto the different solid materials was previously performed (Chrysikopoulos and Aravantinou, 2014) (Schiffenbauer and Stotzky, 1982, Tong et al., 2012), to the best of our knowledge, no study focused on the role of limestone materials on virus inactivation at different experimental conditions. In addition, all previous studies used engineered, pure and synthetic materials to evaluate their role on virus removal. While, the novelty of present research is application of the authentic subsurface materials in batch tests of MS2 inactivation. Therefore, the principal aim of this research was to investigate the inactivation of MS2 virus onto the surfaces of limestone with different particle size distributions under different initial virus concentrations and temperatures under static and dynamic conditions. The obtained experimental data of virus inactivation were

fitted with a log-linear with shoulder and tail kinetic model (Geeraerd et al., 2005). Additionally, to simulate the real environmental conditions, treated wastewater collected from a wastewater treatment plant in Mount Barker, South Australia was used as an aqueous medium to produce biofilm and to determine its influence on surface properties of limestone and consequently MS2 inactivation.

3.4. Results and discussion

3.4.1. Characterization of limestone aquifer material

The calculated specific gravity of limestone aquifer materials was 2.55 g/cm^3. Results of XRD analysis showed that the aquifer materials consisted of a significant amount of calcite with negligible quantities of dolomite and quartz (Fig 3-1a). In addition, based on XRF analysis, the aquifer materials contained 46.41 % CaO, 9.59 % SiO_2, 2.84 % MgO, 1.63 % Fe_2O_3, 0.41 % Al_2O_3, 0.21 % K_2O, 0.20 % SO_3, 0.07 % Na_2O, 0.03 % MnO, 0.02 % P_2O_5 and 38.56 % loss on ignition. Furthermore, results of EDS analysis revealed the presence of O, Ca, C, Mg and Si in the body of aquifer grains (Fig 3-1b). Finally, according to the FTIR spectrum of aquifer materials (Fig 3-1c), three sharp peaks were observed in the region of absorption at 712.66, 872.20 and 1404.32 cm^{-1} attributed to calcite as the highest proportion of aquifer material. A slight peak was also observed between 1000 and 1200 cm^{-1}, indicating the presence of quartz in the limestone aquifer material. Furthermore, the FTIR spectrum of dolomite can be characterized at 727 cm^{-1}. But, in this study no obvious peak was observed in this domain which may be attributed to the low amount of dolomite in the structure of limestone aquifer materials that was confirmed by the results of EDS and XRF techniques.

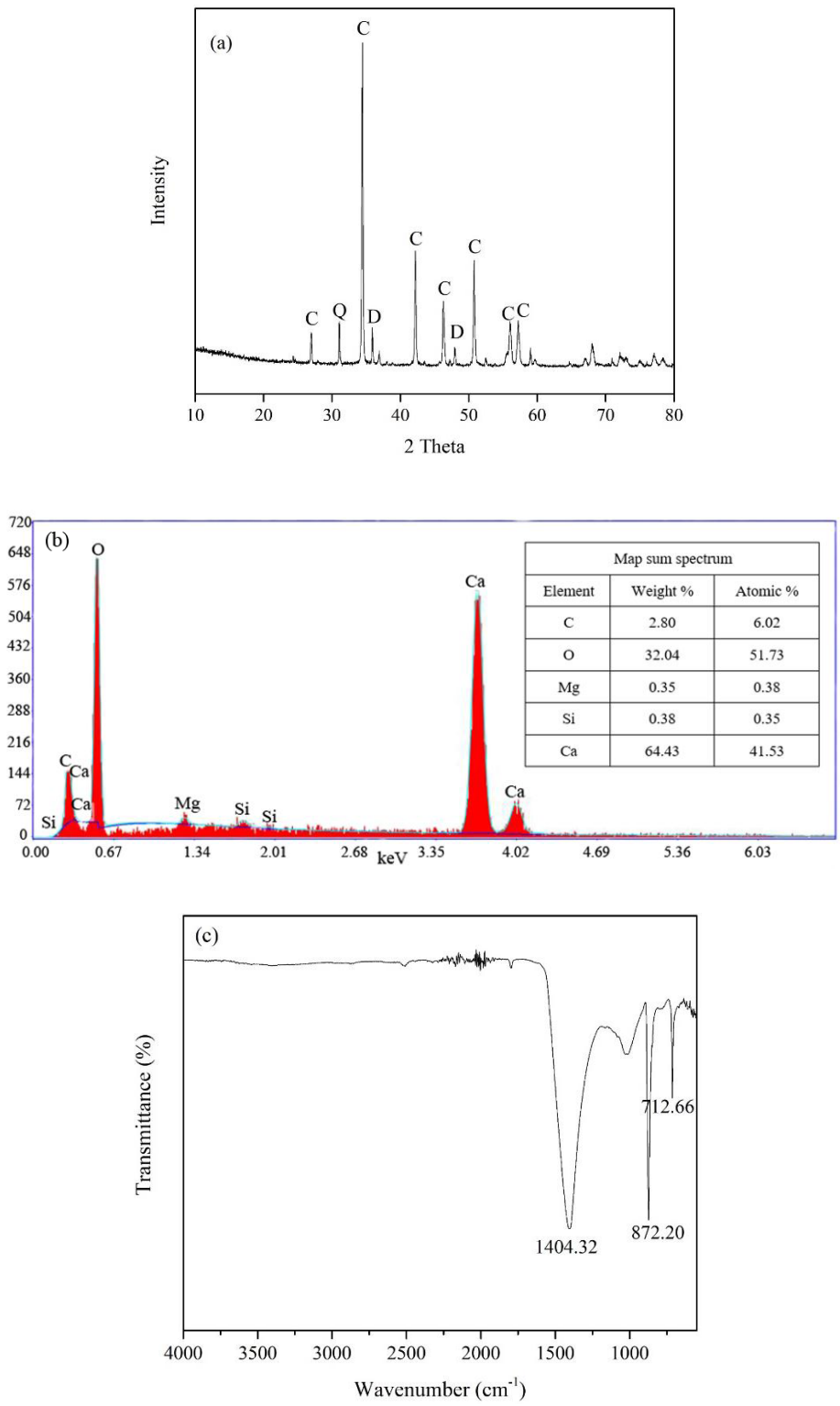

Fig 3-1. XRD diagram (a), EDS (b) and FTIR spectra (c) of limestone aquifer materials (C: calcite, Q: quartz and D: dolomite).

3.4.2. Effect of agitation and temperature

The agitation status and temperature are two most critical factors affecting virus inactivation in the presence of solid surfaces (Chrysikopoulos and Aravantinou, 2014). Fig 3-2 shows the $\log_{10}$ removal of MS2 over the reaction time, due to the inactivation by attachment onto the surfaces of small particle size (0.25–0.50mm) aquifer material under static and dynamic (mixed) incubation conditions. MS2 inactivation rate in the presence of limestone was significantly higher than those of the controls in the absence of limestone. For example, in 4 °C static treatment, MS2 inactivation rate in the control incubation (−0.03) was significantly lower than incubations in the presence of limestone (−0.07; $p < 0.05$). Indeed, in the control experiments, the most likely causes of virus inactivation are dark die off inactivation and attachment to the internal surfaces of reactors. However, in reactive experiments with the presence of solid surfaces, the removal of virus is the sum of the above-mentioned processes together with inactivation by attachment onto the surfaces of substrate. The maximum $\log_{10}$ (N_t/N_0) removal of MS2 at 22 °C in the presence of limestone was −0.38 in the dynamic incubation, compared with −0.15 when incubated statically. Agitation in the dynamic incubation increases contact between virus particles and the limestone surfaces thereby enhancing the chance of collision between these particles and reducing the resistance to mass transfer (Anders and Chrysikopoulos, 2006). Furthermore, this observation can be ascribed to the presence of air-liquid and air-solid interfaces in dynamic conditions, which were not effective in virus inactivation in static conditions. Similar findings have been reported in other studies (Chrysikopoulos and Aravantinou, 2012) (Anders and Chrysikopoulos, 2005). In addition, Fig 3-2 shows that virus inactivation in both static and dynamic experiments was higher at the higher temperature. Accordingly, the maximum virus inactivation was observed with $\log_{10}$ removal of −0.38 at 22 °C under dynamic incubation. While, at 4 °C under dynamic incubation,

the maximum virus $\log_{10}$ removal was −0.12. This may be damage due to high temperature on some viral components that are necessary for infection (Harvey and Ryan, 2004). Bellou et al., (2015) similarly reported a considerable increase in MS2 inactivation when increasing the incubation temperature from 4 to 22 °C (Bellou et al., 2015).

Results of kinetic studies of MS2 inactivation on aquifer material in both control and reactive experiments under static and dynamic incubation conditions, at both 4 and 22 °C are reported in Table 3-1. As can be seen from Table 3-1, the significantly high correlation coefficients (R^2) and low root mean square error (*RMSE*) and sum of squared error (*SSE*) demonstrate the accuracy of the model applied to fit the experimental data of MS2 inactivation. Furthermore, k_{max}, which is a reliable virus inactivation index, of the control experiments, in the absence of limestone, is lower than reactive experiments, where limestone is present. In addition, although no trend was observed for *Sl* (h), by increasing the temperature and agitation, in both control and reactive experiments, the k_{max} (h^{-1}) was higher at room temperature than at 4°C and in dynamic, compared with static incubations.

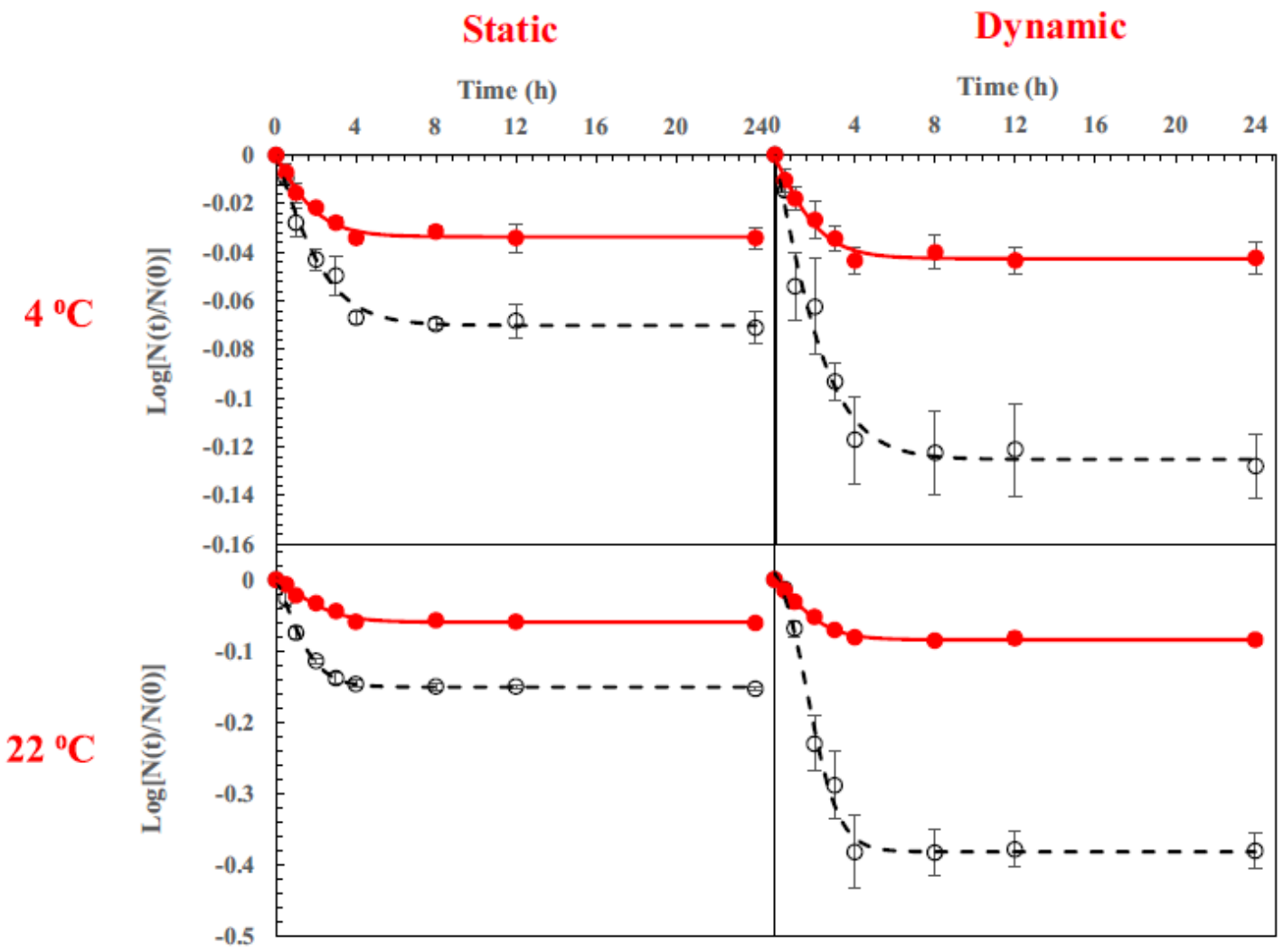

Fig 3-2. Log_{10} removal of MS2 due to attachment on small particle size (0.25 -0.50 mm) limestone aquifer materials incubated under static and dynamic conditions and at 4 and 22°C (initial MS2 concentration: 10^3 PFU/mL), in the presence (o) and absence (●) of limestone substrate. The error bars smaller than dots are not shown.

Table 3-1. Kinetic studies of MS2 inactivation in the presence (reactive) and absence (control) of limestone aquifer material at 4 and 22°C under static and dynamic conditions in RO water (particle size; small (0.25-0.50 mm); medium (0.5-1.0 mm) and coarse (1-2 mm).

Experimental conditions	[a]C_0 (PFU/mL)	Control experiments						Reactive experiments				
		[b]k_{max} (h^{-1})	[c]*Sl (h)*	[d]R^2	[e]*RMSE*	[f]*SSE*	Particle size	k_{max} (h^{-1})	*Sl (h)*	R^2	*RMSE*	*SSE*
4°C static	2.48×10^3	0.74±0.13	0.43±0.34	0.982	0.0024	0.0000	Small	0.64±0.23	0.48±0.28	0.975	0.005	0.0000
4°C dynamic	2.80×10^3	0.78±0.07	0.68±0.07	0.955	0.0038	0.0000	Small	0.69±0.03	0.88±0.75	0.956	0.0130	0.0002
22°C static	3.71×10^3	0.86±0.37	1.05±0.67	0.975	0.0044	0.0000	Small	1.22±0.39	0.65±0.26	0.990	0.0069	0.0001
22°C dynamic	3.28×10^3	0.95±0.65	0.87±0.44	0.983	0.0054	0.0000	Small	1.38±0.72	1.34±0.28	0.982	0.0276	0.0008
22°C dynamic	3.31×10^4	0.73±0.32	0.57±0.68	0.974	0.0061	0.0000	Small	1.35±0.49	2.06±0.25	0.969	0.0246	0.0006
22°C dynamic	3.53×10^5	0.68±0.15	0.71±0.44	0.951	0.0083	0.0001	Small	1.25±0.52	2.08±0.30	0.972	0.0221	0.0004
22°C dynamic	2.73×10^6	0.79±0.14	0.62±0.10	0.935	0.0087	0.0001	Small	1.23±0.25	2.15±0.08	0.960	0.0230	0.0006
22°C dynamic	3.24×10^7	0.66±0.08	0.72±0.48	0.948	0.0069	0.0001	Small	1.13±0.23	2.24±0.12	0.970	0.0186	0.0003
22°C dynamic	3.19×10^3	1.05±0.31	1.38±0.08	0.980	0.0065	0.0000	Medium	1.31±0.08	1.45±0.19	0.988	0.0136	0.0001
22°C dynamic	4.21×10^4	1.03±0.36	1.14±0.39	0.979	0.0055	0.0000	Medium	1.27±0.24	1.55±0.04	0.979	0.0168	0.0003
22°C dynamic	3.48×10^5	0.94±0.03	1.43±0.09	0.974	0.0060	0.0000	Medium	1.18±0.26	1.58±0.14	0.974	0.0164	0.0003
22°C dynamic	4.29×10^6	0.90±0.08	1.35±0.05	0.964	0.0064	0.0000	Medium	1.13±0.11	1.70±0.13	0.980	0.0122	0.0001
22°C dynamic	3.37×10^7	0.89±0.17	1.50±0.75	0.945	0.3236	0.0001	Medium	1.03±0.22	2.02±0.23	0.985	0.0110	0.0001
22°C dynamic	3.50×10^3	0.97±0.15	0.91±0.17	0.975	0.0064	0.0001	Coarse	1.20±0.15	1.72±0.09	0.965	0.0192	0.0004
22°C dynamic	3.93×10^4	0.95±0.31	0.91±0.35	0.983	0.0048	0.0000	Coarse	1.15±0.12	1.04±0.12	0.984	0.0110	0.0001
22°C dynamic	2.80×10^5	0.91±0.31	1.20±0.31	0.962	0.0065	0.0001	Coarse	1.14±0.15	1.83±0.28	0.985	0.0101	0.0001
22°C dynamic	3.18×10^6	0.86±0.09	1.46±0.45	0.972	0.0045	0.0000	Coarse	1.13±0.37	1.81±0.30	0.969	0.0137	0.0002
22°C dynamic	4.40×10^7	0.78±0.06	1.68±0.22	0.940	0.0069	0.0001	Coarse	1.04±0.12	1.73±0.37	0.968	0.0121	0.0001

[a] Initial MS2 concentration. [b] Virus inactivation rate. [c] Shoulder length. [d] Coefficient of determination. [e] Root mean square error. [f] Sum of squared error.

3.4.3. Effect of particle size distributions and initial virus concentrations

In a typical aquifer, the medium consists of materials of different particle sizes, which may influence on the inactivation of microorganisms. This study determined the inactivation of MS2 at five different initial MS2 concentrations (10^3–10^7 PFU/mL) by attachment onto the surfaces of aquifer materials of different particle size distributions (i.e., small, medium and coarse). The results confirmed that the MS2 inactivation in the presence of limestone particles was significantly higher than in those incubations where limestone was absent (Fig 3-3, control), irrespective of the initial concentration of MS2. In addition, an indirect relationship was observed between the particle size and MS2 inactivation rate. At initial virus concentration of 10^3 PFU/mL in three different particle size distributions 0.25-0.50, 0.5-1 and 1-2 mm, the MS2 $\log_{10}$ fraction removal were obtained -0.38, -0.24 and -0.19, respectively. Increasing particle size likely reduces, the available reactive sites decreasing virus inactivation via attachment onto the adsorbent surfaces. Although the grain shape of the aquifer materials with different size distribution was similar since they were obtained from the same source, the number of attachment sites on smaller particles is higher than larger ones. Chrysikopoulos and Aravantinou (2014) in a research on interaction of two bacteriophages MS2 and ΦX174 with quartz sand grains with different diameters also reported higher virus inactivation rates in smaller particle size distributions (Chrysikopoulos and Aravantinou, 2014). Results of kinetic studies of MS2 inactivation using limestone with different particle size distribution are illustrated in Table 3-1. Higher values of k_{max} (h^{-1}) were observed for reactive treatments than the controls, indicating more MS2 inactivation in reactive treatments, compared to the control ones at all initial MS2 concentrations and limestone size distributions.

Furthermore, by decreasing the particle size of aquifer materials, an increase in the value of k_{max} (h^{-1}) was observed.

In addition, MS2 inactivation rate was high at lower initial virus concentrations in both control and reactive experiments. Indeed, when incubated with the small particle size material, the mean MS2 inactivation rate showed a statistically significant decrease from −0.38 to −0.21, ($p = 0.000361$) when the initial MS2 concentration was increased from 10^3 to 10^7 PFU/mL. This observation can be ascribed to increasing virus aggregation in high virus concentrations (Mattle et al., 2011). Increasing the initial virus concentrations in the solution, increases the likelihood of creating a virus sub-population, which leads to the presence of virus with high resistance to inactivation (Mattle et al., 2011). The findings of kinetic studies also showed that k_{max} (h^{-1}) at all particle size distributions, showed a decreasing trend with increasing initial MS2 concentration. However, an indirect relationship was observed between k_{max} (h^{-1}) and *Sl* (h). Where, a sharp increase was observed by increasing initial MS2 concentrations. Similar results were reported by Ng et al., (2016) who investigated the effect of bromide on the photocatalytic inactivation of bacteria in aqueous media (Ng et al., 2016).

Furthermore, contact time is a very crucial factor for the removal of adsorbate molecules onto the solid surfaces (Babaei, 2014, Islam et al., 2019, Ali et al., 2018, Dalvand et al., 2018). Depending on the physical and chemical features of adsorbents and intrinsic nature of viruses, the equilibrium contact time of virus inactivation is quite different. In this study, the inactivation ofMS2 by attachment on the limestone surfaces attained equilibrium at 4 h after which the changes in MS2 inactivation were negligible. However, results of Bellou et al., (2015) showed that hAdV, MS2 and ΦX174 inactivation using the kaolinite and bentonite was a slower process and equilibrated after 7 days (Bellou et al., 2015).

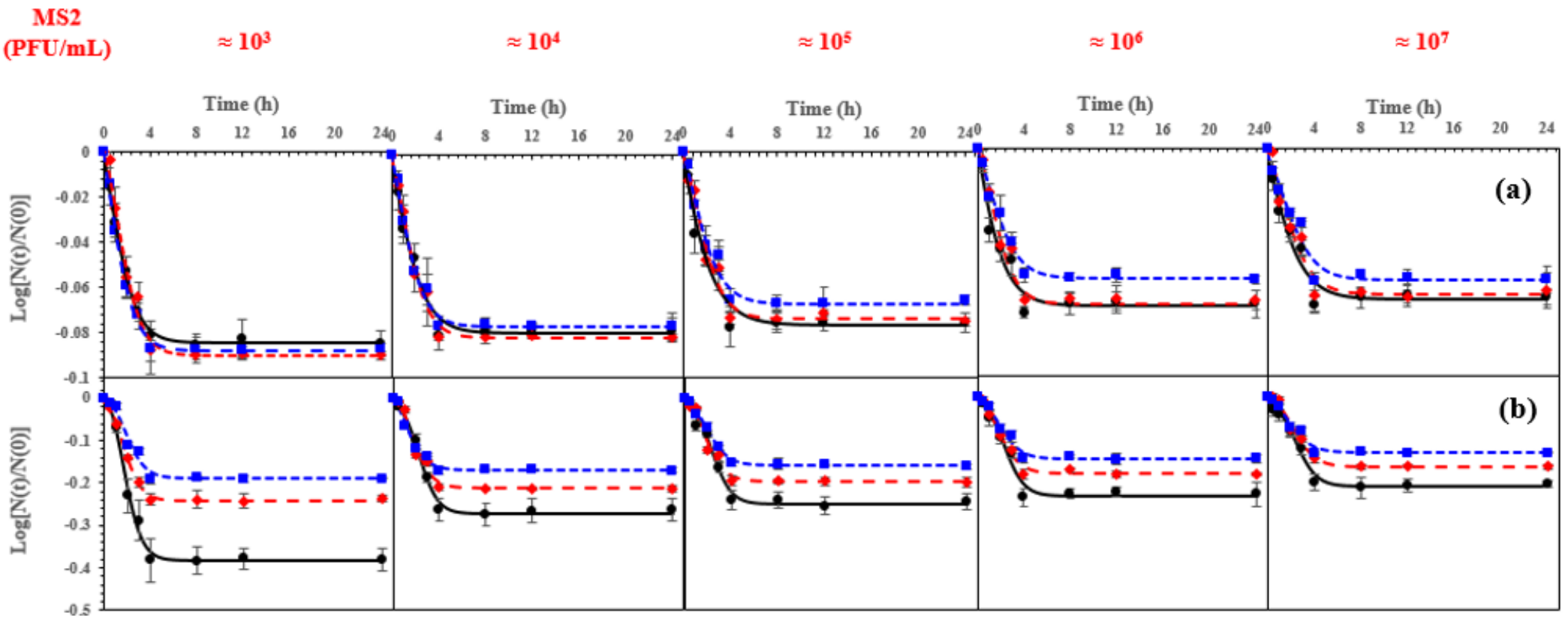

Fig 3-3. MS2 inactivation determined simultaneously in the presence of limestone aquifer materials of different particle size distributions (reactive), small particles (0.25-0.50 mm; ●), medium (0.5-1.0 mm;◆) and coarse (1-2 mm; ■) and in the respective controls in the absence of limestone material. The inactivation rates were determined at five initial MS2 concentrations at 22°C under dynamic conditions. The error bars smaller than dots are not shown.

3.4.4. Effect of biofilm

Limestone aquifer substrate (0.25–0.50 mm) was pre-incubated for 2 months with secondary treated wastewater obtained from Mount Barker Wastewater Treatment Plant, South Australia to condition the surface with biofilm. The chemical and biological properties of wastewater, before and after incubation with the limestone, are presented in Table 3-2. Batch incubation with MS2 were performed to determine the effect of conditioning the limestone on MS2 inactivation under static and dynamic conditions at 4 and 22 °C. Fig 3-4 shows that, irrespective of other incubation conditions, incubation at 22 °C increased the MS2 inactivation rate, which was further increased by agitation. -0.46 and − 1.88 MS2 $\log_{10}$ removal were observed in the presence of the conditioned limestone substrate at 4 °C static and 22 °C dynamic treatments, respectively. Furthermore, results of kinetic studies of MS2 inactivation in conditioned limestone show that the lowest k_{max} 1.53 (h^{-1}) was obtained at 4 °C in the static incubation (Table 3-3). While, dynamic treatment at 22 °C showed the highest k_{max} 1.94 (h^{-1}). In addition, the inactivation rate of virus in limestone conditioned with treated wastewater was higher than those determined with pristine limestone in RO water. Accordingly, in the dynamic treatment at 22 °C, the difference in the mean MS2 inactivation rate in pristine limestone with RO water (−0.38) and conditioned limestone with treated wastewater (−1.88) was statistically significant (p = 0.000002). In the same experimental conditions, the minimum and maximum values of *Sl* (h) were observed at 22 °C dynamic and 4 °C static treatments, respectively. A most likely explanation of this phenomenon is the presence of irregularities and roughness onto the surfaces of conditioned limestone which were created by biofilm. Previous research have reported the role of biofilm in changing the surface properties of granular substrates which provide low velocity regions with less hydrodynamic forces and torques

to adsorb particles, even in unfavorable conditions (Vaidyanathan and Tien, 1988). SEM images of limestone aquifer materials, before and after conditioning with treated wastewater are shown in Plate 3-1. It is clear that conditioning of limestone in treated wastewater caused an enhancement in surface roughness of the limestone, which is attributed to the microbial growth onto the limestone surfaces by creation of a biofilm layer of relatively large thickness. CLSM images of pristine and biofilm-conditioned limestone grains are shown in Plate 3-2. A very thin layer of fluorescent can be seen around the pristine limestone, which is attributed to the negligible amounts of microbial mass. However, the CLSM image of biofilm-conditioned limestone grains shows a thick layer of fluorescent around the substrate, denoting biofilm production.

Dika et al., (2013) similarly observed higher virus attachment on the surfaces of adsorbents by increasing the attachment sites originating from surface irregularities (Dika et al., 2013). Previous research has shown that the deposition of micro and nano-sized colloidal particles was enhanced in the presence of surface roughness (Tripathi et al., 2011, Hoek and Agarwal, 2006, Joo and Aggarwal, 2018). By conditioning limestone particles with treated wastewater, the amount of total carbon increased from 5.22±0.78 to 5.48±0.07 mg/g (Table 3-2), which was due to the production of biofilm on the surfaces of limestone grains, originating from bacterial growth. In addition, around 0.49 ± 0.21 mg/g organic matter was produced in biofilm-conditioned limestone grains, by the conditioning with treated wastewater. In some cases, an increase in organic matter can potentially cause a negative relationship with virus removal onto the substrates, due to blocking the attachment sites. For example, results of Mayotte et al., (2017) showed that increasing organic carbon on sand particles decreased their adsorption capacity towards bacteriophage, because of the blockage of surface attachment sites of sand grains which prevented further MS2 attachment (Mayotte et al., 2017). In contrast, the results presented here showed increasing virus inactivation

in conditioned limestone, which contained higher organic matter. It can be implied that the role of surface irregularities and roughness outweigh the blocking of surface attachment sites with organic matter on virus inactivation. To further elucidate the potential relationship between the presence of biofilm and enhanced virus inactivation, batch experiments were carried out incubating MS2 with conditioned limestone in RO water at 4 and 22 °C under static and dynamic agitation conditions. The lowest and highest MS2 inactivation rates were recorded in 4 °C static and 22 °C dynamic conditions, respectively (Fig 3-5). Comparison of k_{max} (h^{-1}) and $\log_{10}$ removal of MS2 onto either pristine or conditioned limestone in RO or treated wastewater are shown in Fig 3-6. The minimum and maximum for MS2 $\log_{10}$ removal were -0.32 and -1.31 at 4°C static and 22°C dynamic conditions, respectively, which were apparently higher for the pristine limestone incubated in RO water in the same temperature and agitation status. Statically incubating MS2 at 4 °C with limestone conditioned with a biofilm led to a statistically significant increase in MS2 inactivation, when compared to similarly incubated pristine limestone. This result confirmed that the conditioning of limestone increased its potential to adsorb more MS2 from aqueous solution, because of enhanced surface irregularities by biofilm growth.

Zeta potential is another essential parameter which governs the inactivation of MS2 on the substrate surfaces. The obtained zeta potentials of MS2 in RO water and treated wastewater were -20.3±1.44 and -9.1±0.6 mV, respectively, which shows the role of presence of different cations in treated wastewater on charge neutralization of MS2. The zeta potentials of pristine and conditioned limestone were -16.9±1.3 and -13.3±3.2 mV in RO water and -11.2±2.7 and -5.1±0.1 mV in treated wastewater. As can be seen, the zeta potentials of conditioned limestone in both solutions were slightly less negative than pristine limestone, indicating the role of biofilm on decreasing negative surface charges of limestone and consequently decreasing the electrostatic

double layer. Tripathi et al., (2011) observed that biofilm-coated sand particles had less negative values of zeta potential than sand grains, which enhanced nanoparticle retention in columns (Tripathi et al., 2011).

The observed increase in MS2 inactivation using the surfaces of the conditioned limestone in the presence of wastewater compared with the RO water may be associated with the higher ionic strength of the treated wastewater, due to the presence of various cations (e.g. Ca^{2+} and Mg^{2+}). This may contribute to decreasing the thickness of electrostatic double layer, cation bridging, neutralization of negative charges of adsorbent and virus particles and binding between calcium and some carboxyl functional groups onto the virus surfaces (Chu et al., 2003); (Harvey and Ryan, 2004, Huysman and Verstraete, 1993, Rahmatpour et al., 2017). Sasidharan et al., (2016) reported that the presence of Ca^{2+} in solution increased significantly virus inactivation in the surfaces of sand grains (Sasidharan et al., 2016). In addition, Stevenson et al., (2015) showed that the addition of Ca^{2+} led to higher virus inactivation in the surfaces of granular limestone aquifer materials (Stevenson et al., 2015). To test this hypothesis, the amounts of soluble calcium ions (Ca^{2+}) and calcium carbonate in the wastewater conditioning solution were measured. Table 3-2 shows that Ca^{2+} and calcium carbonate concentrations were increased in conditioned limestone incubation, confirming that the limestone dissolution into the aqueous solution was a dominating process. Indeed, the concentrations of Ca^{2+} and calcium carbonate in treated wastewater after incubation with limestone particles showed an increasing trend from 9.55 to 42.55 mg/L and 124 to 151 mg/L, respectively. The concentrations of Ca^{2+} and calcium carbonate in the incubations with treated wastewater were higher than for similar RO water incubations (data not shown). That is attributed to microbial activities increasing the dissolution of limestone. Rinck-Pfeiffer et al., (2000) similarly attributed Ca^{2+} dissolution in limestone-packed columns to the microbial activity (Rinck-

Pfeiffer et al., 2000). The concentration of Mg^{2+} in treated wastewater also increased from 10.63 to 26.13 mg/L, which may be due to the dissolution of dolomite. pH is influential on calcite dissolution. In this study, the initial pH of treated wastewater was 7.21 (Table 3-2), which is quite favorable for dissolution of limestone grains. After conditioning of the limestone particles with treated wastewater, the solution pH increased to 8.43, which can be ascribed to increasing cations in aqueous media. Another effectual process on limestone dissolution in treated wastewater is nitrification, due to this process releasing hydrogen ions (H^+) into the aqueous media. Nitrification was observed during limestone conditioning. NO_3^-N concentration increased from 0.243 to 16.85 mg NO_3^-N /L. While, a simultaneous reduction was observed in NO_2^--N and NH_4^+-N concentrations from 0.028 to 0.005 mg NO_2^--N /L and 64.4 mg NH_4^+-N /L to below detection limit, respectively. Total nitrogen, NH_4^+, NO_3^- and NO_2^- concentrations were determined, before and after limestone conditioning in wastewater (Table 3-2). It is observed that the amount of total nitrogen declined from 74.33 to 23.87 mg N/L, which may be due either to volatilization of NH^+_4 –N or more likely to transformation to microbial biomass on the surfaces of limestone grains

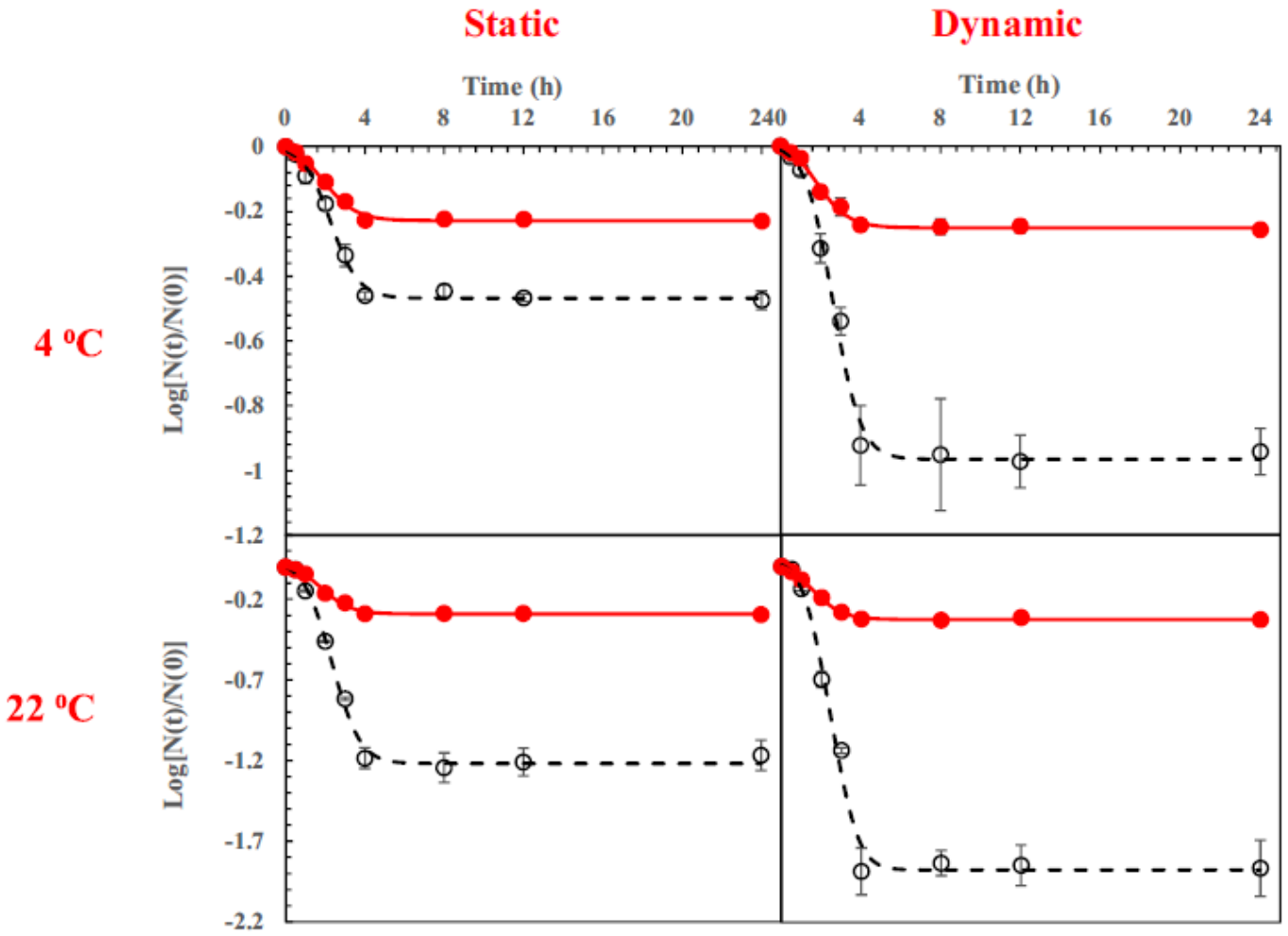

Figs 3-4. MS2 inactivation in the biofilm conditioned, small particle size (0.25-0.50mm) limestone aquifer materials incubated in treated wastewater for 2 months under static and dynamic conditions at 4 and 22°C (initial MS2 concentration 10^3 PFU/mL), in the presence (o) and absence (●) of limestone substrate. The error bars smaller than dots are not shown.

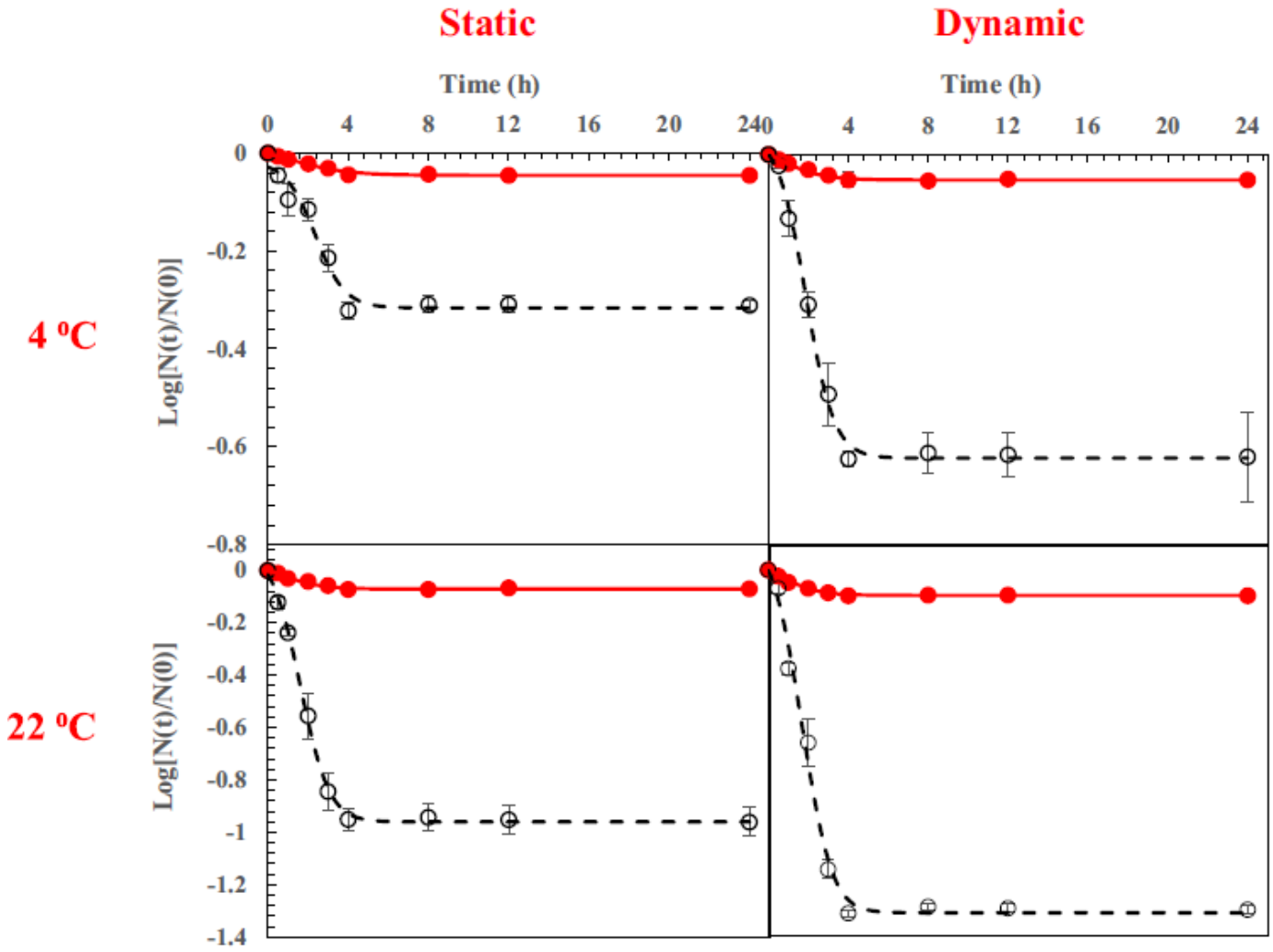

Fig 3-5. MS2 inactivation in the biofilm conditioned, small particle size (0.25-0.50mm) limestone aquifer materials in RO water incubated under static and dynamic conditions and at 4 and 22°C (initial MS2 concentration 10^3 PFU/mL); in the presence (o) and absence (●) of limestone substrate. The error bars smaller than dots are not shown.

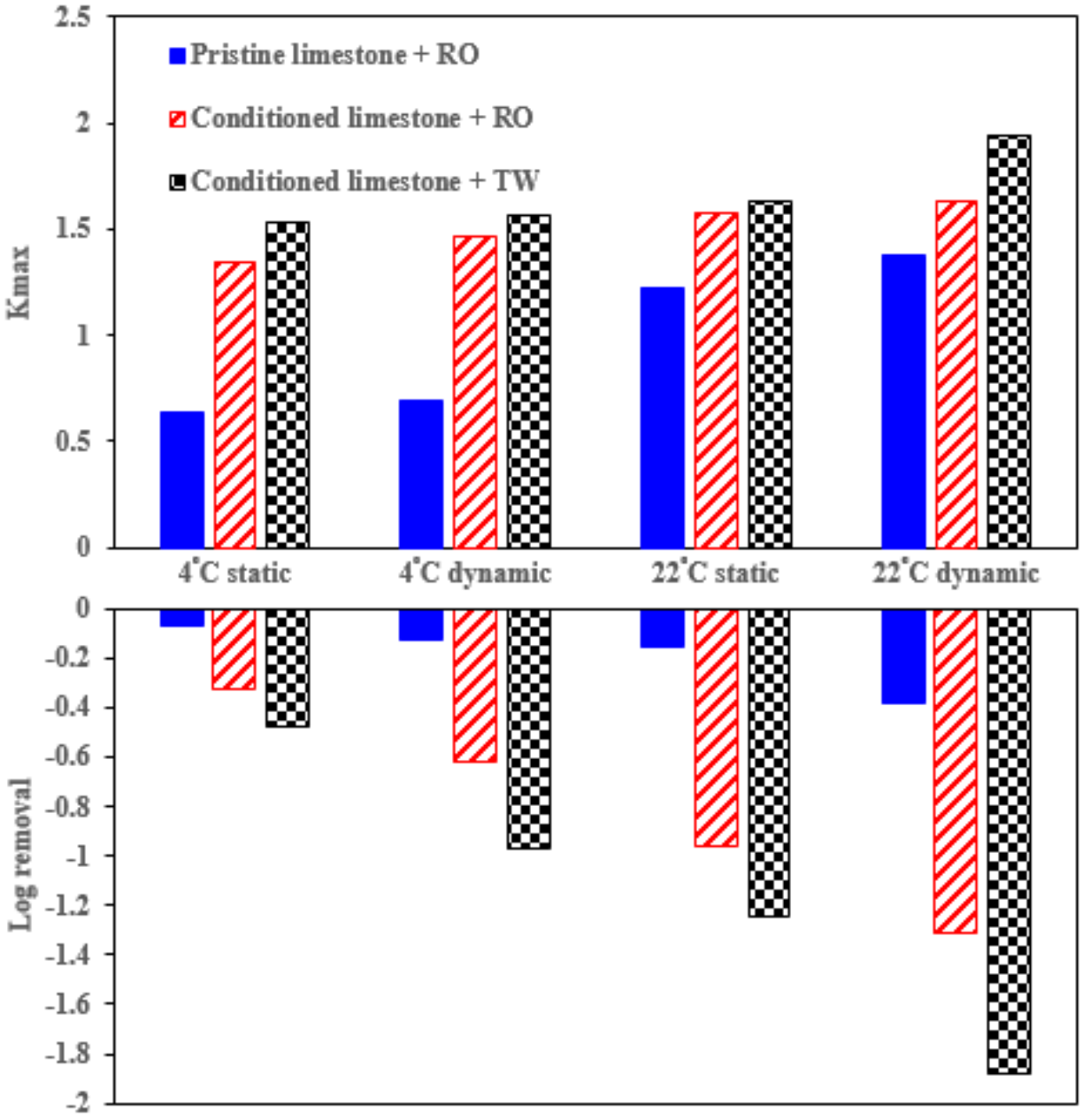

Fig 3-6. Comparison between MS2 inactivation rate (K_{max}) and log removal under different treatments.

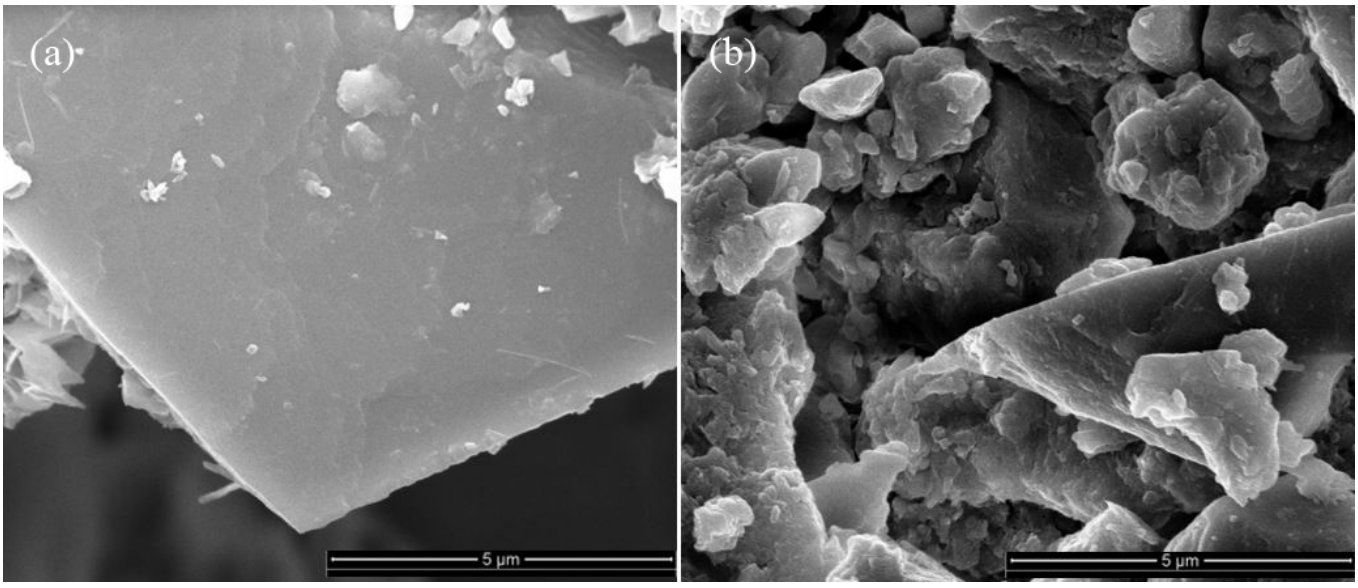

Plate 3-1. SEM images of pristine (a) and biofilm-conditioned limestone particles (b).

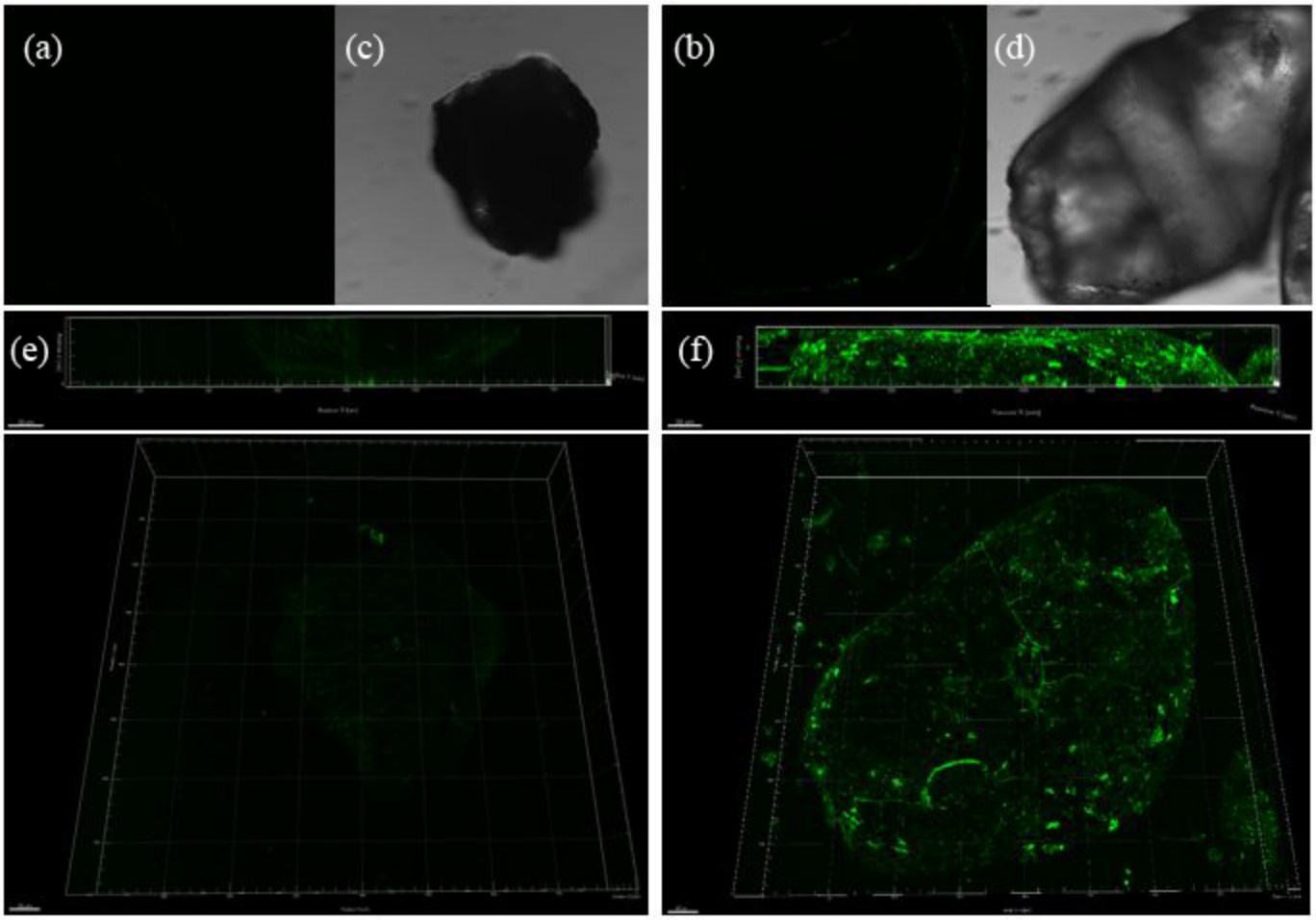

Plate 3-2. CLSM images of (left) pristine and (right) biofilm-conditioned limestone with treated wastewater (a) and (b): confocal slice images through limestone grains, (c) and (d): transmitted light images of limestone shown in (a) and (b), respectively, e and f: 3D view of confocal z-stack data set in Imaris software).

Table 3-2. Chemical and biological parameters of studied treated wastewater, before and after conditioning limestone aquifer material.

Parameter	Before conditioning	After conditioning
	Treated wastewater	
pH	7.21±0.04	8.43±0.02
Total nitrogen (mg/L)	74.33±0.36	23.87±0.21
NH_4-N (mg/L)	64.40±0.1	Below detection limit
NO_2-N (mg/L)	0.028±0	0.005±0
NO_3-N (mg/L)	0.243±0.001	16.85±0.08
PO_4-P(mg/L)	4.31±0.08	0.54±0.001
TOC (mg/L)	24.13±0.9	4.70±0.02
Calcium carbonate (mg/L)	124±7.0	151±10.0
MS2 (PFU/ml)	Below detection limit	Below detection limit
Ca^{2+} (mg/L)	9.55±0.17	42.55±0.27
Mg^{2+}(mg/L)	10.63±0.24	26.13±0.18
	Limestone aquifer material	
Total carbon (mgC/g)	5.22±0.78	5.48±0.07

Table 3-3. Kinetic studies of MS2 inactivation by attachment onto the surfaces of conditioned limestone aquifer material at different temperatures (4 and 22°C) and agitation (static and dynamic) conditions in RO water and treated wastewater aqueous solution (particle size; small (0.25-0.50 mm).

Experimental conditions	[a]C_0 (PFU/mL)	Control experiments					Particle size	Reactive experiments				
		[b]k_{max} (h^{-1})	[c]*Sl (h)*	[d]R^2	[e]*RMSE*	[f]*SSE*		[b]k_{max} (h^{-1})	[c]*Sl (h)*	[d]R^2	[e]*RMSE*	[f]*SSE*
RO water												
4°C static	2.77×10^3	0.83±0.05	1.76±0.25	0.959	0.0042	0.0000	Small	1.34±0.20	2.08±0.21	0.952	0.0347	0.0012
4°C dynamic	3.58×10^3	0.88±0.40	0.92±0.60	0.945	0.0060	0.0000	Small	1.46±0.27	1.42±0.20	0.982	0.0423	0.0020
22°C static	2.91×10^3	0.91±0.25	0.92±0.45	0.947	0.0082	0.0001	Small	1.58±0.34	1.38±0.38	0.989	0.0513	0.0026
22°C dynamic	3.30×10^3	0.96±0.18	0.57±0.28	0.984	0.0056	0.0000	Small	1.63±0.09	0.87±0.15	0.989	0.0684	0.0052
Treated wastewater												
4°C static	3.63×10^3	1.25±0.25	1.73±0.28	0.991	0.0109	0.0001	Small	1.53±0.38	1.95±0.11	0.988	0.0277	0.0008
4°C dynamic	2.72×10^3	1.38±0.62	1.60±0.26	0.990	0.0136	0.0002	Small	1.57±0.32	1.92±0.22	0.968	0.0899	0.0092
22°C static	4.15×10^3	1.41±0.17	1.64±0.13	0.988	0.0162	0.0003	Small	1.63±0.16	1.49±0.18	0.989	0.0686	0.0049
22°C dynamic	3.15×10^3	1.46±0.26	1.39±0.37	0.980	0.0244	0.0006	Small	1.94±0.25	1.34±0.14	0.983	0.1281	0.0191

[a] Initial MS2 concentration. [b] Virus inactivation rate. [c] Shoulder length. [d] Coefficient of determination. [e] Root mean square error. [f] Sum of squared error.

3.4.5. Environmental Implications

The understanding of MS2 inactivation in the aquifer materials is required to use different water resources such as stormwater and treated wastewater in a managed aquifer recharge site. Much research focuses on physically simple and chemically clean substrates like sand grains and different clay minerals interactions with viruses (Chrysikopoulos and Aravantinou, 2012, Bellou et al., 2015). However, the interaction between authentic limestone aquifer materials, which are representative of an authentic limestone-based MAR site with MS2 has not previously been presented. In addition, the presence of biofilm in a MAR site is possible, due to the application of stormwater and treated wastewater containing high TOC and nutrient concentrations. Recent studies have shown the significant effect of biofilm on enhanced retention of nanoparticles and Escherichia coli (*E.coli*) (Tong et al., 2010, Bozorg et al., 2015). However, no study has paid attention to the virus inactivation behavior of biofilm grown onto the surfaces of authentic aquifer materials. The present study mainly focused on MS2 inactivation using pristine and biofilm-coated aquifer materials in RO water and treated wastewater, to mimic the inactivation of virus in a MAR site. Our results revealed the enhanced MS2 inactivation in biofilm-coated aquifer materials compared to pristine one, even when RO water was considered as aqueous media. Therefore, although application of different water streams in MAR may pose the groundwater resources to the risk of pathogenic pollution, the production of biofilm may enhance virus inactivation in groundwater and aquifers.

3.5. Conclusion

In this study, virus inactivation in the limestone grains was studied at different experimental conditions. Results revealed that virus inactivation was completely dependent on adsorbent particle size distribution. As aquifer limestone particle size increased, a sharp decrease occurred in virus inactivation. Furthermore, more virus in RO or wastewater were inactivated in the presence of limestone grains incubated at 22 ˚C than 4 ˚C, indicating a firm relationship between virus inactivation and temperature. Additionally, incubation of limestone aquifer material with treated wastewater caused a significant increase in virus inactivation, due to the enhancement of adsorbent surface roughness and increasing solution ionic strength. Biofilm production onto the substrate surfaces increased the height of roughness that changes the mass transfer rate and lever arms associated with torque balance. These findings were confirmed by the SEM images of pristine and conditioned substrate. Results of the present research provide a valuable insight about the interaction between MS2 bacteriophage with biofilm in natural aquifers.

This chapter provides results from a mechanistic approach to virus interaction with aquifer materials. As mentioned above, in addition to surface attachment, other mechanisms such as blocking and physical straining are effective on retention of virus in aquifers. Furthermore, in addition to the surface properties of aquifer grains, the hydrological features of aquifers are also influenced by biofilm, which may affect virus retention. The influence of these additional mechanisms is unable to be determined using batch studies. Moreover, the detachment of microorganisms onto the substrate would be either reversible or irreversible. The detachment of microorganisms from aquifer materials may potentially threaten groundwater resources via pathogenic contamination.

Therefore, to have a more realistic view of virus attachment behavior in aquifers, the attachment and detachment behavior of virus onto the substrate has to be performed in column experiments with authentic aquifer substrates and aqueous media to find sum effect of the various mechanisms on retention of virus in porous media. In the following chapter, virus transport behavior is determined in saturated and biofilm-conditioned, limestone and sand columns (as a control treatment), to understand the mechanisms influencing virus retention in porous media and determine the relationship between batch and column studies of virus removal using limestone aquifer materials.

4. Combined physical, chemical and biological clogging of managed aquifer recharge and the effect of biofilm on virus transport behavior: A column study

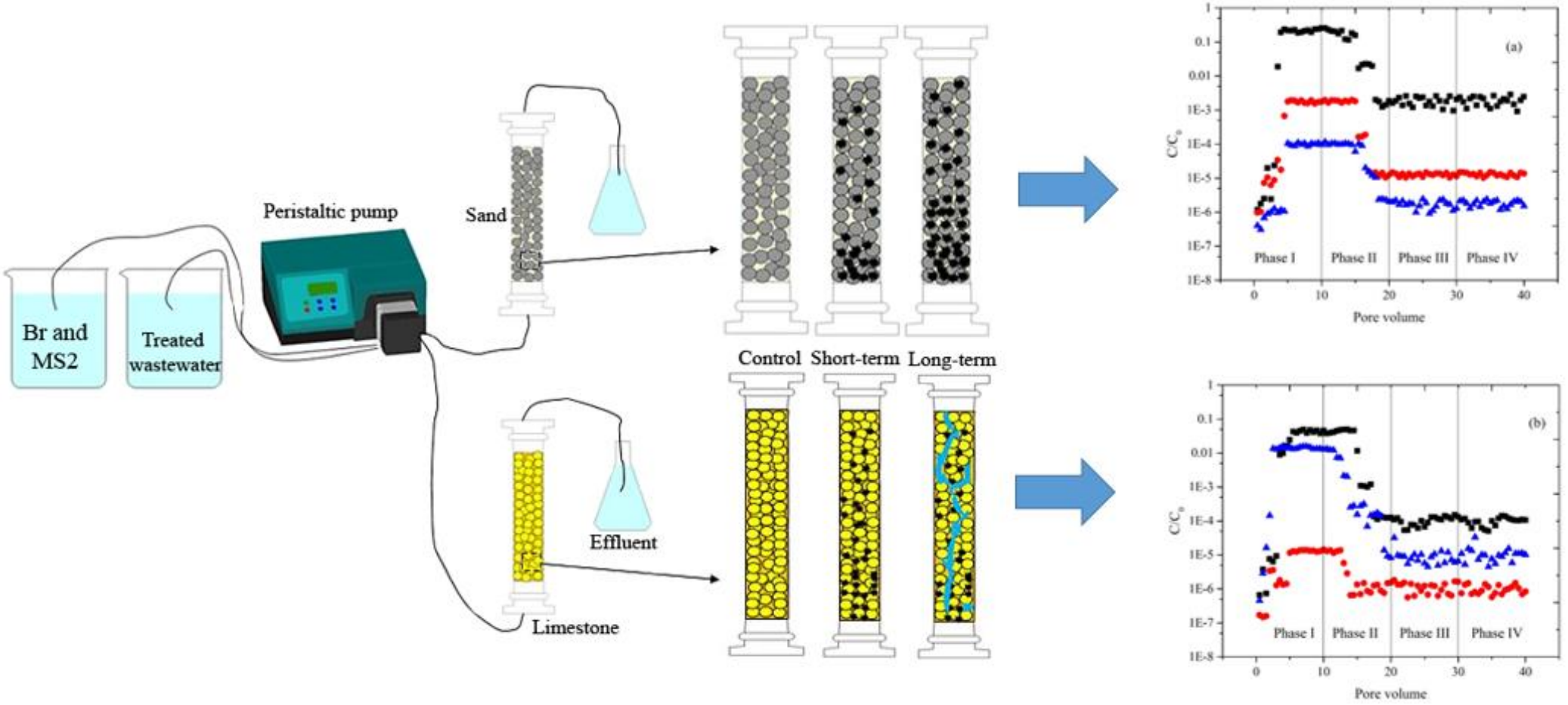

4.1. Highlights

- Study role of irrigation of sand and limestone aquifer sediments with treated wastewater on physical, chemical and biological features.
- Investigation of effect of biofilm growth on transport parameters of tracer.
- Study the effect of biofilm growth on virus retention and detachment behavior in saturated columns.

This Chapter is based on the following publication: Amirhosein Ramazanpour Esfahani, Okke Batelaan, John L. Hutson and Howard J. Fallowfield. Combined physical, chemical and biological clogging of managed aquifer recharge and the effect of biofilm on virus transport behavior: A column study. Journal of Water Process Engineering (Volume 33, 2020, 101115) (DOI: https://doi.org/10.1016/j.jwpe.2019.101115).

4.2. Abstract

In this study, the effect of treated wastewater on physical, chemical and biological clogging of porous media and subsequently transport behavior of solutes and virus was studied. Therefore, transport experiments of bromide (Br^-) and MS2 bacteriophage as tracer and microorganism in sand and limestone-packed columns irrigated with treated wastewater at different short and long-term periods (2 and 8 weeks) were carried out. In addition, some physical, chemical and biological features of columns were measured after irrigation with wastewater. Results revealed that injection of treated wastewater for around 2 weeks not only led to the physical and biological clogging, but also caused a significant increase in MS2 retention in the columns. However, enhancement of limestone column irrigation for 8 weeks increased solutes and pathogenic agents discharge into the effluents. This is due to increased saturated hydraulic conductivity caused by the formation of heterogeneities in the columns, as a result of calcium dissolution and microbial activities. Ultimately, from the findings of this research, it can be postulated that long-term application of recycled water in limestone aquifers will endanger groundwater resources with pathogenic contaminations.

4.3. Introduction

Managed aquifer recharge (MAR) is one of the most promising hydrological techniques for improving groundwater resources whereby surface water is transferred to groundwater aquifers (Bouwer, 2002). The injection of reclaimed water into the aquifers has been extensively performed in various parts of the world such as Australia (Vanderzalm et al., 2010), Israel (Harpaz, 1971) and the United States (Rauch-Williams et al., 2010). One of the most practical limitations, however, of the application of MAR is aquifer clogging. Physical, chemical and biological factors influence aquifer clogging via trapping of suspended solids, gas entrapment, mineral precipitation and microbial biomass production caused by nutrient addition (Thullner, 2010). The process of bio-clogging caused by growth of microbial biomass (e.g., cell and extracellular polymeric substances (EPS)) in the pores of aquifers leads to reduction of hydraulic conductivity, porosity and pore size. Avnimelech and Nevo, (1964) found a direct relationship between bio-clogging of sand aquifers and growth of exo-polymer. In recent years, further research has been performed on the role of microbial activities on bio-clogging of porous media (Avnimelech and Nevo, 1964). Similarly, Xia et al., (2016) reported severe bioclogging in sand columns inoculated with different bacteria, due to the production of EPS (Xia et al., 2016). In another research, Zhong and Wu, (2013) found a significant reduction in hydraulic conductivity of sand-packed column, especially close to the inlet end, by microbial growth and proliferation (Zhong and Wu, 2013).

Another drawback of MAR is the potential presence of pathogens e.g., bacteria, virus and protozoa in stormwater and treated wastewater, even at low concentrations, which may pose a risk to human health (Costán-Longares et al., 2008) from exposure to the reuse water. However, filtration of surface water through soil and aquifer material may act to remove or inactivate bacterial or viral pathogenic organisms within the groundwater potentially offering an efficient cost effective

method of treatment (Mayotte et al., 2017). The inactivation of virus is the loss of the capability to infect or replicate in a susceptible host, due, mainly, to degradation of protein substances in their capsid. Various factors including, solution pH, ionic strength and composition, temperature, light, and redox conditions and presence of different kinds of organic materials affect virus inactivation (Schijven and Hassanizadeh, 2000). While, in porous media, other mechanisms such as attachment/detachment to/from collector grains, straining and blocking also influence their inactivation (Torkzaban and Bradford, 2016). Previous studies have shown the effect of biofilm on transport behavior of solutes and microorganisms, by decreasing hydraulic conductivity and the creation of preferential flow paths (Seifert and Engesgaard, 2007). However, the majority of research on microorganism transport behavior has been carried out in artificially contaminated aqueous solution and porous media –e.g., clean sand grains and glass beads- which are not reliable representations of authentic aquifer materials and groundwater resources (Torkzaban et al., 2006, Torkzaban et al., 2008b, Chu et al., 2001). Moreover, the transport of virus in a chemically heterogeneous porous medium is not well described. Limestone-based aquifer sediments are more physically (e.g, size, roughness, pores) and chemically (e.g, minerals and metal oxides) heterogeneous than clean sand grains, and potentially have a significant influence on microorganisms transport. The results of transport behavior of microorganisms in clean sand columns cannot be readily extrapolated to a carbonaceous aquifer, emphasizing the importance of conducting studies with authentic aquifer substrates.

In most of the studies on microorganism transport in limestone aquifers, the experiments were conducted over a short time-period, which neglected the role of long-term injection of treated wastewater on porous media structure and consequently microorganisms transport behavior (Sasidharan et al., 2017a). Although a few studies focused on long-term irrigation of aquifers by

treated wastewater (Flynn and Sinreich, 2010), no study has been reported on relationship between bio-clogging, preferential flow paths of porous media and virus transport and retention in aquifers.

The main objective of the research reported here was determining the inactivation behavior of MS2 coliphage in pristine and biofilm-coated natural limestone aquifer sediments irrigated with treated wastewater for 2 and 8 weeks. The effects of short and long-term irrigation of aquifer materials with treated wastewater on the physical, chemical and hydraulic properties of limestone aquifer sediments was also studied.

4.4. Results and discussion

4.4.1. Porous media characteristics

The specific gravity (ρ_s) of limestone sediments and sand grains was 2.55 and 2.68 g/cm^3, respectively. XRD analysis of limestone sediments showed that they contained high quantity of calcite with lesser amounts of quartz and dolomite (Fig 4-1). However, sand grains contained > 99 % quartz with negligible amounts of the other minerals. According to EDS spectrum of sand grains, they contained high amounts of Si and O. In contrast, limestone aquifer materials comprised significant amounts of Ca and O and very low quantities of Si, C and Mg. XRF analysis revealed that limestone sediments consisted of 46.41 % CaO, 9.59 % SiO_2, 2.84 % MgO, 1.63 % Fe_2O_3, 0.41 % Al_2O_3, 0.21 % K_2O, 0.20 % SO_3, 0.07 % Na_2O, 0.03 % MnO, 0.02 P_2O_5 and 38.56 % loss on ignition. The sand grains comprised 98.42 % SiO_2, 0.2 % Fe_2O_3, 0.2 % Al_2O_3, with only 1.55 % loss on ignition. Negligible amounts of the other metal oxides were observed in the sand grains.

The FTIR spectra of sand grains and limestone sediments at different segments in each 1 cm are shown in Fig 4-2. As can be seen in the spectra of sand grains, some sharp peaks were observed at 778 cm^{-1} which is ascribed to Si-O-Si intertetrahedral bridging bonds. Moreover, the peaks in the absorption bands of around 1000-1100 cm^{-1} in sand were ascribed to Si-O stretching (Chen et al., 2014). In the limestone sediments, various peaks in the absorption regions of 1400 cm^{-1} were related to calcite. The presence of quartz in the limestone sediments was marked by a slight peak in the range of 1000 to 1200 cm^{-1}. However, the spectra of limestone sediments did not show any peak at 700 cm^{-1}, the absorption region characteristic of dolomite. This finding was also confirmed by the negligible amount of Mg in limestone materials and lack of Mg in the sediment structure.

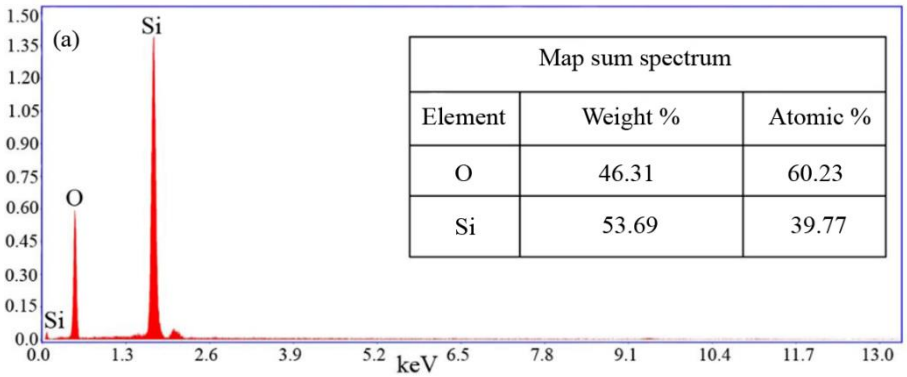

Map sum spectrum		
Element	Weight %	Atomic %
O	46.31	60.23
Si	53.69	39.77

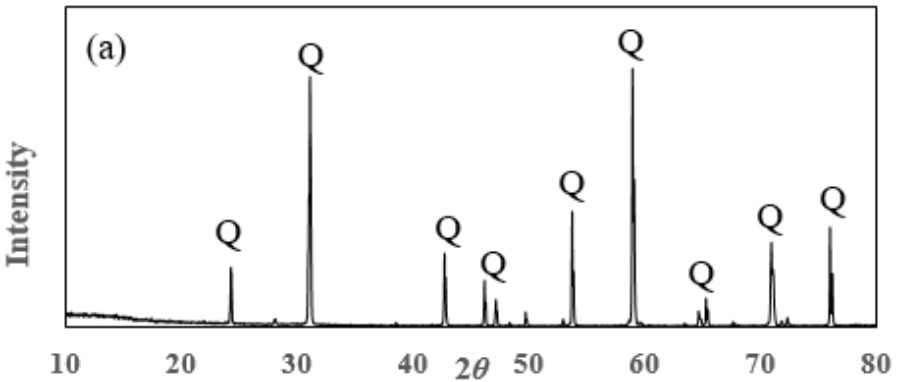

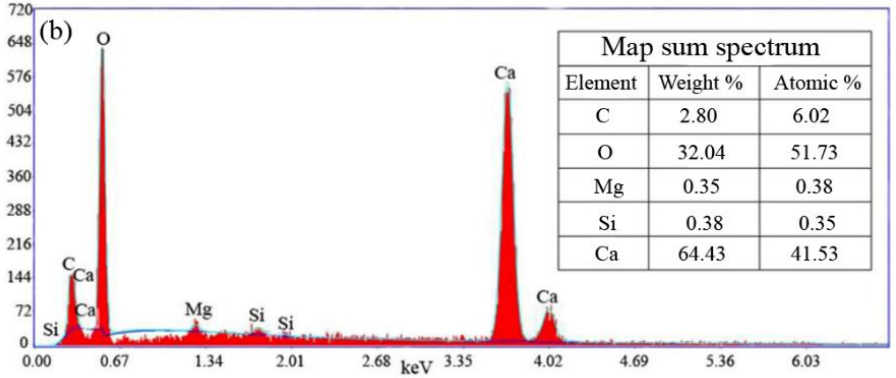

Map sum spectrum		
Element	Weight %	Atomic %
C	2.80	6.02
O	32.04	51.73
Mg	0.35	0.38
Si	0.38	0.35
Ca	64.43	41.53

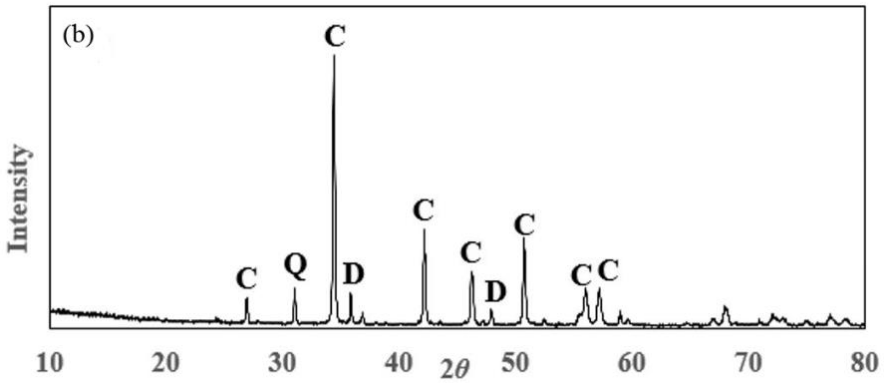

Fig 4-1. EDS spectra (left) and XRD diagrams (right) of sand (a) and limestone aquifer grains (b) (C: calcite, Q: quartz, D: dolomite).

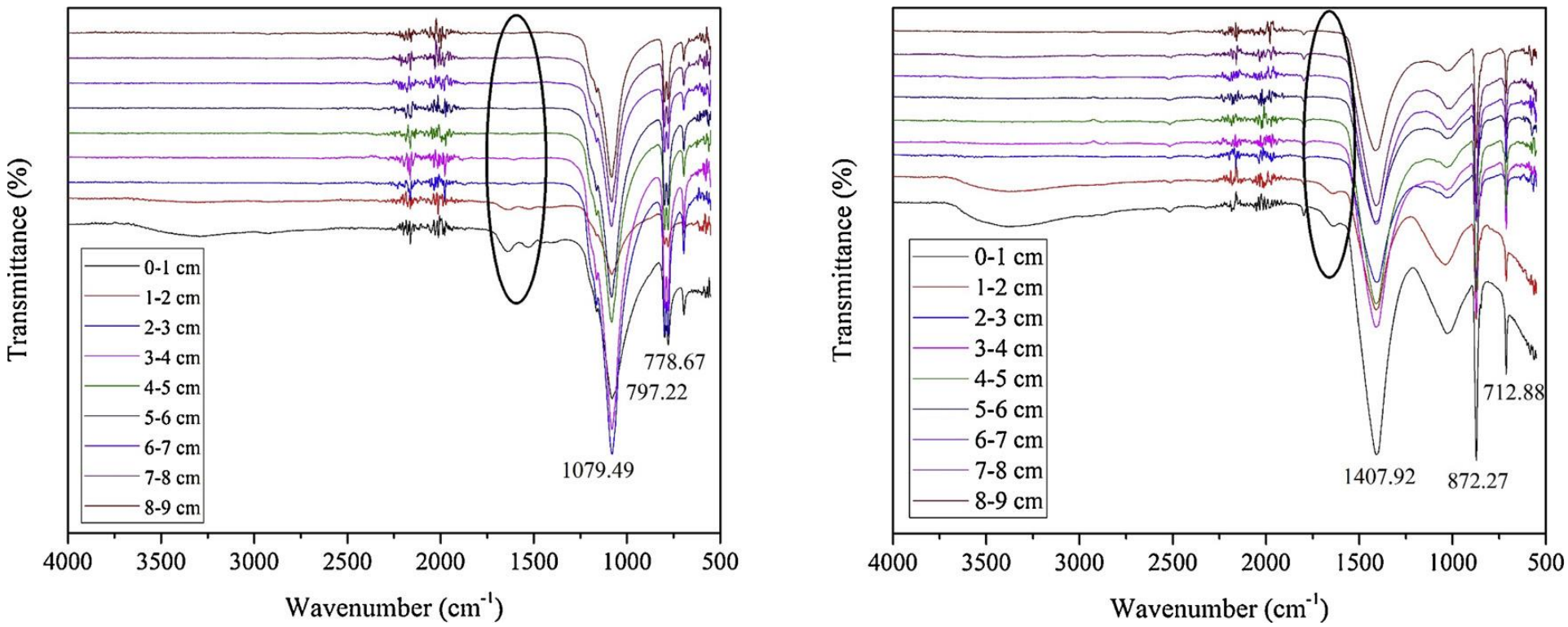

Fig 4-2. FTIR spectra of sand (left) and limestone aquifer grains (right) of different parts of columns irrigated with treated wastewater for 8 week**s.**

4.4.2. Physical, chemical and biological changes in columns

Short (2 weeks) and long-term (8 weeks) irrigation of sand and limestone-packed columns with treated wastewater was performed to develop biofilm onto the surface and interpore of collectors. The chemical and biological characteristics of the treated wastewater applied are reported in Table 4-1. The saturated hydraulic conductivity was measured to determine the effect of wastewater irrigation on physical, chemical and biological pore clogging. The saturated hydraulic conductivity of all columns was measured at the beginning and end of experiments and the results are reported in Fig 4-3 based on C/C_0 ratio. In sand-packed columns, injected with treated wastewater for 2 or 8 weeks, the K_{fin}/K_{ini} values decreased by 38 and 67 %, respectively, which may be due to both physical and biological clogging of interpores. Vandevivere and Baveye, (1992d) in similar research reported that K_s was reduced in sand columns inoculated with *Arthrobacter sp* at 4 mg/g of collectors (Vandevivere and Baveye, 1992d). In contrast, in limestone-packed columns, K_{fin}/K_{ini} value after the 2-week irrigation with wastewater was decreased by 35 %, however, at 8-week treatment an increase was observed in K_{fin}/K_{ini} value, which can be ascribed to the dissolution of calcite in the limestone substrate, due to microbial activities.

To find the role of physical clogging on decreasing K_s of columns, total suspended solids (TSS) and turbidity of influent and effluent samples were measured and the results are reported in Fig 4-3. A considerable decrease occurred in TSS and turbidity of the effluents from both columns after 2 weeks irrigation, likely due to the attachment and entrapment of solids onto the surfaces of collectors. C/C_0 of TSS and turbidity remained constant until 8 weeks. Particles of suspended solids can be attached onto either the inner or outer surfaces of collectors at the inlet end of columns, leading to the considerable reduction in hydraulic conductivity and porosity. Ragusa et al, (1994) showed the significant role of suspended clay particles on hydraulic conductivity with

the application of 5 and 10 g/L of clay resulting 50 % and complete cessation of hydraulic conductivity, respectively (Ragusa et al., 1994).

The quantity of biofilm within the columns is shown in Fig 4-4. The majority of the biomass was produced or accumulated at the inlet end of the columns (0−3 cm), where the concentrations of dissolved oxygen and nutrients were higher. Similar results were reported by Rinck-Pfeiffer et al., (2000) where they observed that the majority of polysaccharide and microbial biomass production was at the inlet end of columns (Rinck-Pfeiffer et al., 2000). Zhong and Wu, (2013) also observed a sudden decrease in total bacteria with increasing distance from inlet end of a sand-packed column (Zhong and Wu, 2013). Vandevivere and Baveye, (1992d) reported an insignificant decline in K_s, when microbial dry weight was less than 4 mg/g, however, an increase in microbial biomass to 10 or 20 mg/g caused one and two order of magnitude decline in K_s, respectively (Vandevivere and Baveye, 1992d). The biofilm in the 2 week irrigation experiments (> 4 mg/g), caused decrease in the K_s of columns. While, since no changes were observed in the amount of TSS and turbidity in 2 and 8-week treatments, it can be postulated that in long-term experiments, the microbial growth and proliferation was the main factor effecting a decrease in saturated hydraulic conductivity of columns.

The columns were sectioned and analyzed using scanning electron microscopy (SEM). The surface and morphological features of sand and limestone grains obtained from columns containing pristine and wastewater irrigated (8 weeks) media are shown in Plate 4-1. A biofilm layer was produced on the formerly sand and limestone particles following irrigation of columns with treated wastewater. Plates 4-2 and 4-3 CLSM images of pristine and biofilm conditioned sand and limestone aquifer material, respectively for 2 and 8 weeks. Accordingly, a very slight fluorescent layer was seen in the CLSM images of pristine sand and limestone grains that can be ascribed to

the low microbial mass in their construction. Moreover, according to CLSM images of biofilm-conditioned sand and limestone grains with treated wastewater for 2 and 8 weeks, a condensed fluorescent layer was observed in biofilm-conditioned substrates which is ascribed to the bonding between ConAAlexa488 and produced biofilm. The FTIR spectra of different layers of sand and limestone grains irrigated with wastewater for 8 weeks, show slight peaks at around 1640 cm^{-1} absorption bands of 0-2 cm layer, which are attributed to protein (Fig 4-2). Similar results have been reported by Cui et al., (2018), who observed a slight peak at 1637 cm^{-1} absorption band related to the protein (Cui et al., 2018).

The changes in TOC concentration of the wastewaters following passage for either 2 or 8 weeks through the sand or limestone columns are shown in Fig 4-5 After 2-week's irrigation, the initial TOC concentration of the wastewater decreased by 59.76 and 69.84 % in sand and limestone columns, respectively; further irrigation for 8 weeks did not substantially increase TOC removal in either the sand (68.44 %) or the limestone column (65.18 %). This is consistent with the removal data for TSS and turbidity through the columns.

The concentrations of total nitrogen (TN), ammonium (NH_4^+-N), nitrate (NO_3^--N) and nitrite (NO_2^--N) in the effluents of all columns are shown in Fig 4-5. After 2 weeks irrigation with treated wastewater, the concentrations of TN decreased by 12.14 and 11.45 % in the effluents from the sand and limestone columns respectively. Furthermore, N-NO_2^- and N-NO_3^- concentrations in the sand column increased by 47.54 and 67.10 %, respectively. Similarly, the N-NO_2^- and NO_3^- concentrations increased by 98.13 and 101.49 %, respectively in the limestone column. The concentrations of N-NH_4^+ in both sand and limestone columns decreased by 37.18 and 56.67 %, respectively. These decreases in both columns were associated with nitrification (Fig 4-5).

Nitrification was greater in limestone than in the sand packed columns likely because of higher alkalinity and pH which can be described by Equations 4-1 & 4-2 below:

$$2NH_4^+ + 3O_2 \rightarrow 2NO_2^- + 4H^+ + 2H_2O \quad (4\text{-}1)$$

$$2NO_2^- + O_2 \rightarrow 2NO_3^- \quad (4\text{-}2)$$

Fig 4-6 shows the variations in pH, alkalinity and Ca^{2+} concentrations in the effluents of sand and limestone-packed columns conditioned for 8 weeks. As Fig 4-6 (a) demonstrates, in sand columns, no significant changes occurred in alkalinity and Ca^{2+} concentrations during irrigation with treated wastewater, while, the solution pH decreased slightly because of nitrification and microbial activity. In contrast, in limestone-packed columns, Ca^{2+} concentrations in the effluents showed an increasing trend over the irrigation period, indicating that calcium dissolution was continuously enhanced until end of experiments (Fig 4-6 b). Furthermore, alkalinity an index of calcite dissolution (Equation 4-3), was consistently increased in the wastewater following passage through the limestone columns.

$$CaCO_3 + CO_2 + H_2O \rightarrow Ca^{2+} + 2HCO_3^- \quad (4\text{-}3)$$

The pH of effluents at the beginning of the experiments was 7.72±0.01, which is in the range for calcite dissolution. However, after 8 weeks irrigation in the limestone column, solution pH was slightly increased to 8.14, although the undeniable index of decreasing pH (i.e., nitrification and microbial oxidation) was observed. However, since nitrification is an acidic process and leads to decreasing solution pH in the close proximity of biological niche, due to the production of hydrogen ions (H^+), the shear forces of water flow can mix it with bulk solution which had a significant role on calcite dissolution and probable preferential paths in limestone column, which is discussed later. Furthermore, microbial respiration of organic carbon produces CO_2 which

caused carbonic acid production and decreases pH leading to calcite dissolution, as shown in Eq (4-4):

$$CH_2O + O_2 \rightarrow CO_2 + H_2O \rightarrow HCO_3^- + H^+ \quad (4\text{-}4)$$

It can be concluded that even though pH values were decreased by microbial oxidation and nitrification processes, calcite dissolution caused a buffering effect on decreasing solution pH in the limestone column.

Table 4-1. Chemical and biological characteristics of treated wastewater from the Mt Barker wastewater treatment plant. Values are mean ± the standard deviation.

Parameter	Value
pH	7.72±0.01
Total nitrogen (mg N/L)	65.41±0.32
Ammonium (mg NH_4-N/L)	47.33±1.23
Nitrate (mg NO_3-N/L)	6.92±0.98
Nitrite(mg NO_2- N/L)	1.90±0.005
Phosphorous (PO_4-P mg/L)	4.92±0.71
TOC (mg/L)	33.57±0.63
Calcium carbonate (mg/L)	98±2
Ca^{2+} (mg/L)	35.01±0.48
Mg^{2+} (mg/L)	12.93±0.01
K^{2+} (mg/L)	19.39±0.01
Na^{+} (mg/L)	88.74±0.69
Turbidity (FTU)	14.66±1.15
TSS (mg/L)	37±3.60
MS2 (Log_{10} PFU/mL)	2.35

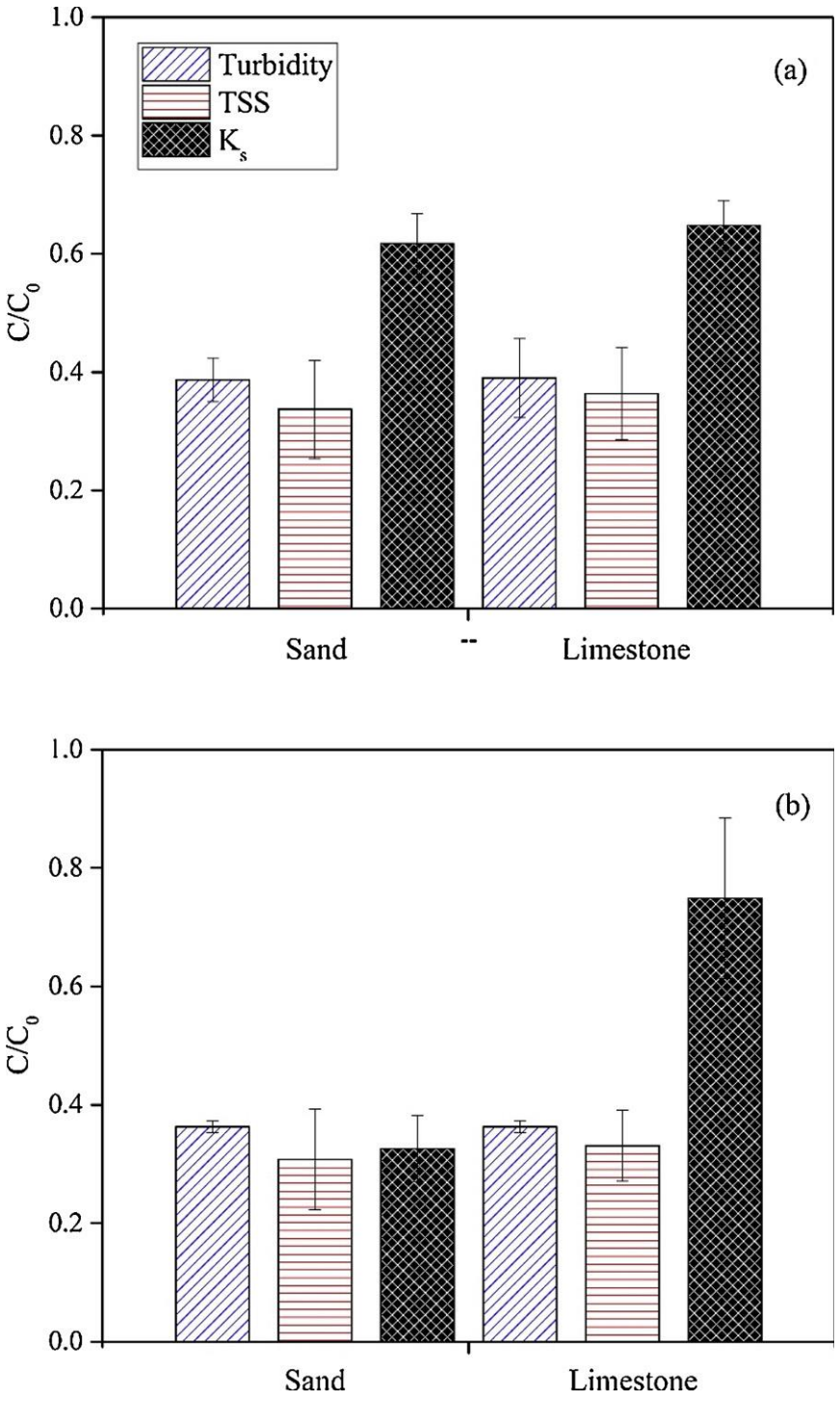

Fig 4-3. Turbidity, total suspended solids (TSS) and saturated hydraulic conductivity of sand and limestone columns after irrigation with treated wastewater for (a) 2 and (b) 8 weeks. Error bars also show the standard deviation (n= 3).

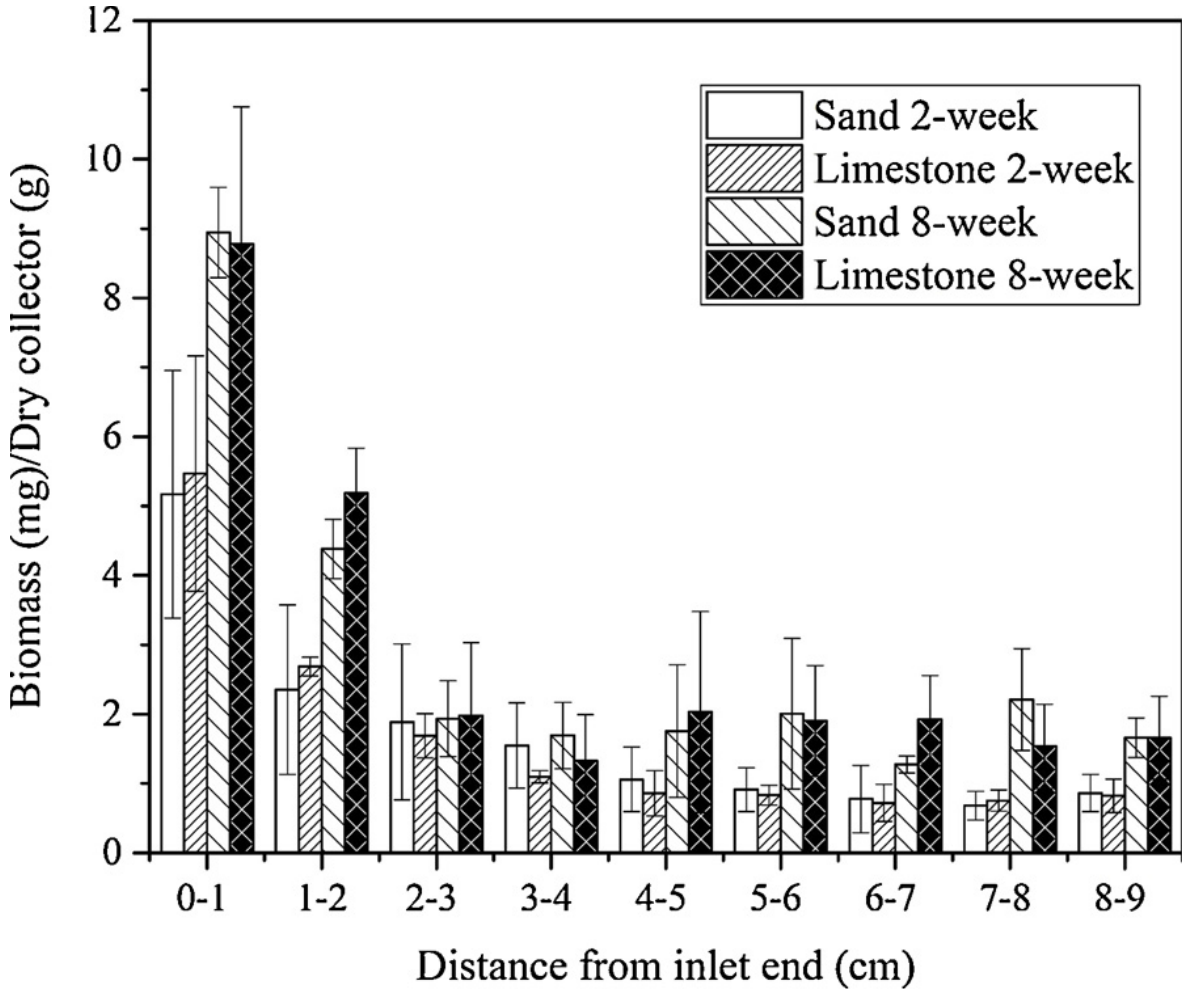

Fig 4-4. Total biomass (mg/g) in sections of the sand and limestone columns after irrigation with treated wastewater for 2 and 8 weeks.

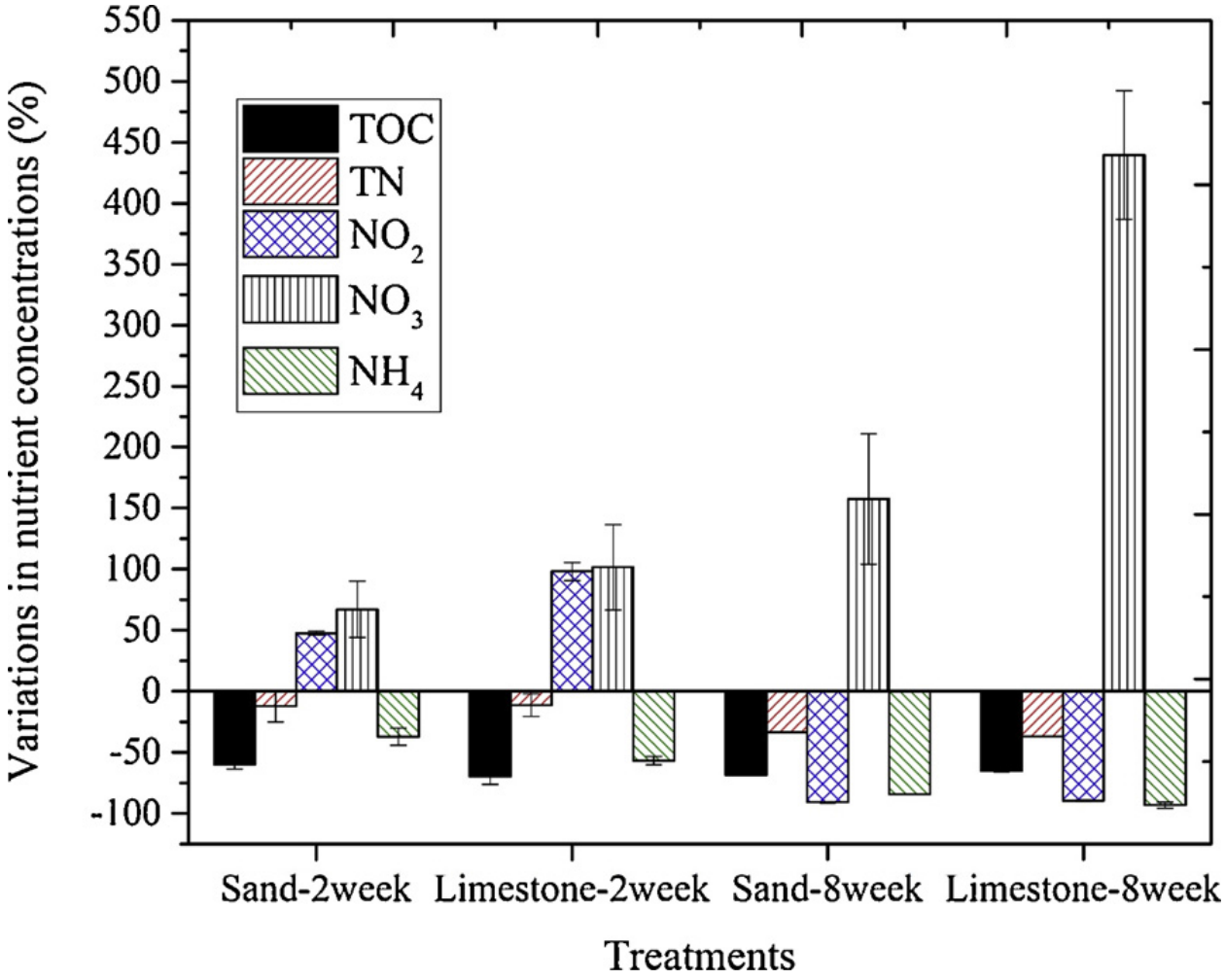

Fig 4-5. Changes in the concentrations of TOC and nitrogen speciation in wastewater following passage through, either sand or limestone columns for 2 and 8 weeks. Error bars also show the standard deviation (n = 3).

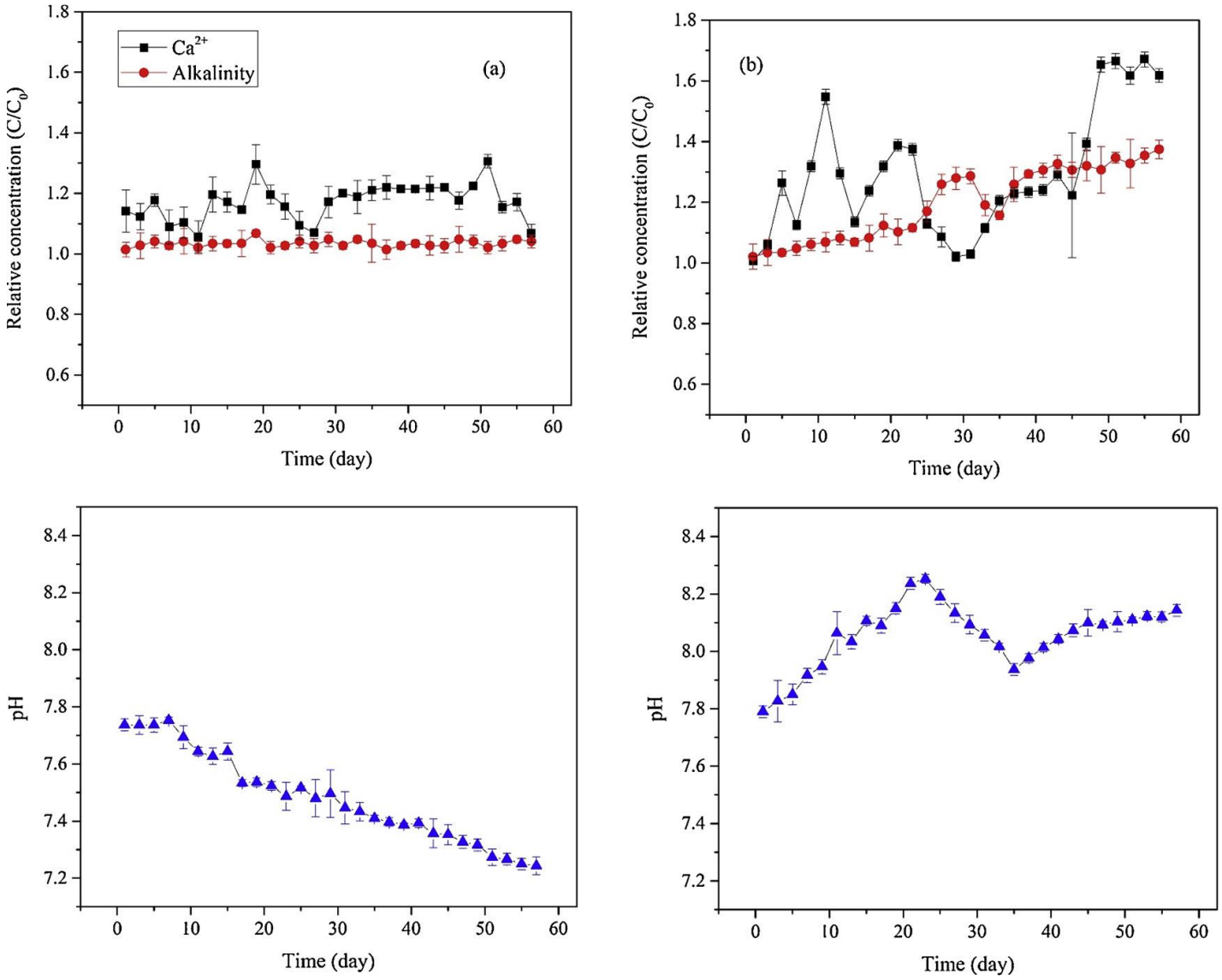

Fig 4-6. Changes in pH, alkalinity and Ca^{2+} concentrations in (a) sand and (b) limestone columns after irrigation with treated wastewater for 8 weeks (circle: alkalinity, square: calcium concentration and triangle: pH of solution). Error bars also show the standard deviation (n = 3).

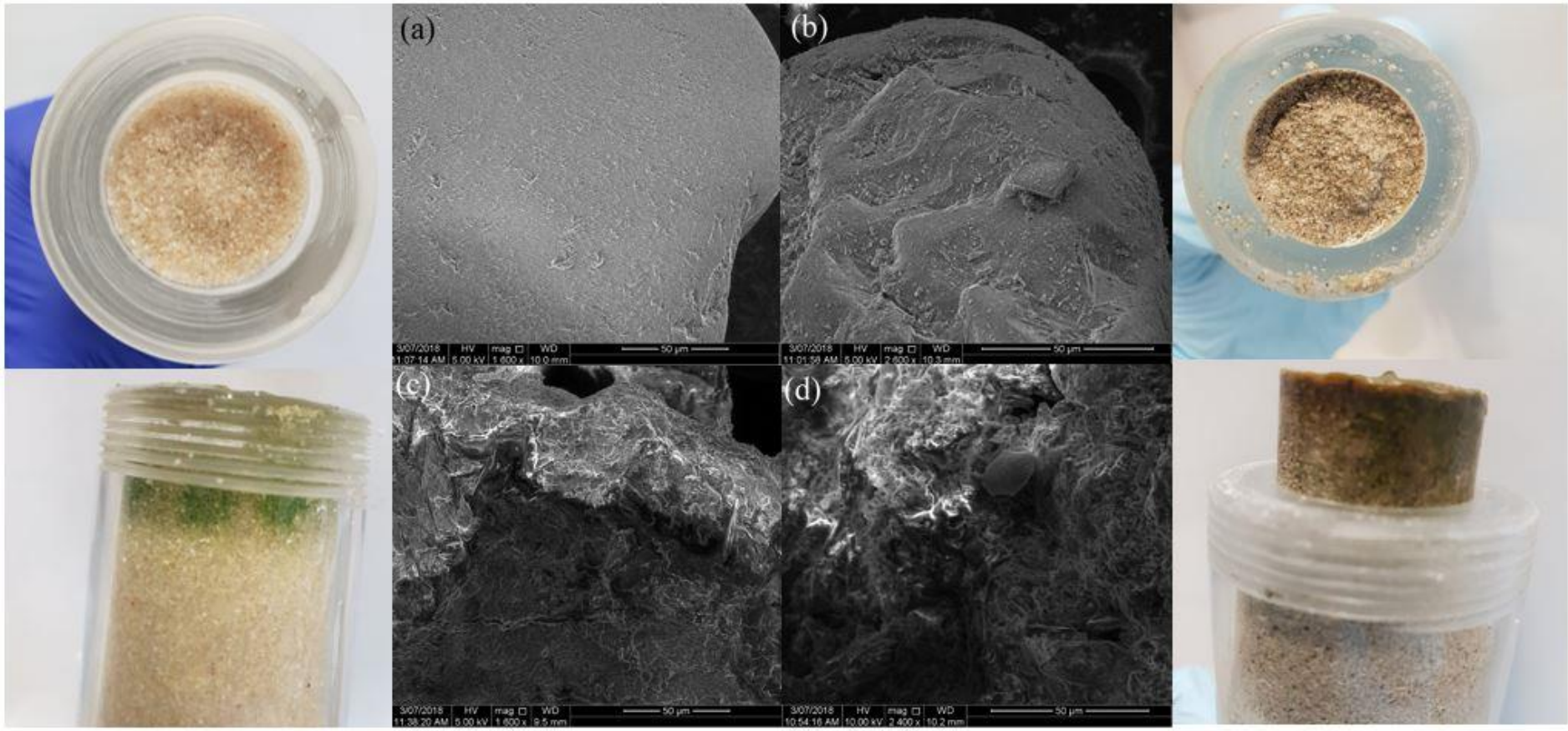

Plate 4-1. SEM images of pristine (a and b) and biofilm-conditioned (c and d) sand (left) and limestone (right) grains obtained from 0-1 cm of columns after irrigation with treated wastewater for 8 weeks.

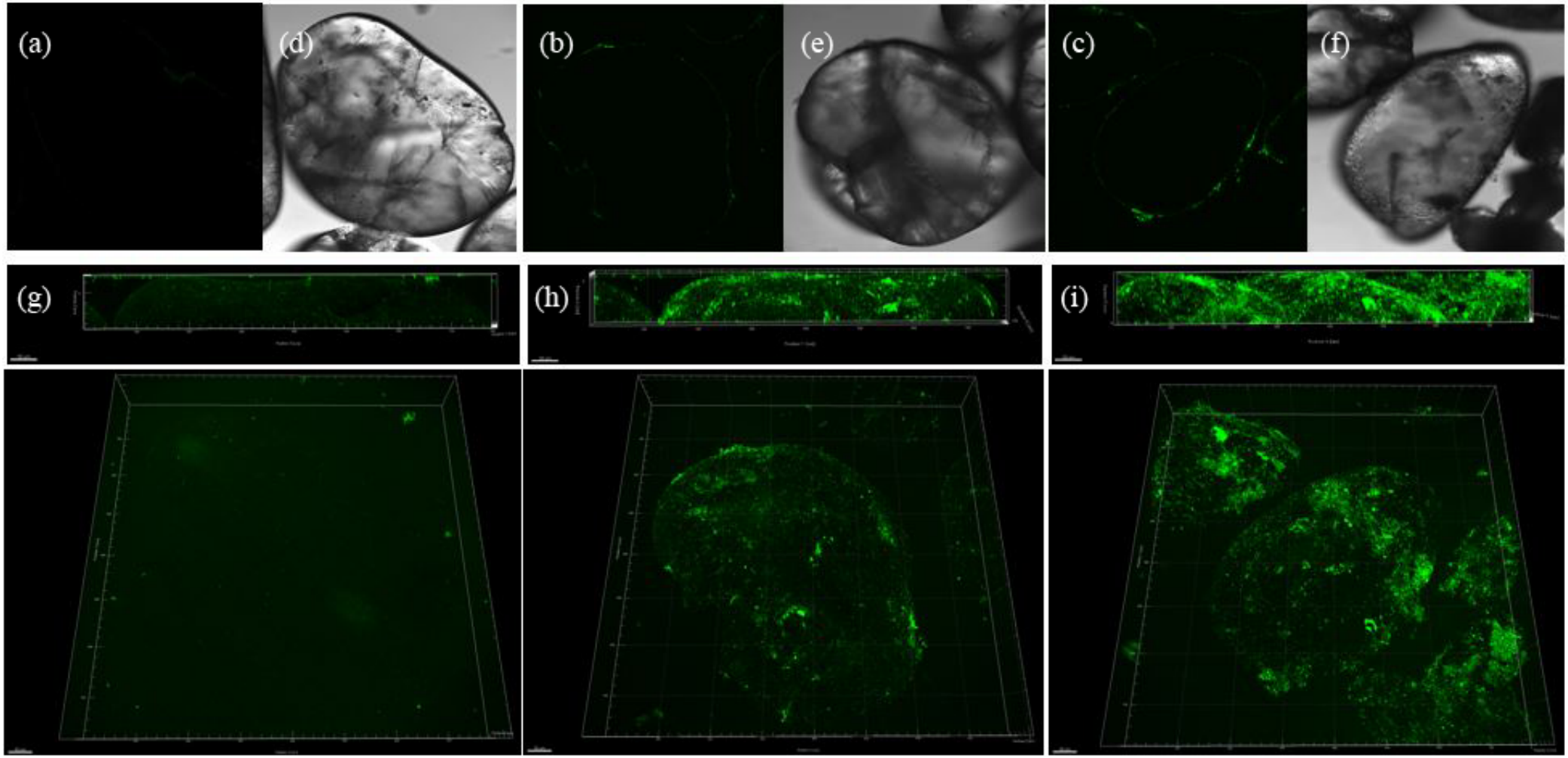

Plate 4-2. CLSM images of (left) pristine, 2week (center) and 8week (right) incubated sand grains obtained from 0−1 cm of columns after irrigation with treated wastewater (a, b and c: confocal slice images through sand grains, d, e and f: transmitted light images of sand grains in a, b and c, respectively, g, h and i: 3D view of confocal z-stack data set in Imaris software).

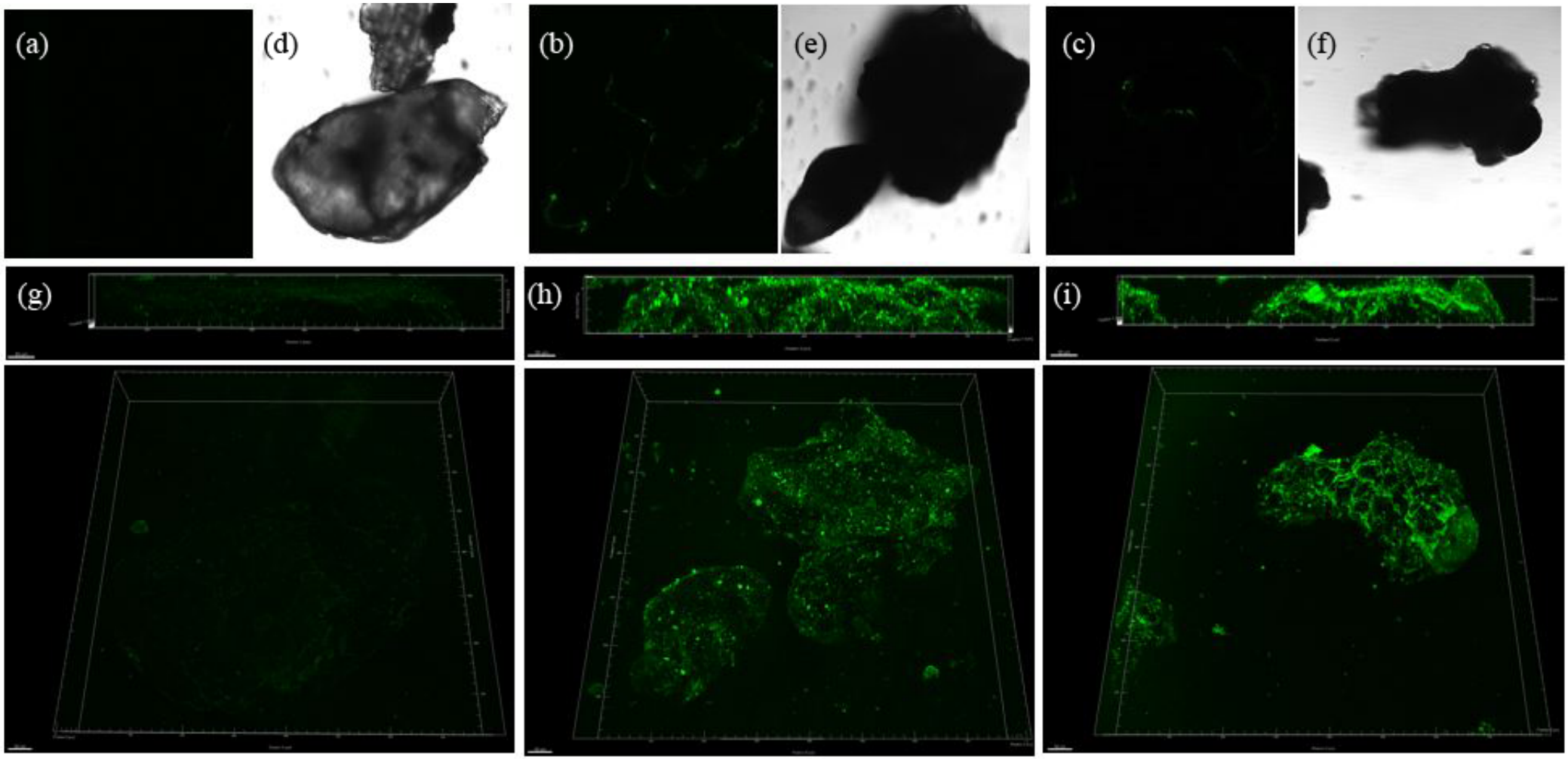

Plate 4-3. CLSM images of (left) pristine, 2week (center) and 8week (right) incubated limestone grains obtained from 0−1 cm of columns after irrigation with treated wastewater (a, b and c: confocal slice images through limestone grains, d, e and f: transmitted light images of limestone grains in a, b and c, respectively, g, h and i: 3D view of confocal z-stack data set in Imaris software).

4.4.3. Transport of tracer

Transport experiments of Br^-, a conservative non-reactive tracer, were performed to determine either presence or absence of preferential flow paths in the columns, due to biofilm growth and related microbial activities. The analytical simulation of Br^- transport was performed using convection-dispersion equation (CDE) model and the results are reported in Table 4-2. Accordingly, high coefficients of determination (R^2) were obtained between measured values and those obtained from application of CDE model, which indicates the accurate characterization of physical features of columns. Although, for heterogeneous porous media, the non-equilibrium model has been previously applied, we selected CDE model for both pristine and biofilm-conditioned columns, because of the simplicity and also for a better comparison between different treatments. The experimental data for Br^- transport were fitted on a mobile-immobile model (MIM) in CXTFIT software. The output showed very unrealistic values of hydrodynamic dispersion, indicating that the MIM was unable to fit the Br^- transport experimental data. Findings of previous studies have shown the ability of CDE model to fit the data relating to tracer transport in preferential flow paths (Zhang et al., 2015b). According to Bejat et al., (2000), ADE would be a very suitable model to study tracer transport in heterogeneous porous media, when fewer fitted parameters are required (Bejat et al., 2000). Fig 4-7 shows the BTCs of Br^- transport in the sand and limestone-packed columns, which were irrigated with treated wastewater in saturated flow conditions at different time intervals. The transport of Br^- was not influenced by chemical sorption, only physical process affected tracer transport. Based on the BTCs of Br^- transport in the pristine column, the symmetric shape of BTC with no tails and C_{max}/C_0 close to 1 reveals lack of any preferential flow paths in sand-packed columns. Furthermore, increasing the injection of treated wastewater for 2 and 8 weeks caused a slightly earlier appearance in BTC of tracer transport, due

to decreasing porosity and saturated hydraulic conductivity via physical and biological clogging. The findings of Seifert and Engesgaard, (2007) also revealed that the biofilm growth in porous media caused the early appearance of tracer in BTCs (Seifert and Engesgaard, 2007). However, the presence of biofilm in sand columns did not cause macropores and physical heterogeneities in the sand columns. Previous studies showed a firm relationship between longitudinal dispersivity (λ) of porous media and saturation status, pore size distribution, pore water velocity and the magnitude of heterogeneity in porous media (Toride et al., 2003). The fitted λ values of sand columns were 0.92, 1.37 and 1.59 (cm) in pristine, columns irrigated with wastewater for 2 and 8 week, respectively. Increasing the amount of biofilm, increased the value of λ. The growth of *Pseudomonas aeruginosa* biofilm in a glass bead-packed column increased λ from 35 to 288 % (Sharp et al., 1999). Biofilm growth also influenced the hydrodynamic dispersion (D). Injection of treated wastewater for 2 and 8 weeks in sand columns, increased D from 0.79 cm^2/min in the pristine column from to 1.27 and 1.67 cm^2/min, respectively Table 4-2,.

CXTFIT optimizes the value of D, or λ. The value of the pore water velocity (ν) depends on the porosity (θ_s), since the water flux density (q), i.e. the application rate, is constant and $\nu = q/\theta_s$. So, if there is microbial clogging then θ_s may decrease. The values in Table 4-2 are obtained by assuming a pre-clogging value of θ_s, assumed constant through the column. If there is clogging then ν would increase and, to have the same BTC, λ values would be lower. If λ is assumed constant through the column, then the shape of the BTC will depend on the mean column porosity, regardless of how porosity is distributed, since at any depth in the column, ν will be inversely related to θ_s, leading to a constant value of D through the column. If we assume that the values of λ are approximately correct and porosity is uniform through the column then the relative values of ν can be used to estimate porosity, since $\theta_s = q/\nu$.

Similar results were also observed for limestone-packed columns, where after 2 weeks irrigation with wastewater, the BTC of Br^- appeared earlier and λ increased from 1.05 to 1.26 (cm). However, in the case of the limestone column irrigated with wastewater for 8 weeks, a sharp increase was observed in the value of λ (5.92 cm). In these columns the value of λ in limestone-packed column was higher than sand-packed one. Indeed, BTC of Br^- commenced at 0.5 PV and showed an asymmetric shape which is a good index for creation of either preferential paths or heterogeneity in column (Fig 4-7). In contrast to previous studies on preferential transport of tracers, a long tail was not observed in the BTC of Br^-, which shows that a macropore was not produced in the limestone column (Koestel and Jorda, 2014). Zhong and Wu, (2013) reported preferential flow paths in sand-packed columns after irrigation with treated wastewater, however in our study, we did not observe early raising and long tails in the BTCs of Br^- in wastewater irrigated sand columns (Zhong and Wu, 2013). In limestone columns, Ca^{2+} dissolution, which resulted from the microbial activities including nitrification, led to the heterogeneities in the column that accelerated transport of Br^-. In a similar research, Wang et al., (2013b) attributed fast movement of Br^- to the creation of artificial macro-pores, which led to the enhancement of tracer transport (Wang et al., 2013b). Advection and dispersion are the two most effective mechanisms of solute transport, which can be distinguished by the Peclet number (P_e). In the case of sand columns and longer irrigation time, lower P_e values were obtained, which shows that the production of biofilm increased the role of diffusion rather than advection in tracer transport, due to the enhanced heterogeneities in the column. The value of P_e in the pristine sand column decreased from 9.76 to 6.53 and 5.65 following irrigation with treated wastewater for 2 and 8 weeks, respectively. In limestone columns, irrigated for 8 weeks, the decrease in P_e value was greater than in the sand columns, which suggests either the creation of preferential flow paths or higher heterogeneity.

Table 4-2. Fitted parameters for Br^- transport using convection-dispersion model in; pristine sand and limestone columns (control) and columns irrigated for 2 or 8 weeks with Mt Barker treated wastewater, where, ρ_b bulk density, D hydrodynamic dispersion, λ dispersivity and P_e Peclect number.

Treatment		*Tracer recovery (%)*	*D (cm^2/min)*	*λ* (cm)	*P_e* (-)	*R^2*	*MSE*
Sand	**Pristine**	92.20	0.79	0.92	9.76	0.96	0.006
	2 week	94.73	1.27	1.37	6.53	0.98	0.004
	8 week	96.14	1.67	1.59	5.65	0.99	0.002
Limestone	**Pristine**	91.12	0.86	1.05	8.59	0.96	0.007
	2 week	94.30	1.21	1.26	7.11	0.98	0.003
	8 week	95.06	8.80	5.92	1.51	0.99	0.002

Table 4-3. Zeta potentials of sand and limestone particles in conditioned treated wastewater at different time periods.

Sample	Conditioning period (day)					
	Control		14		56	
	pH	Zeta potential (mV)	pH	Zeta potential (mV)	pH	Zeta potential (mV)
MS2	7.71	-29.7±0.6	-	-	-	-
Sand	7.71	-44±6.5	7.62	-37.3±4.0	7.24	-21.46±0.2
Limestone	7.71	-16.5±0.4	8.09	-11.26±0.4	8.14	-7.32±0.8

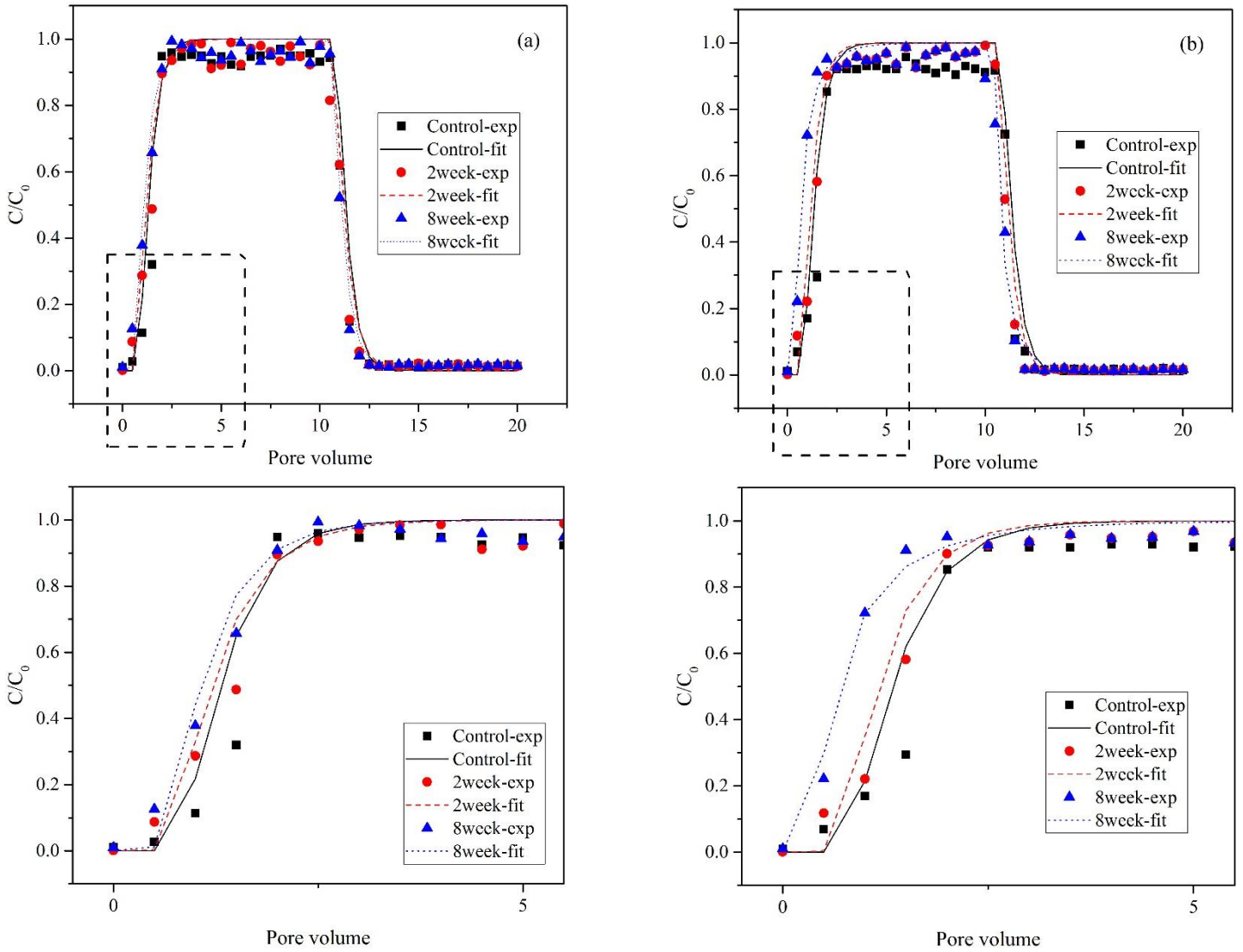

Fig 4-7. Breakthrough curves of Br- transport in (a) sand and (b) limestone columns after flushing with 20 pore volumes (up) and 5 pore volumes (down) of tracer and background solution (square: pristine, circle: 2-week and triangle: 8-week irrigated with treated wastewater experimental data. Solid line: pristine, dashed line: 2-week and dotted line: 8-week irrigated with treated wastewater fitted data).

4.4.5. Transport of MS2

Upon completion of the tracer measurements, MS2 transport experiments were performed in the same columns. Fig 4-8 shows BTCs of MS2 transport in sand (a) and limestone (b) columns, based on relative concentration of MS2 (C/C_0) against pore volumes (PVs). Figure 8 showing MS2 transport is divided into four phases. Phase I was the raising step, when C/C_0 attained the maximum value. Phase II shows decreasing C/C_0 of virus, which was derived from their flushing by background (MS2-free) solution. Phase III and Phase IV show results of detachment of MS2 from columns using RO water and 3 % beef extract solution, respectively. The peak of the graphs (Phases I and II) shows the removal rate of MS2, which is determined by inactivation by attachment onto the collector surfaces and environmental factors. In fact, the higher the peak, the lower the MS2 removal rate. Based on the figure for sand and limestone-packed columns, between 1 and 5 MS2 log removal rates were observed, indicating the high attachment of MS2 onto the surfaces of collectors (Fig 4-9). According to the BTCs of the pristine treatment, the log removal of MS2 in sand and limestone columns were 0.59 and 1.30, respectively. However, after injection of treated wastewater for two weeks, log removal in sand and limestone columns increased to 2.71 and 4.84, respectively. This phenomenon can be ascribed to the high physical and biological clogging of these treatments, compared to the pristine ones, due to microbial activities and suspended solid materials deposition, causing a significant decrease in K_s and porosity that enhanced MS2 retention in porous media. Furthermore, the increase in various cation concentrations (especially Ca^{2+}) in the wastewater irrigated limestone columns, caused a greater increase in virus attachment to limestone collectors than to sand grains. An increase in ionic strength of solution can lead to further virus attachment to solid surfaces due to charge screening and the binding of Ca^{2+} onto anionic groups of MS2 surfaces (Sasidharan et al., 2014). Jiang et al.,

(2012) observed a significant retention in ZnO nanoparticles by increasing Ca^{2+} concentration from 0.1-1 mM. In addition, the increased virus attachment onto the limestone compared with the sand grains surfaces is due to the presence of different metal oxides (e.g., CaO, MgO, Al_2O_3, Fe_2O_3) in the structure of the aquifer substrates, which caused charge heterogeneities (Jiang et al., 2012). In some cases, the distribution of negative and positive charges on collector surfaces leads to the enhancement of virus attachment by one order of magnitude when compared to collectors without charge heterogeneities (Schijven and Hassanizadeh, 2000). As mentioned in the previous section, increasing microbial activities not only changed pore geometry, but also caused growth of biofilm onto the surfaces of collectors that led to higher MS2 retention, through trapping into the surface roughness. In general, the importance of microorganism's attachment and straining in porous media depends on colloidal particle characteristics, surface features and size distribution of collector grains, ionic strength of solution and hydrodynamic conditions (Bradford and Torkzaban, 2013).

In addition to surface attachment, straining is another effective mechanism of virus retention in porous media, which is defined as trapping of particles into the pores between collectors (McDowell-Boyer et al., 1986). The collector and colloid features determine the intensity of colloidal particle straining (Bradford et al., 2013). Natural porous media like soil profiles generally contain different particles with various diameters from nanometer to micrometer. However, in this experiment, the collectors were in the range of 0.25 to 0.50 mm, which reduced the possibility of MS2 straining. Generally, when the ratio of particles to collectors is higher than 0.002, the role of straining on particle retention would be significant (Bradford et al., 2003). In this study, since the ratio of MS2 to collectors (25 nm diameter) is around 0.00016, straining was not significant mechanism on MS2 trapping in the columns.

Fig 4-9 represents the log removal rates of MS2 at sand and limestone columns either pristine or irrigated with treated wastewater for 2 and 8 weeks. Accordingly, in sand columns, higher virus retention was observed in 8-week treatment (4 log removal), in comparison with pristine and 2-week treatments, due to enhanced biological clogging by microbial growth and proliferation. Several research papers have reported colloidal particle retention in biofilm-coated porous media (Jian-Zhou et al., 2015, Lerner et al., 2012, Tong et al., 2010). In fact, biofilm production can alter surface features of porous media grains by creating irregularities and surface roughness, which improve particle deposition in unfavorable conditions through production of low flow velocity regions (Vaidyanathan and Tien, 1988). Furthermore, based on Table 4-3, the zeta potentials of biofilm coated-sand and limestone grains were less negative than pristine materials, which may lead to a decrease in the electrostatic double layer (EDL) between porous media grains and negatively-charged MS2. Results of Tripathi et al., (2011) showed that by increasing aging biofilm on the surfaces of sand grains, the values of zeta potentials became less negative (Tripathi et al., 2011). In addition, for limestone treatments, the intensity of increasing zeta potentials was higher than sand particles, due to the dissolution of divalent cations in the solution.

However, unlike the sand column, after long-term irrigation of the limestone-packed column with treated wastewater, the removal rate of MS2 was lower than for the 2-week treatment. According to Fig 4-9, a lower MS2 removal rate (1.79) was observed in 8-week, compared to 2-week treatment (4.84), which can be ascribed to the calcite dissolution, producing physical heterogeneities in the column and accelerated MS2 transport. However, the removal rate of MS2 in the 8-week treatment was higher than in the pristine one, due to the production of biofilm in the column that caused MS2 removal by surface attachment and physical straining.

In addition, after the end of the transport tests, the potential of MS2 detachment from sand and limestone grains was evaluated using injection of 10 PVs RO water (Fig 4-8, Phase III) followed by 10 PVs 3 % Beef extract solution (Fig 4-8, Phase IV). The detachment behavior of viruses in natural systems is of great importance; heavy rain can decrease the ionic strength of porous media (e.g., soil and aquifer) and result in remobilization of virus particles. Therefore, viruses can remain viable for a long-time period, their infection should be considered after remobilization of infectious attached viruses (de Roda Husman et al., 2009). In general, a significant difference between peak and tail-end of BTCs shows the irreversible attachment of virus particles. In all experiments, a long tail was observed which shows the virus detachment. However, the height of tail shows the intensity of virus detachment from collectors, in which the lower tail shows lower detachment. Furthermore, the slope of the tail shows virus inactivation, which is higher with steeper slope. Results of the retained and released MS2 in Phases I, II, III and IV are reported in Table 4-4. Accordingly, in all columns, very small amounts of MS2 were detached from porous media grains, which indicated the generally irreversible attachment of virus onto the collector surfaces. Similar results have been reported by Sasidharan et al., (2017a) who observed very low detachment of several bacteriophages (e.g., MS2, PRD1 and φX174) from aquifer sediments, which was attributed to the irreversible attachment of virus onto the collectors (Sasidharan et al., 2017a). Furthermore, the slope of the tail was similar for all experimental conditions, indicating an insignificant effect of ionic strength of solution on inactivation of attached particles. Sadeghi et al., (2011) reported that the inactivation of attached PRD1 bacteriophage was not significantly affected by pH and ionic strength of solution (Sadeghi et al., 2011). However, different experimental conditions represented different virus detachment behaviors. In fact, in pristine and short-term experiments, the values of M_{irr} in limestone were relatively higher than sand packed

columns, which shows the higher attachment of virus to limestone than to sand surfaces. Furthermore, in case of sand columns, by increasing the injection of treated wastewater and consequently biofilm production, fewer MS2 were detached from collectors, implying the significant role of biofilm on irreversible attachment of MS2. Indeed, the amounts of M_{irr} that were obtained 75.583 and 99.989 % in pristine and long irrigation columns, respectively. But, for limestone columns, a completely different trend was observed. Short-term injection of treated wastewater caused an increase in M_{irr} from 95.41 to 99.999 %, compared to the pristine column. While, further increase in injection of treated wastewater for 56 days, decreased M_{irr} to 98.568 %. A slight increase in M_{irr} in the short-term treatment compared to the pristine, would be due to the role of biofilm in improvement of MS2 attachment. While, decreasing M_{irr} in long-term column was due to the presence of macropores and preferential flow paths, which increased detachment and releasing MS2 from the column.

Table 4-4. Mass balance information for MS2 attachment and detachment behavior in columns irrigated by treated wastewater for 2 and 8 weeks (M_{eff}: eluted virus, M_s: retained virus, M_{irr}: 100-M_{eff}-M_{III}-M_{IV}, M_{III}: detached virus by RO water and M_{IV}: detached virus by 3% Beef extract solution.

Treatment		***Retention (%)***			***Release (%)***	
		M_{eff}	M_s	M_{irr}	M_{III}	M_{IV}
Sand	**Pristine**	24.08	75.92	75.547	0.184	0.189
	2 week	0.195	99.805	99.803	0.001	0.001
	8 week	0.011	99.989	99.989	0.000	0.000
Limestone	**Pristine**	4.57	95.43	95.41	0.010	0.010
	2 week	0.001	99.999	99.999	0.000	0.000
	8 week	1.43	98.570	98.568	0.001	0.001

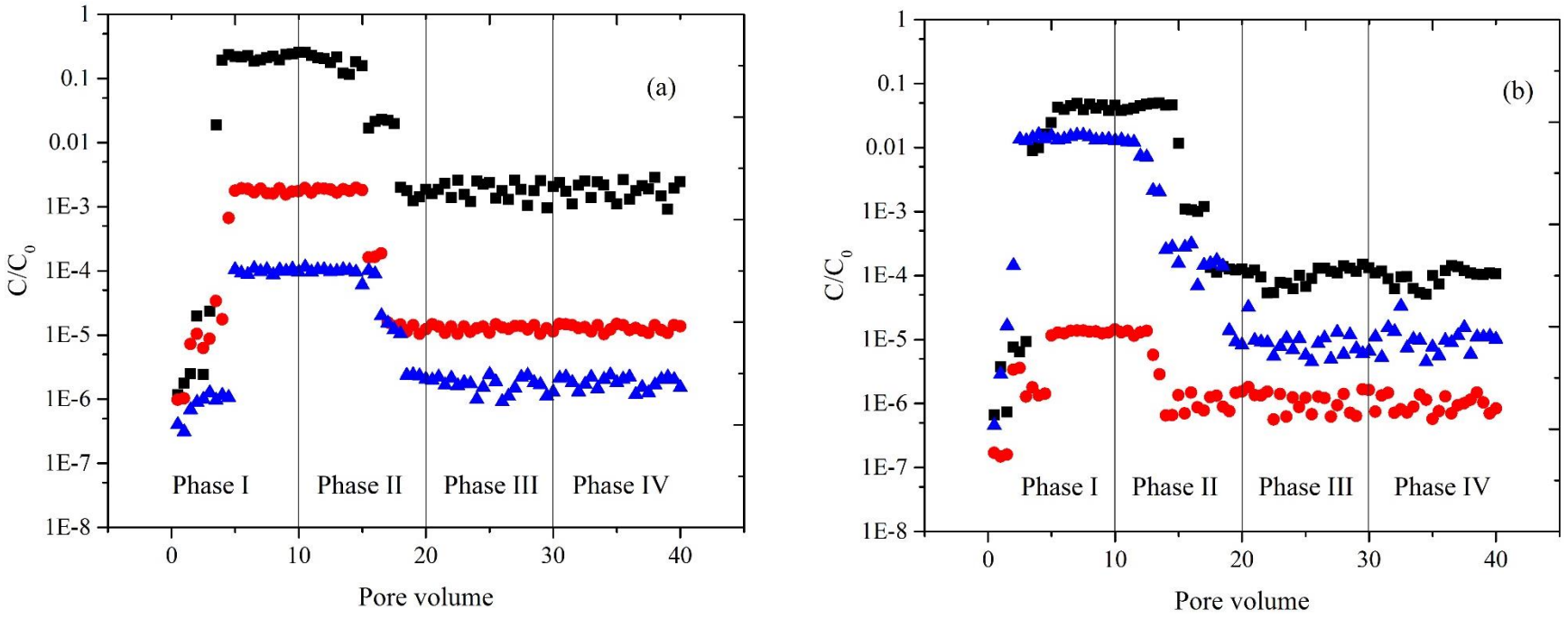

Fig 4-8. Breakthrough curves of MS2 transport in (a) sand and (b) limestone columns (square: control, circle: 2-week and triangle: 8-week irrigated with treated wastewater experimental data).

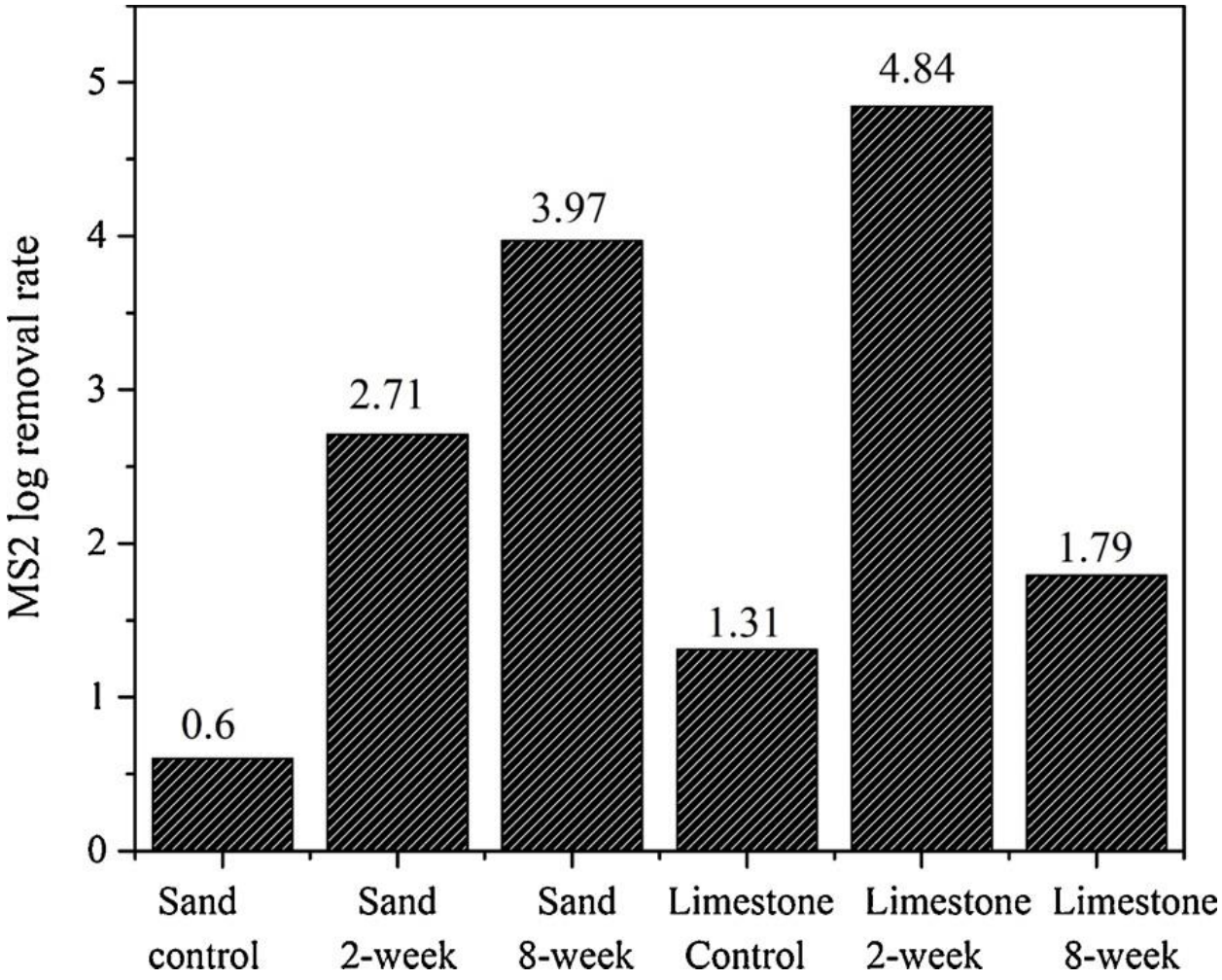

Fig 4-9. MS2 log removal rates in pristine and biofilm-conditioned sand and limestone columns irrigated with treated wastewater for 2 and 8 weeks.

4.5. Conclusion

In this study, we investigated the effect of short and long-term irrigation of limestone and sand-packed columns with treated wastewater on column clogging and also transport behavior of Br^- and MS2 in these columns. Application of treated wastewater caused severe physical and biological clogging in both sand and limestone columns, which were confirmed by findings of state-of-art analyses (SEM and CLSM images). Results indicated continuous K_s reduction in sand columns, while K_s of limestone columns decreased in the first two weeks of the experiment, which was followed by a slight increase until the end of the experiments, due to calcite dissolution by microbial activities. Moreover, findings of tracer transports indicated increasing heterogeneities in both sand and limestone columns, due to the growth and proliferation of biofilm. In addition, in short-term irrigation application, higher MS2 removal was observed in limestone than in sand columns, because of calcite dissolution and presence of various mono and divalent cations in the solution. Biofilms developed in sandy aquifers, as a consequence of nutrient enrichment from the addition of wastewater, entraped microorganisms impeding transport through the aquifer. However, the long-term application of treated wastewater in limestone aquifers has more risk than in sandy aquifers, due to the role of preferential flow in enhancing transport of pathogenic agents through the aquifer to the point of abstraction for above ground irrigation.

In this chapter, the effect of biofilm growth and proliferation on hydrological features of porous media and retention behavior of virus was studied. Regarding lack of studies on the relationship between physical, chemical and biological clogging of column and virus transport behavior, the findings of this study took a bridging gap. Previous studies just focused on individual effect of application of treated wastewater or synthetic solution on either clogging of porous media or transport behavior of colloidal particles. But, this chapter shares unique information about the

potential of danger for human infection by pathogenic agents thereby application of reused water in calcareous MAR sites via preferential flow paths caused by microbial activities. In addition, the dominant mechanisms of virus in the columns conditioned by biofilm with different ages were presented. However, in recent years, groundwater contamination with engineered nanoparticles, due to the widespread application of nanomaterials, has drawn the attention of environmentalists. So, the study of interaction between native aquifer materials and engineered nanoparticles in different physicochemical conditions is of great importance. Little is known regarding the role of biofilm on changing the surface properties and porosity of media and its effect on GONPs transport and retention. The following chapter presents results of research on transport and retention of GONPs in pristine and biofilm-conditioned porous media.

5. Transport and retention of graphene oxide nanoparticles in sandy and carbonaceous aquifer sediments: Effect of physicochemical factors and natural biofilm

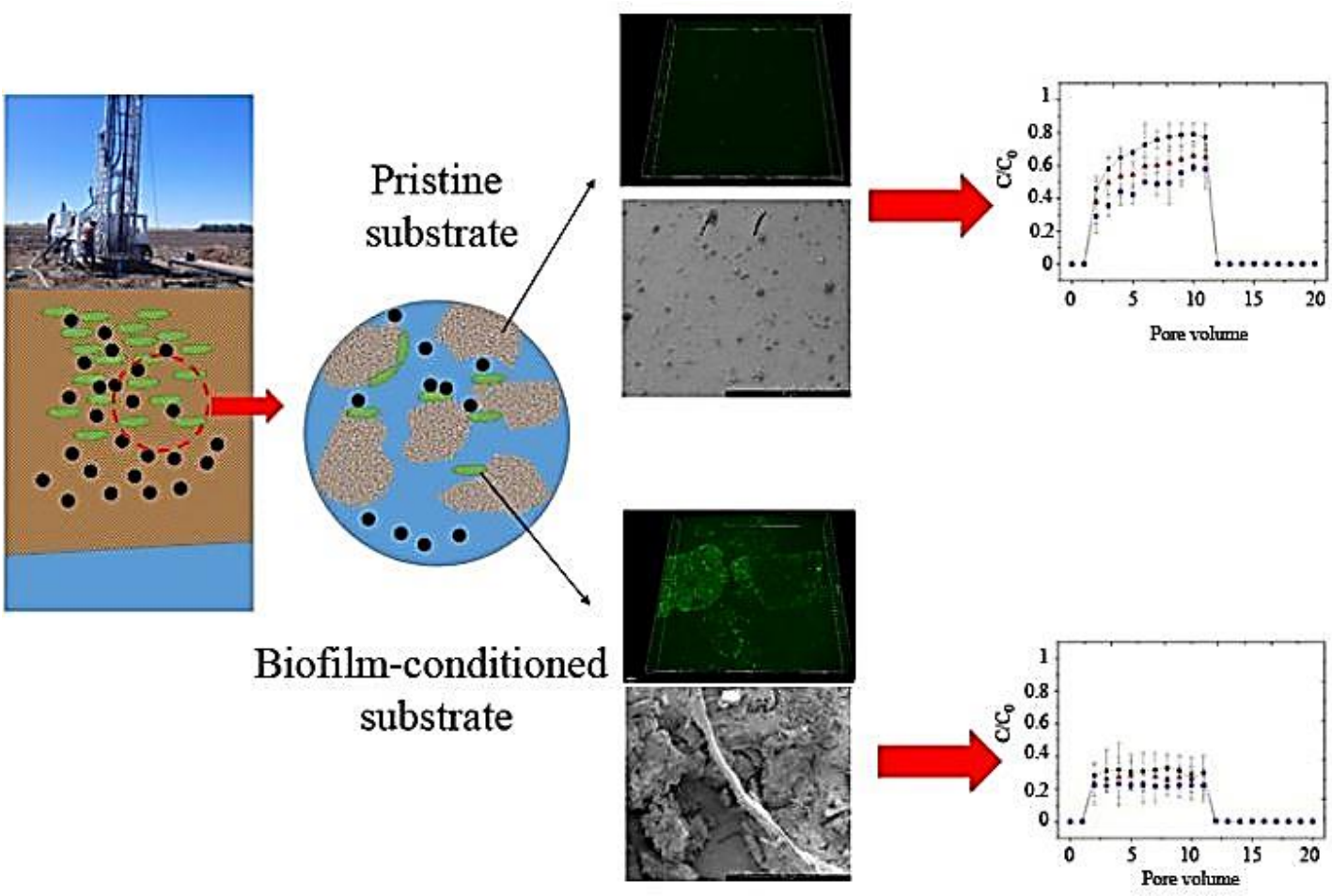

Graphical abstract

5.1. Highlights

- Presence of metal oxides in the structure of sediments had a significant influence on attachment and transport and retention behavior of GONPs in porous media.
- Higher temperature caused an enhancement in attachment of GONPs onto the surfaces of collectors and also retention in saturated porous media.
- The presence of natural biofilm in porous media led to the enhanced retention of GONPs near inlet end of columns.

This Chapter is based on the following publication: Amirhosein Ramazanpour Esfahani, Okke Batelaan, John L. Hutson and Howard J. Fallowfield. Transport and retention of graphene oxide nanoparticles in sandy and carbonaceous aquifer sediments: Effect of physicochemical factors and natural biofilm. Journal of Environmental Management (Under review).

5.2. Abstract

The study of transport and retention of graphene oxide nanoparticles (GONPs) has increased as GONPs find more applications. This study focused on the effect of different porous media (sand grains, quartz sediments and limestone sediments) with various mineralogical features on batch sorption and transport and retention behavior of GONPs at different temperatures, ionic strength and compositions. Furthermore, parallel transport experiments were carried out to determine the role of natural biofilm on the retention of nanoparticles in porous media. The retention rate of GONPs at 22°C was higher than at 4°C. Furthermore, increasing ionic strength favored GONPs retention onto the surfaces of collectors. The presence of Ca^{2+} in the solution had more impact than Na^{+} on GONPs retention in porous media. The retention profiles (RPs) of GONPs in pristine porous media at low ionic strength were linear, which contrasted with hyper-exponential shape of RPs at high ionic strength. The results showed that higher GONPs retention rate was observed in natural porous media than in sand, due to the presence of metal oxides heterogeneities. The presence of biofilm on porous media increased the retention rate of GONPs when compared to the pristine material. The size-distribution analysis of retained GONPs showed decreasing particle diameter with increasing distance from column inlet at high ionic strength and equal diameter at low ionic strength conditions.

5.3. Introduction

In recent years, nanotechnology which considers specific physicochemical features of surface areas of engineered nanoparticles (ENPs) has grown rapidly. Although ENPs offer new opportunities, their high toxicity and persistence in the environment is cause for concern (Gerber et al., 2013, Kreyling et al., 2006). Graphene oxide (GO) is a graphene-based nanomaterial, increasingly used in a wide range of industries (Salas et al., 2010), with high solubility in water. The production and use of GO has led to its abundance in groundwater resources, which causes detrimental effects on humans, aquatics organisms and bacterial cells (Akhavan and Ghaderi, 2010, Chang et al., 2011). Therefore, to determine the potential risk and detrimental environmental effects of GONPs, knowledge about their transport and retention behavior in porous media, effective physicochemical factors and mechanisms is a critical necessity.

Currently, numerous studies have been performed to determine the influence of different physicochemical factors such as initial nanoparticle concentration (Sun et al., 2015), ionic strength and composition (Qi et al., 2014c), temperature (Wang et al., 2017b) and collector grain sizes and heterogeneities (Chen et al., 2018, Dong et al., 2016) on transport behavior of GONPs in porous media. However, the influence of other factors such as physical and chemical heterogeneities and surface properties of porous media require elucidation. The ability of nanoparticles to pass through porous media grains with different mineralogical features has been shown (Neukum et al., 2014, Adrian et al., 2018, Makselon et al., 2017, Esfahani et al., 2014). The majority of the previous studies on transport and retention of GO nanoparticles, however, have been carried out in sand grains and natural soil, which is not the representative of natural material present in complex aquifers (Fan et al., 2015, Sun et al., 2015, Qi et al., 2014b).

Population growth, expanding urbanization and climate change, increase demand on drinking water resources, which leads to depletion of groundwater resources. To date, a wide number of methods have been applied for compensation of groundwater shortage, in which managed aquifer recharge (MAR), which is defined as injection of low quality water resources into the aquifers has been proposed as a promising approach (Ayuso-Gabella et al., 2011). However, the source input water such as stormwater and treated wastewater in MAR sites may contain high volumes of pathogenic agents or engineered nanoparticles which may potentially threaten the groundwater resources. Aquifers consist of different sedimentary materials such as quartz, dolomite, and carbonate. Carbonates (e.g., calcite and dolomite) are the most important sinks for storing drinking water resources. Therefore, more attention is needed on the transport behavior of GONPs in limestone aquifer materials. The surface properties of aquifer materials are potential factors that control fate and transport of nanoparticles. Most of previous research on nanoparticle transport have been carried out in simple and clean porous media with smooth and regular surfaces. However, there are some efforts on making more chemical complexity on porous media surfaces. Qi et al., (2019) coated sand grains with different types of iron oxide to find the role of chemical heterogeneities on GONPs retention behavior (Qi et al., 2019). A typical aquifer material contains various types of complex metal oxides, which likely have a significant effect on nanoparticle retention. Consequently, in the study presented here, we collected authentic carbonaceous and quartz materials from two sites within an aquifer extensively used for MAR schemes to determine the influence of their chemical and physical complexity on the transport behavior and mechanisms of GONPs retention in porous media.

In recent years, there has been a widespread interest in study of transport and deposition of nanoparticles in biofilm-conditioned porous media. Most studies reported the enhanced retention

of nanoparticles in porous media conditioned with biofilm. However, in almost all experiments, a synthetic biofilm was produced by a specific bacteria such as *Pseudomonas aeruginosa* (Basnet et al., 2016), *Bacillus subtilis and Pseudomonas putida* (He et al., 2017). In a typical aquifer, however, there is a diverse range of microorganisms capable of creating a biofilm with varied characteristics on the media grains. In the present study, we used a natural biofilm produced by treated wastewater from Mount Barker, South Australia to determine its effect on attachment and detachment of GONPs in natural porous media. Finally, the main objectives of the research are to determine: 1) the role of mineralogical features of porous media on attachment, transport and retention behavior of GONPs, 2) the effect of temperature, ionic strength and composition on transport and retention behavior of GONPs in porous media and 3) the effect of natural biofilm on transport of GONPs in porous media.

5.4. Results and discussion

5.4.1. Characterization of porous media

XRD diagrams of porous media grains are illustrated in Fig 5-1. Accordingly, sand grains contain around 99 % quartz. Quartz sediments consisted of a large amount of quartz and trace amounts of calcite and aragonite. In addition, the XRD pattern of limestone sediments exhibited several sharp peaks related to calcite with two slight peaks, which indicated the presence of quartz and dolomite in the structure of sediments. The results of XRF analysis revealed that sand comprised 98.42 % SiO_2, 0.02 % Al_2O_3, 0.02 % Fe_2O_3 with only 1.55 % loss on ignition. Moreover, 65.10 % SiO_2, 14.76 % CaO, 2.72 % Fe_2O_3, 1.69 % Al_2O_3, 0.89 % SO_3, 0.85 % MgO, 0.60 % K_2O, 0.34 % Na_2O, 0.03 % MnO, 0.01 P_2O_5 and 12.80 % loss on ignition were observed in the structure of quartz sediments. The limestone sediments contained 46.41 % CaO, 9.59 % SiO_2, 2.84 % MgO, 1.63 %

Fe_2O_3, 0.41 % Al_2O_3, 0.21 % K_2O, 0.20 % SO_3, 0.07 % Na_2O, 0.03 % MnO, 0.02 P_2O_5 and 38.56 % loss on ignition. The elemental analysis of the minerals was performed using EDS technique. According to Fig 5-1 (a), the main elements in the structure of sand were Si and O. However, Fig 5-1 (b) shows less Si in the body of quartz sediments and the other constituents were O and Ca. In addition, limestone sediments contained significant amounts of O and Ca and lesser proportions of C, Si and Mg.

FTIR spectra of pristine and biofilm-conditioned sand, quartz and limestone sediments are shown in Fig 5-2. As can be seen, in the spectra of pristine and biofilm-conditioned sand, two peaks were observed at 797.32 and 778.62 cm^{-1} and 796.56 and 778.47 cm^{-1}, respectively, which may be due to the Si-O-Si intertetrahedral bridging bonds. Other defined peaks were also observed in the 1079.86 and 1079.49 cm^{-1} absorption bands of pristine and biofilm-conditioned sand spectra which are related to Si-O stretching (Chen et al., 2014). In addition, similar peaks were observed in FTIR spectra of quartz sediments which revealed Si-O symmetric stretch and Si-O-Si intertetrahedral bridging bonds. However, extra peaks were seen in the absorption bands at 1409.20 and 1413.19 cm^{-1} of pristine and biofilm-conditioned quartz sediments spectra, respectively, which indicate the presence of calcite. Additionally, the intensity of calcite peaks in pristine (1404.32 cm^{-1}) and biofilm-conditioned (1409.39 cm^{-1}) limestone sediments was higher than quartz, which is in line with the results of XRD and EDS. Moreover, the slight peaks related to quartz were seen in the absorption band ranging from 1000 to 1200. Although the XRD diagram of limestone sediments showed a weak peak of dolomite, no peak was seen in the FTIR spectra of limestone sediments, indicating the trace amount of dolomite in the structure of minerals.

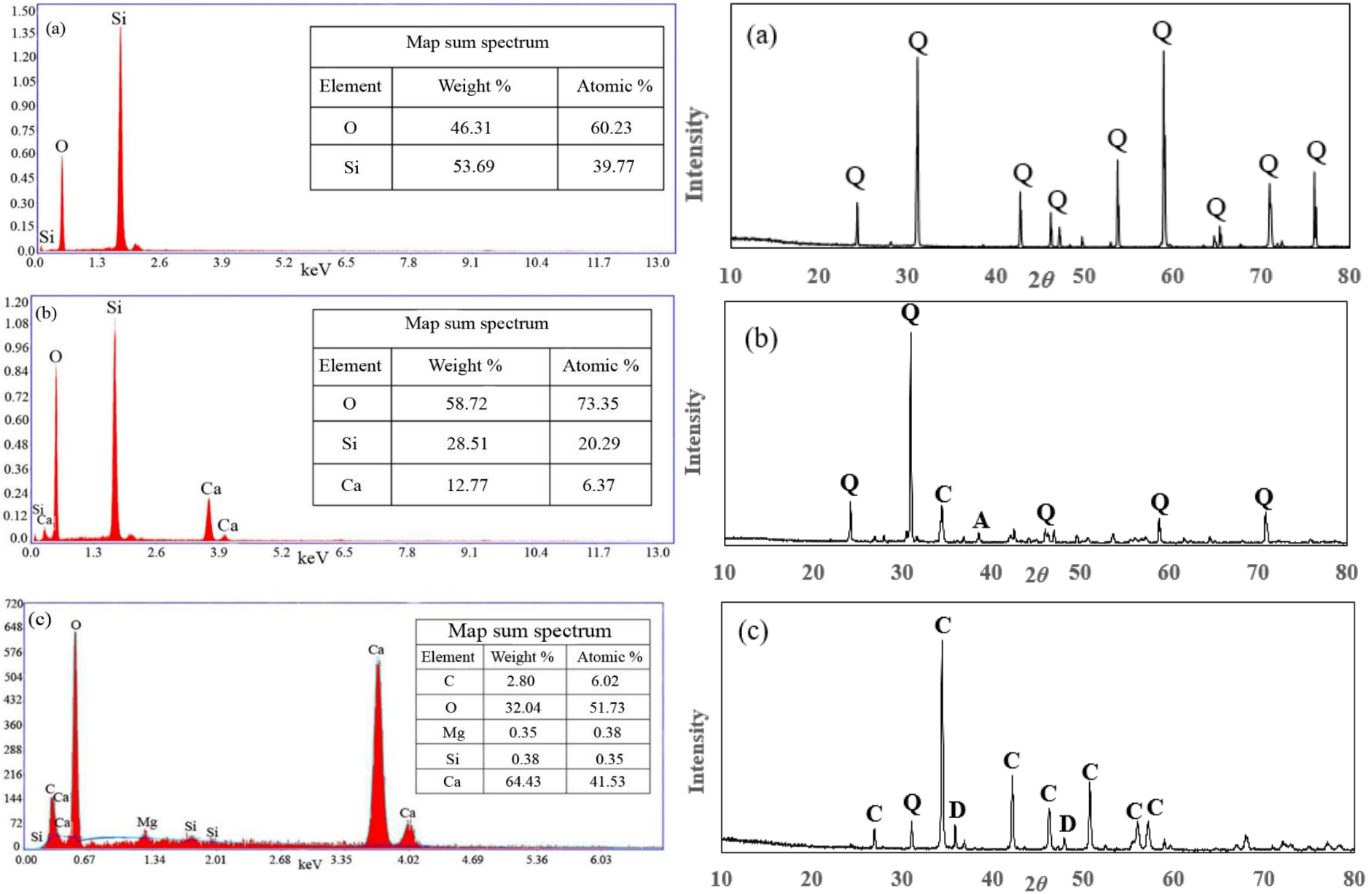

Fig 5-1. EDS spectra (left) and XRD diagrams (right) of (a) sand, (b) quartz sediments and (c) limestone sediments.

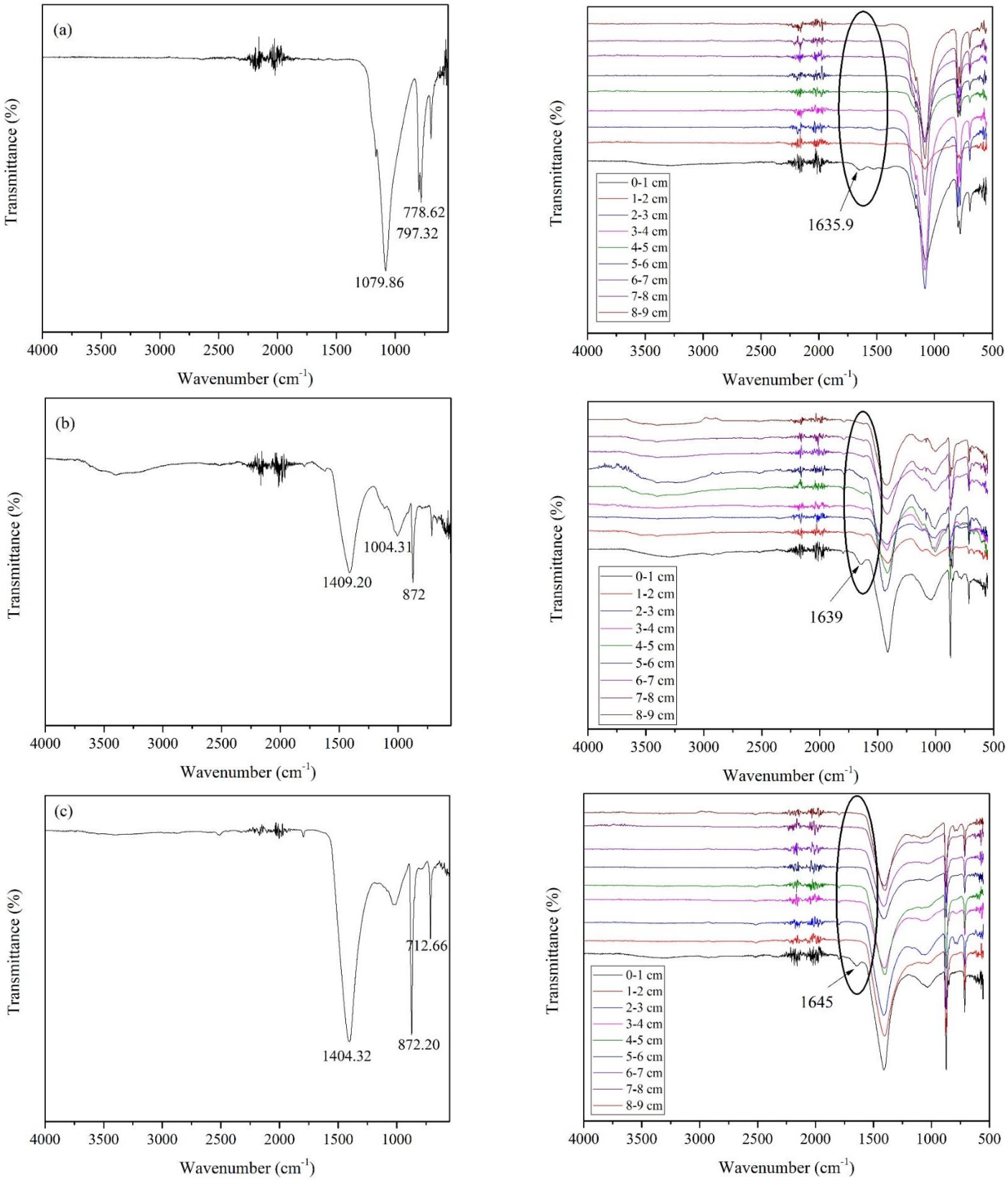

Fig 5-2. FTIR spectra of pristine (left) and biofilm-conditioned (right) (a) sand, (b) quartz sediments and (c) limestone sediments excavated from different parts of columns irrigated with treated wastewater.

5.4.2. Colloidal stability

Fig 5-3 shows the colloidal stability of GONPs based on Abs/Abs_0 which represents the absorption measured at time *t* minutes (Abs) and the initial absorbance (Abs_0) of GONPs, respectively against time. GONPs showed a high stability in water at both temperatures. The lowest value of Abs/Abs_0 was 0.9 at 22 °C and 10 mM NaCl. The stability of GONPs was slightly lower at 22 °C than at 4 °C. Similarly, the results of Wang et al., (2017b) showed higher GONPs aggregation at higher temperature(Wang et al., 2017b). However, an increase in the ionic strength (IS) of the GONP suspension caused a significant decrease in colloidal stability of GONPs in the studied period. The Abs/Abs_0 value decreased from 0.9 to 0.5 by increasing the IS of solution from 10 to 50 mM NaCl. High IS of a solution has a significant impact on collision between particles which stimulates their sedimentation. In addition, the colloidal stability of GONPs decreased in 10 mM NaCl from 0.9, to 0.6 in 1 mM $CaCl_2$. This observation shows that divalent cations have more influence than monovalent ones on the colloidal stability of nanoparticles.

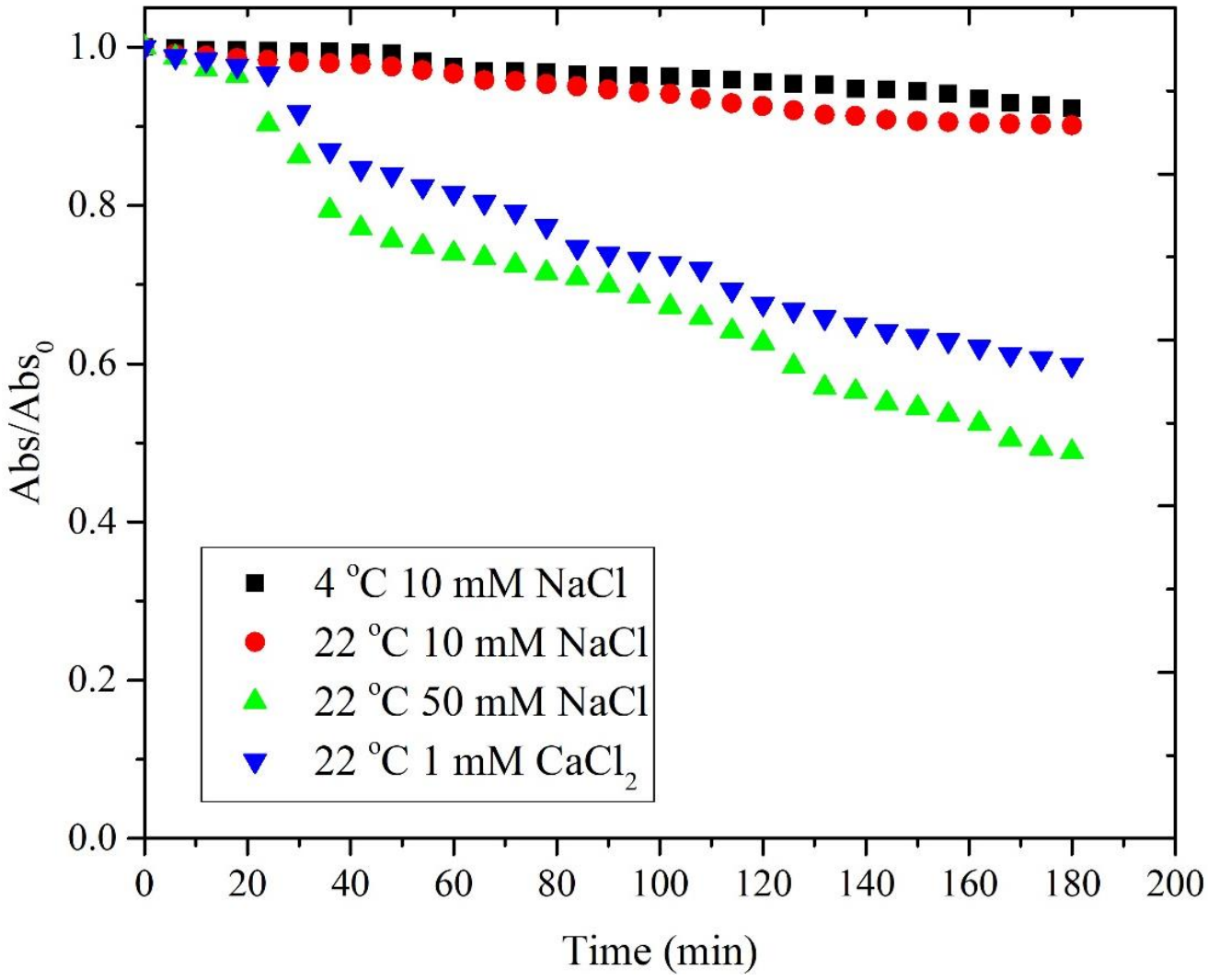

Fig 5-3. Colloidal stability of GONPs at different 4 and 22 °C temperature (GONPs concentration: 25 mg/L and IS: 10 mM NaCl, 50 mM NaCl and 1 mM $CaCl_2$).

3.3. Effect of temperature and ionic strength and compositions on GONPs sorption

The sorption behavior of GONPs onto different adsorbents was studied in several batch experiments at different temperature and ionic strength to determine the attachment of GONPs on collectors without role of pore structure. Fig 5-4 reveals normalized GONPs concentration (C/C_0, where C_0 and C are the initial and residual GONPs concentrations (mg/L) at time t, respectively). The results of control experiments (without adsorbents) showed negligible attachment of GONPs onto the internal walls of experimental glass tubes (data not shown). Fig 5-4 a shows that the attachment of GONPs onto the surfaces of adsorbents was endothermic which showed an increasing trend by enhancement of temperature from 4 to 22 °C. The cause of the higher GONPs attachment at higher temperature would be the endothermic nature of GONPs attachment. Previous studies have illustrated a reduction in nanoparticle colloidal stability with increasing temperature (Majedi et al., 2014). Increased temperature decreases electrostatic repulsion of nanoparticles, which coincides with increasing random Brownian motion and enhanced nanoparticle retention on substrate. Table 5-2 shows the zeta potentials of GONPs and all porous media at different experimental conditions. The zeta potentials of GONPs were less negative at 22°C (-31.3±0.5 mV) compared with 4°C (-36.4±2.2 mV). Different effects of temperature on electrokinetic properties of solid surfaces have been reported in the literature (Castro and Tufenkji, 2007, Sasidharan et al., 2017b). Sasidharan et al., (2017b) observed an insignificant effect of temperature on electrokinetic properties of virus, latex nanoparticles and sand grains (Sasidharan et al., 2017b). In contrast, findings of Wang et al., (2017b) showed that following an increase in temperature from 6 to 24°C, zeta potentials of GONPs and sand grains became less negative (Wang et al., 2017b). In our study, zeta potentials of GONPs and porous media were less negative at higher temperature, which may be due to the surface-exchange reaction of particles (Valdivieso et al., 2006). An increase in

temperature may prevent desorption of protons, which decreases the negative charges on the surfaces of GONPs and substrate.

Moreover, irrespective of temperature, GONPs attachment in the different porous media used here was in the following order: limestone sediments > quartz sediments > sand. The low attachment of GONPs in sand grains is likely associated with the unique surface charge screen and lack of charge heterogeneities, due to the removal of metal oxides and hydroxides in the preparation step. However, based on the results of XRF analysis, in quartz and limestone sediments, different iron, magnesium and aluminum oxides were present, which have an increasing effect on the attachment of nanoparticles. Indeed, iron and aluminum oxyhydroxides on surfaces of collectors provide positive charges that favor GONPs attachment (Tian et al., 2012). The results of DLVO interaction energies of GONPs attachment onto the sand grains show that no primary energy minimum value was obtained for sand grains at both temperature, indicating lack of attachment of GONPs on primary energy minimum. Fisher Power and Cheng, (2018) found the significant effect of low amount of iron/aluminum oxides on increasing retention of TiO_2 nanoparticles in natural sediments (Fisher-Power and Cheng, 2018).

In addition, a sharp increase was observed in GONPs sorption on the collectors by increasing ionic strength from 1 to 50 mM NaCl. An increase in ionic strength not only leads to the aggregation of nanoparticles, but also causes compression of electrostatic repulsive layer on the surfaces of substrate, decreasing the surface potentials of both nanoparticles and substrates, which enhances retention of nanoparticles. In addition, increasing the ionic strength of solution increases the effect of nanoscale heterogeneities of collectors on GONPs retention (Bradford and Torkzaban, 2013). Furthermore, cation bridging between nanoparticles and negatively-charged surfaces of collectors can be caused by presence of Ca^{2+} in solution which acts in favor of nanoparticle deposition (Liang

et al., 2013). Dong et al., (2017) reported the possibility of attachment of GONPs onto the limestone surfaces thereby bridging between –OH group of GONPs and Ca^{2+} of limestone even at unfavorable attachment conditions (Dong et al., 2017).

Moreover, at low ionic strength, 1 mM $CaCl_2$ had a greater effect than 10 mM NaCl on attachment rate of GONPs onto the surfaces of collectors. This observation is in line with Schulze-Hardy rule, which describes higher charge screening by higher valence cations. These results are consistent with previous studies, which have shown that divalent cations had more ability than monovalent ones to increase the deposition rate of GONPs and the other nanoparticles (Chen et al., 2012). Results of DLVO studies show that the Φ_{max} values were decreased by increasing ionic strength from 10 to 50 mM NaCl. In addition, more negative Φ_{min2} values were obtained at higher ionic strength which shows that increasing ionic strength of solution caused more attachment of GONPs onto the surfaces of collectors at secondary energy minimum.

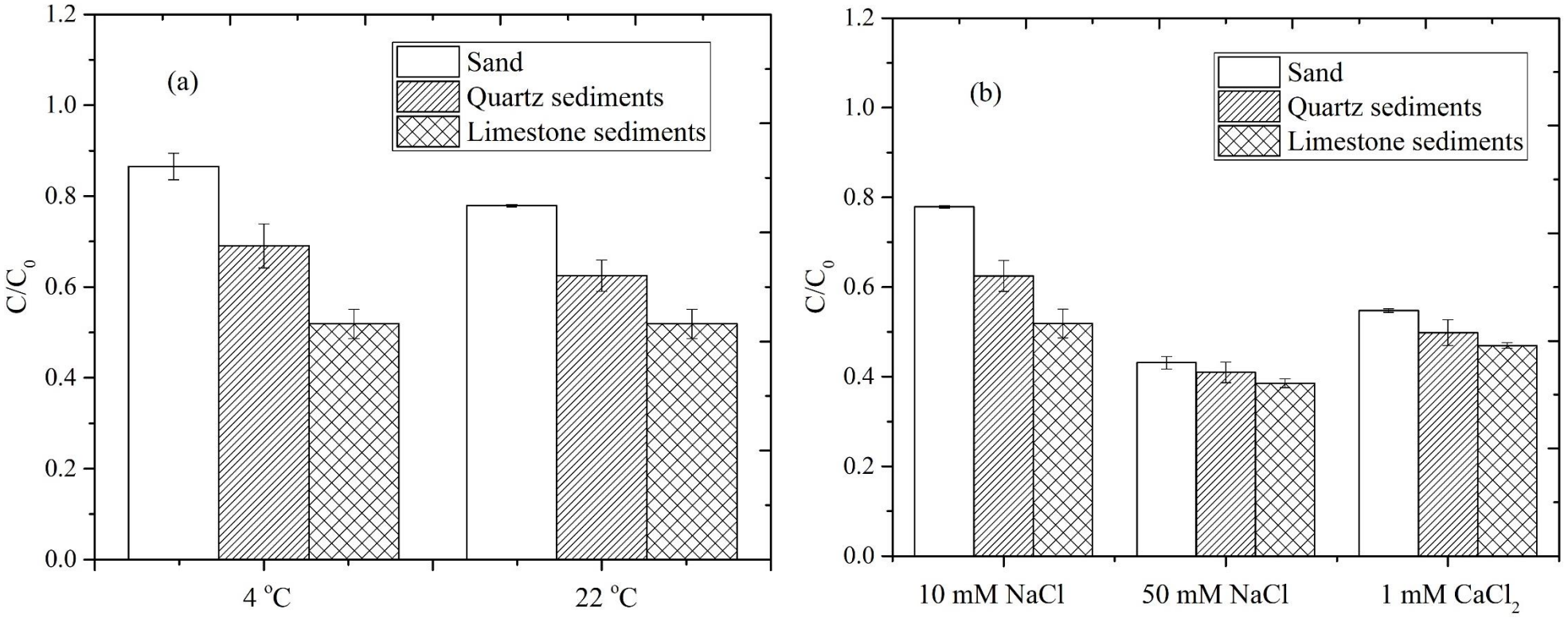

Fig 5-4. Bar charts of GONPs attachment onto the surfaces of sand, quartz sediments and limestone sediments at different (a) temperatures (4 and 22 °C) and (b) ionic strength and compositions (10 and 50 mM NaCl and 1 mM $CaCl_2$). The Y-axis represents the relative nanoparticle concentrations (C_0 and C are the initial and residual GONPs concentrations (mg/L), respectively). Error bars also show the standard deviation (n=3).

5.4.3. Transport of GONPs in pristine porous media

The porous media mineralogical features have a significant influence on the transport and retention behavior of nanoparticles. In this study, three different substrates, sand, quartz sediments and limestone sediments were used as porous media. The experiments were performed at 4 and 22°C using 10, 50 mM NaCl and 1 mM $CaCl_2$. Fig 5-5 shows the BTCs of GONPs in the different porous media as a function of relative concentration (C/C_0) against pore volume. C_{max}/C_0 of GONPs in all treatments was lower than 1 which was attributed to the attachment of nanoparticles onto the surfaces of collectors. Dong et al., (2016) observed higher peak of BTCs of tracer in comparison with GONPs in saturated and unsaturated structured heterogeneous sand columns (Dong et al., 2016). In contrast with other research, which has reported retardation of nanoparticles BTCs (Liang et al., 2013), compared to tracer, in the study reported here no retardation in the BTCs of GONPs in any porous media was observed, which may be due to the high mobility of nanoparticles in porous media. The shape of BTCs of GONPs at both temperatures and for all porous media showed an increasing trend with injection of nanoparticles, which was a good index of blocking in porous media. A similar mechanism has been reported in previous research considering GONPs transport in porous media (Feriancikova and Xu, 2012, Dong et al., 2017). Our results showed that higher GONPs deposition was observed at the higher incubation temperature in all columns. Results of Sotirelis and Chrysicopoulos, (2015) also showed that the attachment of GONPs onto the sand grain surfaces at 25°C was higher than at 4°C (Sotirelis and Chrysikopoulos, 2015). Furthermore, the temperature-dependent aggregation of nanoparticles is another effective mechanism for particle retention in porous media (Su et al., 2017). Results of Wang et al., (2017b) showed that decreasing temperature did not cause a significant change in deposition of GONPs in

coarse porous media (0.9-1 mm); whereas, in fine porous media (0.3-0.4 mm) (which is similar to the porous media size distribution of our study) a remarkable decrease was observed in GONPs retention by decreasing temperature from 24 to 6°C (Wang et al., 2017b).

Aqueous ionic strength and composition are the other critical agents, controlling the attachment behavior of nanoparticles onto the surfaces of substrate. In our study, a series of experiments were carried out at 10 and 50 mM NaCl and 1 mM $CaCl_2$ to study the effect of increasing ionic strength and composition on retention of GONPs at different porous media. The mass balance calculations for GONP (effluent, retained and total) are presented in Table 5-1. The mass balance calculations demonstrated >90 % recovery of GONPs from eluted and retained sections which indicated lack of particle attachment on primary energy minimum. According to Table 5-1 by increasing ionic strength from 10 to 50 mM NaCl at 22 °C, a significant decrease was observed in GONPs transport in which C_{max}/C_0 in sand (0.79 to 0.23), quartz (0.66 to 0.19) and limestone sediments (0.58 to 0.17). In addition, application of 1 mM $CaCl_2$ in the solution led to higher GONPs retention, than 10 mM NaCl which shows the greater influence of divalent than monovalent cations on GONPs retention in porous media. Furthermore, under conditions of higher ionic strength (i.e., 50 mM NaCl and 1 mM $CaCl_2$) the shape of BTCs of GONPs changed decreasing which may be due to the role of ripening (the deposition of suspended nanoparticles onto the retained ones as further attachment sites) on GONPs deposition. Chen et al., (2018) found the effect of ripening on retention of GONPs in sand-packed columns with an increase in ionic strength from 1 to 50 mM NaCl (Chen et al., 2018). Moreover, in another study, Liang et al., (2019) found that by increasing $CaCl_2$ concentration from 0.33 to 0.4 mM, ripening was the main mechanism of GONPs retention in sand packed columns (Liang et al., 2019).

Figs 5-5 c and d show the retention profiles (RPs) of GONPs in the three substrates based on $C/C_0/g_{collector}$ (C and C_0 are the residual and initial GONPs concentrations, respectively) against distance from inlet end (cm) at 4 and 22 °C, respectively. It is obvious that higher GONPs retention was observed at higher temperature, which is in line with the results of BTCs analyses. At 4 and 22°C, the retained GONPs in sand, quartz and limestone sediments increased from 11.00, 27.05 and 41.64 % to 19.57, 34.87 and 47.11 %, respectively (Table 5-1). The shapes of RPs in all columns were linear which show the equal amounts of retained nanoparticles in different parts of columns (Figs 5-5 c and d). However, slightly more GONPs was retained in the first 3 cm of quartz and limestone sediments column which may be due to the presence of different metal oxides onto the surfaces of collectors. In addition, a very different shape was obtained for RPs of GONPs at high ionic strength (Figs 5-6 c and d). The hyper-exponential shape of RPs indicates higher particle attachment onto the inlet end of column, compared to the deeper areas. Furthermore, the RP shape, in some cases, determines the governing mechanisms on nanoparticle attachment onto the substrate surfaces. In previous study, the hyper-exponential shape of RPs of nanoparticles and microorganisms has been attributed to different processes such as aggregation of particles (Chen and Elimelech, 2006), straining (Bradford and Bettahar, 2006), chemical heterogeneities of particles and collectors (Tufenkji and Elimelech, 2005b) and the hydrodynamic characteristics of system (Bradford et al., 2009). While, finding the percentage of contribution of each parameter on the RPs of nanoparticle is not so easy.

According to the literature, ripening and straining are the most plausible mechanisms of particle retention in porous media, when RP has a hyper-exponential shape which shows the depth-dependence of colloidal particles deposition in porous media (Bradford et al., 2002). The most important conditions for observing the role of straining on nanoparticle retention would be the

ratio of diameters of nanoparticles to collectors. Bradford et al., (2002) reported that at a ratio of higher than 0.002, the role of straining on particle retention is significant (Bradford et al., 2002). Results of hydrodynamic studies of GONPs showed that the hydrodynamic diameters of GONPs at 10 mM NaCl and at 4 and 22°C were 368±97 and 422±115 nm, respectively and at 50 mM NaCl and 1 mM $CaCl_2$ were 684±126 and 579±104 nm which shows that the d_p/d_c is around 0.0010, 0.0011, 0.0018 and 0.0015 indicating that the straining was significant at high ionic strength.

After end of experiments, the hydrodynamic diameters (D_H) of GONPs in the influent and porous media were measured which would be an appropriate index to represent the size distribution of nanoparticles in a comparative way (Chowdhury et al., 2013). Fig 5-7 shows size distribution of retained nanoparticles at different IS. In case of low IS, no significant changes were observed in the size distribution of retained particles in different parts of columns which indicates lack of straining on GONPs retention (Figs 5-7 a and b). However, at high IS, a decreasing trend was observed in size distribution of retained GONPs by increasing distance from inlet end (Figs 5-7 c and d). This phenomenon justifies the hyper-exponential shape of RPs which showed the retention of larger particles in the inlet end of columns. Decreasing GONPs size distribution with increasing travel distance would be due to the different factors such as repining, straining, aggregation, enhanced collision efficiency of particles and the combination of these factors. Different results have been reported about size-selective retention behavior of nanoparticles in porous media in the literature. In the study of Sun et al., (2015) the size of retained GONPs in sand-packed columns increased by further distance from column inlet, which was attributed to the higher attachment of finer colloidal particles than larger one, based on colloidal filtration theory (Sun et al., 2015). However, Jiang et al., (2012) found that by increasing the distance from column inlet, the size distribution of ZnO nanoparticles showed a decreasing trend which was due to simultaneous

aggregation and straining of particles (Jiang et al., 2012). Furthermore, Wang et al., (2015) reported similar results in retention of larger aggregates of goethite nanoparticles in the inlet end of column which showed a decreasing trend to the outlet end (Wang et al., 2015). Indeed, the greatest size of retained nanoparticles was observed in the inlet end of column. This finding shows that the nanoparticle size increased in columns which caused pore throat straining in the column inlet when injected into the columns. The aggregation of GONPs led to the higher retention of nanoparticles on large aggregated that narrowed the grain-grain contacts and trapping more nanoparticles in this area (Saleh et al., 2007). So, it would be the possible cause of the creation of large aggregates found in the column inlet. Moreover, by further injection of nanoparticles into the column, the suspended particles can be deposited onto the previously retained nanoparticles which create a thick layer of nanoparticles in the column inlet (Bradford et al., 2002). Indeed, it is anticipated that the continuous injection of GONPs in the column led to the high particle-particle collision in the column inlet which increased the particle deposition and size of deposited particles (Bradford et al., 2007)

Table 5-1. Zeta potentials, hydrodynamic diameter (D_H) of nanoparticles, DLVO and mass balance calculations of GONPs in all porous media.

No	Treatment	Temperature	Ionic strength	D_H [a](nm)	Zeta potential (mV)		Ψ_{max} [b](kT)	Ψ_{min2} [b](kT)	M_{eff} (%)	M_{ret} (%)	M_{loss} (%)	C_{max}/C_0
					GONPs	Collectors						
1	Sand	4°C	10 mM NaCl	368±97	-36.4±2.2	-48.1±3.2	216.82	-0.48	78.79	11.00	10.21	0.92
2	Quartz sediments	4°C	10 mM NaCl	368±97	-36.4±2.2	-41.2±2.1	ND[c]	ND	62.61	27.05	10.34	0.70
3	Limestone sediments	4°C	10 mM NaCl	368±97	-36.4±2.2	-22.4±1.4	ND	ND	55.07	41.64	3.29	0.63
4	Sand	22°C	10 mM NaCl	422±115	-31.3±0.5	-46.1±3.1	157.88	-0.42	69.99	19.57	10.44	0.79
5	Quartz sediments	22°C	10 mM NaCl	422±115	-31.3±0.5	-28.8±1.5	ND	ND	57.30	34.88	7.82	0.66
6	Limestone sediments	22°C	10 mM NaCl	422±115	-31.3±0.5	-17.2±3.4	ND	ND	47.39	47.11	5.50	0.58
7	Sand	22°C	50 mM NaCl	684±126	-23.2±3.4	-33.5±3.3	91.53	-6.89	21.74	72.25	6.01	0.23
8	Quartz sediments	22°C	50 mM NaCl	684±126	-23.2±3.4	-21.7±0.2	ND	ND	16.74	76.52	6.74	0.19
9	Limestone sediments	22°C	50 mM NaCl	684±126	-23.2±3.4	-12.4±1.8	ND	ND	14.24	79.84	5.92	0.17
10	Sand	22°C	1 mM $CaCl_2$	579±104	-26.6±0.3	-38.2±4.1	121.12	-5.31	25.10	70.43	4.46	0.29
11	Quartz sediments	22°C	1 mM $CaCl_2$	579±104	-26.6±0.3	-22.3±1.5	ND	ND	20.10	74.16	5.74	0.23
12	Limestone sediments	22°C	1 mM $CaCl_2$	579±104	-26.6±0.3	-14.5±2.2	ND	ND	17.83	76.36	5.80	0.20
13	Sand-Biofilm	22°C	10 mM NaCl	422±115	-31.3±0.5	-25.2±6.3	121.57	-0.80	30.57	-	-	0.32
14	Quartz sediments-Biofilm	22°C	10 mM NaCl	422±115	-31.3±0.5	-15.5±4.2	ND	ND	26.06	-	-	0.28
15	Limestone sediments-Biofilm	22°C	10 mM NaCl	422±115	-31.3±0.5	-9.6±4.13	ND	ND	22.63	-	-	0.23

[a] Hydrodynamic diameter of GONPs obtained by DLS.

b Relative maximum energy barrier and secondary energy minimum between GONPs and sand grains (kT) in which *k* is the Boltzmann constant and *T* is temperature.

[c] Not determined.

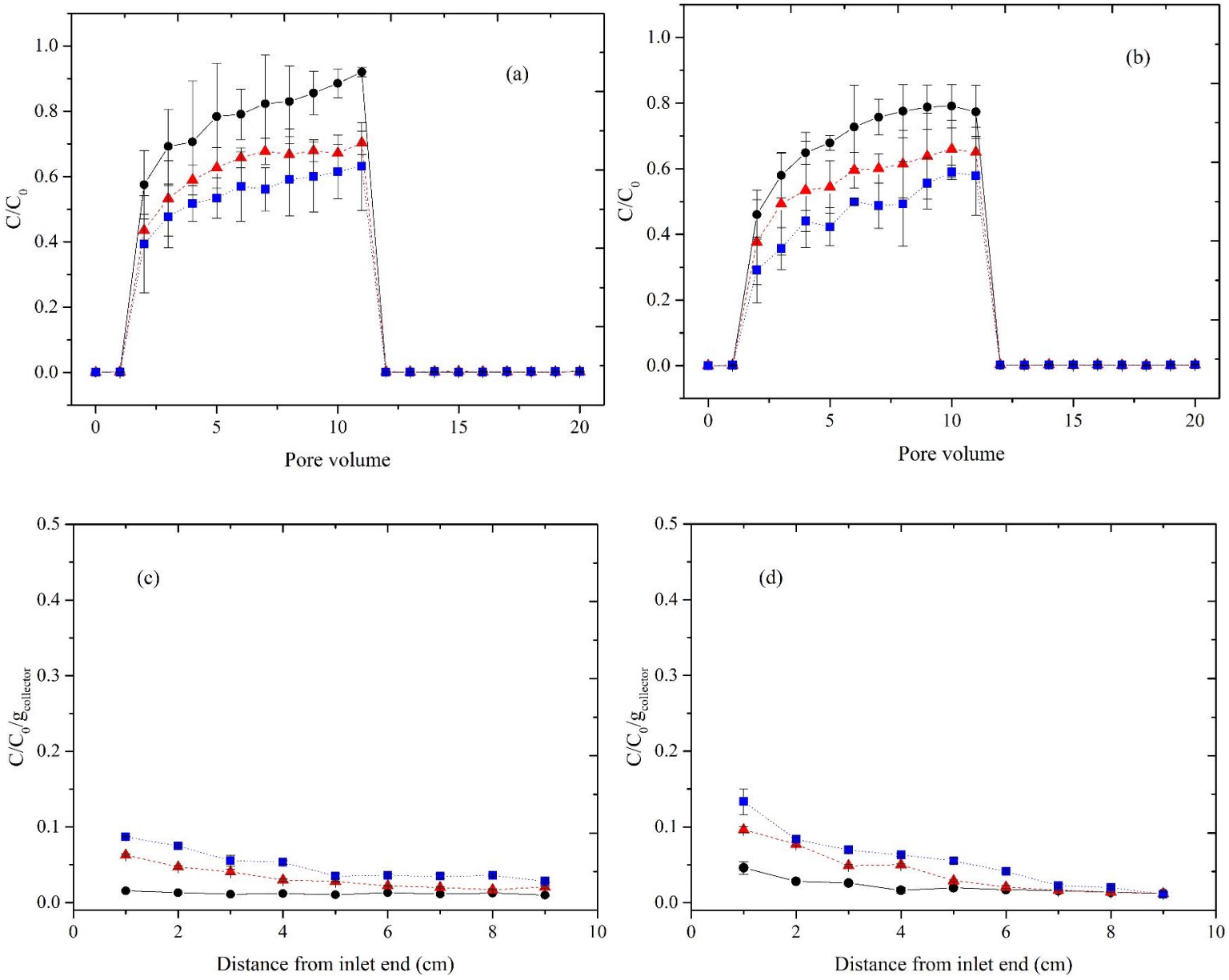

Fig 5-5. Breakthrough curves (a and b) and retention profiles (c and d) of GONPs at 4 °C (left) and 22 °C (right) at IS = 10 mM NaCl, pH = 7.5 and flow velocity = 5 m/day (●: sand, ▲: quartz sediments and ■: limestone sediments). Error bars also show the standard deviation (n=3).

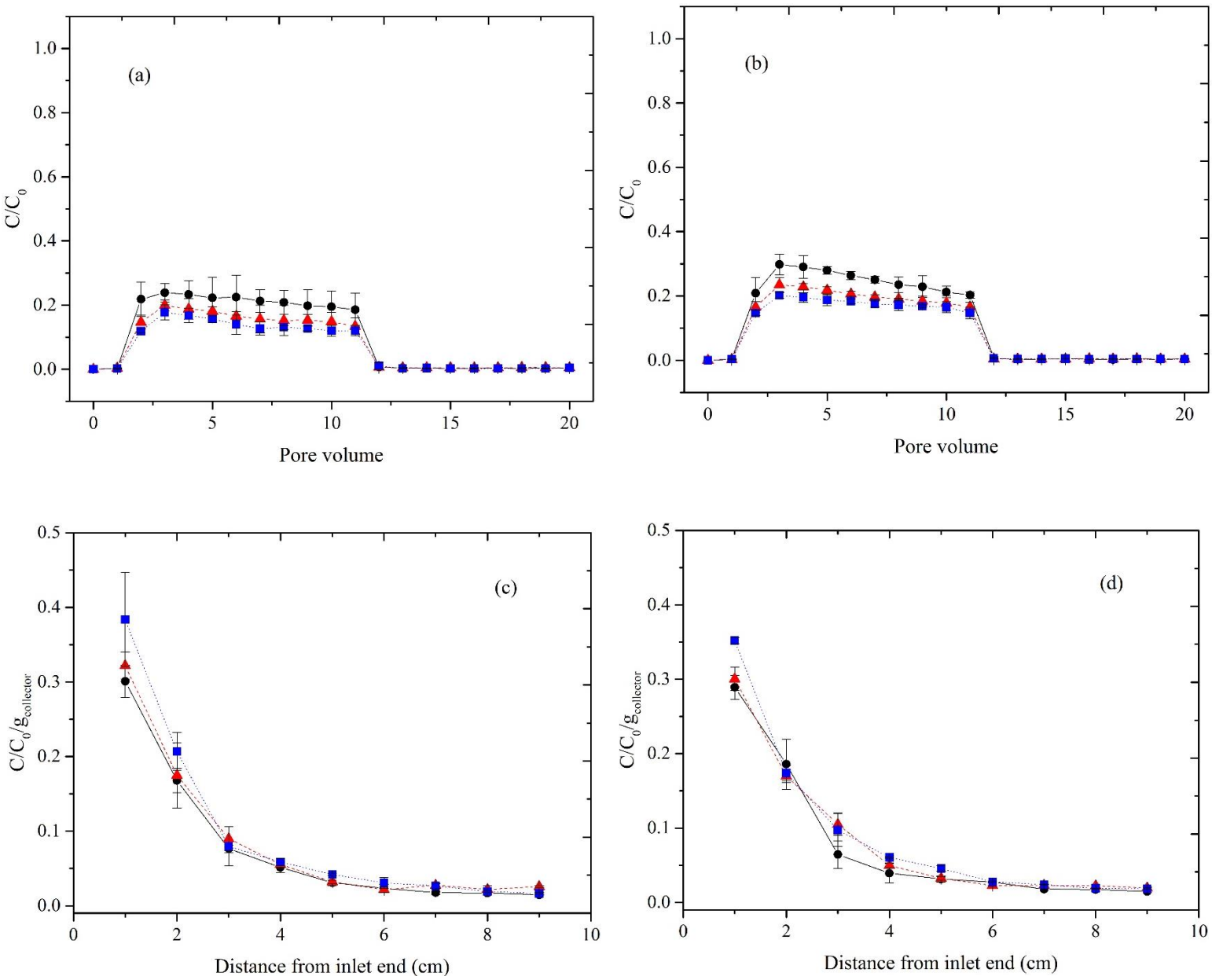

Fig 5-6. Breakthrough curves (a and b) and retention profiles (c and d) of GONPs at 50 mM NaCl (left) and 1 mM $CaCl_2$ (right) at pH = 7.5, flow velocity = 5 m/day and temperature = 22 °C (●: sand, ▲: quartz sediments and ■: limestone sediments). Error bars also show the standard deviation (n=3).

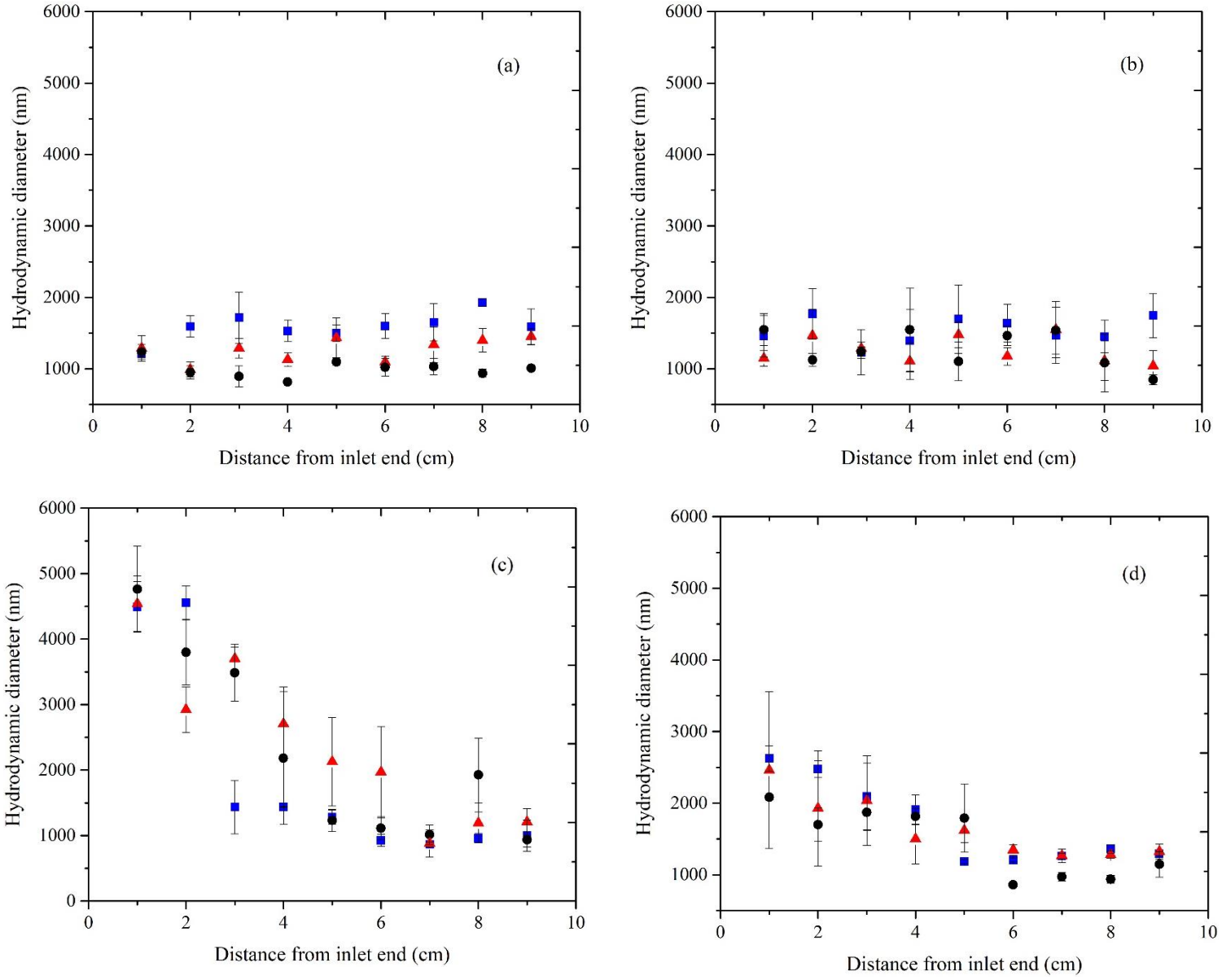

Fig 5-7. Size distribution of retained nanoparticles at (a) 10 mM NaCl and 4 °C, (b) 10 mM NaCl 22 °C, (c) 50 mM NaCl 22 °C and (d) 1 mM $CaCl_2$ 22 °C. (●: sand, ▲: quartz sediments and ■: limestone sediments). Error bars also show the standard deviation (n=3).

5.4.4. Transport of GONPs in biofilm-conditioned porous media

Transport experiments of GONPs in biofilm-conditioned porous media were performed at 22°C (Fig 5-8). The presence of biofilm significantly increased the retention of GONPs in columns, irrespective of the mineralogical features of porous media. Based on Table 5-1, by conditioning surfaces of pristine sand, quartz and limestone sediments with biofilm, C_{max}/C_0 of GONPs BTCs decreased from 0.79, 0.66 and 0.58 to 0.32, 0.28 and 0.23, respectively. Furthermore, the recovered GONPs in sand, quartz sediments and limestone sediments decreased from 69.99, 57.30 and 47.39 % to 30.57, 26.06 and 22.63 %, respectively. Recently, a number of studies have reported enhanced nanoparticle retention in biofilm-conditioned porous media (Lerner et al., 2012, Kurlanda-Witek et al., 2015). One of the reasons of high colloidal particle attachment onto the surfaces of collectors would be less negative surface charges (zeta potentials) of collectors in biofilm-conditioned media than the pristine ones, indicating the role of biofilm on surface charge neutralization of collectors and decreasing electrostatic repulsive forces. Han et al., (2016) attributed the higher ZnO nanoparticle retention in biofilm-conditioned compared with the pristine porous media to the differences in energy barrier height (Han et al., 2016). The derived Φ_{max} for sand grains show a strong primary energy barrier against GONPs retention in the biofilm-conditioned column. However, results shown in Table 5-1 indicated that there was a difference between eluted GONPs in pristine and biofilm-conditioned columns. Therefore, a major discrepancy between BTC and DLVO results confirm the role of other mechanisms on the retention of GONPs in collectors.

It is widely reported that the natural organic matter (NOM) contains large numbers of functional groups such as amino, hydroxyl and carboxyl (Schulten and Schnitzer, 1993). Based on previous research, GONPs have an interaction with surface functional groups of NOM, even under unfavorable conditions (Chowdhury et al., 2014). In this study, it was possible to identify the

bonding between GONPs and produced microbial mass onto the surfaces of collectors, especially in limestone columns where the dissolution of calcite led to the presence of higher Ca^{2+} and bonding between GONPs, Ca^{2+} and microbial mass.

The higher GONPs retention may also be enhanced by the surface physical heterogeneities in biofilm-conditioned columns, which have a critical role in colloidal particle retention, even in unfavorable electrostatic conditions. Biofilm creates surface charge heterogeneities and surface roughness which produce some low velocity regions on collector surfaces with fewer hydrodynamic forces and torques, providing favorable conditions for nanoparticle deposition (Vaidyanathan and Tien, 1988, Taneda, 1979). Indeed, the created roughness by biofilm decreases the height of the energy barrier and primary minimum depth which changes the lever arms to decrease the applied hydrodynamic torque and improve the resisting adhesive torque (Bradford et al., 2013, Bradford and Torkzaban, 2013). Plate 5-1 shows SEM images of pristine and biofilm-conditioned collector surfaces of all porous media. Rougher surfaces were observed in biofilm-conditioned grains, compared to pristine, which can be attributed to the production of microbial mass. Jang et al., (2013) found higher roughness onto the surfaces of biofilm-conditioned sand grains, which caused greater retention of ZnO nanoparticles (Jiang et al., 2013). Moreover, metal oxides have the ability to interact with bacteria surface polymers such as extracellular polymeric substances (EPS) and macromolecules through hydrogen bonding (Jiang et al., 2013). It is possible that surface polymers were produced by bacterial biofilm, which may interact with anionic surface groups of GONPs, leading to interaction between NP-polymer onto the surfaces of collectors.

In addition to decreasing the surface charges and increasing physical heterogeneities of collectors, physical straining is another possible mechanism influencing retention by biofilm-conditioned media. It has been well-documented that the presence of biofilm at the inlet end of column covers

the substrate surfaces and fills interpores. It has been shown that the growth of biofilm in the interpores fills pore vacancies and changes the geometry and hydraulic features of column (Dupin and McCarty, 2000).

To test this hypothesis, the amounts of produced biofilm in different parts of columns was measured (Fig 5-9). As can be seen, more biofilm was produced at the inlet ends of columns, however, at increasing the distances from the column inlet, the amount of biofilm decreased, which may be attributable to nutrient and oxygen limitation. The spatial distribution of biofilm in the column was further demonstrated by determining the FTIR spectra of sand, quartz and limestone sediments after incubation with treated wastewater, which show a slight peak in the absorption bands of 1635.9, 1639 and 1645 cm^{-1}, respectively, which implied the production of protein. However, there was no peak in the same absorption bands of biofilm-conditioned limestone grains with increasing distance from inlet end of columns; suggesting negligible amounts of biofilm were present. Similar results have been reported by (Cui et al., 2018). 2 and 3D CLSM images of pristine and biofilm-conditioned different porous media obtained from 0-1 surfaces of columns are represented in Plates 5-2 and 5-3. The 2 and 3D images of pristine substrate show a very low amount of biofilm, which is marked by a thin fluorescent layer around the substrate in the 3D images. However, the biofilm-conditioned substrates show a thick fluorescent layer in both 2 and 3D images, indicating the production of biofilm onto the surfaces.

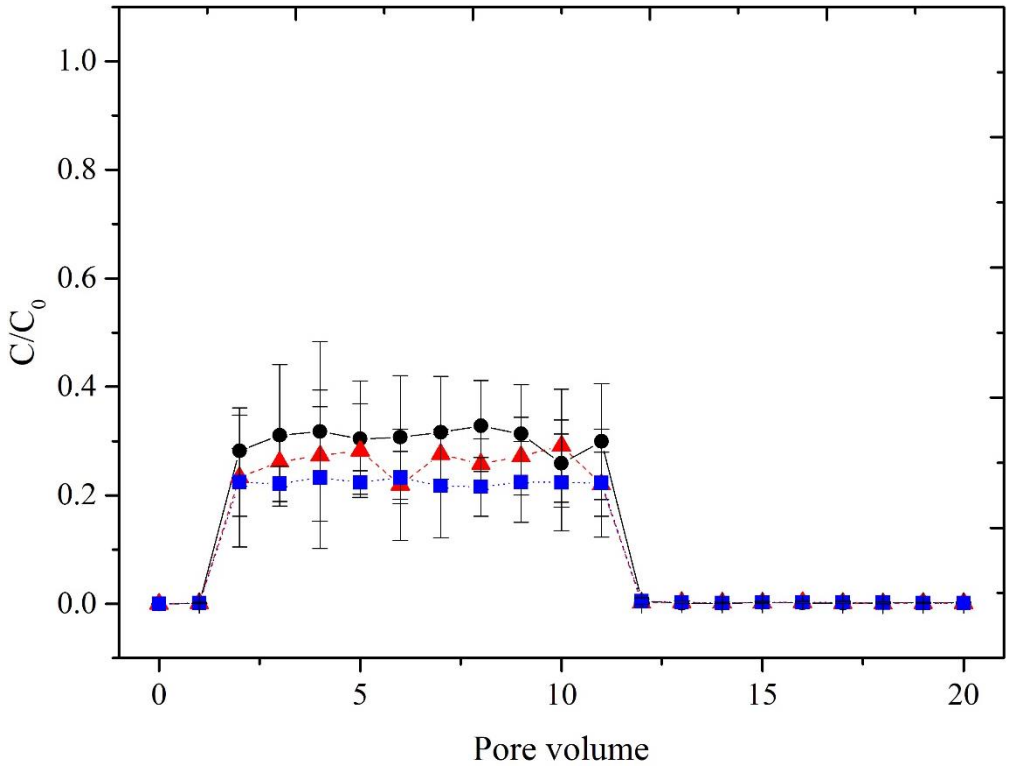

Fig 5-8. Breakthrough curve of GONPs in biofilm-conditioned porous media at 10 mM NaCl and 22 °C (●: sand, ▲: quartz sediments and ■: limestone sediments).

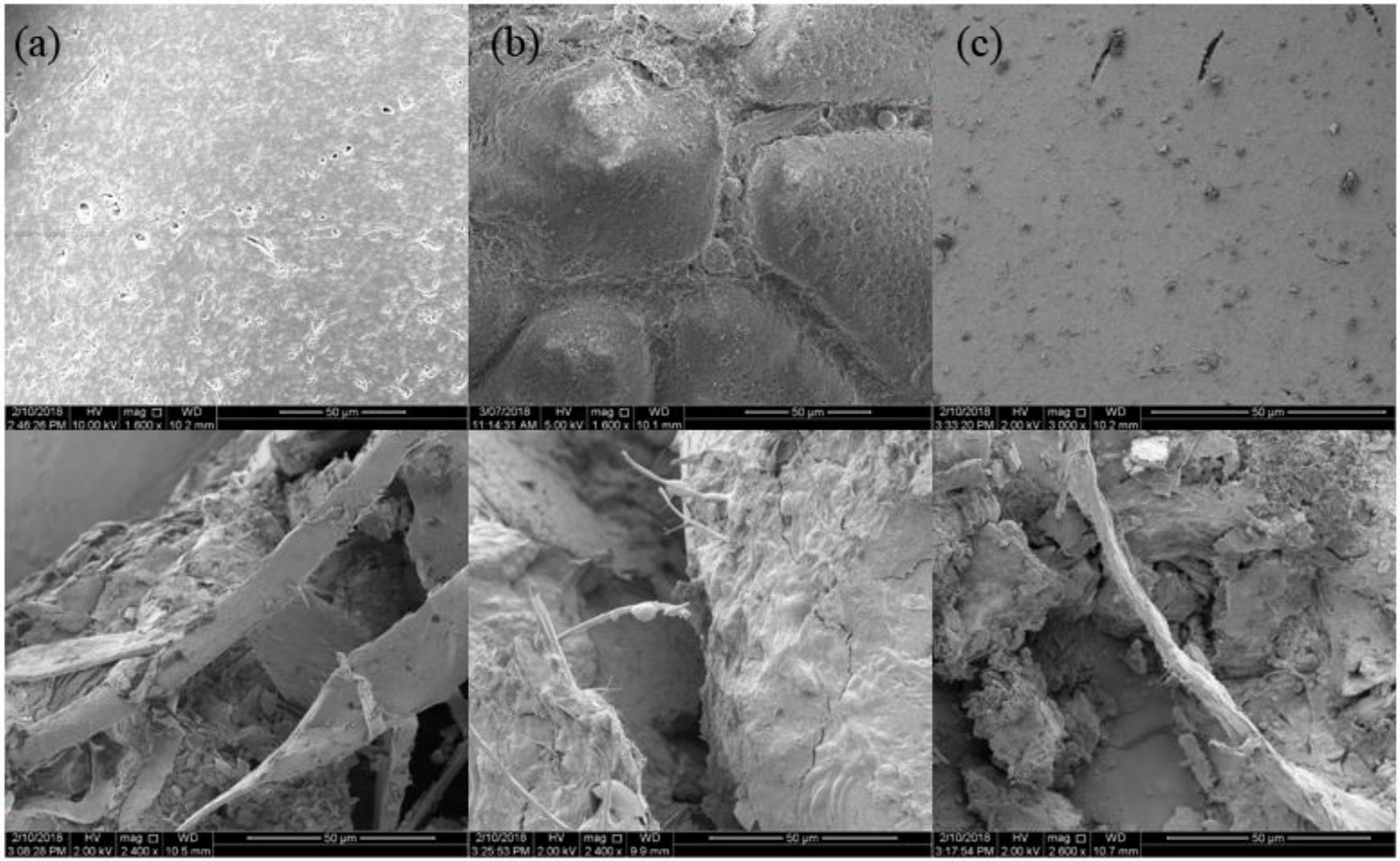

Plate 5-1. SEM images of substrates extracted 0-1 cm from the column inlet. Pristine (first row) and equivalent biofilm-conditioned material (second row); (a) sand, (b) quartz sediments and (c) limestone sediments.

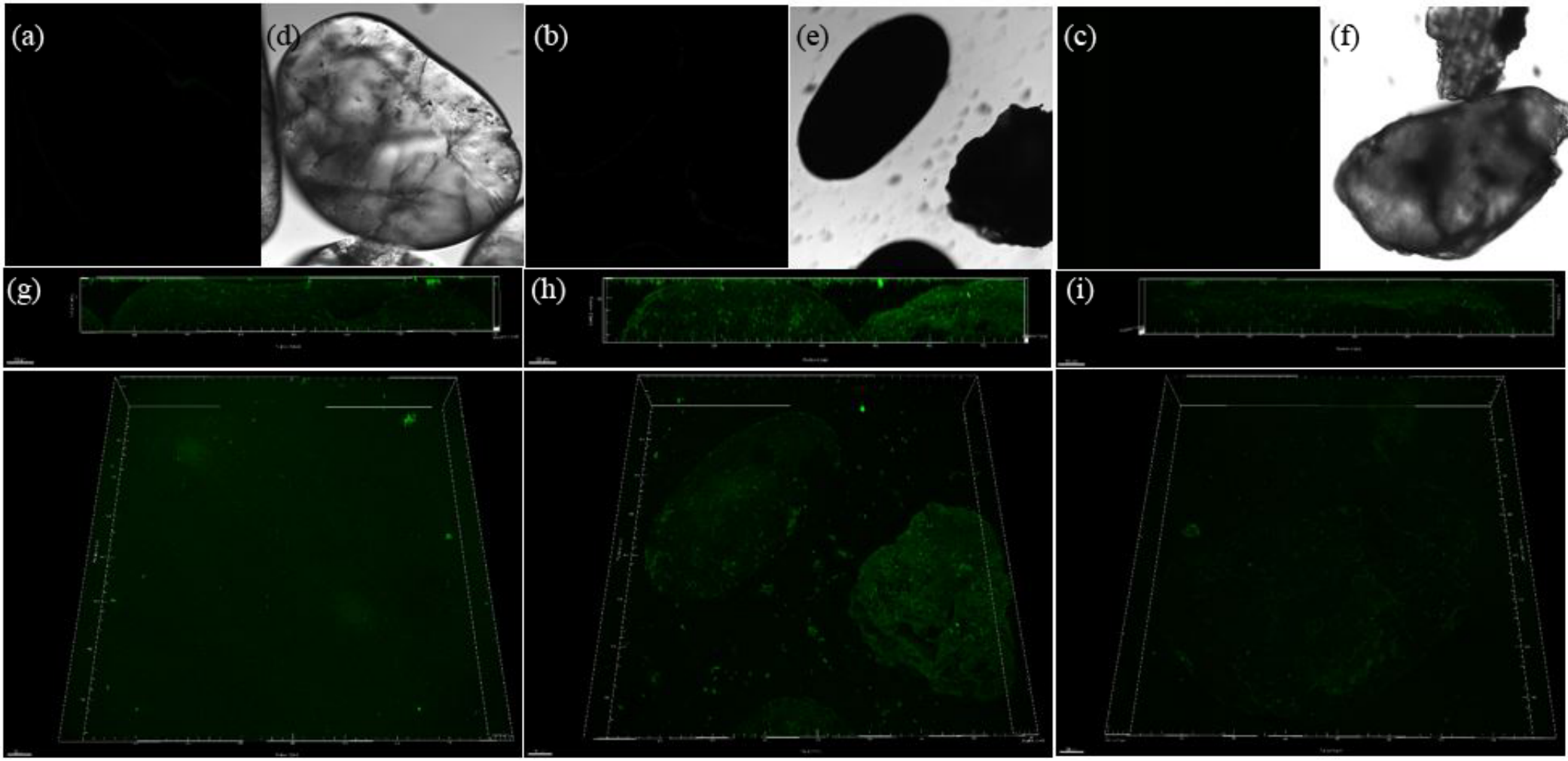

Plate 5-2. CLSM images of (left) pristine sand grains, (center) quartz sediments and (right) limestone sediments: (a), (b) and (c): confocal slice images through sand grains, quartz sediments and limestone sediments, (d), (e) and (f): transmitted light images of the sand grains, quartz sediments and limestone sediments shown in (a), (b) and (c), respectively; (g), (h) and (i): 3D image of confocal z-stack data set in Imaris software.

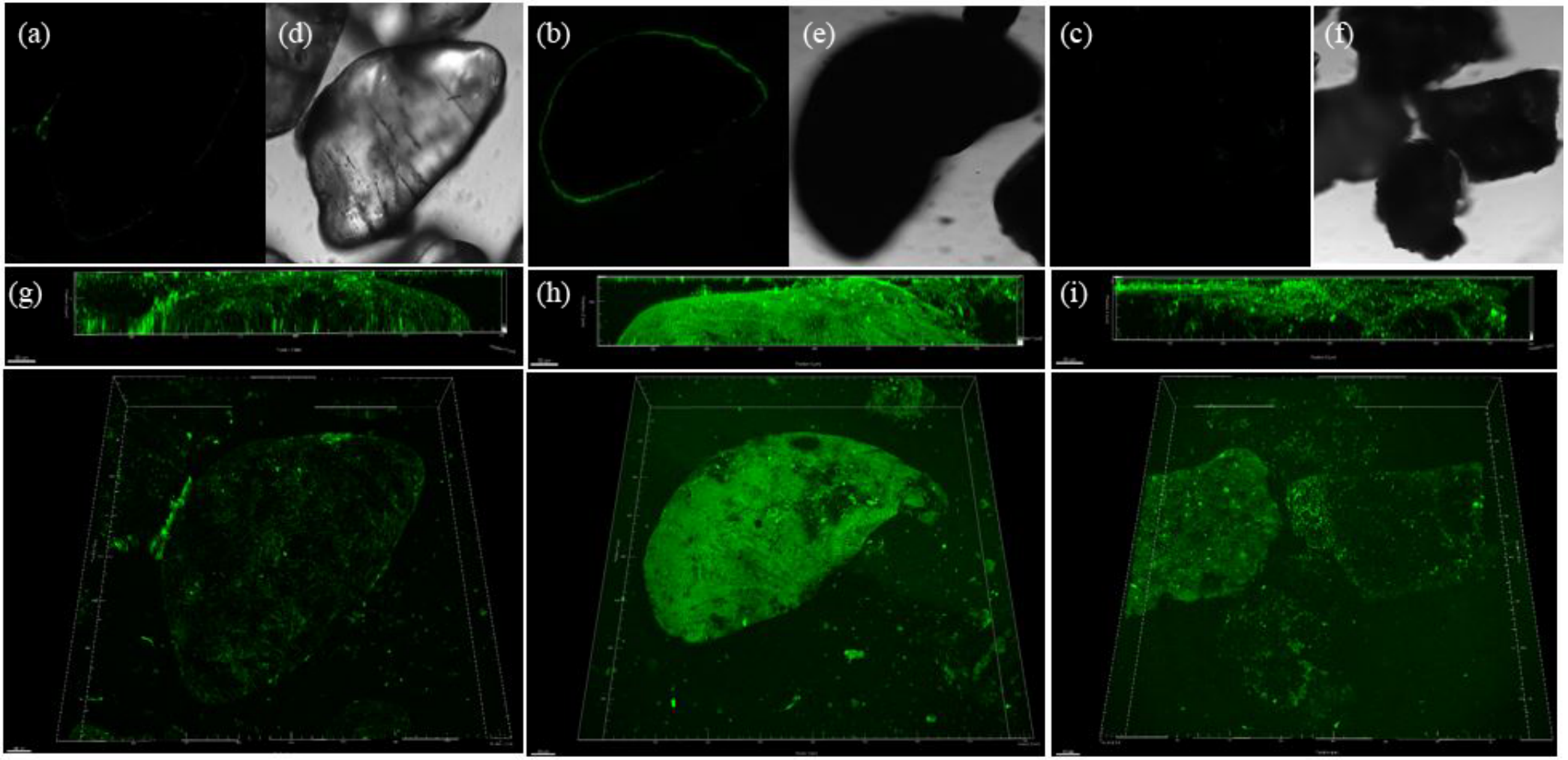

Plate 5-3. CLSM images of sand (left), quartz sediments (center) and limestone sediments (right) incubated obtained from material extracted 0-1 cm from the inlet of the columns (a), (b) and (c): confocal slice images through sand, quartz sediments and limestone sediments, respectively, (d), (e) and (f): transmitted light images of the sand, quartz sediments and limestone sediments in a, b and c, respectively **,** (g), (h) and (i): 3D image of confocal z-stack data set in Imaris software.

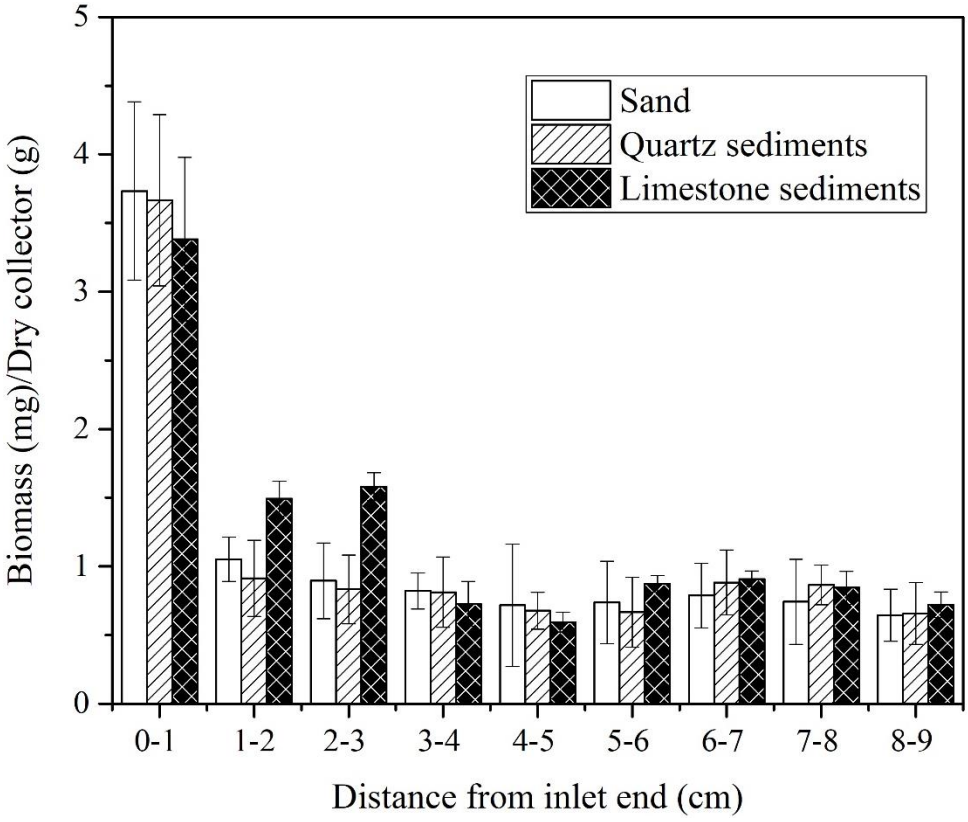

Fig 5-9. The produced biofilm in different parts of sand, quartz sediments and limestone sediments columns conditioned with treated wastewater.

5.5. Conclusion

A fundamental understanding about interaction between GONPs with native aquifer materials and natural biofilm attached onto the substrates provides a good view about risk of groundwater contamination with engineered nanoparticles. Therefore, the batch sorption and column experiments of GONPs in saturated columns containing different mineralogical collectors were performed at different physicochemical conditions. Results of batch and column experiments revealed the high dependence of GONPs retention onto the surfaces of collectors to the temperature, IS and cation type, in which the higher temperature, IS and cation valence, the higher GONPs retention. However, the high GONPs retention was observed in biofilm-conditioned porous media, because of the pore throat straining, surface physical roughness and surface charge neutralization and decreasing zeta potential and porosity of collectors. Moreover, the size distribution of retained GONPs showed the relatively equal size of retained particles at low IS. However, at high IS, by increasing the distance from column inlet end, the size distribution of retained GONPs decreased. Finally, although biofilm decreases the porosity of aquifers in MAR site, it would act as a natural bio-filter to protect groundwater resource nanoparticle toxicity.

This chapter gave readers the novel ideas about the mechanisms of transport and retention of GONPs in natural sediments, which would be applicable in designing a typical MAR site. That was the first study performed the effect of chemical heterogeneities of native aquifer sediments on transport and retention of GONPs in porous media. Furthermore, although several papers have been reported on the effect of synthetic biofilm from a typical microorganism (He et al., 2017, Jian-Zhou et al., 2015), the findings of this research showed transport behavior of GONPs affected by natural biofilm obtained by treated wastewater. The presence of other colloidal particles in aquifers has the potential to interact and effect their respective transport and retention behavior. In

majority of applied stormwater and treated wastewater in MAR sites, high amounts of microorganisms and engineered nanoparticles have been observed (Sidhu et al., 2012). It is likely that the transport behavior of engineered nanoparticles in a multiple colloid system is significantly different. In the following chapter, g the role of co-presence of different sized microorganisms on GONPs retention in porous media is investigated.

6. Effect of bacteria and virus on transport and retention of graphene oxide nanoparticles in natural limestone sediments

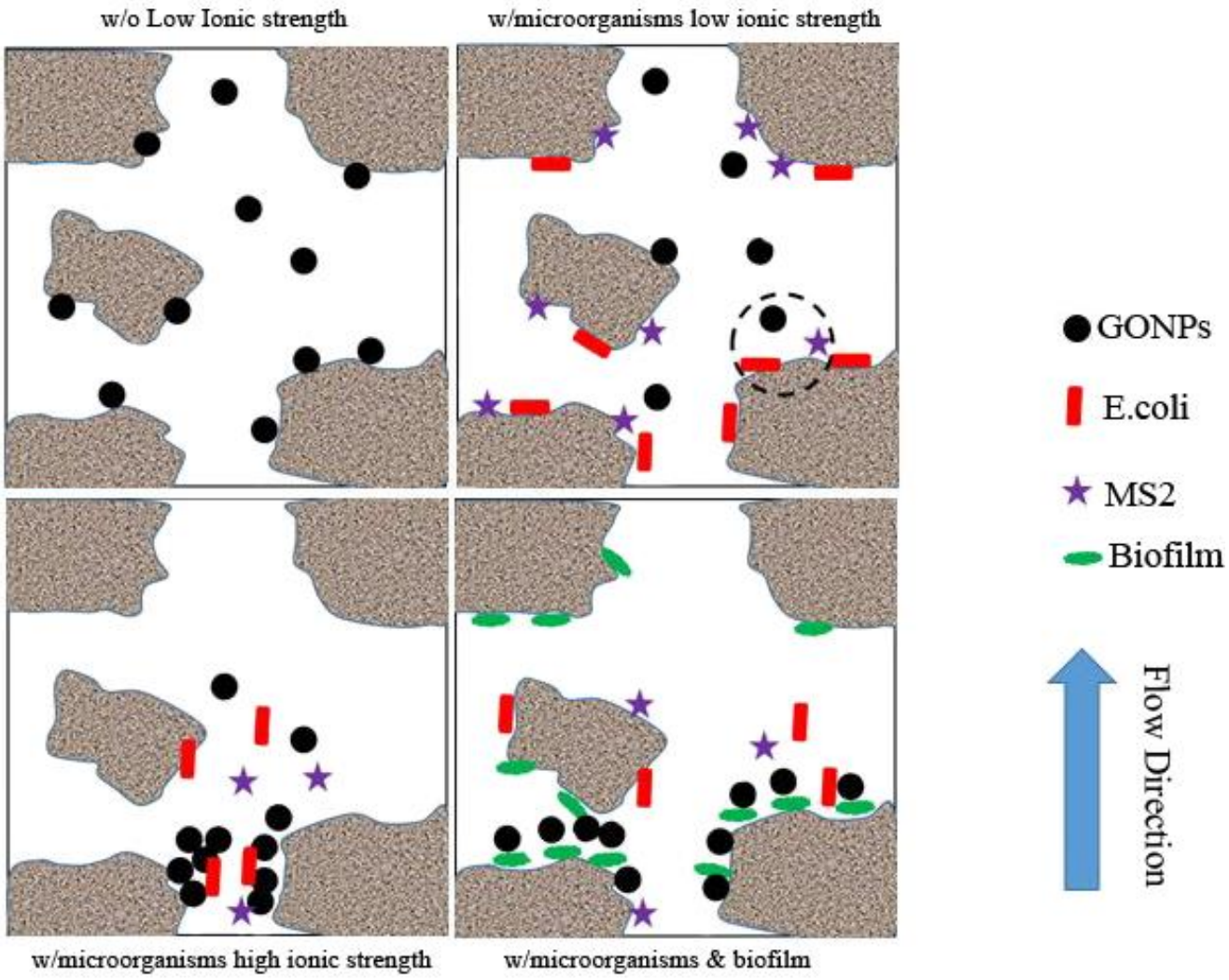

Graphical abstract

6.1. Highlights

- Biofilms reduce transport of graphene oxide nanoparticles (GONPs) in porous media.
- At high ionic strength, GONPs co-transported with microorganisms was not changed.
- At low ionic strength, GONPs co-transported with microorganisms was enhanced.
- Pre-saturation of porous media with microorganisms enhanced transport of GONPs.

This Chapter is based on the following publication: Amirhosein Ramazanpour Esfahani, Okke Batelaan, John L. Hutson and Howard J. Fallowfield. Effect of bacteria and virus on transport and retention of graphene oxide nanoparticles in natural limestone sediments. Chemosphere (Volume 248, 2020, 125929) (DOI: https://doi.org/10.1016/j.chemosphere.2020.125929).

6.2. Abstract

This research was conducted to evaluate the effect of co-transport of different-sized microorganisms on graphene oxide nanoparticles (GONPs) transport and retention in saturated pristine and biofilm-conditioned limestone columns. The transport and retention behavior of GONPs was studied in columns in the presence of MS2 -as a nano-sized- and *Escherichia coli* (*E.coli*) -as a micro-sized- microorganisms at low and high ionic strength conditions. Results showed no changes in GONPs transport and retention at high ionic strength in the presence of MS2 or *E.coli*, which was attributed to the effect of the high concentration of divalent cation on aggregation of nanoparticles and microorganisms. Furthermore, simultaneous enhanced transport and decreased retention of GONPs in column was observed in the co-presence of microorganisms at low ionic strength. Results revealed that the main mechanism governing increasing GONPs transport in porous media was occupation of reactive surface sites of collectors by microorganisms, which prevented attachment of nanoparticles. The pre-saturation of columns with MS2 and *E.coli* caused increasing transport of GONPs in the columns, due to the occupation of surface reactive sites. In addition, at low ionic strength conditions, the size-distribution of retained nanoparticles was not changed throughout the column. Moreover, conditioning limestone collectors with natural biofilm resulted in the same eluted nanoparticle rates (i.e., in the presence or absence of microorganisms) by straining of GONPs in the inlet end of columns which shows that the biofilm acts as a bio-filter against discharging nanoparticles into the effluents. Finally, from the obtained results, it can be postulated that the presence of microorganisms in a MAR site causes risk of groundwater pollution by toxic nanoparticles.

6.3. Introduction

Groundwater is one of the essential components of water resources which is extensively used in agricultural, domestic and manufacturing activities. Managed aquifer recharge (MAR), defined as the storage of excessive water in the subsurface environment for subsequent reuse, has been proposed as a promising technique to compensate groundwater shortage (Zhang et al., 2015a). MAR has been widely used in different parts of the world such as Australia, the United States, the Netherland and Israel (Rinck-Pfeiffer et al., 2000). However, in some cases, the injected water for MAR has several chemical and physical components that may have negative effects on the hydrochemistry of groundwater resources and cause pathogenic and engineered nanoparticle contamination (Vanderzalm et al., 2010).

Like other nanoparticles, large amounts of graphene oxide (GO) have been discharged into soil and water resources from manufacturing, application and disposal processes. Several studies have shown the ability of graphene oxide nanoparticles (GONPs) to transport organic pollutants and heavy metals in soil, leading to groundwater contamination (Qi et al., 2014a, Qi et al., 2014b, Ding et al., 2014). Furthermore, the toxicity of GONPs to the environmental resources and human health being has been documented in the literature (Hu et al., 2011, Akhavan and Ghaderi, 2010, Singh et al., 2011).

In recent years, there has been widespread attention on transport and retention of GONPs in porous media. GONPs transport can be affected by a wide spectrum of environmental factors such as flow rate, initial particle concentration, organic matter, ionic strength and composition and porous media size distribution (Xia et al., 2015, Chen et al., 2018). The majority of studies on GONPs transport only focused on single transport of nanoparticles in porous media, which is unrealistic in a natural aqueous environment. Potentially, there are a wide range of organic and inorganic

colloids in the subsurface environment that could have an interaction with GONPs transport and retention.

Recently, the co-present effect of various colloidal particles on nanoparticle transport has drawn great attention. Chowdhury et al., (2012) found a decrease in TiO_2 retention affected by bacteria in glass bead columns due to the effect on electrosteric and electrostatic forces (Chowdhury et al., 2012). Similarly, enhanced transport of plutonium colloids in porous media was observed when smectite clay particles were in the suspension (Abdel-Fattah et al., 2013).

The size and surface features of colloidal particles are two important factors affecting nanoparticle retention. In the subsurface environment, different-sized colloids ranging from nano to micro are ubiquitous. May and Li, (2013) reported varying retention rates for colloidal particles of differing sizes (May and Li, 2013). He et al., (2018) showed that nano and micro-sized plastic particles had varying influences on the deposition of bacteria in sand-packed columns (He et al., 2018). Most studies on co-transport experiments were performed in clean sand or glass bead columns, which are largely unrepresentative of natural aquifers. Natural aquifer sediments contain large quantities of metal oxide/hydroxides, which provide favorable attachment sites for particle deposition (Fisher-Power and Cheng, 2018). Therefore, the co-transport of nanoparticles with microorganisms in native aquifer materials requires investigation.

Currently, the co-transport of GONPs with inorganic particles such as carboxylate-modified polystyrene latex microspheres with different size distributions has been reported (Peng et al., 2017), which is not representative of microorganisms present in the natural subsurface environment. Therefore, in order to simulate natural groundwater conditions, different-sized microorganisms such as the F-RNA coliphage MS2 and *E.coli* were used to study co-transport behavior of GONPs. To the best of our knowledge, this is the first research that focuses on the role

of microorganisms on transport and retention of GONPs in porous media. Uniquely, our cotransport study uses natural limestone sediments, permitting a more relevant assessment of the potential risk of toxicity of nanoparticles in water reused following storage and transport in carbonaceous aquifers.

6.4. Results and discussion

6.4.1. Porous media characterization

XRD diagram of limestone sediments is represented in Fig 6-1 a which shows that sediments mainly consisted of calcite and insignificant amounts of dolomite and quartz. Furthermore, the results of XRF analysis revealed that the limestone sediments contained 46.41 % CaO, 9.59 % SiO_2, 2.84 % MgO, 1.63 % Fe_2O_3, 0.41 % Al_2O_3, 0.21 % K_2O, 0.20 % SO_3, 0.07 % Na_2O, 0.03 % MnO, 0.02 P_2O_5 and 38.56 % loss on ignition. The major ion composition of the aquifer materials (Fig 6-1 b) was O, Ca, C, Mg and Si. The FTIR spectrum of limestone sediments (Fig 6-1 c), shows a sharp peak in 1404.32 cm^{-1} absorption region which can be ascribed to the calcite. Furthermore, the slight peak in the absorption range of 1000-1200 cm^{-1} was attributed to the presence of quartz in the structure of limestone grains. No significant peak was observed in the absorption region 700 cm^{-1} suggesting little magnesium was present.

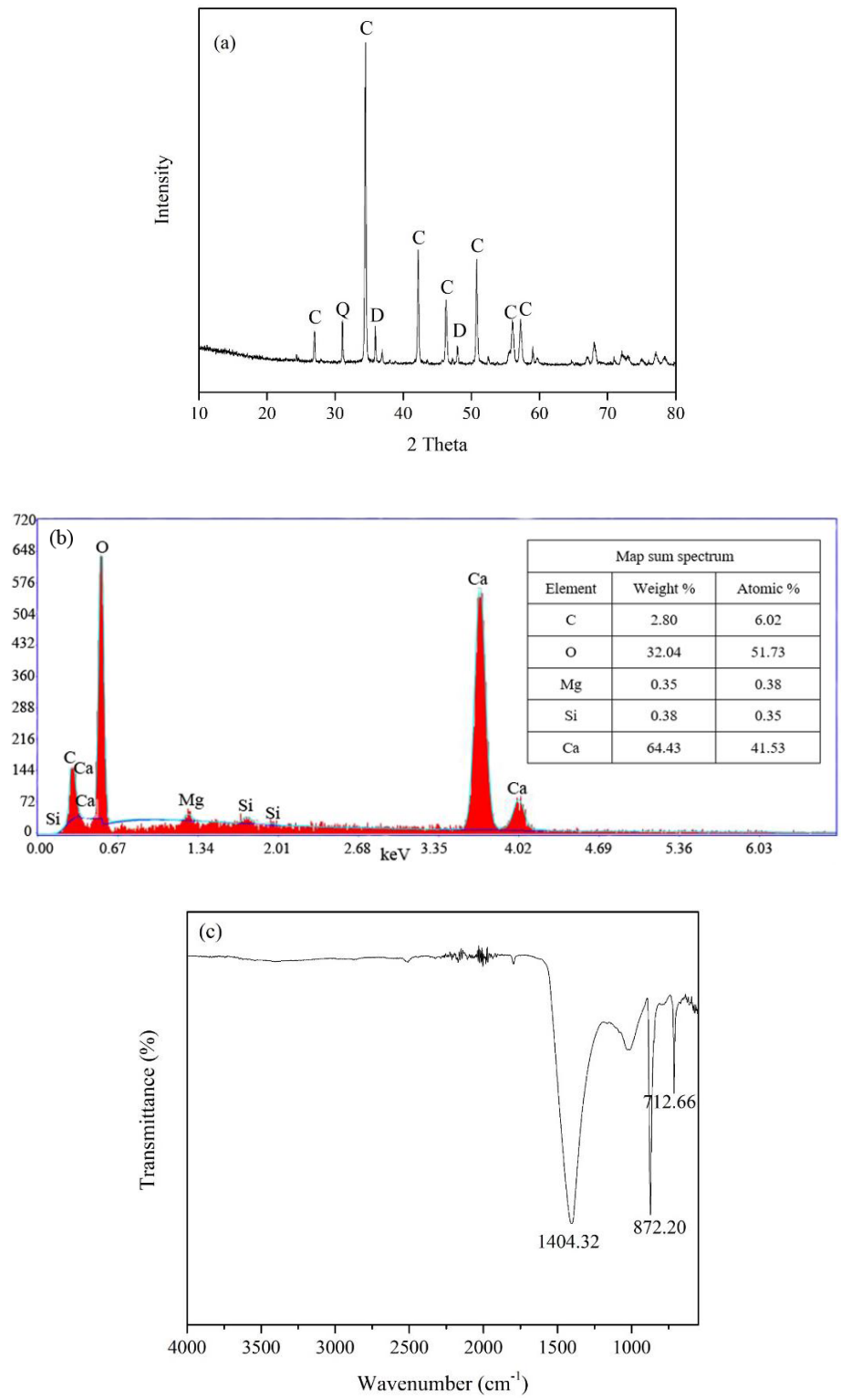

Fig 6-1. XRD diagram (a), EDS (b) and FTIR spectra (c) of limestone aquifer materials (C: calcite, Q: quartz and D: dolomite).

6.4.2. GONPs stability in the presence and absence of microorganisms

The results of GONPs stability at 10 mM NaCl and 5 mM $CaCl_2$ as representatives of low and high ionic strengths, respectively are reported in Fig 6-2 based on Abs/Abs_0 (226 nm) against time (min). GONPs showed relatively good stability at low ionic strength, with decrease to approximately 0.90 at the end of the experiments. However, at high ionic strength, a sharp decrease was observed in GONP stability from 1 to 0.3 over 3 h. Wu et al., (2013) reported high stability of GONPs in a solution containing Na^+ (Wu et al., 2013). The main mechanism of GONPs aggregation was charge screening resisting the proton separation from GONPs surfaces via the electric field produced by free ions in aqueous media. However, the presence of Ca^{2+} in the solution caused enhanced aggregation kinetics of GONPs, due to the sum of charge screening of surfaces of GONPs and interaction with surface functional groups for cross-linking. Furthermore, at both ionic strengths, the presence of microorganisms did not change the colloidal stability status of nanoparticles. The photographs of GONPs vials with and without microorganisms (Fig 6-2 c and d) show the low stability of nanoparticles at high IS, which led to the creation of large aggregate. In contrast, the stability of the nanoparticles in the respective treatment were similar irrespective of the presence of microorganisms.

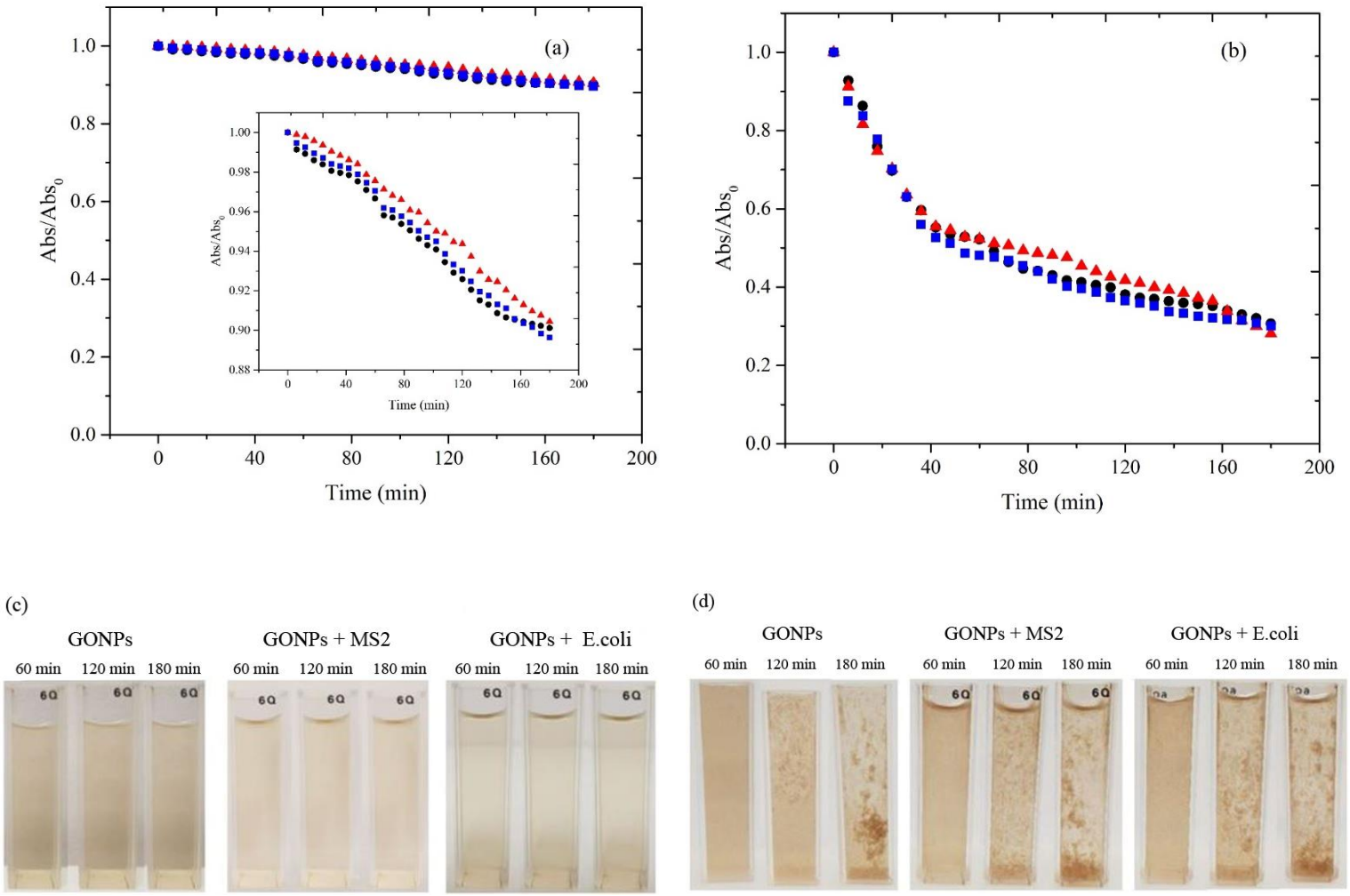

Fig 6-2. Sedimentation curves (a and b) and photographs showing colloidal stability (c and d) of GONPs either individual or in the presence of MS2 and *E.coli* at 10 mM NaCl (left) and 5 mM $CaCl_2$ (right) (●: individual GONPs, ▲: GONPs + MS2 and ■: GONPs + *E.coli*). The results of sedimentation curves are based on the ratio of the absorbance of GONPs suspensions at time t and initial GONPs absorbance at 226 nm wavelength using a UV-visible spectrophotometer. (The insert figure represents the Y-axis data plotted in the range of 0.88-1).

6.4.3. Transport of GONPs in the presence of *E.coli* and MS2 in favorable and unfavorable attachment conditions

In order to determine the role of microorganisms on transport and retention of GONPs in limestone aquifer sediments, the experiments were carried out in electrostatically favorable, high ionic strength (5 mM $CaCl_2$), attachment conditions. According to Fig 6-3 a, the descending shape of BTCs of GONPs was observed in either the presence or absence of microorganisms. This was attributed to the role of ripening on GONPs retention in porous media by which the attached particles act as further attachment sites for suspended particles. Furthermore, the C_{max}/C_0 of GONPs in the presence of both MS2 and *E.coli* were similar to the control treatments in the absence of these microorganisms. 5.96 % of GONPs were recovered in individual suspension, whereas in the presence of MS2 and *E.coli* in the suspension 7.09 and 6.63 % of GONPs were recovered, respectively. This observation confirms that the presence of MS2 or *E.coli* in the suspension of GONPs at high ionic strength did not change the retention behavior of GONPs. The high attachment of nanoparticles onto the surfaces of collectors at high ionic strength has been previously reported in the literature (Kamrani et al., 2018, Adrian et al., 2018). This phenomenon is due to the enhanced compression of the electrostatic double layer on the collector surfaces. This has a direct relationship with changes in DLVO interaction energies between nanoparticles and porous media collectors. Increasing attachment rate of colloidal particles with an enhancement in the ionic strength of the solution has been ascribed to increasing primary and secondary energy minima (Tufenkji and Elimelech, 2005a).

The retention profiles (RPs) of GONPs in the presence and absence of MS2 or *E.coli* are presented in Fig 6-3, as the relative concentration (C/C_0) of GONPs per unit mass of collector (g) plotted against distance from inlet end (cm). Similar to the results of transport experiments, no significant

differences were observed between the retention profiles of GONPs in the presence or absence of MS2 or *E.coli*. This shows a lack of effect of the co-presence of these microorganisms in the suspension on the transport and retention behavior of GONPs. Accordingly, a hyper-exponential curve was obtained for RPs of GONPs both in the presence and the absence of MS2 or *E.coli*. The most likely explanation is pore throat straining of nanoparticle aggregates at the inlet end of column and ripening, which showed a decreasing trend with distance from the injection point. Chen et al., (2018) also attributed the hyper-exponential curve of the RP for GONPs at 50 mM NaCl to pore throat straining of nanoparticles in porous media (Chen et al., 2018). The straining can be caused when the ratio of diameters of nanoparticles to collectors is ≥0.002 (Torkzaban et al., 2008a). In this study, the measured hydrodynamic diameter (D_H) of the GONPs at high ionic strength conditions was 1826.66 ± 735 nm and the size distribution of collector is 0.25-0.50 mm which will give the ratio of 0.005 against the collector surfaces. It is worth noting that the presence of either MS2 or *E.coli* did not affect the amount of nanoparticles retained onto the surfaces of collectors, which may be because of the role of ionic strength on aggregation of the microorganisms in solution.

Transport and retention experiments of GONPs in aquifer sediments with and without MS2 or *E.coli* were carried out at low ionic strength (10 mM NaCl), which is electrostatically unfavorable for GONPs retention (Fig 6-3 b). The BTCs of GONPs were ascending which show lower GONPs retention by continuing the injection of nanoparticles (Fig 6-3 b). The ascending trend of BTCs of GONPs has been attributed to the blocking, which always produces an increase in the relative concentrations of nanoparticles in the effluents because of filling surface attachment sites (Adrian et al., 2018). Similar research has also reported the role of blocking on retention of GONPs onto the surfaces of collectors (Liang et al., 2019, Dong et al., 2017). However, lower GONPs retention

was observed at low ionic strength, which is explained by the more negative values of zeta potentials of collectors and colloidal particles at lower ionic strength. Indeed, the negative zeta potentials of collectors, nanoparticles, MS2 and *E.coli* demonstrate the electrostatic repulsive forces between colloidal particles and collectors. Previous studies have shown higher particle retention in porous media by increasing the ionic strength (Esfahani et al., 2014, Chowdhury et al., 2011). In addition, at low ionic strength, higher GONPs transport was observed in the presence of MS2 and *E.coli*, compared to the control treatments. Cotransport of MS2 and *E.coli* with GONPs, increased the recovered percentage of GONPs from 44.96 % in their absence to 60.08 and 57.04 %, respectively. Overall, at low ionic strength conditions, the co-presence of MS2 and *E.coli* with nanoparticles enhanced their transport in porous media, which will be discussed below.

The RPs of GONPs were obtained at low ionic strength to investigate the effect of MS2 or *E.coli* on GONPs retention rate. The quantity of retained nanoparticles was opposed their BTCs, the presence of MS2 or *E.coli* in low ionic strength solution reduced the retention of GONPs. In contrast to the high ionic strength conditions (above) the shape of the curve for retained GONPs in the absence of MS2 or *E.coli* was linear (Fig 6-3 a). This observation shows that different mechanisms govern particle retention in low and high ionic strength conditions. The presence of MS2 or *E.coli* in the nanoparticle suspension led to a decrease in their retention in porous media.

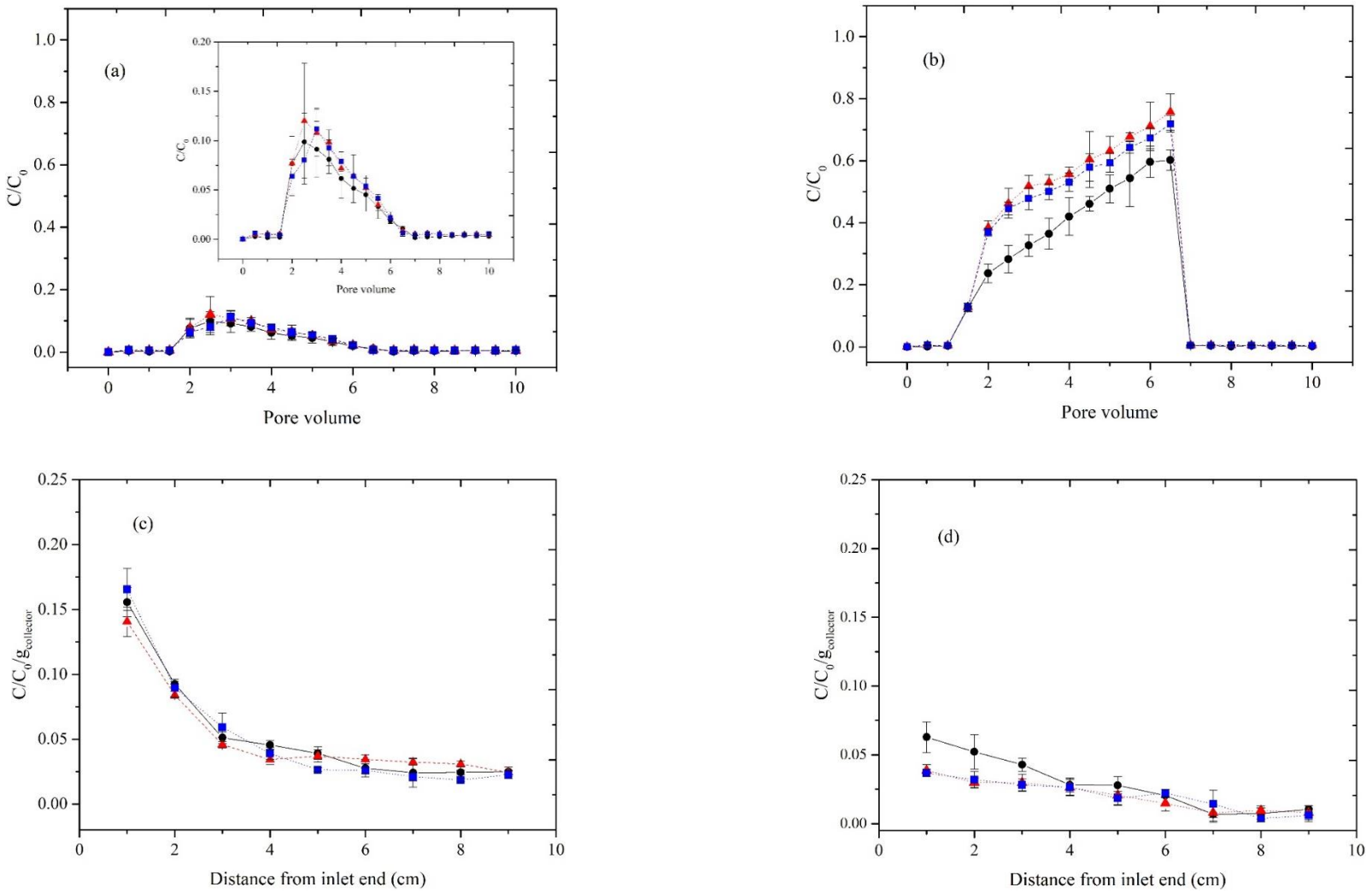

Fig 6-3. Breakthrough curves (a and b) and retention profiles (c and d) of GONPs in the presence and absence of MS2 and *E.coli* in saturated limestone-packed column at high (left) and low ionic strength (right) (●: individual GONPs, ▲: GONPs + MS2 and ■: GONPs + *E.coli*) (experimental conditions: pH: 7.5, flow velocity: 5 m/day and temperature: 22 °C). (The insert figure in Fig 6-3a represents the same figure with Y-axis range of 0-0.2).

Table 6-1. Mass balance calculations of GONPs in pristine and biofilm-conditioned porous media with and without co-presence of microorganisms.

Number	Treatment	Solution	Porous media	Zeta potentials (mV)		Mass balance			
				GONPs	Collectors	M_{eff} (%)	M_{ret} (%)	M_{loss} (%)	C_{max}/C_0
1	GONPs	10 mM NaCl	Pristine	-31.3±0.5	-17.2±3.4	44.96	48.39	6.65	0.60
2	GONPs + MS2	10 mM NaCl	Pristine	-32.7±0.6	-17.2±3.4	60.08	34.59	5.32	0.75
3	GONPs + *E.coli*	10 mM NaCl	Pristine	-34.3±1.4	-17.2±3.4	57.04	35.30	7.65	0.71
4	GONPs	10 mM NaCl	Pre-MS2	-31.3±0.5	-17.2±3.4	60.40	35.11	4.49	0.77
5	GONPs	10 mM NaCl	Pre-*E.coli*	-31.3±0.5	-17.2±3.4	56.16	38.49	5.35	0.71
6	GONPs	5 mM $CaCl_2$	Pristine	-4.6±3.9	-10.4±2.4	5.96	91.30	2.74	0.09
7	GONPs + MS2	5 mM $CaCl_2$	Pristine	-6.5±0.4	-10.4±2.4	7.09	87.14	5.76	0.12
8	GONPs + *E.coli*	5 mM $CaCl_2$	Pristine	-8.7±0.4	-10.4±2.4	6.63	88.23	5.14	0.11
9	GONPs	5 mM $CaCl_2$	Pre-MS2	-4.6±3.9	-10.4±2.4	6.61	85.80	7.59	0.12
10	GONPs	5 mM $CaCl_2$	Pre-*E.coli*	-4.6±3.9	-10.4±2.4	5.67	85.68	8.65	0.08
11	GONPs	10 mM NaCl	Biofilm-conditioned	-31.3±0.5	-13.5±1.6	19.44	-	-	0.20
12	GONPs + MS2	10 mM NaCl	Biofilm-conditioned	-31.3±0.5	-13.5±1.6	23.47	-	-	0.23
13	GONPs + *E.coli*	10 mM NaCl	Biofilm-conditioned	-31.3±0.5	-13.5±1.6	21.82	-	-	0.21

6.4.4. Mechanisms governing on GONPs retention

Previous research has shown the effect of colloidal particles on the agglomeration status of the other suspended colloids, which has a direct relationship with transport and deposition behavior in porous media. Chowdhury et al., (2012) reported enhanced TiO_2 dispersion in solution in the presence of *E.coli* at pH 5 and 10 mM KCl (Chowdhury et al., 2012). However, by increasing solution pH to 7, no changes were observed in the aggregation status of TiO_2 by *E.coli*. In our study, GONPs, *E.coli* and MS2 had negative zeta potential values, which may potentially affect the aggregation status of GONPs through enhanced dispersion and transport in the columns. Table 6-1 shows that the co-presence of *E.coli* and MS2 in the suspension did not change significantly the zeta potentials of GONPs. In fact, the zeta potentials of GONPs, together with MS2 and *E.coli* at low ionic strength were -31.3±0.5, -32.7±0.6 and -34.3±1.4 mV, respectively. Furthermore, SEM images of GONPs size and morphology, either individually or affected by *E.coli* or MS2, are shown in Fig 6-4. Nanoparticles were aggregated in high ionic strength solution and the co-presence of *E.coli* or MS2 in the suspension did not change their aggregation status. In addition, a similar trend was observed for low ionic strength solution in which the aggregation status of individual GONPs, together with *E.coli* or MS2 were relatively similar, which shows that the aggregation status of nanoparticles is independent of the co-presence of *E.coli* or MS2. Therefore, other mechanisms would influence enhanced transport of GONPs affected by the *E.coli* or MS2. The hydrodynamic diameter (D_H) of retained GONPs were larger in the suspension at high ionic strength, potentially due to enhanced aggregation of nanoparticles, caused by a decrease in the electrostatic double layer.

The changes in the D_H of GONPs were derived from changing the zeta potentials of nanoparticles, which has a significant effect on particle dispersion in solution. The zeta potential of individual GONPs was -4.6±3.9, while in the presence of MS2 and *E.coli* were obtained -6.5±0.4 and -8.7±0.4 mV, respectively. However, at low IS, the GONPs zeta potential was more negative, predicating fewer retained GONPs in a low ionic strength solution compared with a high ionic strength solution. Furthermore, at low IS, the size of retained nanoparticles did not significantly change with increasing distance from the column inlet and a uniform trend throughout the column was observed for D_H of retained nanoparticles. Apart from the shapes of BTCs and RPs of nanoparticles, the relatively uniform distribution of retained nanoparticles reveals the role of blocking of nanoparticles (increasing particle transport by passing time) in the column. However, at high IS, a very different trend was observed (Fig 6-5) shows the D_H of retained nanoparticles decreased from 5147.3 nm at the column inlet (0-1cm) to 1858.7 nm 8-9cm from the inlet. The size-selective retention of nanoparticles in porous media shows the dominant mechanism of particle deposition in high IS solutions. At high ionic strength, the decreasing trend in the diameter of retained nanoparticles is a good index of the influence of aggregation, ripening and physical straining on the deposition of nanoparticles. Jiang et al., (2012) reported a decrease in the diameter of retained nanoparticles in sand grains as the distance from inlet end increased, which was attributed to the aggregation and straining of nanoparticles (Jiang et al., 2012). Straining is defined as colloidal particle trapping in a pore throat which prevents passage of the particles (McDowell-Boyer et al., 1986). Considering the size distribution of collectors (0.25-0.50 mm) and the ratio of colloidal particles to collectors, the physical straining in porous media was significant only in the high ionic strength solution.

The cotransport of colloidal particles can either increase or decrease the transport of the other colloidal particles in porous media. Previous research revealed that colloidal particles such as nanoparticles (Cai et al., 2013), humic acid (Wang et al., 2008) and anions (Wu et al., 2010) in suspension compete with each other to occupy surface reactive sites of collectors and caused enhanced transport of the colloids in porous media. Liu et al., (2015) reported the role of cetyl trimethylammonium bromide (CTAB) ion in increasing transport of graphene oxide in porous media, through competition by occupying reactive surface sites (Liu et al., 2015). In contrast, higher retention of carboxylate-modified polystyrene latex microspheres occurred after pre-equilibration of sand grains with GONPs, since the number of attachment sites increase following deposition of GONPs (Peng et al., 2017).

E.coli or MS2, when cotransported with GONPs, may occupy active surface sites, which either prevent GONPs retention or act as additional surface sites to enhance GONPs deposition. So, decreasing surface reactive sites of collectors occupied by *E.coli* or MS2 would lead to enhanced transport of graphene oxide in columns. Higher IS of solution also leads to greater retention of *E.coli* or MS2, therefore it is expected there would be enhanced GONPs transport with concomitant decreases in retention in a high ionic strength solution in porous media covered with *E.coli* or MS2. To test this hypothesis, a column was pre-saturated with 5 PVs of *E.coli* or MS2, followed by injection of 5 PVs GONPs and 5 PVs background solution. Columns pre-saturated with *E.coli* or MS2, in comparison with pristine column, followed by the injection of individual nanoparticle suspension gave enhanced recovered and less retained GONPs.

The results of experiments where columns containing limestone substrate were pre-equilibrated with *E.coli* or MS2 at high and low IS are reported in Fig 6-6. As can be seen, the higher BTCs were observed for GONPs in pre-equilibrated columns with *E.coli* or MS2, compared to the

pristine column. At low IS, the C_{max}/C_0 of GONPs in pristine and pre-equilibrated columns with MS2 and *E.coil* are 0.60, 0.77 and 0.71, respectively. Furthermore, the retention profiles of GONPs in columns with and without pre-equilibration were similar, indicating similar mechanisms contributing in particle retention. The results revealed the role of blocking of surface sites of collectors by *E.coli* or MS2 on increasing transport of GONPs through the columns. However, at high IS, pre-equilibration of columns with *E.coli* or MS2 did not cause a significant change in transport and retention behavior of GONPs. The BTCs and transport behavior of MS2 and *E.coli* at both IS are reported in Fig 6-7. The majority of *E.coli* or MS2 were attached onto the surfaces of collectors, which may be due to the surface attachment to metal oxide/hydroxides. At low ionic strength, 96.47 and 82.12% of MS2 and *E. coli* were retained in collectors, respectively. However, at high ionic strength, 99.93 and 99.53% of MS2 and *E. coli*, were retained, respectively Foppen and Schijven, (2005) showed that the presence of only 5 % calcite in sand-packed columns decreased the C_{max}/C_0 of *E.coli* to 0.15 (Foppen and Schijven, 2005). In high IS solution, a sharp increase in the retention of *E.coli* and MS2 was observed, which was due to the role of different mono and divalent cations on compression of electrostatic double layer. Although more retention sites were occupied by *E.coli* or MS2, the eluted GONPs in high IS were less than low IS solution, due to the aggregation behavior of GONPs in solutions of different ionic strength, which has a significant influence on their transport in porous media. Furthermore, comparing the transport behavior of GONPs and *E.coli* or MS2 revealed that the microorganisms had higher retention rates than the nanoparticles, which demonstrates the occupation of surface reactive sites of collectors by these microorganisms. Consequently, the opportunity for GONPs to be retained onto the collector surfaces was decreased, in the copresence of *E.coli* or MS2 in the suspension.

Although both microorganisms enhanced transport of GONPs in porous media in unfavorable attachment conditions, the relative size of microorganisms did not have a significant influence on the intensity of GONPs transport. Indeed, MS2 and *E.coli* led to 15.12 and 12.08 % increase in percentage recovered mass of GONPs in the effluents, respectively. However, contrasting results have been reported by Cai et al., (2016) where the application of 0.2 and 2 μm colloidal particles caused 24 and 7 % enhancement in the transport of $nTiO_2$ in sand-packed columns (Cai et al., 2016). The effect of size of co-transported particles on the retention of nanoparticles is beyond the scope of this study.

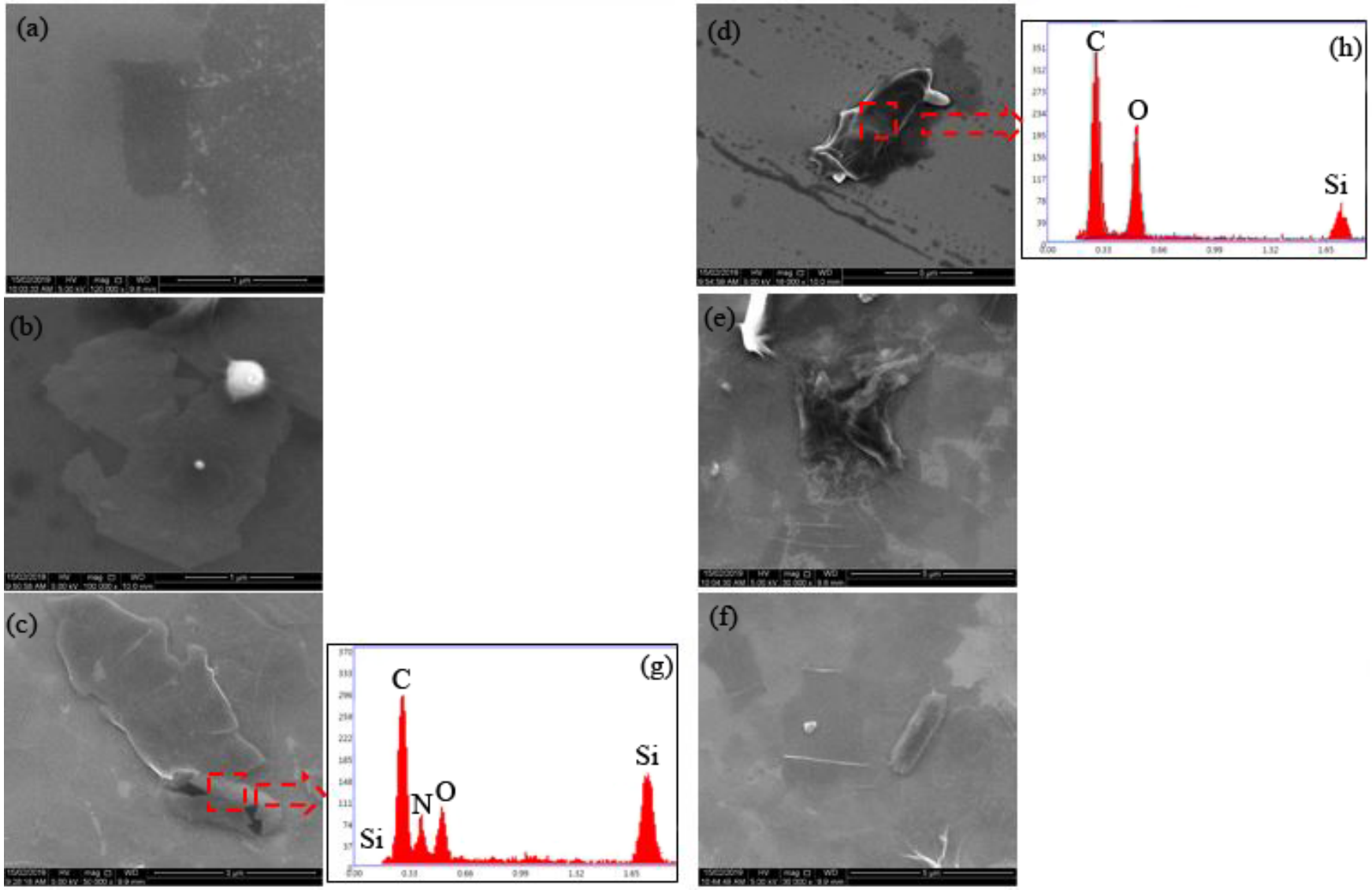

Fig 6-4. SEM images of (a) individual GONPs (b) GONPs + MS2, (c) GONPs + E.coli at low ionic strength and (d) individual GONPs, (e) GONPs + MS2 and (f) GONPs + E.coli at high ionic strength, (g) EDS spectrum of E.coli and (h) EDS spectrum of GONPs.

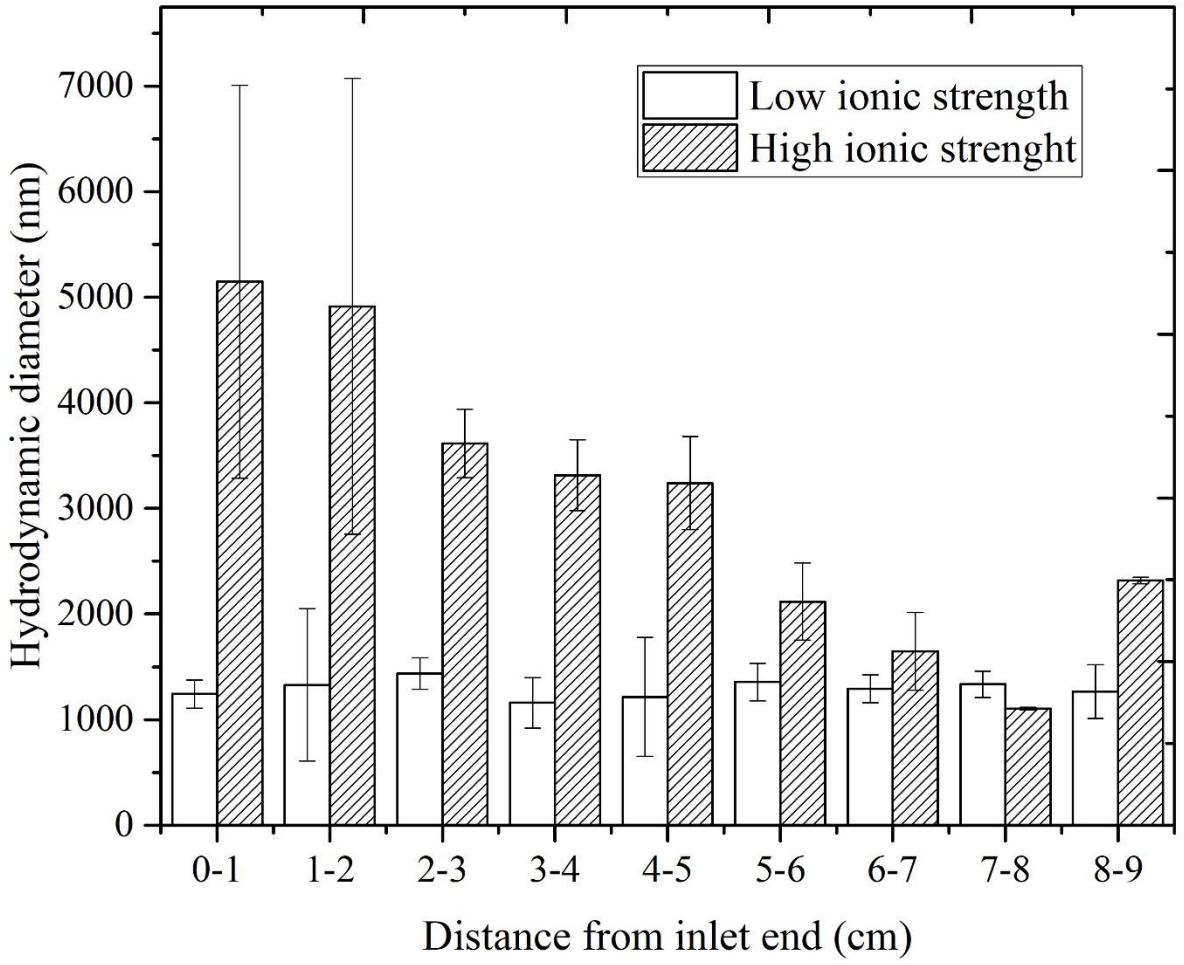

Fig 6-5. Size distribution of retained GONPs at different distance from column inlet end at low and high ionic strength conditions.

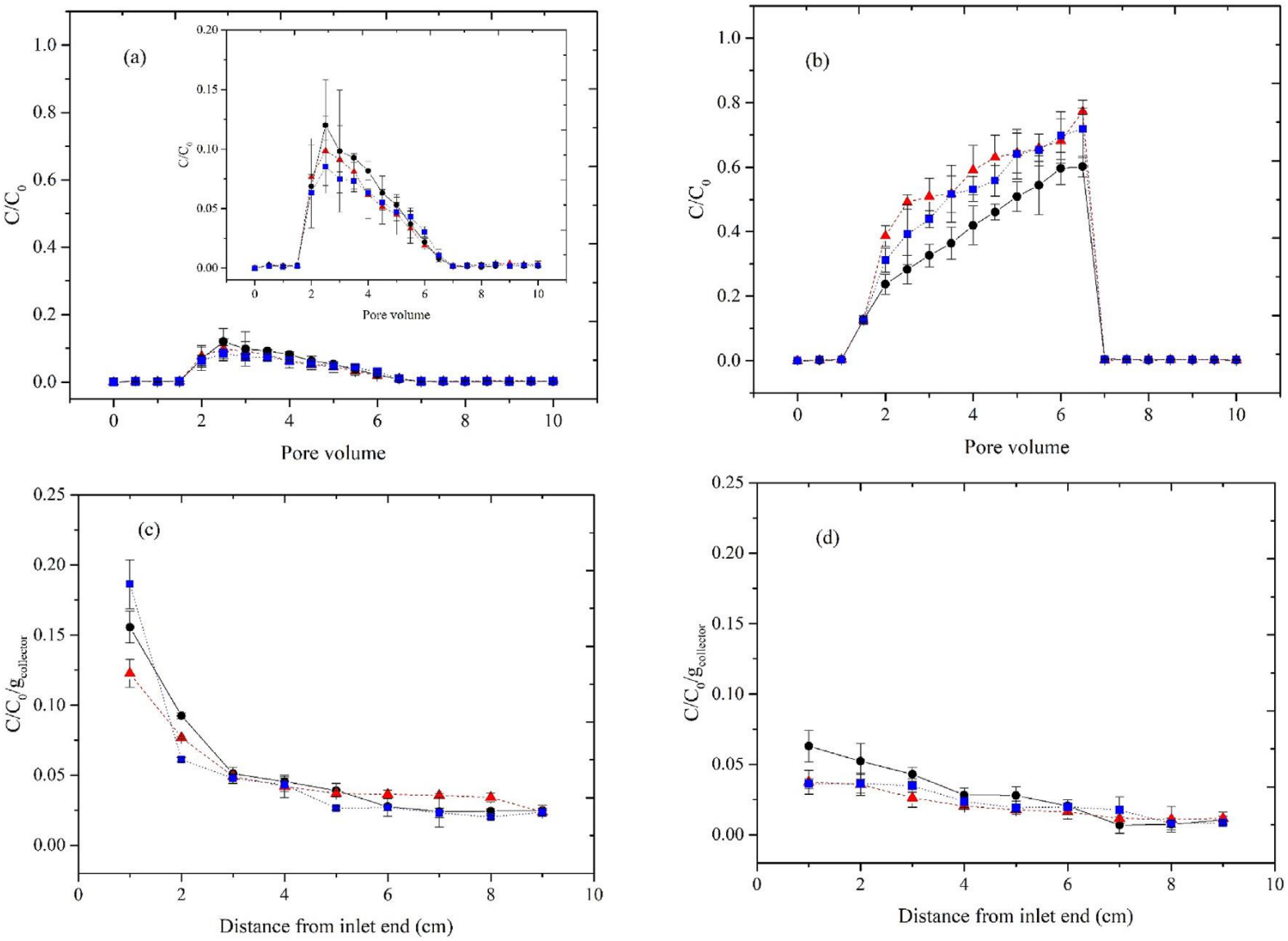

Fig 6-6. Breakthrough curves (a and b) and retention profiles (c and d) of GONPs at high (left) and low (right) ionic strength conditions pre-equilibrated with MS2 and *E.coli* (●: individual GONPs, ▲: GONPs + MS2 and ■: GONPs + *E.coli*) (experimental conditions: pH: 7.5, flow velocity: 5 m/day and temperature: 22 °C). (The insert figure in Fig 6-6a represents the same figure with Y-axis range of 0-0.2).

.

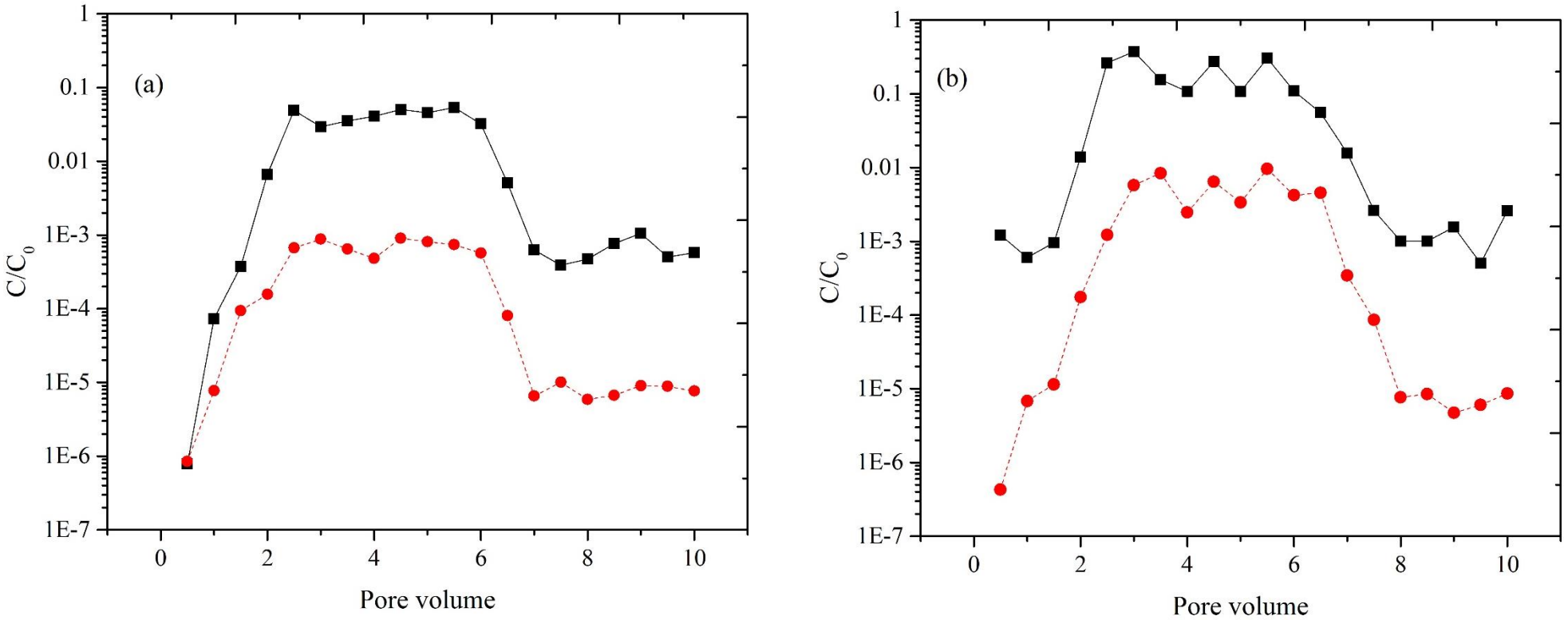

Fig 6-7. Breakthrough curves (BTCs) of (a) MS2 and (b) *E.coli* in limestone packed columns at low and high ionic strength conditions. (■ low ionic strength and ● high ionic strength); experimental conditions: pH: 7.5, flow velocity: 5 m/day, temperature: 22 °C, initial MS2 concentration: 10^7 PFU/mL and initial *E.coli* concentration: 10^8 MPM/100 mL.

6.4.5. Co-transport of MS2 and *E.coli* with GONPs in biofilm-conditioned porous media

GONPs transport experiments were performed with and without MS2 and *E.coli* in biofilm-conditioned porous media in low ionic strength conditions. The BTC of GONPs is reported in Fig 6-8 which shows that the presence of different-sized microorganisms had a negligible influence on transport behavior of GONPs in biofilm-conditioned porous media. Specifically, the co-presence of MS2 and *E.coli* in GONPs suspension slightly increased nanoparticle mass percentage recovery from 19.44 % to 23.47 and 21.82 %, respectively. It is obvious that the presence of biofilm caused higher GONPs retention, in comparison with pristine porous media.

One of the reasons for high GONPs retention in the biofilm-conditioned columns was the charge neutralization of limestone grains by the conditioning biofilm. The presence of biofilm decreased the zeta potential of collectors, which led to compression of electrostatic double layer of collectors and increasing GONPs attachment. Furthermore, changes in the surface irregularities of porous media grains, due to the biofilm growth has a significant influence on GONPs retention in porous media. Biofilm increased the surface roughness and irregularities of limestone, which provides suitable positions for trapping nanoparticles, even in unfavorable electrostatic attachment conditions. The SEM images of pristine and biofilm-conditioned limestone grains are represented in Plate 6-1, which shows the rougher surfaces of biofilm-conditioned limestone, compared to the control treatment, which can be ascribed to the production of microbial mass. The presence of biofilm is clearly demonstrated in the CLSM images. The 3-dimensional (3D) images of pristine and biofilm-conditioned limestone grains are shown in Plate 6-2. The biofilm distribution on the surfaces of the substrate was heterogeneous. Furthermore, the amount of microbial mass around

pristine limestone grains was small confirmed by the very thin layer of fluorescent. In contrast, the layer of fluorescent around the biofilm-conditioned limestone grains was very thick (Plate 6-2 b) confirming the development of biofilm onto the surfaces of substrate, derived from incubation with the treated wastewater.

Moreover, another possible cause for the high GONPs retention at the inlet end of column may be the growth and proliferation of natural biofilm derived from treated wastewater, which attached onto the surfaces of collectors and filled pore vacancies. In order to demonstrate the production of biofilm by treated wastewater, the amount of produced biomass was measured and the results reported in Fig 6-9. The quantity of biofilm at the inlet end of columns was higher than the other parts, which showed a decreasing trend with increasing distance from the column inlet. The significant quantities of biofilm in the column inlet were likely due to the abundance of oxygen and nutrients (e.g., N, P, C) at the inlet end of columns, which stimulated biofilm growth. The ratio of nanoparticles to collector grains is lower than threshold for straining (see above), indicating an insignificant effect of straining on particle retention in pristine porous media. Therefore, the role of straining was of significance in the biofilm-conditioned porous media compared to the pristine media, due to the biological clogging of porous media by biofilm growth and proliferation in pore vacancies, confirmation of production of biofilm into the column was further provided by FTIR spectra of limestone grains after conditioning with treated wastewater Fig 6-10. The peak at the 1641.3 cm^{-1} absorption band shown in the spectrum of biofilm-conditioned limestone obtained from 0-1 cm at the inlet end is ascribed to the protein. However, the other sections of the columns did not show a significant peak in the same absorption band, suggesting less biomass was produced in these sections in the presence of treated wastewater. The results of FTIR analysis confirmed the

presence of higher biomass in the column inlet, compared to the other parts of column which led to the higher retention of GONPs close to the inlet end of column.

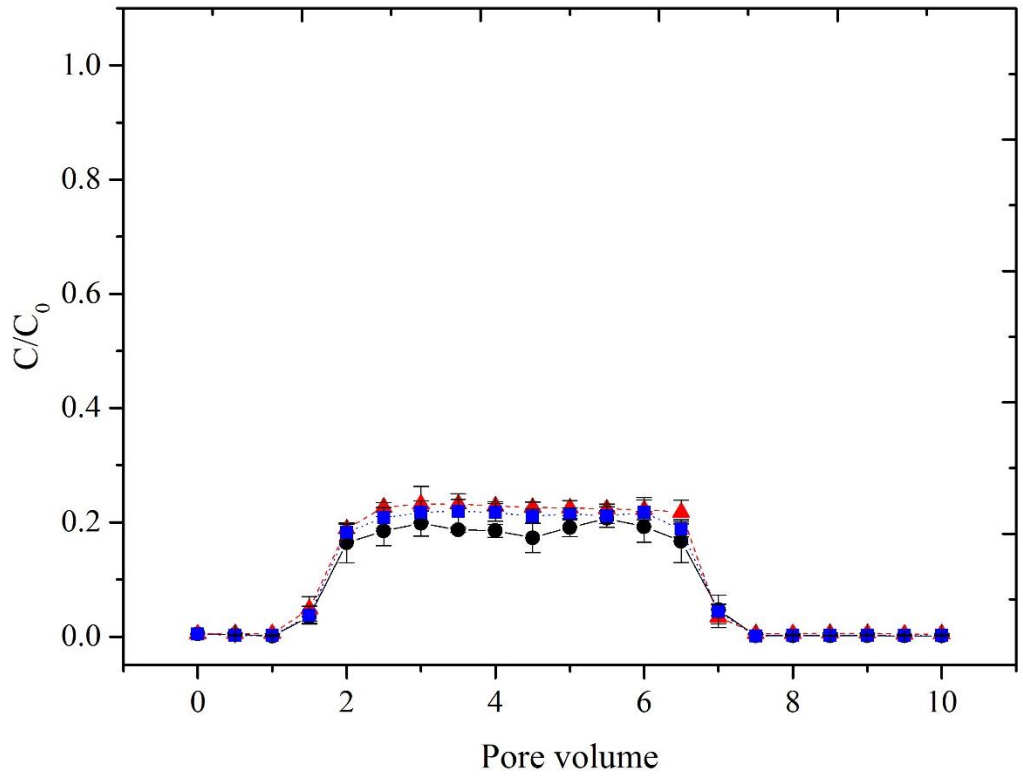

Fig 6-8. Breakthrough curves of GONPs in the presence or absence of MS2 and *E.coli* in biofilm-conditioned limestone-packed column (●: individual GONPs, ▲: GONPs + MS2 and ■: GONPs + *E.coli*) (experimental conditions: pH = 7.5, flow velocity: 5 m/day and temperature: 22 °C).

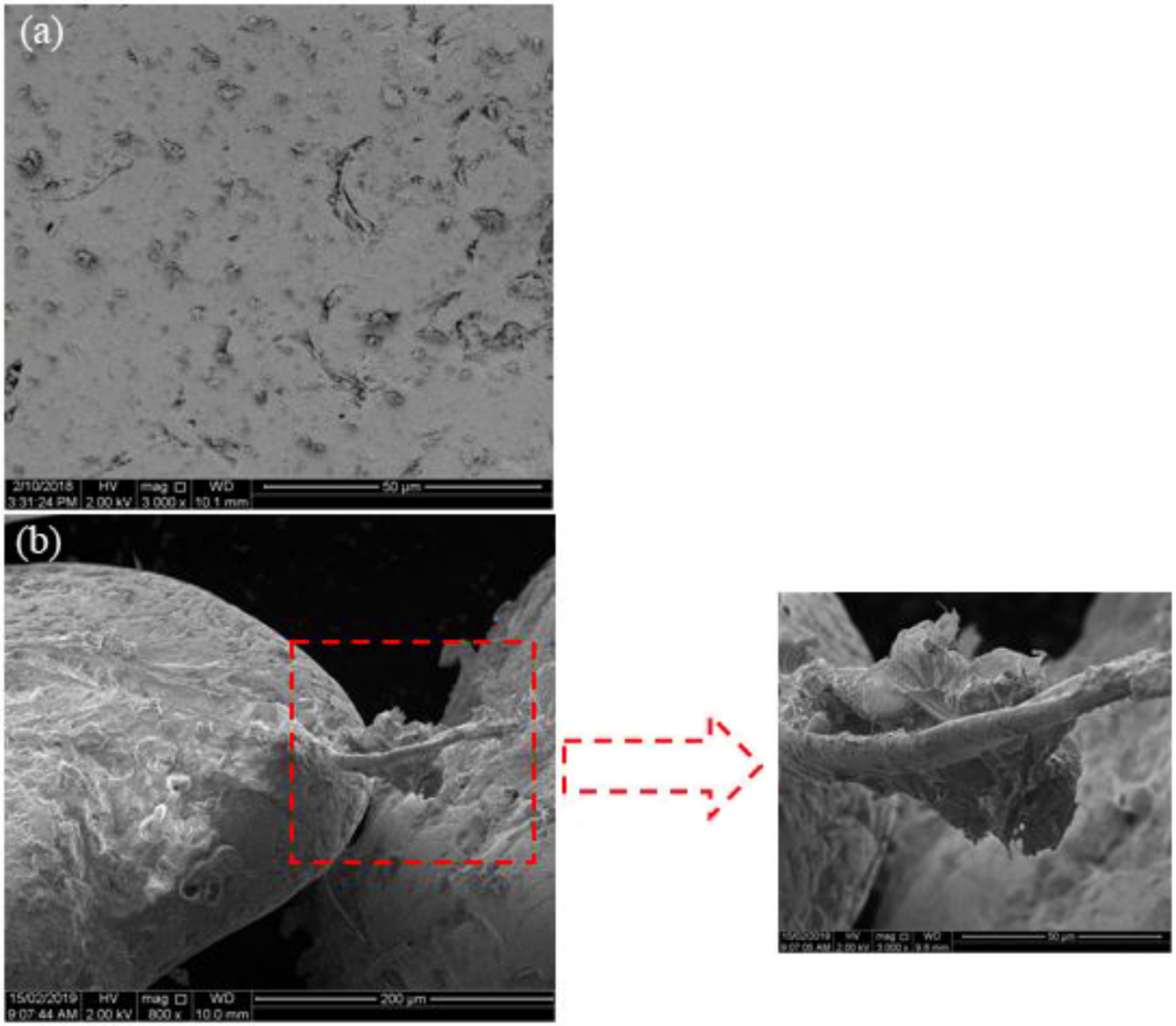

Plate 6-1. SEM images of (a) pristine and (b) biofilm-conditioned limestone obtained from 0-1 cm of inlet end of column.

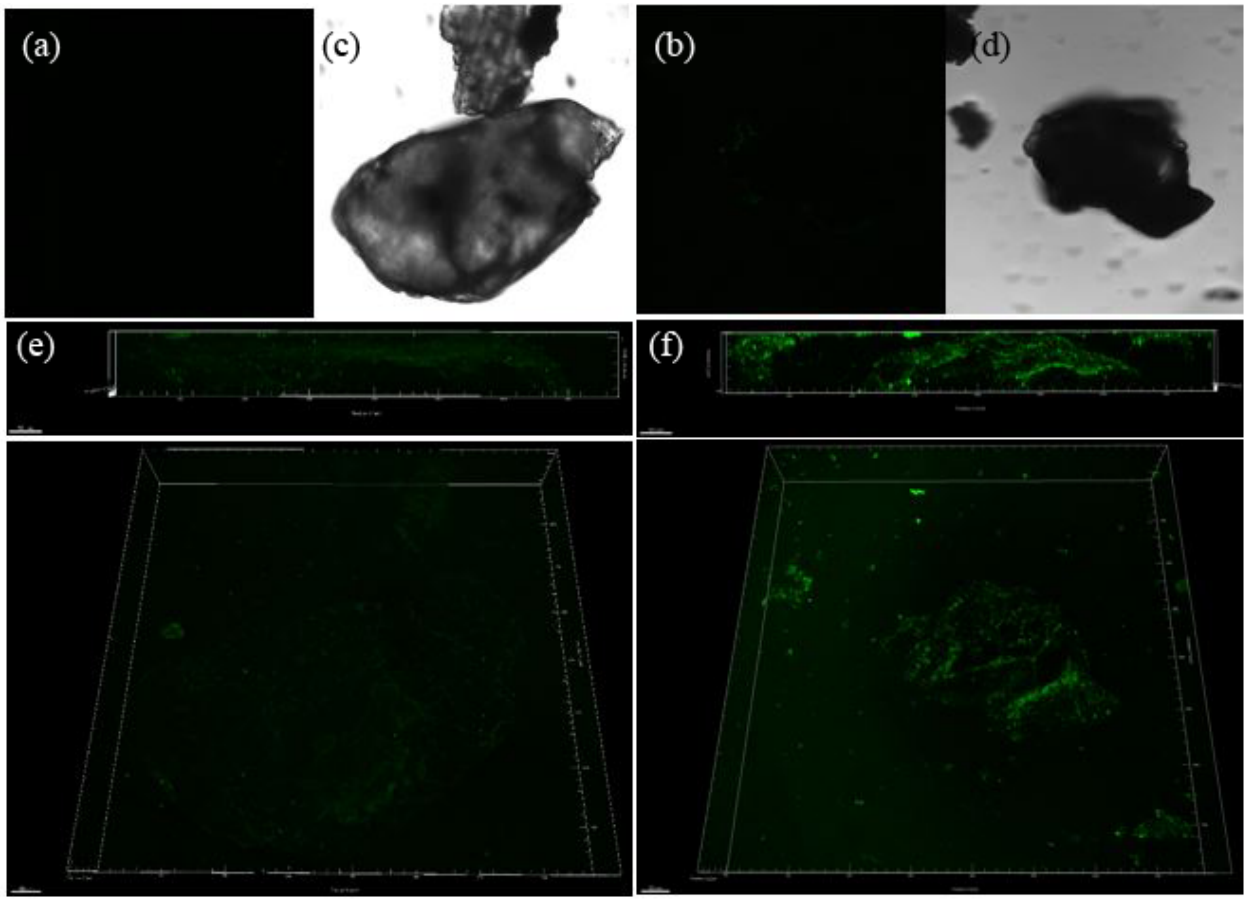

Plate 6-2. CLSM images of (a) pristine and (b) biofilm-conditioned limestone obtained from material extracted 0-1 cm of inlet end of column (a) and (b): confocal slice images through pristine and biofilm-conditioned limestone, (c) and (d): transmitted light images of pristine and biofilm-conditioned limestone in (a) and (b), respectively, (e) and (f): 3D view of confocal z-stack data set in Imaris software).

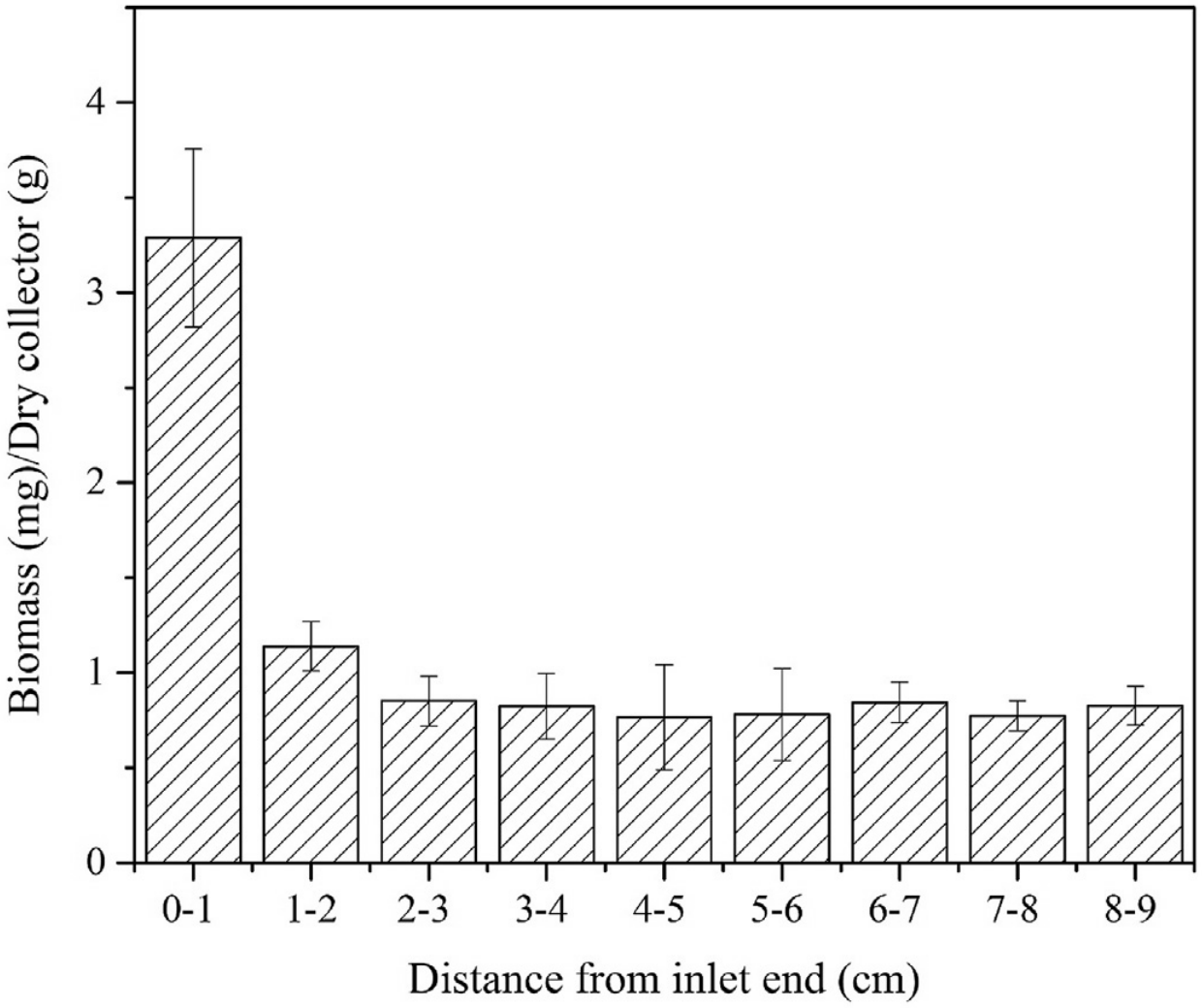

Fig 6-9. The biofilm biomass in 1 cm sections (0-9 cm) of the limestone packed columns conditioned with treated wastewater for 10 days.

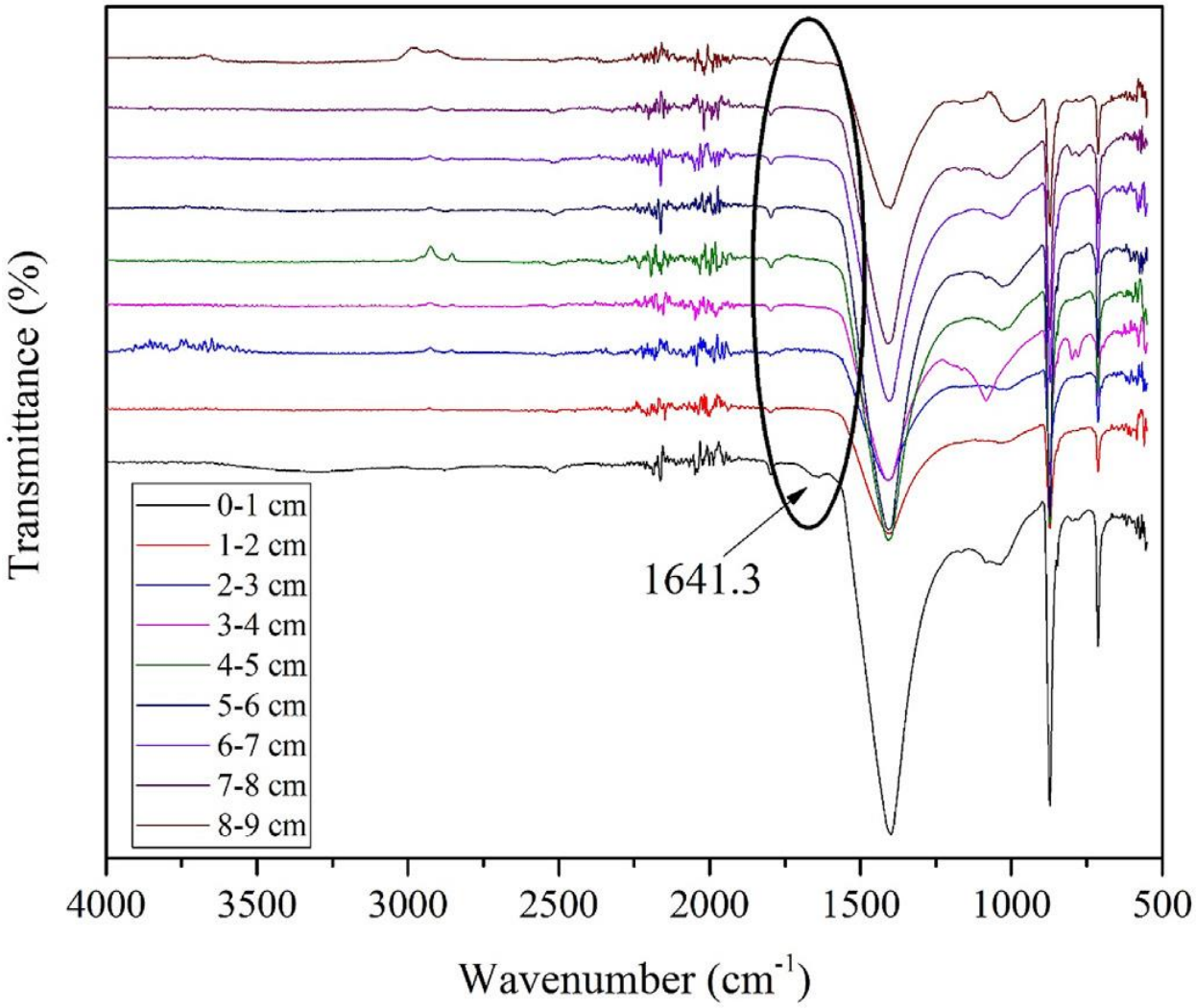

Fig 6-10. FTIR spectra of different parts of excavated limestone packed columns conditioned with treated wastewater for 10 days.

6.5. Conclusion

The present study investigated transport and retention behavior of GONPs in the presence and absence of MS2 and *E.coli* in natural limestone aquifer sediments at low and high ionic strength conditions. Results revealed no significant changes in GONPs transport and retention with co-presence of MS2 and *E.coli* at high ionic strength. However, at low ionic strength, the co-presence of MS2 and *E.coli* caused an enhancement in the transport of GONPs in porous media. The main mechanism governing GONPs transport and retention in porous media was the blocking of surface reactive sites by *E.coli* or MS2 that prevented further attachment of GONPs and consequently enhanced nanoparticle transport in porous media. Additionally, the same BTCs GONPs were obtained with and without co-presence of MS2 and *E.coli* in biofilm-coated porous media, due to the pore throat straining of particles in the column inlet end. Ultimately, our results indicate that the presence of microorganisms of different sizes in a typical managed aquifer recharge site has similar effects on enhanced transport of GONPs, which may threaten environmental water resources.

7. General conclusion

This chapter summarizes the results and discusses all of the experimental chapters. Noteworthy to say that the detailed discussion has been mentioned at the end of each chapter. Below, a summary of results with area for future applications are presented.

This research investigated the interaction between authentic aquifer substrates and MS2-F-RNA bacteriophage and engineered nanoparticles in the presence of natural biofilm in both batch and column systems to find their potential effect on human health being through infection. Presently, there is limited research on the attachment behavior of MS2 on native aquifer materials that determines the fate of virus in MAR sites. Batch studies with aquifer substrate and MS2 presented novel information on the influence of biofilm on inactivation rates of MS2 via attachment onto the surfaces of native aquifer materials. The results of batch studies showed the high affinity of MS2 bacteriophage to surfaces of limestone aquifer materials (Chapter 3). Higher temperature favored virus attachment and inactivation, due to the damage to the viral components of microorganisms (Harvey and Ryan, 2004). The virus in aquifers can be in either static or dynamic states, depending on the flow rate conditions within the aquifer, which may affect the virus inactivation rate. The results revealed higher virus inactivation in dynamic rather than static conditions, likely due to increasing collision between adsorbent surfaces and virus particles and creation of air-water and air-solid interactions, which are absent in static conditions. Previously, little attention has been afforded in the literature to the role of biofilm, which naturally occurs in MAR schemes, on inactivation rates of virus. The inactivation rate of MS2 onto the biofilm-conditioned limestone was higher than pristine substrate, which indicates the significant role of surface physical heterogeneities on virus entrapment and inactivation. Moreover, a higher MS2 inactivation rate

was seen in treated wastewater than RO water samples, due to the presence of different cations such as K^+, Na^+, Mg^{2+} and Ca^{2+}.

Transport experiments of bacteriophage in columns packed with sediments from managed aquifer recharge site have recently been reported (Sasidharan et al., 2017a). However, the effect of natural biofilm on attachment and detachment behavior of bacteriophage was not investigated. A previous study had also shown, that biofilm, produced by long-term irrigation of limestone-packed columns with treated wastewater, created preferential flow paths in the columns due to limestone dissolution (Rinck-Pfeiffer, 2000). The effect of biofilm induced limestone dissolution and the subsequent creation of preferential flow paths on virus transport behavior was not considered. This is an important issue for MAR schemes since preferential flow may reduce virus retardation/inactivation, increasing the risk of human exposure to virus upon subsequent water reuse.

In Chapter 4, the transport behavior of tracer and virus was reported for pristine sand and limestone aquifer-packed columns and for ones similarly packed in which biofilm was developed, on the surfaces and interpores of the substrates, by short and long-term irrigation with treated wastewater. The surface, hydrological and hydro-geochemical characteristics of columns were determined. The results showed a significant effect of biofilm on the enhancement of physical and biological clogging. Severe clogging was observed in the first 3 cm from the column inlet end, because of growth and proliferation of biofilm-derived from treated wastewater. Several processes, such as biofilm growth and entrapment of suspended solid particles filling vacant spaces between collectors, lead to the clogging of both sand and limestone porous media. However, in limestone columns, nitrification by autotrophic bacteria was observed, producing abundant hydrogen ions in solution, which caused calcite dissolution following long-term injection of treated wastewater.

Moreover, the conservative tracer appeared earlier in the BTCs in the biofilm-conditioned limestone columns than the pristine control columns. Indeed, the greater the amount of biofilm, the earlier the appearance of the tracer in the BTCs. The analytical simulation of tracer transport showed increases in the hydrodynamic dispersion, pore water velocity and longitudinal dispersivity of columns by increasing biofilm growth, in which the role of dispersivity in biofilm-conditioned columns outweigh advection on tracer transport. The BTCs of virus, showed greater virus attachment in limestone aquifer sediments than in sand, due to the presence of different metal oxides on the limestone aquifer surfaces. Retention of MS2 was enhanced in the presence of biofilm, in both sand and limestone columns, independent of the duration of irrigation with treated wastewater. Tracer and MS2 transport experiments demonstrated that the presence of biofilm changed the structure of the limestone columns. Significantly, a higher discharge of MS2 was observed in the effluents of biofilm conditioned limestone columns compared to pristine control ones, due to the creation of preferential flow paths created by calcite dissolution by a nitrifying biofilm. This finding has not been reported elsewhere in the literature.

Chapter 5 reported results of the transport and retention of GONPs in saturated porous media with different mineralogical features (e.g., sand, quartz sediments and limestone sediment) either pristine or biofilm-conditioned. Many studies have reported the effect of porous media characteristics (i.e., chemical and physical heterogeneities) on the enhanced retention of nanoparticles in porous media (Qi et al., 2019, Wang et al., 2017a), however, the author is unaware of any published study on the transport and retention behavior of GONPs in natural aquifer sediments. This study provides new information on the transport of GONPs in sandy and carbonaceous aquifer sediments. Temperature is an influential parameter on particle transport in porous media, which should not be neglected (Wang et al., 2019). The seasonal and diurnal solar

irradiation, the temperature of soil, aquifer and subsurface environment will vary (Wang et al., 2017b). Furthermore, heavy rain and the subsequent discharge of stormwater containing various types and concentrations of mono and poly-valent cations may alter the solution chemistry of aqueous matrix, which may significantly affect the transport and retention behavior of nanoparticles. The role of temperature and ionic strength on colloidal stability of GONPs was investigated. The results showed a significant dependence of the transport behavior of GONPs in porous media on temperature and ionic strength of solution, which may enable the prediction of nanoparticle transport in the aquifers in winter and summer. It was shown that the colloidal stabilities of GONPs were dependent on the temperature and ionic strength of solution. By increasing the temperature and ionic strength and also the valence of cations in solution, a decrease was observed in the colloidal stability of GONPs thereby increasing aggregation, due to decreasing the electrostatic double layer around GONPs. Although DLVO theory revealed unfavorable conditions for attachment of GONPs onto the surfaces of collectors, a large amount of nanoparticles were retained in biofilm-conditioned porous media. Metal oxides and clay minerals are abundant on natural sediments, which increase the number of favorable attachment sites and decrease the energy barrier against attachment of nanoparticles (Bradford and Torkzaban, 2012). Apart from intrinsic nature of natural sediments, the surface characteristics of substrate govern the mechanisms and transport behavior of nanoparticles. According to the literature, the transport experiments of GONPs in porous media were performed in the media conditioned with biofilm synthesized using an artificially media such as *Pseudomonas Putida* (Jian-Zhou et al., 2015). However, the research reported here uniquely determines the effect on the transport of nanoparticles in biofilm naturally induced on authentic aquifer material. The presence of biofilm on the surfaces of substrate caused a significant enhancement in the retention rate of GONPs,

compared to the same pristine substrates, due to changes in the surface properties of porous media via increasing the zeta potentials of substrate and decreasing the porosity of columns. The results presented here showed that the attachment rate of GONPs has a direct relationship with sum of physical (roughness and irregularities), chemical (pH, ionic strength and composition, etc) and the hydrological features of porous media.

The results of research on the co-transport of GONPs with different-sized microorganisms, the virus MS2 and *E.coli*, in pristine and biofilm-coated limestone-packed columns were reported in Chapter 6. The author is unaware of any other published study reporting the effect of co-presence of microorganisms and GONPs in suspension on transport and retention behavior of GONPs in an authentic aquifer substrate. The results revealed the less retardation of GONPs in aquifers at low ionic strength of solution which caused the danger of human exposure to the engineered nanoparticles thereby application of reused water. Greater discharge and less retention of GONPs in pristine limestone aquifer grains were observed, when MS2 and *E.coli* were concomitantly present in the nanoparticle suspension. The presence of these microorganisms did not change the colloidal stability of nanoparticles, which was confirmed through measurements of zeta potentials and SEM images of GONPs. The main mechanism of enhanced discharge of nanoparticles from porous media was occupation of surface reactive sites of media by MS2 and *E.coli*, which prevented the attachment of nanoparticles and simultaneously enhanced their transport. The retention of GONPs was independent of the size of the co-transported microorganism. Significantly, the presence of biofilm did not change the quantity of GONPs eluted from columns, when solely present in suspension or in the co-presence of microorganisms. The observation suggests that biofilm acted as a protective layer in limestone-packed columns reducing the

discharge of GONPs from column, in either the presence or absence of the co-transported microorganisms.

The findings of this research can be applied for designing a MAR site in order to predict the contamination of water resources for reuse purposes. First of all, long-term application of treated wastewater containing various amounts and sorts of pathogenic agents and engineered nanoparticles in limestone aquifers can potentially cause risk for human health thereby creation of preferential flow paths, due to the calcite dissolution and less retardation of pathogenic agents and engineered nanoparticles by aquifers. It indicates the importance of paying serious attention to the presence of different pathogenic and nanoparticles in influent water while designing a MAR site. In addition, since the transport behavior of colloidal particles in porous media with different flow pathways is different, the findings of this study can be useful in designing a MAR site in carbonaceous aquifer which predict the possibility of groundwater pollution by penetration of contaminants through either preferential flow paths or fractures. Furthermore, although biofilm growth and proliferation induced by treated wastewater in a MAR site would exacerbate the hydraulic properties of aquifers via decreasing the porosity and hydraulic conductivity of aquifers, it can act as a bio-filter to trap virus, bacteria and nanoparticles to prevent their discharge into the environmental resources. Treatment of source water contaminated by different harmful microorganisms and toxic nanoparticles is important to prevent further environmental problems. Up to now, several methods have been used to filtrate input water resources before use in MAR sites. Filtration is a remediation technique which has been used for improving the quality of drinking water. Results of this study revealed that the production of biofilm in a typical MAR site would protect the safety of groundwater resources for re-use application. Therefore, understanding the relationship between changing in hydraulic properties of aquifers by application of treated

wastewater and biofilm growth in discharging pathogenic agents and engineered nanoparticles contributes to this management of human exposure risk. Proposed future research directions can be summarized as follows:

- Examination of the effect of natural biofilm on transport behavior of microorganisms and engineered nanoparticles in a 2 or 3-dimensional system for better understanding in natural environments.
- Determine the influence of different characteristics of biofilm (e.g., thickness, hydrophobicity and etc.,) on the attachment/detachment of colloidal particles onto the substrate.
- Study numerical modeling of nanoparticle and microorganisms transport in biofilm-conditioned porous media to understand the effect of biofilm on quantitative retention of colloidal particles.
- Examine the age of biofilm on the hydrological properties of porous media (e.g., saturated hydraulic conductivity, porosity etc.,) and subsequently transport and retention of microorganisms and engineered nanoparticles.
- Determine the microbiological composition of the natural biofilm and the respective contribution of microbial assemblages on the retention behavior of microorganisms and engineered nanoparticles.
- Determine the long-term influence of natural biofilm in porous media on the transport and retention of soluble nanoparticles affected by natural biofilm media.
- Modeling biofilm growth and proliferation in porous media to give a better picture on the intensity of aquifer clogging.

References

ABBOTT, A., RUTTER, P. & BERKELEY, R. 1983. The influence of ionic strength, pH and a protein layer on the interaction between Streptococcus mutans and glass surfaces. *Microbiology,* 129**,** 439-445.

ABDEL-FATTAH, A. I., ZHOU, D., BOUKHALFA, H., TARIMALA, S., WARE, S. D. & KELLER, A. A. 2013. Dispersion stability and electrokinetic properties of intrinsic plutonium colloids: implications for subsurface transport. *Environmental science & technology,* 47**,** 5626-5634.

ABUZERR, S., DARWISH, M. & MAHVI, A. H. 2018. Simultaneous removal of cationic methylene blue and anionic reactive red 198 dyes using magnetic activated carbon nanoparticles: equilibrium, and kinetics analysis. *Water Science and Technology,* 2017**,** 534-545.

ADRIAN, Y. F., SCHNEIDEWIND, U., BRADFORD, S. A., SIMUNEK, J., FERNANDEZ-STEEGER, T. M. & AZZAM, R. 2018. Transport and retention of surfactant-and polymer-stabilized engineered silver nanoparticles in silicate-dominated aquifer material. *Environmental Pollution,* 236**,** 195e207.

AGARWALA, M., CHOUDHURY, B. & YADAV, R. 2014. Comparative study of antibiofilm activity of copper oxide and iron oxide nanoparticles against multidrug resistant biofilm forming uropathogens. *Indian journal of microbiology,* 54**,** 365-368.

AKHAVAN, O. & GHADERI, E. 2010. Toxicity of graphene and graphene oxide nanowalls against bacteria. *ACS nano,* 4**,** 5731-5736.

ALI, S. N., EL-SHAFEY, E.-S. I., AL-BUSAFI, S. & AL-LAWATI, H. A. 2018. Adsorption of chlorpheniramine and ibuprofen on surface functionalized activated carbons from

deionized water and spiked hospital wastewater. *Journal of Environmental Chemical Engineering***,** 102860.

ANDERS, R. & CHRYSIKOPOULOS, C. 2005. Virus fate and transport during artificial recharge with recycled water. *Water Resources Research,* 41.

ANDERS, R. & CHRYSIKOPOULOS, C. V. 2006. Evaluation of the factors controlling the time-dependent inactivation rate coefficients of bacteriophage MS2 and PRD1. *Environmental science & technology,* 40**,** 3237-3242.

ANGELAKIS, A. & GIKAS, P. 2014. Water reuse: overview of current practices and trends in the world with emphasis on EU states. *Water Utility Journal,* 8**,** 67-78.

AVNIMELECH, Y. & NEVO, Z. 1964. Biological clogging of sands. *Soil Science,* 98**,** 222-226.

AYUSO-GABELLA, N., PAGE, D., MASCIOPINTO, C., AHARONI, A., SALGOT, M. & WINTGENS, T. 2011. Quantifying the effect of Managed Aquifer Recharge on the microbiological human health risks of irrigating crops with recycled water. *Agricultural Water Management,* 99**,** 93-102.

BABAEI, A. A. 2014. Kinetic modeling of methylene blue adsorption onto acid-activated spent tea: A comparison between linear and non-linear regression analysis. *Journal of Advances in Environmental Health Research,* 2**,** 129-208.

BABAEI, A. A., BAHRAMI, M., FARROKHIAN FIROUZI, A., RAMAZANPOUR ESFAHANI, A. & ALIDOKHT, L. 2015. Adsorption of cadmium onto modified nanosized magnetite: kinetic modeling, isotherm studies, and process optimization. *Desalination and Water Treatment,* 56**,** 3380-3392.

BAGARELLO, V., IOVINO, M. & ELRICK, D. 2004. A simplified falling-head technique for rapid determination of field-saturated hydraulic conductivity. *Soil Science Society of America Journal,* 68**,** 66-73.

BASNET, M., GERSHANOV, A., WILKINSON, K. J., GHOSHAL, S. & TUFENKJI, N. 2016. Interaction between palladium-doped zerovalent iron nanoparticles and biofilm in granular porous media: characterization, transport and viability. *Environmental Science: Nano,* 3**,** 127-137.

BAVEYE, P. & VALOCCHI, A. 1989. An evaluation of mathematical models of the transport of biologically reacting solutes in saturated soils and aquifers. *Water Resources Research,* 25**,** 1413-1421.

BAVEYE, P., VANDEVIVERE, P., HOYLE, B. L., DELEO, P. C. & DE LOZADA, D. S. 1998. Environmental impact and mechanisms of the biological clogging of saturated soils and aquifer materials. *Critical reviews in environmental science and technology,* 28**,** 123-191.

BECKWITH, C. W. & BAIRD, A. J. 2001. Effect of biogenic gas bubbles on water flow through poorly decomposed blanket peat. *Water Resources Research,* 37**,** 551-558.

BEJAT, L., PERFECT, E., QUISENBERRY, V., COYNE, M. S. & HASZLER, G. 2000. Solute transport as related to soil structure in unsaturated intact soil blocks. *Soil Science Society of America Journal,* 64**,** 818-826.

BELLOU, M. I., SYNGOUNA, V. I., TSELEPI, M. A., KOKKINOS, P. A., PAPARRODOPOULOS, S. C., VANTARAKIS, A. & CHRYSIKOPOULOS, C. V. 2015. Interaction of human adenoviruses and coliphages with kaolinite and bentonite. *Science of the Total Environment,* 517**,** 86-95.

BERGSTRÖM, L. 1997. Hamaker constants of inorganic materials. *Advances in colloid and interface science,* 70**,** 125-169.

BHATTACHARJEE, S., RYAN, J. N. & ELIMELECH, M. 2002. Virus transport in physically and geochemically heterogeneous subsurface porous media. *Journal of Contaminant Hydrology,* 57**,** 161-187.

BOUWER, H. 2002. Artificial recharge of groundwater: hydrogeology and engineering. *Hydrogeology Journal,* 10**,** 121-142.

BOZORG, A., GATES, I. D. & SEN, A. 2015. Impact of biofilm on bacterial transport and deposition in porous media. *Journal of contaminant hydrology,* 183**,** 109-120.

BRADFORD, S. A. & BETTAHAR, M. 2006. Concentration dependent transport of colloids in saturated porous media. *Journal of Contaminant Hydrology,* 82**,** 99-117.

BRADFORD, S. A., KIM, H. N., HAZNEDAROGLU, B. Z., TORKZABAN, S. & WALKER, S. L. 2009. Coupled factors influencing concentration-dependent colloid transport and retention in saturated porous media. *Environmental science & technology,* 43**,** 6996-7002.

BRADFORD, S. A., SIMUNEK, J., BETTAHAR, M., VAN GENUCHTEN, M. T. & YATES, S. R. 2003. Modeling colloid attachment, straining, and exclusion in saturated porous media. *Environmental science & technology,* 37**,** 2242-2250.

BRADFORD, S. A., TADASSA, Y. F. & JIN, Y. 2006. Transport of coliphage in the presence and absence of manure suspension. *Journal of environmental quality,* 35**,** 1692-1701.

BRADFORD, S. A. & TORKZABAN, S. 2012. Colloid adhesive parameters for chemically heterogeneous porous media. *Langmuir,* 28**,** 13643-13651.

BRADFORD, S. A. & TORKZABAN, S. 2013. Colloid interaction energies for physically and chemically heterogeneous porous media. *Langmuir,* 29**,** 3668-3676.

BRADFORD, S. A., TORKZABAN, S. & SHAPIRO, A. 2013. A theoretical analysis of colloid attachment and straining in chemically heterogeneous porous media. *Langmuir,* 29**,** 6944-6952.

BRADFORD, S. A., TORKZABAN, S. & WALKER, S. L. 2007. Coupling of physical and chemical mechanisms of colloid straining in saturated porous media. *Water Research,* 41**,** 3012-3024.

BRADFORD, S. A., YATES, S. R., BETTAHAR, M. & SIMUNEK, J. 2002. Physical factors affecting the transport and fate of colloids in saturated porous media. *Water Resources Research,* 38.

BROWN, L. R. 2010. Microbial enhanced oil recovery (MEOR). *Current opinion in Microbiology,* 13**,** 316-320.

BUIJSE, M. Mechanisms of wormholing in carbonate acidizing. International Symposium on Oilfield Chemistry, 1997. Society of Petroleum Engineers.

CAGLE, G. D. 1975. Fine structure and distribution of extracellular polymer surrounding selected aerobic bacteria. *Canadian journal of microbiology,* 21**,** 395-408.

CAI, L., PENG, S., WU, D. & TONG, M. 2016. Effect of different-sized colloids on the transport and deposition of titanium dioxide nanoparticles in quartz sand. *Environmental Pollution,* 208**,** 637-644.

CAI, L., TONG, M., MA, H. & KIM, H. 2013. Cotransport of titanium dioxide and fullerene nanoparticles in saturated porous media. *Environmental science & technology,* 47**,** 5703-5710.

CAI, L., TONG, M., WANG, X. & KIM, H. 2014. Influence of clay particles on the transport and retention of titanium dioxide nanoparticles in quartz sand. *Environmental science & technology,* 48**,** 7323-7332.

CALDERER, M., MARTÍ, V., DE PABLO, J., GUIVERNAU, M., PRENAFETA-BOLDÚ, F. X. & VIÑAS, M. 2014. Effects of enhanced denitrification on hydrodynamics and microbial community structure in a soil column system. *Chemosphere,* 111**,** 112-119.

CASTRO, F. D. & TUFENKJI, N. 2007. Relevance of nontoxigenic strains as surrogates for Escherichia coli O157: H7 in groundwater contamination potential: Role of temperature and cell acclimation time. *Environmental science & technology,* 41**,** 4332-4338.

CEDERVALL, T., LYNCH, I., LINDMAN, S., BERGGÅRD, T., THULIN, E., NILSSON, H., DAWSON, K. A. & LINSE, S. 2007. Understanding the nanoparticle–protein corona using methods to quantify exchange rates and affinities of proteins for nanoparticles. *Proceedings of the National Academy of Sciences,* 104**,** 2050-2055.

CHANG, Y., YANG, S.-T., LIU, J.-H., DONG, E., WANG, Y., CAO, A., LIU, Y. & WANG, H. 2011. In vitro toxicity evaluation of graphene oxide on A549 cells. *Toxicology letters,* 200**,** 201-210.

CHEN, C., SHANG, J., ZHENG, X., ZHAO, K., YAN, C., SHARMA, P. & LIU, K. 2018. Effect of physicochemical factors on transport and retention of graphene oxide in saturated media. *Environmental pollution (Barking, Essex: 1987),* 236**,** 168-176.

CHEN, K. L. & ELIMELECH, M. 2006. Aggregation and deposition kinetics of fullerene (C60) nanoparticles. *Langmuir,* 22**,** 10994-11001.

CHEN, K. L. & ELIMELECH, M. 2007. Influence of humic acid on the aggregation kinetics of fullerene (C60) nanoparticles in monovalent and divalent electrolyte solutions. *Journal of Colloid and Interface Science,* 309**,** 126-134.

CHEN, L., SABATINI, D. A. & KIBBEY, T. C. 2012. Transport and retention of fullerene (nC60) nanoparticles in unsaturated porous media: Effects of solution chemistry and solid phase coating. *Journal of contaminant hydrology,* 138**,** 104-112.

CHEN, Y., FURMANN, A., MASTALERZ, M. & SCHIMMELMANN, A. 2014. Quantitative analysis of shales by KBr-FTIR and micro-FTIR. *Fuel,* 116**,** 538-549.

CHOWDHURY, I., CWIERTNY, D. M. & WALKER, S. L. 2012. Combined factors influencing the aggregation and deposition of nano-TiO2 in the presence of humic acid and bacteria. *Environmental science & technology,* 46**,** 6968-6976.

CHOWDHURY, I., DUCH, M. C., MANSUKHANI, N. D., HERSAM, M. C. & BOUCHARD, D. 2013. Colloidal properties and stability of graphene oxide nanomaterials in the aquatic environment. *Environmental science & technology,* 47**,** 6288-6296.

CHOWDHURY, I., DUCH, M. C., MANSUKHANI, N. D., HERSAM, M. C. & BOUCHARD, D. 2014. Interactions of graphene oxide nanomaterials with natural organic matter and metal oxide surfaces. *Environmental science & technology,* 48**,** 9382-9390.

CHOWDHURY, I., HONG, Y., HONDA, R. J. & WALKER, S. L. 2011. Mechanisms of TiO2 nanoparticle transport in porous media: Role of solution chemistry, nanoparticle concentration, and flowrate. *Journal of colloid and interface science,* 360**,** 548-555.

CHRYSIKOPOULOS, C. V. & ARAVANTINOU, A. F. 2012. Virus inactivation in the presence of quartz sand under static and dynamic batch conditions at different temperatures. *Journal of hazardous materials,* 233**,** 148-157.

CHRYSIKOPOULOS, C. V. & ARAVANTINOU, A. F. 2014. Virus attachment onto quartz sand: Role of grain size and temperature. *Journal of Environmental Chemical Engineering,* 2**,** 796-801.

CHRYSIKOPOULOS, C. V. & SIM, Y. 1996. One-dimensional virus transport in homogeneous porous media with time-dependent distribution coefficient. *Journal of Hydrology,* 185**,** 199-219.

CHRYSIKOPOULOS, C. V. & SYNGOUNA, V. I. 2012. Attachment of bacteriophages MS2 and ΦX174 onto kaolinite and montmorillonite: Extended-DLVO interactions. *Colloids and Surfaces B: Biointerfaces,* 92**,** 74-83.

CHU, Y., JIN, Y., BAUMANN, T. & YATES, M. V. 2003. Effect of soil properties on saturated and unsaturated virus transport through columns. *Journal of Environmental Quality,* 32**,** 2017-2025.

CHU, Y., JIN, Y., FLURY, M. & YATES, M. V. 2001. Mechanisms of virus removal during transport in unsaturated porous media. *Water Resources Research,* 37**,** 253-263.

CONNOR, J. A., PAQUETTE, S., MCHUGH, T., GIE, E., HEMINGWAY, M. & BIANCHI, G. 2017. Application of natural resource valuation concepts for development of sustainable remediation plans for groundwater. *Journal of environmental management,* 204**,** 721-729.

COSTÁN-LONGARES, A., MONTEMAYOR, M., PAYÁN, A., MÉNDEZ, J., JOFRE, J., MUJERIEGO, R. & LUCENA, F. 2008. Microbial indicators and pathogens: removal, relationships and predictive capabilities in water reclamation facilities. *Water research,* 42**,** 4439-4448.

CUI, X., CHEN, C., SUN, S., ZHOU, D., NDAYISENGA, F., HUO, M., ZHU, S., ZHANG, L. & CRITTENDEN, J. C. 2018. Acceleration of saturated porous media clogging and silicon

dissolution due to low concentrations of Al (III) in the recharge of reclaimed water. *Water Research*.

CUNNINGHAM, A. B., CHARACKLIS, W. G., ABEDEEN, F. & CRAWFORD, D. 1991. Influence of biofilm accumulation on porous media hydrodynamics. *Environmental science & technology,* 25**,** 1305-1311.

DALVAND, A., KHOOBI, M., NABIZADEH, R., GANJALI, M. R., GHOLIBEGLOO, E. & MAHVI, A. H. 2018. Reactive Dye Adsorption from Aqueous Solution on HPEI-Modified Fe 3 O 4 Nanoparticle as a Superadsorbent: Characterization, Modeling, and Optimization. *Journal of Polymers and the Environment,* 26**,** 3470-3483.

DE RODA HUSMAN, A., LODDER, W., RUTJES, S., SCHIJVEN, J. & TEUNIS, P. 2009. Long-term inactivation study of three enteroviruses in artificial surface and groundwaters, using PCR and cell culture. *Applied and Environmental Microbiology,* 75**,** 1050-1057.

DEAN, W. E. 1974. Determination of carbonate and organic matter in calcareous sediments and sedimentary rocks by loss on ignition; comparison with other methods. *Journal of Sedimentary Research,* 44**,** 242-248.

DEBARTOLOMEIS, J. & CABELLI, V. J. 1991. Evaluation of an Escherichia coli host strain for enumeration of F male-specific bacteriophages. *Applied and Environmental Microbiology,* 57**,** 1301-1305.

DERAGUIN, B. & LANDAU, L. 1941. Theory of the stability of strongly charged lyophobic sols and of the adhesion of strongly charged particles in solution of electrolytes. *Acta Physicochim: USSR,* 14**,** 633-662.

DERJAGUIN, B. V. & LANDAU, L. 1993. Theory of the stability of strongly charged lyophobic sols and of the adhesion of strongly charged particles in solutions of electrolytes. *Progress in Surface Science,* 43**,** 30-59.

DIJK, P. E., BERKOWITZ, B. & YECHIELI, Y. 2002. Measurement and analysis of dissolution patterns in rock fractures. *Water resources research,* 38.

DIKA, C., LY-CHATAIN, M., FRANCIUS, G., DUVAL, J. & GANTZER, C. 2013. Non-DLVO adhesion of F-specific RNA bacteriophages to abiotic surfaces: importance of surface roughness, hydrophobic and electrostatic interactions. *Colloids and Surfaces A: Physicochemical and Engineering Aspects,* 435**,** 178-187.

DILLON, P. 2009. Water recycling via managed aquifer recharge in Australia. *Boletín geológico y minero,* 120**,** 121-130.

DILLON, P., FERNANDEZ, E. E. & TUINHOF, A. 2012. Management of aquifer recharge and discharge processes and aquifer storage equilibrium. IAH contribution to GEF-FAO Groundwater Governance Thematic Paper 4.

DILLON, P., TOZE, S., PAGE, D., VANDERZALM, J., BEKELE, E., SIDHU, J. & RINCK-PFEIFFER, S. 2010. Managed aquifer recharge: rediscovering nature as a leading edge technology. *Water science and technology,* 62**,** 2338-2345.

DILLON, P. J., HICKINBOTHAM, M. R. & PAVELIC, P. 1994. Review of international experience in injecting water into aquifers for storage and reuse. *Water Down Under 94: Groundwater Papers; Preprints of Papers***,** 13.

DING, Z., HU, X., MORALES, V. L. & GAO, B. 2014. Filtration and transport of heavy metals in graphene oxide enabled sand columns. *Chemical Engineering Journal,* 257**,** 248-252.

DONG, S., SHI, X., GAO, B., WU, J., SUN, Y., GUO, H., XU, H. & WU, J. 2016. Retention and release of graphene oxide in structured heterogeneous porous media under saturated and unsaturated conditions. *Environmental science & technology,* 50**,** 10397-10405.

DONG, S., SUN, Y., GAO, B., SHI, X., XU, H., WU, J. & WU, J. 2017. Retention and transport of graphene oxide in water-saturated limestone media. *Chemosphere,* 180**,** 506-512.

DREWES, J. E. 2009. Ground water replenishment with recycled water—water quality improvements during managed aquifer recharge. *Groundwater,* 47**,** 502-505.

DU, X., FANG, Y., WANG, Z., HOU, J. & YE, X. 2014. The prediction methods for potential suspended solids clogging types during managed aquifer recharge. *Water,* 6**,** 961-975.

DUPIN, H. J. & MCCARTY, P. L. 2000. Impact of colony morphologies and disinfection on biological clogging in porous media. *Environmental science & technology,* 34**,** 1513-1520.

ERIKSSON, N., GUPTA, A. & DESTOUNI, G. 1997. Comparative analysis of laboratory and field tracer tests for investigating preferential flow and transport in mining waste rock. *Journal of Hydrology,* 194**,** 143-163.

ESFAHANI, A. R., FIROUZI, A. F., SAYYAD, G. & KIASAT, A. 2013. Lead removal from aqueous solutions using polyacrylicacid-Stabilized zero-Valent iron nanoparticles. *Research Journal of Environmental and Earth Sciences,* 5**,** 548-555.

ESFAHANI, A. R., FIROUZI, A. F., SAYYAD, G. & KIASAT, A. 2014. Transport and retention of polymer-stabilized zero-valent iron nanoparticles in saturated porous media: effects of initial particle concentration and ionic strength. *Journal of Industrial and Engineering Chemistry,* 20**,** 2671-2679.

FABREGA, J., RENSHAW, J. C. & LEAD, J. R. 2009. Interactions of silver nanoparticles with Pseudomonas putida biofilms. *Environmental science & technology,* 43**,** 9004-9009.

FAN, W., JIANG, X., YANG, W., GENG, Z., HUO, M., LIU, Z. & ZHOU, H. 2015. Transport of graphene oxide in saturated porous media: effect of cation composition in mixed Na–Ca electrolyte systems. *Science of the Total Environment,* 511**,** 509-515.

FEDERATION, W. E. & ASSOCIATION, A. P. H. 2005. Standard methods for the examination of water and wastewater. *American Public Health Association (APHA): Washington, DC, USA.*

FERIANCIKOVA, L. & XU, S. 2012. Deposition and remobilization of graphene oxide within saturated sand packs. *Journal of hazardous materials,* 235**,** 194-200.

FISHER-POWER, L. M. & CHENG, T. 2018. Nanoscale Titanium Dioxide (nTiO2) Transport in Natural Sediments: Importance of Soil Organic Matter and Fe/Al Oxyhydroxides. *Environmental science & technology,* 52**,** 2668-2676.

FLYNN, R. M. & SINREICH, M. 2010. Characterisation of virus transport and attenuation in epikarst using short pulse and prolonged injection multi-tracer testing. *water research,* 44**,** 1138-1149.

FONTES, D. E., MILLS, A., HORNBERGER, G. & HERMAN, J. 1991. Physical and chemical factors influencing transport of microorganisms through porous media. *Appl. Environ. Microbiol.,* 57**,** 2473-2481.

FOPPEN, J. & SCHIJVEN, J. 2005. Transport of E. coli in columns of geochemically heterogeneous sediment. *Water Research,* 39**,** 3082-3088.

GEE, G. W. & BAUDER, J. W. 1986. *Particle-size analysis 1,* Soil Science Society of America, American Society of Agronomy.

GEERAERD, A., VALDRAMIDIS, V. & VAN IMPE, J. 2005. GInaFiT, a freeware tool to assess non-log-linear microbial survivor curves. *International journal of food microbiology,* 102**,** 95-105.

GERBER, A., BUNDSCHUH, M., KLINGELHOFER, D. & GRONEBERG, D. A. 2013. Gold nanoparticles: recent aspects for human toxicology. *Journal of occupational medicine and toxicology,* 8**,** 32.

GODINEZ, I. G. & DARNAULT, C. J. 2011. Aggregation and transport of nano-TiO2 in saturated porous media: effects of pH, surfactants and flow velocity. *Water research,* 45**,** 839-851.

GUPTA, R. P. & SWARTZENDRUBER, D. 1962. Flow-Associated Reduction in the Hydraulic Conductivity of Quartz Sand 1. *Soil Science Society of America Journal,* 26**,** 6-10.

HAN, Y., HWANG, G., KIM, D., BRADFORD, S. A., LEE, B., EOM, I., KIM, P. J., CHOI, S. Q. & KIM, H. 2016. Transport, retention, and long-term release behavior of ZnO nanoparticle aggregates in saturated quartz sand: Role of solution pH and biofilm coating. *Water research,* 90**,** 247-257.

HARPAZ, Y. 1971. Artificial ground-water recharge by means of wells in Israel. *Journal of the Hydraulics Division,* 97**,** 1947-1964.

HARVEY, R. W. & RYAN, J. N. 2004. Use of PRD1 bacteriophage in groundwater viral transport, inactivation, and attachment studies. *FEMS Microbiology Ecology,* 49**,** 3-16.

HE, J.-Z., WANG, D.-J., FANG, H., FU, Q.-L. & ZHOU, D.-M. 2017. Inhibited transport of graphene oxide nanoparticles in granular quartz sand coated with Bacillus subtilis and Pseudomonas putida biofilms. *Chemosphere,* 169**,** 1-8.

HE, L., WU, D., RONG, H., LI, M., TONG, M. & KIM, H. 2018. Influence of Nano-and Microplastic Particles on the Transport and Deposition Behaviors of Bacteria in Quartz Sand. *Environmental science & technology,* 52**,** 11555-11563.

HIJIKATA, N., TEZUKA, R., KAZAMA, S., OTAKI, M., USHIJIMA, K., ITO, R., OKABE, S., SANO, D. & FUNAMIZU, N. 2016. Bactericidal and virucidal mechanisms in the alkaline disinfection of compost using calcium lime and ash. *Journal of environmental management,* 181**,** 721-727.

HILL, A., ZHU, D. & WANG, Y. 1995. The effect of wormholing on the fluid loss coefficient in acid fracturing. *SPE Production & Facilities,* 10**,** 257-264.

HOEK, E. M. & AGARWAL, G. K. 2006. Extended DLVO interactions between spherical particles and rough surfaces. *Journal of Colloid and Interface science,* 298**,** 50-58.

HU, W., PENG, C., LV, M., LI, X., ZHANG, Y., CHEN, N., FAN, C. & HUANG, Q. 2011. Protein corona-mediated mitigation of cytotoxicity of graphene oxide. *ACS nano,* 5**,** 3693-3700.

HUNDESA, A., DE MOTES, C. M., BOFILL-MAS, S., ALBINANA-GIMENEZ, N. & GIRONES, R. 2006. Identification of human and animal adenoviruses and polyomaviruses for determination of sources of fecal contamination in the environment. *Applied and environmental microbiology,* 72**,** 7886-7893.

HUYSMAN, F. & VERSTRAETE, W. 1993. Effect of cell surface characteristics on the adhesion of bacteria to soil particles. *Biology and fertility of soils,* 16**,** 21-26.

ISLAM, M. T., HYDER, A. G., SAENZ-ARANA, R., HERNANDEZ, C., GUINTO, T., AHSAN, M. A., ALVARADO-TENORIO, B. & NOVERON, J. C. 2019. Removal of methylene

blue and tetracycline from water using peanut shell derived adsorbent prepared by sulfuric acid reflux. *Journal of Environmental Chemical Engineering,* 7**,** 102816.

ISRAELACHVILI, J. 1992. Intermolecular and surface forces, Acad. *Press, Darmstadt*.

JAHN, A. & NIELSEN, P. 1995. Extraction of extracellular polymeric substances (EPS) from biofilms using a cation exchange resin. *Water science and technology,* 32**,** 157-164.

JANJAROEN, D., LING, F., MONROY, G., DERLON, N., MOGENROTH, E., BOPPART, S. A., LIU, W.-T. & NGUYEN, T. H. 2013. Roles of ionic strength and biofilm roughness on adhesion kinetics of Escherichia coli onto groundwater biofilm grown on PVC surfaces. *Water research,* 47**,** 2531-2542.

JASTRZĘBSKA, A. M., KURTYCZ, P. & OLSZYNA, A. R. 2012. Recent advances in graphene family materials toxicity investigations. *Journal of Nanoparticle Research,* 14**,** 1320.

JEONG, H. Y., JUN, S.-C., CHEON, J.-Y. & PARK, M. 2018. A review on clogging mechanisms and managements in aquifer storage and recovery (ASR) applications. *Geosciences Journal,* 22**,** 667-679.

JIAN-ZHOU, H., CHENG-CHENG, L., DENG-JUN, W. & ZHOU, D.-M. 2015. Biofilms and extracellular polymeric substances mediate the transport of graphene oxide nanoparticles in saturated porous media. *Journal of hazardous materials,* 300**,** 467-474.

JIANG, X., TONG, M., LU, R. & KIM, H. 2012. Transport and deposition of ZnO nanoparticles in saturated porous media. *Colloids and Surfaces A: Physicochemical and Engineering Aspects,* 401**,** 29-37.

JIANG, X., WANG, X., TONG, M. & KIM, H. 2013. Initial transport and retention behaviors of ZnO nanoparticles in quartz sand porous media coated with Escherichia coli biofilm. *Environmental pollution,* 174**,** 38-49.

JOO, S. H. & AGGARWAL, S. 2018. Factors impacting the interactions of engineered nanoparticles with bacterial cells and biofilms: Mechanistic insights and state of knowledge. *Journal of environmental management,* 225**,** 62-74.

KAMRANI, S., REZAEI, M., KORD, M. & BAALOUSHA, M. 2018. Transport and retention of carbon dots (CDs) in saturated and unsaturated porous media: Role of ionic strength, pH, and collector grain size. *Water research,* 133**,** 338-347.

KANEL, S. R., FLORY, J., MEYERHOEFER, A., FRALEY, J. L., SIZEMORE, I. E. & GOLTZ, M. N. 2015. Influence of natural organic matter on fate and transport of silver nanoparticles in saturated porous media: laboratory experiments and modeling. *Journal of Nanoparticle Research,* 17**,** 154.

KOESTEL, J. & JORDA, H. 2014. What determines the strength of preferential transport in undisturbed soil under steady-state flow? *Geoderma,* 217**,** 144-160.

KONIKOW, L. F., AUGUST, L. & VOSS, C. 2001. Effects of clay dispersion on aquifer storage and recovery in coastal aquifers. *Transport in porous media,* 43**,** 45-64.

KREYLING, W. G., SEMMLER-BEHNKE, M. & MÖLLER, W. 2006. Health implications of nanoparticles. *Journal of Nanoparticle Research,* 8**,** 543-562.

KURLANDA-WITEK, H., NGWENYA, B. & BUTLER, I. 2015. The influence of biofilms on the mobility of bare and capped zinc oxide nanoparticles in saturated sand and glass beads. *Journal of contaminant hydrology,* 179**,** 160-170.

LANCE, J. & WHISLER, F. 1972. Nitrogen Balance in Soil Columns Intermittently Flooded with Secondary Sewage Effluent 1. *Journal of Environmental quality,* 1**,** 180-186.

LANPHERE, J. D., LUTH, C. J. & WALKER, S. L. 2013. Effects of solution chemistry on the transport of graphene oxide in saturated porous media. *Environmental science & technology,* 47**,** 4255-4261.

LAZAROVA, V., LEVINE, B., SACK, J., CIRELLI, G., JEFFREY, P., MUNTAU, H., SALGOT, M. & BRISSAUD, F. 2001. Role of water reuse for enhancing integrated water management in Europe and Mediterranean countries. *Water Science and Technology,* 43**,** 25-33.

LEE, S.-H. & KIM, S.-J. 2002. Detection of infectious enteroviruses and adenoviruses in tap water in urban areas in Korea. *Water Research,* 36**,** 248-256.

LERNER, R. N., LU, Q., ZENG, H. & LIU, Y. 2012. The effects of biofilm on the transport of stabilized zerovalent iron nanoparticles in saturated porous media. *Water research,* 46**,** 975-985.

LIANG, L., KORTE, N., GU, B., PULS, R. & REETER, C. 2000. Geochemical and microbial reactions affecting the long-term performance of in situ 'iron barriers'. *Advances in Environmental Research,* 4**,** 273-286.

LIANG, Y., BRADFORD, S. A., ŠIMŮNEK, J. & KLUMPP, E. 2019. Mechanisms of graphene oxide aggregation, retention, and release in quartz sand. *Science of the Total Environment,* 656**,** 70-79.

LIANG, Y., BRADFORD, S. A., SIMUNEK, J., VEREECKEN, H. & KLUMPP, E. 2013. Sensitivity of the transport and retention of stabilized silver nanoparticles to physicochemical factors. *water research,* 47**,** 2572-2582.

LIPSON, S. M. & STOTZKY, G. 1983. Adsorption of reovirus to clay minerals: effects of cation-exchange capacity, cation saturation, and surface area. *Applied and Environmental Microbiology,* 46**,** 673-682.

LIU, L., GAO, B., WU, L., SUN, Y. & ZHOU, Z. 2015. Effects of surfactant type and concentration on graphene retention and transport in saturated porous media. *Chemical Engineering Journal,* 262**,** 1187-1191.

MA, C., HUANGFU, X., HE, Q., MA, J. & HUANG, R. 2018. Deposition of engineered nanoparticles (ENPs) on surfaces in aquatic systems: a review of interaction forces, experimental approaches, and influencing factors. *Environmental Science and Pollution Research***,** 1-26.

MACLER, B. A. & MERKLE, J. C. 2000. Current knowledge on groundwater microbial pathogens and their control. *Hydrogeology Journal,* 8**,** 29-40.

MAJEDI, S. M., KELLY, B. C. & LEE, H. K. 2014. Combined effects of water temperature and chemistry on the environmental fate and behavior of nanosized zinc oxide. *Science of The Total Environment,* 496**,** 585-593.

MAJKIĆ-DURSUN, B., PETKOVIĆ, A. & DIMKIĆ, M. 2015. The effect of iron oxidation in the groundwater of the alluvial aquifer of the Velika Morava River, Serbia, on the clogging of water supply wells. *J. Serb. Chem. Soc.,* 80**,** 947-957.

MAKSELON, J., ZHOU, D., ENGELHARDT, I., JACQUES, D. & KLUMPP, E. 2017. Experimental and numerical investigations of silver nanoparticle transport under variable flow and ionic strength in soil. *Environmental science & technology,* 51**,** 2096-2104.

MALGARESI, G., ZHANG, H., CHRYSIKOPOULOS, C. & BEDRIKOVETSKY, P. 2019. Cotransport of Suspended Colloids and Nanoparticles in Porous Media. *Transport in Porous Media***,** 1-25.

MALLANTS, D. 2014. Field-scale solute transport parameters derived from tracer tests in large undisturbed soil columns. *Soil research,* 52**,** 13-26.

MARSHALL, K. 1971. Sorptive interactions between soil particles and microorganisms. *Soil biochemistry,* 2**,** 409-445.

MARTIN, R. 2013. Clogging issues associated with managed aquifer recharge methods. *IAH Commission on Managing Aquifer Recharge*.

MATTISON, N. T., O'CARROLL, D. M., KERRY ROWE, R. & PETERSEN, E. J. 2011. Impact of porous media grain size on the transport of multi-walled carbon nanotubes. *Environmental science & technology,* 45**,** 9765-9775.

MATTLE, M. J., CROUZY, B., BRENNECKE, M., R. WIGGINTON, K., PERONA, P. & KOHN, T. 2011. Impact of virus aggregation on inactivation by peracetic acid and implications for other disinfectants. *Environmental science & technology,* 45**,** 7710-7717.

MAXWELL, R. M., WELTY, C. & TOMPSON, A. F. 2003. Streamline-based simulation of virus transport resulting from long term artificial recharge in a heterogeneous aquifer. *Advances in Water Resources,* 26**,** 1075-1096.

MAY, R. & LI, Y. 2013. The effects of particle size on the deposition of fluorescent nanoparticles in porous media: Direct observation using laser scanning cytometry. *Colloids and surfaces A: Physicochemical and engineering aspects,* 418**,** 84-91.

MAYOTTE, J. M., HÖLTING, L. & BISHOP, K. 2017. Reduced removal of bacteriophage MS2 in during basin infiltration managed aquifer recharge as basin sand is exposed to infiltration water. *Hydrological processes,* 31**,** 1690-1701.

MAYS, D. C. & HUNT, J. R. 2005. Hydrodynamic aspects of particle clogging in porous media. *Environmental science & technology,* 39**,** 577-584.

MAYS, D. C. & HUNT, J. R. 2007. Hydrodynamic and chemical factors in clogging by montmorillonite in porous media. *Environmental science & technology,* 41**,** 5666-5671.

MCCARTY, P. L. 1993. In situ bioremediation of chlorinated solvents. *Current opinion in biotechnology,* 4**,** 323-330.

MCCARTY, P. L., GOLTZ, M. N., HOPKINS, G. D., DOLAN, M. E., ALLAN, J. P., KAWAKAMI, B. T. & CARROTHERS, T. 1998. Full-scale evaluation of in situ cometabolic degradation of trichloroethylene in groundwater through toluene injection. *Environmental Science & Technology,* 32**,** 88-100.

MCDOWELL-BOYER, L. M., HUNT, J. R. & SITAR, N. 1986. Particle transport through porous media. *Water Resources Research,* 22**,** 1901-1921.

MONDAL, P. K. & SLEEP, B. E. 2013. Virus and virus-sized microsphere transport in a dolomite rock fracture. *Water Resources Research,* 49**,** 808-824.

MORONES, J. R., ELECHIGUERRA, J. L., CAMACHO, A., HOLT, K., KOURI, J. B., RAMÍREZ, J. T. & YACAMAN, M. J. 2005. The bactericidal effect of silver nanoparticles. *Nanotechnology,* 16**,** 2346.

MORRIS, C. & MOONEY, S. 2004. A high-resolution system for the quantification of preferential flow in undisturbed soil using observations of tracers. *Geoderma,* 118**,** 133-143.

MOZES, N., MARCHAL, F., HERMESSE, M., VAN HAECHT, J., REULIAUX, L., LEONARD, A. & ROUXHET, P. 1987. Immobilization of microorganisms by adhesion: interplay of electrostatic and nonelectrostatic interactions. *Biotechnology and Bioengineering,* 30**,** 439-450.

MUELLER, N. C. & NOWACK, B. 2008. Exposure modeling of engineered nanoparticles in the environment. *Environmental science & technology,* 42**,** 4447-4453.

NASCIMENTO, A., TOTOLA, M., SOUZA, C., BORGES, M. & BORGES, A. 2006. Temporal and spatial dynamics of blocking and ripening effects on bacterial transport through a porous system: A possible explanation for CFT deviation. *Colloids and Surfaces B: Biointerfaces,* 53**,** 241-244.

NEUKUM, C., BRAUN, A. & AZZAM, R. 2014. Transport of engineered silver (Ag) nanoparticles through partially fractured sandstones. *Journal of contaminant hydrology,* 164**,** 181-192.

NG, T. W., LI, B., CHOW, A. & WONG, P. K. 2016. Effects of bromide on inactivation efficacy and disinfection byproduct formation in photocatalytic inactivation. *Journal of Photochemistry and Photobiology A: Chemistry,* 324**,** 145-151.

NOBLE, R. T., LEE, I. M. & SCHIFF, K. C. 2004. Inactivation of indicator micro-organisms from various sources of faecal contamination in seawater and freshwater. *Journal of applied microbiology,* 96**,** 464-472.

OBERDORFER, J. A. & PETERSON, F. L. 1985. Waste-water injection: geochemical and biogeochemical clogging processes. *Groundwater,* 23**,** 753-761.

PAGE, D., BEKELE, E., VANDERZALM, J. & SIDHU, J. 2018. Managed aquifer recharge (MAR) in sustainable urban water management. *Water,* 10**,** 239.

PAGE, D., MIOTLIŃSKI, K., DILLON, P., TAYLOR, R., WAKELIN, S., LEVETT, K., BARRY, K. & PAVELIC, P. 2011. Water quality requirements for sustaining aquifer storage and recovery operations in a low permeability fractured rock aquifer. *Journal of environmental management,* 92**,** 2410-2418.

PAGE, D., VANDERZALM, J., MIOTLIŃSKI, K., BARRY, K., DILLON, P., LAWRIE, K. & BRODIE, R. S. 2014. Determining treatment requirements for turbid river water to avoid clogging of aquifer storage and recovery wells in siliceous alluvium. *Water research,* 66**,** 99-110.

PAL, S., TAK, Y. K. & SONG, J. M. 2007. Does the antibacterial activity of silver nanoparticles depend on the shape of the nanoparticle? A study of the gram-negative bacterium Escherichia coli. *Appl. Environ. Microbiol.,* 73**,** 1712-1720.

PANG, L., FARKAS, K., BENNETT, G., VARSANI, A., EASINGWOOD, R., TILLEY, R., NOWOSTAWSKA, U. & LIN, S. 2014. Mimicking filtration and transport of rotavirus and adenovirus in sand media using DNA-labeled, protein-coated silica nanoparticles. *Water research,* 62**,** 167-179.

PENG, S., WU, D., GE, Z., TONG, M. & KIM, H. 2017. Influence of graphene oxide on the transport and deposition behaviors of colloids in saturated porous media. *Environmental pollution,* 225**,** 141-149.

PEULEN, T.-O. & WILKINSON, K. J. 2011. Diffusion of nanoparticles in a biofilm. *Environmental science & technology,* 45**,** 3367-3373.

PHAM, M., MINTZ, E. A. & NGUYEN, T. H. 2009. Deposition kinetics of bacteriophage MS2 to natural organic matter: Role of divalent cations. *Journal of colloid and interface science,* 338**,** 1-9.

PLATZER, C. & MAUCH, K. 1997. Soil clogging in vertical flow reed beds-Mechanisms, parameters, consequences and..... solutions? *Water Science and Technology,* 35**,** 175-181.

PULS, R. W. & POWELL, R. M. 1992. Transport of inorganic colloids through natural aquifer material: Implications for contaminant transport. *Environmental Science & Technology,* 26**,** 614-621.

QI, Z., DU, T., MA, P., LIU, F. & CHEN, W. 2019. Transport of graphene oxide in saturated quartz sand containing iron oxides. *Science of The Total Environment,* 657**,** 1450-1459.

QI, Z., HOU, L., ZHU, D., JI, R. & CHEN, W. 2014a. Enhanced transport of phenanthrene and 1-naphthol by colloidal graphene oxide nanoparticles in saturated soil. *Environmental science & technology,* 48**,** 10136-10144.

QI, Z., ZHANG, L. & CHEN, W. 2014b. Transport of graphene oxide nanoparticles in saturated sandy soil. *Environmental Science: Processes & Impacts,* 16**,** 2268-2277.

QI, Z., ZHANG, L., WANG, F., HOU, L. & CHEN, W. 2014c. Factors controlling transport of graphene oxide nanoparticles in saturated sand columns. *Environmental toxicology and chemistry,* 33**,** 998-1004.

RAGUSA, S., DE ZOYSA, D. & RENGASAMY, P. 1994. The effect of microorganisms, salinity and turbidity on hydraulic conductivity of irrigation channel soil. *Irrigation Science,* 15**,** 159-166.

RAHMATPOUR, S., SHIRVANI, M., MOSADDEGHI, M. R. & BAZARGANIPOUR, M. 2017. Retention of silver nano-particles and silver ions in calcareous soils: Influence of soil properties. *Journal of environmental management,* 193**,** 136-145.

RAUCH-WILLIAMS, T., HOPPE-JONES, C. & DREWES, J. 2010. The role of organic matter in the removal of emerging trace organic chemicals during managed aquifer recharge. *Water research,* 44**,** 449-460.

RENGASAMY, P., MCLEOD, A. & RAGUSA, S. 1996. Effects of dispersible soil clay and algae on seepage prevention from small dams. *Agricultural water management,* 29**,** 117-127.

RENSLOW, R. S., MAJORS, P. D., MCLEAN, J. S., FREDRICKSON, J. K., AHMED, B. & BEYENAL, H. 2010. In situ effective diffusion coefficient profiles in live biofilms using pulsed-field gradient nuclear magnetic resonance. *Biotechnology and Bioengineering,* 106**,** 928-937.

REYNOLDS, K. A., MENA, K. D. & GERBA, C. P. 2008. Risk of waterborne illness via drinking water in the United States. *Reviews of environmental contamination and toxicology*. Springer.

RINCK-PFEIFFER, S., RAGUSA, S., SZTAJNBOK, P. & VANDEVELDE, T. 2000. Interrelationships between biological, chemical, and physical processes as an analog to clogging in aquifer storage and recovery (ASR) wells. *Water Research,* 34**,** 2110-2118.

RINCK-PFEIFFER, S. M. 2000. *Physical and biochemical clogging processes arising from aquifer storage and recovery (ASR) with treated wastewater*. Flinders University of South Australia, School of Chemistry, Physics & Earth ….

SADEGHI, G., SCHIJVEN, J. F., BEHRENDS, T., HASSANIZADEH, S. M., GERRITSE, J. & KLEINGELD, P. J. 2011. Systematic study of effects of pH and ionic strength on attachment of phage PRD1. *Groundwater,* 49**,** 12-19.

SAHA, A. K., SINHA, A. & PASUPULETI, S. 2019. Modification, characterization and investigations of key factors controlling the transport of modified nano zero-valent iron (nZVI) in porous media. *Environmental technology,* 40**,** 1543-1556.

SAHLE-DEMESSIE, E. & TADESSE, H. 2011. Kinetics and equilibrium adsorption of nano-TiO2 particles on synthetic biofilm. *Surface Science,* 605**,** 1177-1184.

SAIERS, J. E. 2002. Laboratory observations and mathematical modeling of colloid-facilitated contaminant transport in chemically heterogeneous systems. *Water resources research,* 38.

SALAS, E. C., SUN, Z., LÜTTGE, A. & TOUR, J. M. 2010. Reduction of graphene oxide via bacterial respiration. *ACS nano,* 4**,** 4852-4856.

SALEH, N., SIRK, K., LIU, Y., PHENRAT, T., DUFOUR, B., MATYJASZEWSKI, K., TILTON, R. D. & LOWRY, G. V. 2007. Surface modifications enhance nanoiron transport and NAPL targeting in saturated porous media. *Environmental Engineering Science,* 24**,** 45-57.

SASIDHARAN, S., BRADFORD, S. A., ŠIMŮNEK, J., TORKZABAN, S. & VANDERZALM, J. 2017a. Transport and fate of viruses in sediment and stormwater from a Managed Aquifer Recharge site. *Journal of Hydrology,* 555**,** 724-735.

SASIDHARAN, S., TORKZABAN, S., BRADFORD, S. A., COOK, P. G. & GUPTA, V. V. 2017b. Temperature dependency of virus and nanoparticle transport and retention in saturated porous media. *Journal of contaminant hydrology,* 196**,** 10-20.

SASIDHARAN, S., TORKZABAN, S., BRADFORD, S. A., DILLON, P. J. & COOK, P. G. 2014. Coupled effects of hydrodynamic and solution chemistry on long-term nanoparticle transport and deposition in saturated porous media. *Colloids and surfaces A: physicochemical and engineering aspects,* 457**,** 169-179.

SASIDHARAN, S., TORKZABAN, S., BRADFORD, S. A., KOOKANA, R., PAGE, D. & COOK, P. G. 2016. Transport and retention of bacteria and viruses in biochar-amended sand. *Science of the Total Environment,* 548**,** 100-109.

SCANDURA, J. & SOBSEY, M. 1997. Viral and bacterial contamination of groundwater from on-site sewage treatment systems. *Water Science and Technology,* 35**,** 141-146.

SCHIFFENBAUER, M. & STOTZKY, G. 1982. Adsorption of coliphages T1 and T7 to clay minerals. *Applied and Environmental Microbiology,* 43**,** 590-596.

SCHIJVEN, J. F. & HASSANIZADEH, S. M. 2000. Removal of viruses by soil passage: Overview of modeling, processes, and parameters. *Critical reviews in environmental science and technology,* 30**,** 49-127.

SCHROTH, B. K. & SPOSITO, G. 1996. Surface charge properties of kaolinite. *MRS Online Proceedings Library Archive,* 432.

SCHULTEN, H.-R. & SCHNITZER, M. 1993. A state of the art structural concept for humic substances. *Naturwissenschaften,* 80**,** 29-30.

SEIFERT, D. & ENGESGAARD, P. 2007. Use of tracer tests to investigate changes in flow and transport properties due to bioclogging of porous media. *Journal of contaminant hydrology,* 93**,** 58-71.

SEKI, K., SUKO, T. & MIYAZAKI, T. Bioclogging of glass beads by bacteria and fungi. Trans. World Congr. Soil Sci. Symposium, 2002. 1244-1.

SHARP, R., CUNNINGHAM, A., KOMLOS, J. & BILLMAYER, J. 1999. Observation of thick biofilm accumulation and structure in porous media and corresponding hydrodynamic and mass transfer effects. *Water Science and Technology,* 39**,** 195-201.

SIDHU, J., HODGERS, L., AHMED, W., CHONG, M. & TOZE, S. 2012. Prevalence of human pathogens and indicators in stormwater runoff in Brisbane, Australia. *water research,* 46**,** 6652-6660.

SINGH, S. K., SINGH, M. K., NAYAK, M. K., KUMARI, S., GRÁCIO, J. & DASH, D. 2011. Characterization of graphene oxide by flow cytometry and assessment of its cellular toxicity. *Journal of biomedical nanotechnology,* 7**,** 30-31.

SINTON, L. W., HALL, C. H., LYNCH, P. A. & DAVIES-COLLEY, R. J. 2002. Sunlight inactivation of fecal indicator bacteria and bacteriophages from waste stabilization pond effluent in fresh and saline waters. *Applied and environmental microbiology,* 68**,** 1122-1131.

SIRIWARDENE, N., DELETIC, A. & FLETCHER, T. 2007. Clogging of stormwater gravel infiltration systems and filters: Insights from a laboratory study. *Water research,* 41**,** 1433-1440.

SMIRNOVA, T., DIDENKO, L., AZIZBEKYAN, R. & ROMANOVA, Y. M. 2010. Structural and functional characteristics of bacterial biofilms. *Microbiology,* 79**,** 413-423.

SOTIRELIS, N. P. & CHRYSIKOPOULOS, C. V. 2015. Interaction between graphene oxide nanoparticles and quartz sand. *Environmental science & technology,* 49**,** 13413-13421.

STEVENSON, M. E., SOMMER, R., LINDNER, G., FARNLEITNER, A. H., TOZE, S., KIRSCHNER, A. K., BLASCHKE, A. P. & SIDHU, J. P. 2015. Attachment and detachment behavior of human Adenovirus and surrogates in fine granular limestone aquifer material. *Journal of environmental quality,* 44**,** 1392-1401.

STEVIK, T. K., AA, K., AUSLAND, G. & HANSSEN, J. F. 2004. Retention and removal of pathogenic bacteria in wastewater percolating through porous media: a review. *Water research,* 38**,** 1355-1367.

STUYFZAND, P. J. 2011. Hydrogeochemical processes during riverbank filtration and artificial recharge of polluted surface waters: zonation, identification, and quantification. *Riverbank Filtration for Water Security in Desert Countries.* Springer.

SU, Y., GAO, B. & MAO, L. 2017. Concurrent agglomeration and straining govern the transport of 14C-labeled few-layer graphene in saturated porous media. *Water research,* 115**,** 84-93.

SUN, Y., GAO, B., BRADFORD, S. A., WU, L., CHEN, H., SHI, X. & WU, J. 2015. Transport, retention, and size perturbation of graphene oxide in saturated porous media: effects of input concentration and grain size. *water research,* 68**,** 24-33.

SYMONDS, E. M., GRIFFIN, D. W. & BREITBART, M. 2009. Eukaryotic viruses in wastewater samples from the United States. *Appl. Environ. Microbiol.,* 75**,** 1402-1409.

SYNGOUNA, V. I. & CHRYSIKOPOULOS, C. V. 2013. Cotransport of clay colloids and viruses in water saturated porous media. *Colloids and surfaces A: Physicochemical and engineering aspects,* 416**,** 56-65.

TANEDA, S. 1979. Visualization of separating Stokes flows. *Journal of the Physical Society of Japan,* 46**,** 1935-1942.

TAYLOR, S. W. & JAFFÉ, P. R. 1990. Biofilm growth and the related changes in the physical properties of a porous medium: 1. Experimental investigation. *Water resources research,* 26**,** 2153-2159.

THOMPSON, S. S., FLURY, M., YATES, M. V. & JURY, W. A. 1998. Role of the air-water-solid interface in bacteriophage sorption experiments. *Applied and environmental microbiology,* 64**,** 304-309.

THULLNER, M. 2010. Comparison of bioclogging effects in saturated porous media within one- and two-dimensional flow systems. *Ecological Engineering,* 36**,** 176-196.

TIAN, Y., GAO, B., WANG, Y., MORALES, V. L., CARPENA, R. M., HUANG, Q. & YANG, L. 2012. Deposition and transport of functionalized carbon nanotubes in water-saturated sand columns. *Journal of hazardous materials,* 213**,** 265-272.

TONG, M., DING, J., SHEN, Y. & ZHU, P. 2010. Influence of biofilm on the transport of fullerene (C60) nanoparticles in porous media. *water research,* 44**,** 1094-1103.

TONG, M., SHEN, Y., YANG, H. & KIM, H. 2012. Deposition kinetics of MS2 bacteriophages on clay mineral surfaces. *Colloids and Surfaces B: Biointerfaces,* 92**,** 340-347.

TORIDE, N., INOUE, M. & LEIJ, F. J. 2003. Hydrodynamic dispersion in an unsaturated dune sand. *Soil Science Society of America Journal,* 67**,** 703-712.

TORKZABAN, S. & BRADFORD, S. A. 2016. Critical role of surface roughness on colloid retention and release in porous media. *Water research,* 88**,** 274-284.

TORKZABAN, S., BRADFORD, S. A., VAN GENUCHTEN, M. T. & WALKER, S. L. 2008a. Colloid transport in unsaturated porous media: The role of water content and ionic strength on particle straining. *Journal of Contaminant Hydrology,* 96**,** 113-127.

TORKZABAN, S., HASSANIZADEH, S., SCHIJVEN, J., DE BRUIN, H. & DE RODA HUSMAN, A. 2006. Virus transport in saturated and unsaturated sand columns. *Vadose Zone Journal,* 5**,** 877-885.

TORKZABAN, S., TAZEHKAND, S. S., WALKER, S. L. & BRADFORD, S. A. 2008b. Transport and fate of bacteria in porous media: Coupled effects of chemical conditions and pore space geometry. *Water Resources Research,* 44.

TOZE, S. 1999. PCR and the detection of microbial pathogens in water and wastewater. *Water Research,* 33**,** 3545-3556.

TRIPATHI, S., CHAMPAGNE, D. & TUFENKJI, N. 2011. Transport behavior of selected nanoparticles with different surface coatings in granular porous media coated with Pseudomonas aeruginosa biofilm. *Environmental science & technology,* 46**,** 6942-6949.

TUFENKJI, N. & ELIMELECH, M. 2005a. Breakdown of colloid filtration theory: Role of the secondary energy minimum and surface charge heterogeneities. *Langmuir,* 21**,** 841-852.

TUFENKJI, N. & ELIMELECH, M. 2005b. Spatial distributions of Cryptosporidium oocysts in porous media: Evidence for dual mode deposition. *Environmental science & technology,* 39**,** 3620-3629.

TUFENKJI, N., MILLER, G. F., RYAN, J. N., HARVEY, R. W. & ELIMELECH, M. 2004. Transport of Cryptosporidium oocysts in porous media: Role of straining and physicochemical filtration. *Environmental science & technology,* 38**,** 5932-5938.

TZORAKI, O., DOKOU, Z., CHRISTODOULOU, G., GAGANIS, P. & KARATZAS, G. 2018. Assessing the efficiency of a coastal Managed Aquifer Recharge (MAR) system in Cyprus. *Science of the Total Environment,* 626**,** 875-886.

VAIDYANATHAN, R. & TIEN, C. 1988. Hydrosol deposition in granular beds. *Chemical Engineering Science,* 43**,** 289-302.

VALDIVIESO, A. L., BAHENA, J. R., SONG, S. & URBINA, R. H. 2006. Temperature effect on the zeta potential and fluoride adsorption at the α-Al2O3/aqueous solution interface. *Journal of Colloid and Interface Science,* 298**,** 1-5.

VAN BEEK, C. & VAN DER KOOIJ, D. 1982. Sulfate-reducing bacteria in ground water from clogging and nonclogging shallow wells in the Netherlands river region. *Groundwater,* 20**,** 298-302.

VANDERZALM, J., PAGE, D., BARRY, K. & DILLON, P. 2010. A comparison of the geochemical response to different managed aquifer recharge operations for injection of urban stormwater in a carbonate aquifer. *Applied Geochemistry,* 25**,** 1350-1360.

VANDERZALM, J. L., PAGE, D. W., BARRY, K. E., SCHEIDERICH, K., GONZALEZ, D. & DILLON, P. J. 2016. Probabilistic approach to evaluation of metal (loid) fate during stormwater aquifer storage and recovery. *CLEAN–Soil, Air, Water,* 44**,** 1672-1684.

VANDEVIVERE, P. & BAVEYE, P. 1992a. Effect of bacterial extracellular polymers on the saturated hydraulic conductivity of sand columns. *Appl. Environ. Microbiol.,* 58**,** 1690-1698.

VANDEVIVERE, P. & BAVEYE, P. 1992b. Relationship between transport of bacteria and their clogging efficiency in sand columns. *Appl. Environ. Microbiol.,* 58**,** 2523-2530.

VANDEVIVERE, P. & BAVEYE, P. 1992c. Sampling method for the observation of microorganisms in unconsolidated porous media via scanning electron microscopy. *Soil Science,* 153**,** 482-485.

VANDEVIVERE, P. & BAVEYE, P. 1992d. Saturated hydraulic conductivity reduction caused by aerobic bacteria in sand columns. *Soil Science Society of America Journal,* 56**,** 1-13.

VASILIADOU, I. A. & CHRYSIKOPOULOS, C. V. 2011. Cotransport of Pseudomonas putida and kaolinite particles through water-saturated columns packed with glass beads. *Water Resources Research,* 47.

VEERAPANENI, S. & WIESNER, M. R. 1997. Deposit morphology and head loss development in porous media. *Environmental science & technology,* 31**,** 2738-2744.

WANG, D., JIN, Y. & JAISI, D. P. 2015. Effect of size-selective retention on the cotransport of hydroxyapatite and goethite nanoparticles in saturated porous media. *Environmental science & technology,* 49**,** 8461-8470.

WANG, D., JIN, Y., PARK, C. M., HEO, J., BAI, X., AICH, N. & SU, C. 2018. Modeling the Transport of the "New-Horizon" Reduced Graphene Oxide—Metal Oxide Nanohybrids in Water-Saturated Porous Media. *Environmental science & technology,* 52**,** 4610-4622.

WANG, D., SHEN, C., JIN, Y., SU, C., CHU, L. & ZHOU, D. 2017a. Role of solution chemistry in the retention and release of graphene oxide nanomaterials in uncoated and iron oxide-coated sand. *Science of the Total Environment,* 579**,** 776-785.

WANG, M., GAO, B., TANG, D., SUN, H., YIN, X. & YU, C. 2017b. Effects of temperature on graphene oxide deposition and transport in saturated porous media. *Journal of hazardous materials,* 331**,** 28-35.

WANG, M., YU, C., TANG, D., CHEN, J. & GAO, B. 2019. Effects of Surfactant and Electrolyte Concentrations, Cation Valence, and Temperature on Graphene Oxide Retention and Transport in Saturated Porous Media. *Water, Air, & Soil Pollution,* 230**,** 21.

WANG, P., SHI, Q., LIANG, H., STEUERMAN, D. W., STUCKY, G. D. & KELLER, A. A. 2008. Enhanced environmental mobility of carbon nanotubes in the presence of humic acid and their removal from aqueous solution. *small,* 4**,** 2166-2170.

WANG, S., SUN, H., ANG, H.-M. & TADÉ, M. 2013a. Adsorptive remediation of environmental pollutants using novel graphene-based nanomaterials. *Chemical Engineering Journal,* 226**,** 336-347.

WANG, Y., BRADFORD, S. A. & ŠIMŮNEK, J. 2013b. Transport and fate of microorganisms in soils with preferential flow under different solution chemistry conditions. *Water Resources Research,* 49**,** 2424-2436.

WANG, Z., DU, X., YANG, Y. & YE, X. 2012. Surface clogging process modeling of suspended solids during urban stormwater aquifer recharge. *Journal of Environmental Sciences,* 24**,** 1418-1424.

WENG, S., DUNKIN, N., SCHWAB, K. J., MCQUARRIE, J., BELL, K. & JACANGELO, J. G. 2018. Infectivity reduction efficacy of UV irradiation and peracetic acid-UV combined treatment on MS2 bacteriophage and murine norovirus in secondary wastewater effluent. *Journal of environmental management,* 221**,** 1-9.

WU, B., WANG, Y., LEE, Y.-H., HORST, A., WANG, Z., CHEN, D.-R., SURESHKUMAR, R. & TANG, Y. J. 2010. Comparative eco-toxicities of nano-ZnO particles under aquatic and aerosol exposure modes. *Environmental Science & Technology,* 44**,** 1484-1489.

WU, L., LIU, L., GAO, B., MUÑOZ-CARPENA, R., ZHANG, M., CHEN, H., ZHOU, Z. & WANG, H. 2013. Aggregation kinetics of graphene oxides in aqueous solutions: experiments, mechanisms, and modeling. *Langmuir,* 29**,** 15174-15181.

XIA, L., ZHENG, X., SHAO, H., XIN, J., SUN, Z. & WANG, L. 2016. Effects of bacterial cells and two types of extracellular polymers on bioclogging of sand columns. *Journal of Hydrology,* 535**,** 293-300.

XIA, T., FORTNER, J. D., ZHU, D., QI, Z. & CHEN, W. 2015. Transport of sulfide-reduced graphene oxide in saturated quartz sand: Cation-dependent retention mechanisms. *Environmental science & technology,* 49**,** 11468-11475.

YANG, H., KIM, H. & TONG, M. 2012a. Influence of humic acid on the transport behavior of bacteria in quartz sand. *Colloids and Surfaces B: Biointerfaces,* 91**,** 122-129.

YANG, H., TONG, M. & KIM, H. 2012b. Influence of bentonite particles on representative gram negative and gram positive bacterial deposition in porous media. *Environmental science & technology,* 46**,** 11627-11634.

YANG, H., TONG, M. & KIM, H. 2013. Effect of carbon nanotubes on the transport and retention of bacteria in saturated porous media. *Environmental science & technology,* 47**,** 11537-11544.

YATES, M. V., GERBA, C. P. & KELLEY, L. M. 1985. Virus persistence in groundwater. *Appl. Environ. Microbiol.,* 49**,** 778-781.

ZÄNKER, H. & SCHIERZ, A. 2012. Engineered nanoparticles and their identification among natural nanoparticles. *Annual review of analytical chemistry,* 5**,** 107-132.

ZHANG, D., ZHOU, C.-H., LIN, C.-X., TONG, D.-S. & YU, W.-H. 2010. Synthesis of clay minerals. *Applied Clay Science,* 50**,** 1-11.

ZHANG, W., HUAN, Y., YU, X., LIU, D. & ZHOU, J. 2015a. Multi-component transport and transformation in deep confined aquifer during groundwater artificial recharge. *Journal of environmental management,* 152**,** 109-119.

ZHANG, Z., PENG, X., ZHOU, H., LIN, H. & SUN, H. 2015b. Characterizing preferential flow in cracked paddy soils using computed tomography and breakthrough curve. *Soil and Tillage Research,* 146**,** 53-65.

ZHONG, X. & WU, Y. 2013. Bioclogging in porous media under continuous-flow condition. *Environmental earth sciences,* 68**,** 2417-2425.

ZHOU, C. H. 2011. An overview on strategies towards clay-based designer catalysts for green and sustainable catalysis. *Applied Clay Science,* 53**,** 87-96.